SPACECRAFT DESIGN PROJECT LOW EARTH ORBIT COMMUNICATIONS SATELLITE

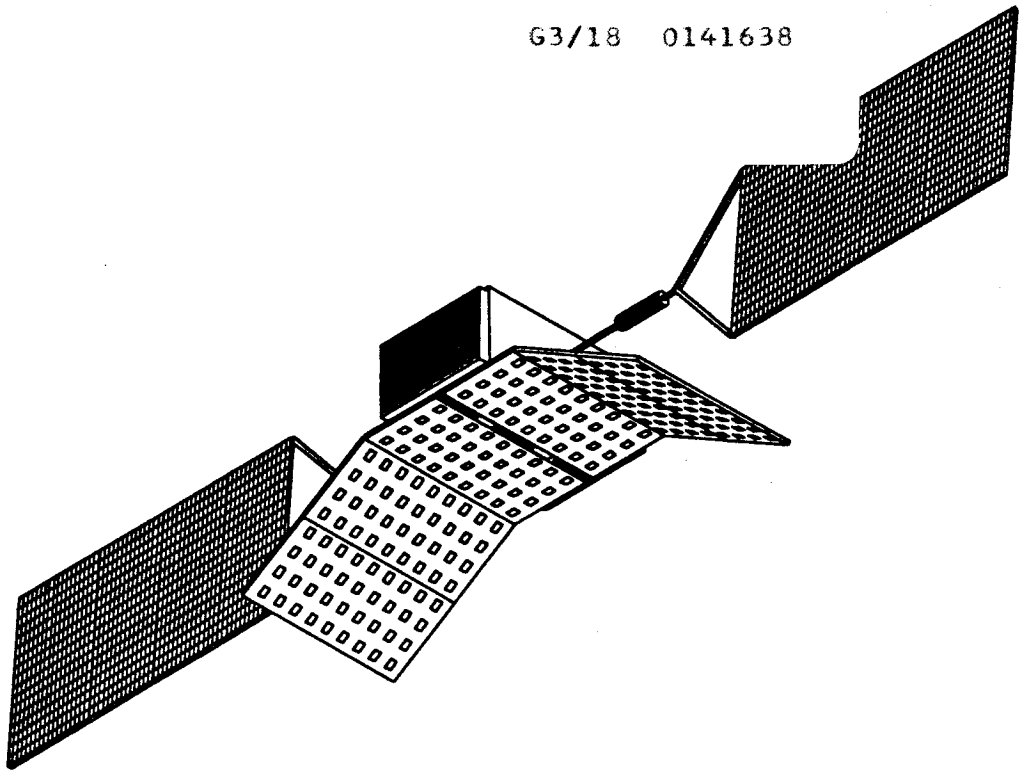

December 1991

NAVAL POSTGRADUATE SCHOOL
MONTEREY, CALIFORNIA

THIS PAGE INTENTIONALLY LEFT BLANK

SPACECRAFT DESIGN PROJECT TEAM

Dave Moroney	System Manager
Dave Lashbrook	Documentation
Barry McKibben	Orbital Analysis
Nigel Gardener	Configuration Manager
Thane Rivers	Launch Vehicle Integration
Greg Nottingham	Structure
Bill Golden	Payload
Bill Barfield	Telemetry,Tracking & Control
Joe Bruening	Electrical Power
Dave Wood	Thermal Control
Dave Pauls	Attitude Control
Walt Bell	Propulsion
Denise Price	Test and Evaluation Manager
Craig Baldwin	Cost Analysis

COURSE
AE-4871
Advanced Spacecraft Design
Fall 1991
Course Instructor
Prof. B. Agrawal

This project was sponsored by the NASA/Universities Space Research Association
Advanced Design Program

ACKNOWLEDGMENTS

The design team would like to express its sincere appreciation to Professor Brij Agrawal for his guidance and assistance throughout the 11 week project. We also wish to thank Dr. Edward Euler, and Mr. Dan Sakoda of the Naval Postgraduate School for their continuing assistance. Mr. Tony Navarra and Mr. Bob Wiedeman of Loral Aerospace Corporation provided the FCC Licensing Request for the GLOBALSTAR Communications System which served as the conceptual basis for the project. Additionally, they provided access to the commercial engineers who were developing the GLOBALSTAR system. The Lockheed FSAT Project Office devoted an entire day to conceptual and detailed design discussions, and remained available for consultation throughout the project. Specifically, the following people's assistance were invaluable: Mr. Larry Van Erdun for structural analysis; Mr. Bill Rust for power and solar array design; Mr. Marty Gerbasi and Mr. Larry Tong for thermal analysis and design; Mr. Jim Kim and Mr. Bruce Simpson for dynamics and attitude control design; and Mr. Kevin Vogler for development of the cost breakdown structure. Finally, we appreciate the comments and interest expressed by Dr. Kim Arron of the Jet Propulsion Laboratory.

TABLE OF CONTENTS

I. INTRODUCTION

A. PURPOSE

This report is the final product of the spacecraft design project completed to fulfill the academic requirements of the Spacecraft Design and Integration II course (AE-4871) taught at the U.S. Naval Postgraduate School.

B. BACKGROUND

The Spacecraft Design and Integration II course is intended to provide students detailed design experience in selection and design of both satellite system and subsystem components, and their location and integration into a final spacecraft configuration. The design team pursued a design to support a Low Earth Orbiting (LEO) communications system currently under development by the Loral Cellular Systems, Corporation.

Each of the 14 team members was assigned both primary and secondary duties in program management or system design. Hardware selection, spacecraft component design, analysis and integration were accomplished within the constraints imposed by the 11 week academic schedule and the available design facilities.

C. PROGRAM CONCEPT

On June 3, 1991 Loral Cellular Systems, Corporation of Palo Alto, California submitted to the Federal Communications Commission a licensing request for authority to construct their proposed GLOBALSTAR communications system [Ref 1]. The request

proposed a joint effort between Loral Aerospace Corp., which will provide for aerospace systems development, and QUALCOMM, Inc., which has expertise in the area of ground communications system technologies.

GLOBALSTAR is a satellite system designed to provide global Radio-Determination Satellite Services (RDSS) for real time position location and tracking, and voice and data services to mobile users. Rather than being a completely self sufficient system, GLOBALSTAR is intended to be integrated into the existing Public Switched Telephone Network (PSTN), Personal Communications Networks, and private, specialized and cellular networks. By complimenting existing carriers' networks, GLOBALSTAR is designed to make RDSS, voice, data, fax and freeze frame video available to users anywhere in the world.

In the licensing request, Loral defines the GLOBALSTAR program concept which is comprised of three distinct but interrelated segments: the space segment, the ground segment, and the mobile user segment. Figure I-1 depicts the integration of these three segments.

1. Space Segment

The GLOBALSTAR space segment is intended to consist of an on-orbit constellation of operational and dormant spare satellites. Loral plans a two phased program acquisition approach for the manufacture, procurement, and deployment of the space segment. For this design project, the first of Loral's phases, a smaller constellation optimized to provide coverage primarily for the continental United States, has been eliminated, and instead, the design goal was to develop a system to provide

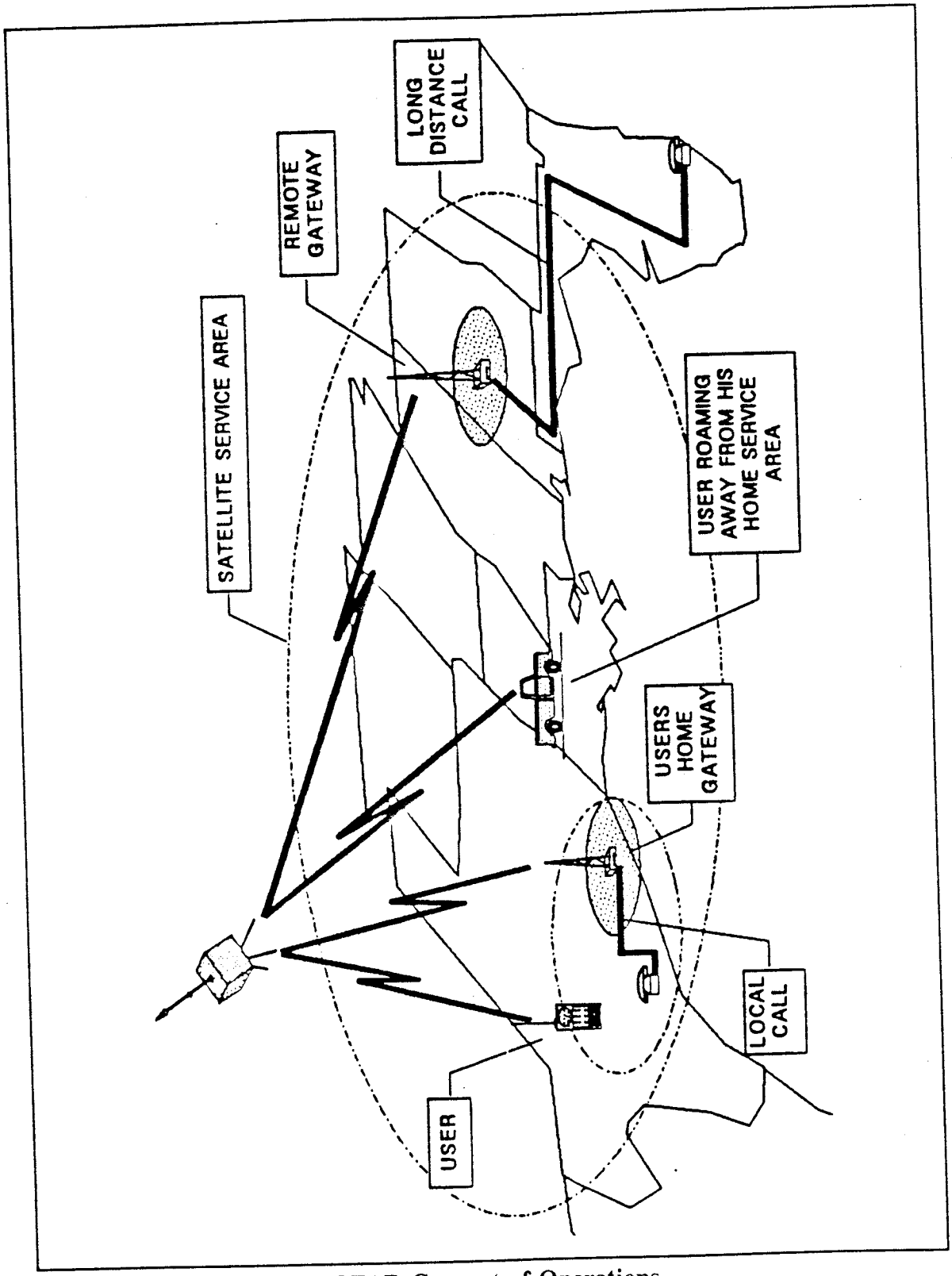

Figure I-1. GLOBALSTAR Concept of Operations

global coverage, which was Loral's second phase. Thus, the design is based on a constellation of 48 operational satellites in circular LEO orbit, with no on-orbit spares.

The communications payload designed by Loral for the GLOBALSTAR program is the sole payload incorporated into the design. Documentation contained in the licensing request provided the basis for determination of the payload supportability requirements which were the primary driver in the design process. Consequently, the launch vehicles intended for use in the GLOBALSTAR program, specifically Delta and Ariane, are also the launch vehicles on which this design is based.

Development of a single satellite configuration to fulfill the requirements of the space segment was the primary focus of the design project.

2. Ground Segment

The ground segment is identical in concept and design to the ground segment proposed by Loral. Key elements of the ground segment are: multiple gateway stations, two Telemetry, Tracking and Control stations located in the Continental United States (CONUS) with potential additional overseas stations positioned to provide continuous satellite-ground command link, a Satellite Operation Control Center (SOCC), and a Network Control Center (NCC).

a. Gateway Stations

Gateway stations link the orbiting satellite constellation and the PSTN. Stations are distributed throughout CONUS and the world and are installed and serviced by commercial communications carriers. Mobile users not serviced by an existing

communications system are linked to gateways via the space segment. Most gateways are directly connected to the land mobile communications network which in turn provides access to the PSTN. In addition to the routing of voice and date communications, the gateways provide RDSS functions in conjunction with user terminals.

b. Telemetry, Tracking and Control Stations (TT&C Stations)

TT&C stations are located on both the east and west coasts of CONUS as well as potential sites overseas. The stations perform tracking and ranging operations as well as satellite systems' performance monitoring to ensure proper maintenance of the on-orbit satellite constellation. A two-way link allows system status information to be downlinked and commands to be sent via uplink. Satellite ephemeris are transmitted to the SOCC for distribution to the gateways to allow them to acquire and track overhead satellites.

c. Satellite Operation Control Center (SOCC)

Tracking and ranging data provided by the TT&C stations are processed at the SOCC for acquisition, synchronization and satellite and beam handoff coordination between gateways. Individual satellite station-keeping maneuvers are planned and executed from the SOCC via TT&C stations.

d. Network Control Center (NCC)

The communications network is managed by the Network Control Center which performs the management functions of registration, verification, billing and

network data base distribution and resources management. Initial plans call for one NCC located in CONUS with options for the construction of additional international centers.

3. User Segment

Currently, three types of user equipment are envisioned to support the GLOBALSTAR concept. These include: hand-held or vehicle-mounted units strictly for RDSS services; hand-held units for voice and data services; and finally vehicle-mounted units for voice and data services. The GLOBALSTAR user segment concept and design has been adopted in this design.

D. SATELLITE DESCRIPTION

1. Statement of Work and Design / Performance Specification

The Statement of Work, presented in Appendix A, was generated based on the system information contained in Ref 1. Initial system design and performance specifications, presented in Table I.1, were also derived from payload supportability requirements delineated in Ref 1.

2. Operational Orbit

A constellation of 48 operational satellites, positioned in a Walker Delta pattern, provides the requirements for global coverage and redundancy. There is no allocation for on-orbit spares. The operational orbit is circular with an altitude of 750 nautical miles (nmi). Eight planes containing six satellites each, are oriented with 45 degree spacing between planes, 60 degree separation between consecutive satellites within each plane, and 7.5 degree sparation between adjacent satellites in neighboring planes.

Table I.1 Design and Performance Specifications

ORBIT ALTITUDE ECCENTRICITY COVERAGE	 750 nmi (1389 km) 0 (CIRCULAR) 75o N / S LATITUDE
LAUNCH VEHICLE	DELTA and ARIANE
MISSION LIFE	5 YEARS
INITIAL LAUNCH DATE	01 JULY 1996
STATION KEEPING STABILIZATION POINTING ACCURACY	 3 AXIS STABILIZATION + / - 1.0o ALL AXES
ELECTRICAL BUS OPERATION	 28 VDC CONTINUOUS (100%) DURING ECLIPSE PERIODS
THERMAL CONTROL	600 Watts FOR 33 MINUTES MAXIMUM
PAYLOAD MISSION POWER REQUIREMENTS MASS	 DIRECT VOICE AND DATA RELAY NETWORK; VOICE AND DATA LINK POSITION LOCATION 800 Watts FOR 20 MINUTES PEAK (50 Watts) NOMINAL 60 kg

Orbital period is 113.54 minutes at an inclination of 52 degrees. The spacecraft environment in the operational orbit imposes no significant design constraints.

3. Launch Vehicle Integration

To provide scheduling flexibility, the spacecraft is compatible with both the Delta and Ariane launch vehicles. Since the Delta 7925 launch vehicle places the most

stringent mass, volume and launch load restrictions, this paper is primarily concerned with satellite design compatibility with that launch vehicle.

A Satellite Launch Dispenser (SLD) designed specifically for the Delta 7925, allows a single launch vehicle to place an entire plane of the constellation on orbit. The SLD resembles a chest of drawers which ejects each satellite individually into its respective location in the operational orbit plane. By designing the deployment mechanism to pyrotechnically decouple the satellites from the SLD and to deploy them via load carrying rails, significant advantages over the standard stacked deployment technique are enjoyed. Specifically: a failure precluding the deployment of a single satellite does not adversely effect the deployment of subsequent satellites, and development of a single optimum satellite structural design is achieved. The SLD precludes the necessity to either develop different configurations for each satellite in the stack based on applied loads imposed by the satellites stacked above it; or to structurally over-design upper stack satellites to withstand the mass loads imposed on the lowest satellite in the stack.

4. Structure

The central structure consists of a frame of rectangular cross sectional aluminum tubing. Attached to the central frame on four sides are aluminum honeycomb panels that provide the mounting surfaces for low heat generating equipment. On the remaining two sides of the central frame, the thermal control cold plates provide both a thermal conduction means and a structural attachment surface for equipment requiring

higher heat dissipation characteristics. A circular support ring, structurally connected to the bottom panel of the spacecraft, supports the propellant tank.

5. Payload

The RDSS, voice and data communications payload is identical to the payload incorporated in the LORAL GLOBALSTAR System A design.

6. Telemetry, Tracking and Control

The TT&C system receives uplink commands from the terrestrial TT&C stations and downlinks telemetry data from various spacecraft systems. The on-board capability to store data for future execution provides for limited semi-autonomous operation. Command uplink and downlink frequencies bracket the C-Band spectrum allocated for the payload, using 6.5 GHz and 5.2 GHz, respectively. Telemetry and control data rates of 1000 and 500 bits/second require bandwidths of 500 Hz and 250 Hz, respectively.

Data encryption is used to prevent unauthorized communication with the spacecraft. Double redundancy is provided for the key components of Remote Tracking (RTU) and Command (RCU) Units, and the micro-strip antennas. The RCU's, which serve as the TT&C microprocessors also provide data bus protocol functions.

7. Electrical Power

A regulated dual bus system provides a constant 28 volts to the electrical components of all spacecraft systems. The solar array consists of BSFR silicon cells mounted on two fully interchangeable wings of 4 collapsible panels each. The arrays are

sized to provide a minimum nominal power of 600 watts at summer solstice End of Life (EOL). To augment the solar array when power loadings exceed the array's capabilities, and to provide 100% operation during eclipse, a nickel-hydrogen (NiH_2) battery is incorporated. Composed of 23 NiH_2 cells each rated at 40 A-hr, the battery is physically divided into four sections for integration purposes. The number of cells is based on a nominal 40% Depth of Discharge (DOD) with a maximum allowable DOD of 60%.

8. Thermal Control

Both active and passive thermal control mechanisms are employed to maintain thermal balance on-orbit. Two banks of louvers are mounted on two satellite exterior faces to dissipate the peak heat loads and provide linear temperature control over a 15 C temperature range. Temperature sensitive bimetallic actuators that do not require electrical power control the louvers. Combinations of heaters and thermal blankets are applied as necessary to appropriate components.

9. Attitude Control

A bias momentum wheel controls satellite attitude about the pitch and roll axes. A backup momentum wheel is included for redundancy. Magnetic torque rods are incorporated for roll control and desaturation of the momentum wheel, which is required approximately ever 17 hours. Propulsion system thrusters provide a backup mode for desaturation. Attitude sensors consist of a single solar aspect sensor, a two-axis scanning Earth Horizon sensor, and a two-axis magnetometer. All attitude control system communications are monitored and processed by the attitude control computer.

10. Propulsion

Monopropellant hydrazine, contained in a single spherical nitrogen pressurized propellant tank, is used by six 2.2 newton thrusters for station-keeping and backup momentum wheel desaturation.

E. REFERENCES

1. LORAL Cellular Systems, Corp., *Application of Loral Cellular Systems, Corp. Before the Federal Communications Commission*, Washington, D.C., June 3, 1991

THIS PAGE INTENTIONALLY LEFT BLANK

II. ORBIT DETERMINATION AND ANALYSIS

A. INTRODUCTION

A constellation of satellites placed into Low Earth Orbit (LEO) will provide mobile communications services to customers worldwide. The constellation provides the coverage required by the design and performance specifications, while minimizing the number of satellites and therefore, cost. For redundancy, and to preclude the need for on-orbit spares a minimum of two satellites are in view at any one time. The first operational launch is scheduled for 1 July 1996.

1. Operational Requirements

The constellation must provide one hundred percent coverage of the Earth's surface between 75 degrees north latitude and 75 degrees south latitude. Full service operations are supported for users with satellite elevation angles from 90 degrees (directly overhead) down to 10 degrees above the horizon. Degraded service may be achieved at elevation angles less than 10 degrees, depending upon the height of any obstructions along the line of sight between the user and the satellite. This situation will only occur at latitudes above 75 degrees.

2. Orbital Analysis Software

Orbits and ground coverages were analyzed using three orbital analysis programs. The following programs provided graphical and computational orbital analysis

tools such as satellite sensor ground coverage circles, ground track analysis, astrodynamic calculations, and perturbation analysis:

- Orbital Workbench - version 1.01 (Cygnus Engineering, 408-773-8366)
- OrbitView - version 2.0 (Cygnus Engineering)
- Personal Computer Satellite Orbit Analysis Package (PCSOAP) - version 5.3 (The Aerospace Corporation, 213-336-9380)

B. OPERATIONAL ORBIT CONSIDERATIONS

Environmental factors and cost were carefully weighed against optimization of mission requirements. Van Allen and solar radiation levels, space debris locations, atomic oxygen concentrations and atmospheric drag were all taken into account when selecting the orbits.

1. Van Allen Radiation Belt

The Van Allen Radiation Belt, which begins at an altitude of approximately 1,000 kilometers, can seriously effect LEO satellites. Electrons and protons are trapped within the Earth's magnetic field lines, with the protons dominating the lower altitude regions. As orbital radius increases out to approximately three and one half Earth radii, the radiation in the Van Allen Belt continuously increases. At higher altitudes, heavy shielding is required around electronic components driving up the weight and cost of the spacecraft. Solar array degradation is also increased in high radiation environments.

In accordance with the design specification, the operational orbital altitude of the constellation is 1389 kilometers (750 nautical miles), equating to an orbital radius of 1.22 Earth radii. The radiation level experienced by the satellites at that altitude is lower than the radiation level normally experienced by a geosynchronous satellite. Only minimal radiation

shielding of electronic components is necessary and solar array degradation over the lifetime of the spacecraft does not have a significant adverse impact on the design. Lowering the orbital altitude to reduce radiation degradation is not financially desireable since to do so will increase the number of satellites necessary to provide the required coverage.

2. Space Debris

Debris is made up of both natural micro-meteoroids and man made objects from prior space launches. Most of the man made debris in LEO is intentionally deorbited so that it completely burns up in the Earth's atmosphere; however, there are still thousands of items which were not controllable that have been discarded in space. The orbital altitude of 1389 kilometers is relatively free from trackable space debris (greater than 10 centimeters in diameter). Micro-meteoroids pose the highest collision risk factor. Collisions with micro-meteoroids are a random event and cannot be predicted or avoided. Currently, probability of satellite collision with space debris at the operational altitude is less than one chance in one million.

3. Expected Solar Activity

Solar activity follows a cycle of approximately eleven years duration between solar maximums. Activity increases for about four years until reaching a maximum and then decreases for about seven years until reaching a minimum. The cycle is currently near a maximum. Solar activity will begin to decrease, reaching a minimum around 1998-1999 and then begin increasing again, reaching its next maximum around 2002.

The initial constellation is scheduled to be operational from 1996 to 2001. Over the five year lifetime of the satellites, solar activity should be minimal at the beginning of life

(BOL) and near a maximum at the end of life (EOL). High solar activity may interfere with satellite communications at that time.

4. Atomic Oxygen and Atmospheric Drag

Atomic oxygen (AO) causes degradation of spacecraft surfaces and changes in their emissivity and absorbtivity. It is produced by the dissociation of oxygen molecules in the upper atmosphere. At an altitude of 500 kilometers, the concentration of AO is 88 percent, but begins to decrease above 800 kilometers.

At the constellation's operational altitude, there exist only 100 particles per cubic centimeter during low solar activity and 10^5 particles per cubic centimeter during solar maximum. Towards the EOL of the satellites, AO concentrations may accelerate the degradation processes as ultraviolet radiation from the sun increases molecular dissociation. Total on-orbit atmospheric density is less than 10^{-13} kg/m^3 during solar maximum and less than 10^{-14} kg/m^3 nominally. Thus, atomic oxygen is of minimal concern for most of the life of the initial constellation and atmospheric drag is negligible.

C. OPERATIONAL ORBIT SELECTION

1. Constellation Design

Design specifications, based on payload performance optimization, allowed no flexibility in operational orbit altitude or eccentricity, which were fixed at 1389 kilometers and circular, respectively. The constellation was designed to minimize the total number of satellites necessary to provide 100 percent coverage between 75 degrees north and 75 degrees south latitudes. At the specified operational altitude, the total number of satellites in the

constellation is 48. Van Allen Radiation Belts were taken into consideration as well as possible debris locations. The selected constellation is shown in Figure II-1.

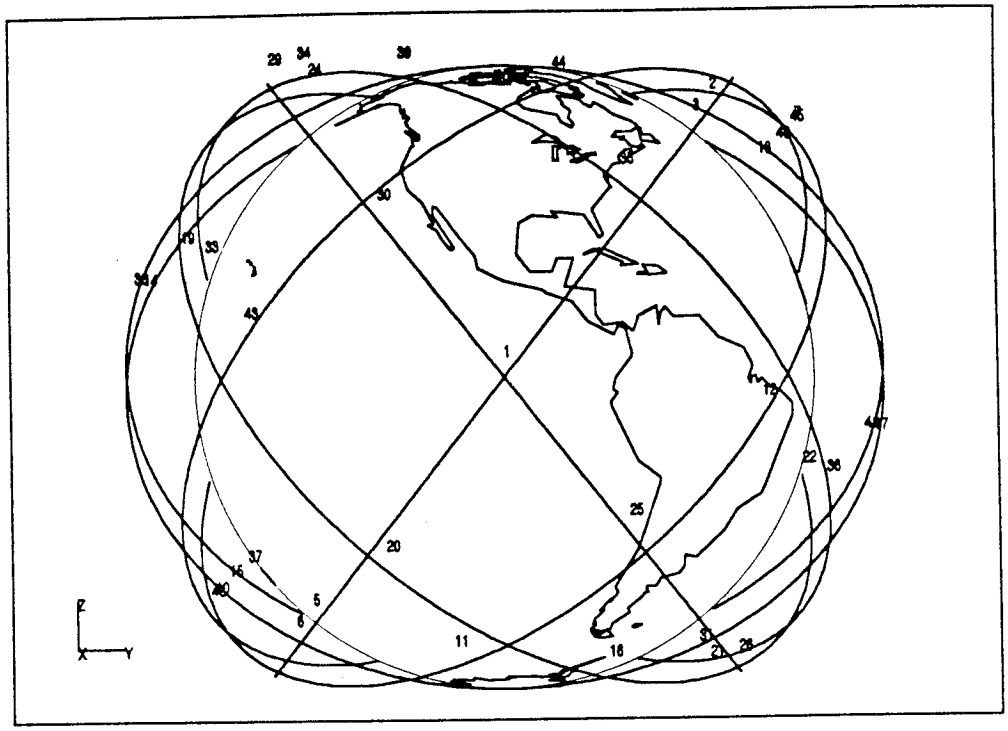

Figure II-1. Constellation Orbital Planes

a. Number of Planes

Eight orbital planes are used, separated by 45 degrees of the ascending nodes. Payload antenna footprint at equatorial nadir determined the number of planes. Overlap was determined to allow for a minimum of two satellites in view at all times.

b. Number of Satellites per Plane

Six satellites are evenly spaced throughout each orbital plane. Again, communications payload coverage determined the number of satellites per plane, and overlap was determined to allow for a minimum of two satellites in view at all times.

c. *Phasing of Satellites*

Satellites are evenly spaced within each plane and are out of phase between adjacent planes for collision avoidance. The Walker Delta Pattern of the constellation is 48/8/1 at an inclination of 52 degrees. The Pattern Unit (PU) is determined by dividing 360 degrees by the total number of satellites; the PU is 7.5 for this constellation.[Ref. 1]

(1) Within the Same Orbital Plane. The phasing between satellites within the same orbital plane is 60 degrees. This is easily determined by dividing 360 degrees by the number of satellites in the plane. Using the Walker Delta Pattern, phasing can be determined by multiplying the PU by the number of orbital planes.

(2) Between Adjacent Orbital Planes. The phasing of satellites between adjacent orbital planes is 7.5 degrees in true anomaly and can be determined from the Walker Delta Pattern. The satellites must be phased by an integral factor of the PU. For this constellation, the integral factor is unity (the last number of the Walker Delta Pattern). Phasing of satellites between adjacent orbital planes ensures collision avoidance since separation is maximized at their Closest Points of Approach (CPA).

d. *Inclination*

Design specifications requiring full service to users between 75 degrees north and south latitudes determined the inclination of the orbital planes. An inclination of 52 degrees provides full communications payload coverage at these high latitudes. Higher inclination orbits require a larger propellant expenditure to achieve. Lower inclinations do not provide adequate high latitude coverage.

2. Ephemeris Parameters

The ephemeris parameters common to all satellites are listed in Table II.1 and those unique to each satellite are listed in Table II.2.

Table II.1. Constellation Ephemeris Parameters

Altitude (km):	1389.0
Semi-major axis (km):	7767.15
Inclination (deg):	52.0
Eccentricity:	0.0
Period (min):	113.54

3. Perturbations

Perturbations of the orbits were analyzed using the Orbital Workbench software. All of the perturbing forces are cyclic except for solar pressure. This requires station keeping within the orbital plane to maintain separation between the satellites but does not require any out of plane (inclination) station keeping. Analysis results are in Appendix J.

D. GROUND COVERAGE

The constellation of satellites provides one hundred percent ground coverage between 75 degrees north and 75 degrees south latitudes. The representative ground track of one satellite over a 72 hour period is depicted in Figure II-2. Each satellite passes over the same point on the ground every 72 hours.

Table II.2. Individual Satellite Ephemeris Parameters

Satellite (plane/ number)	Right Ascension (deg)	True Anomaly (deg)	Satellite (plane/ number)	Right Ascension (deg)	True Anomaly (deg)
1-1	0.0	0.0	5-1	180.0	30.0
1-2	0.0	60.0	5-2	180.0	90.0
1-3	0.0	120.0	5-3	180.0	150.0
1-4	0.0	180.0	5-4	180.0	210.0
1-5	0.0	240.0	5-5	180.0	270.0
1-6	0.0	300.0	5-6	180.0	330.0
2-1	45.0	7.5	6-1	225.0	37.5
2-2	45.0	67.5	6-2	225.0	97.5
2-3	45.0	127.5	6-3	225.0	157.5
2-4	45.0	187.5	6-4	225.0	217.5
2-5	45.0	247.5	6-5	225.0	277.5
2-6	45.0	307.5	6-6	225.0	337.5
3-1	90.0	15.0	7-1	270.0	45.0
3-2	90.0	75.0	7-2	270.0	105.0
3-3	90.0	135.0	7-3	270.0	165.0
3-4	90.0	195.0	7-4	270.0	225.0
3-5	90.0	255.0	7-5	270.0	285.0
3-6	90.0	315.0	7-6	270.0	345.0
4-1	135.0	22.5	8-1	315.0	52.5
4-2	135.0	82.5	8-2	315.0	112.5
4-3	135.0	142.5	8-3	315.0	172.5
4-4	135.0	202.5	8-4	315.0	232.5
4-5	135.0	262.5	8-5	315.0	292.5
4-6	135.0	322.5	8-6	315.0	352.5

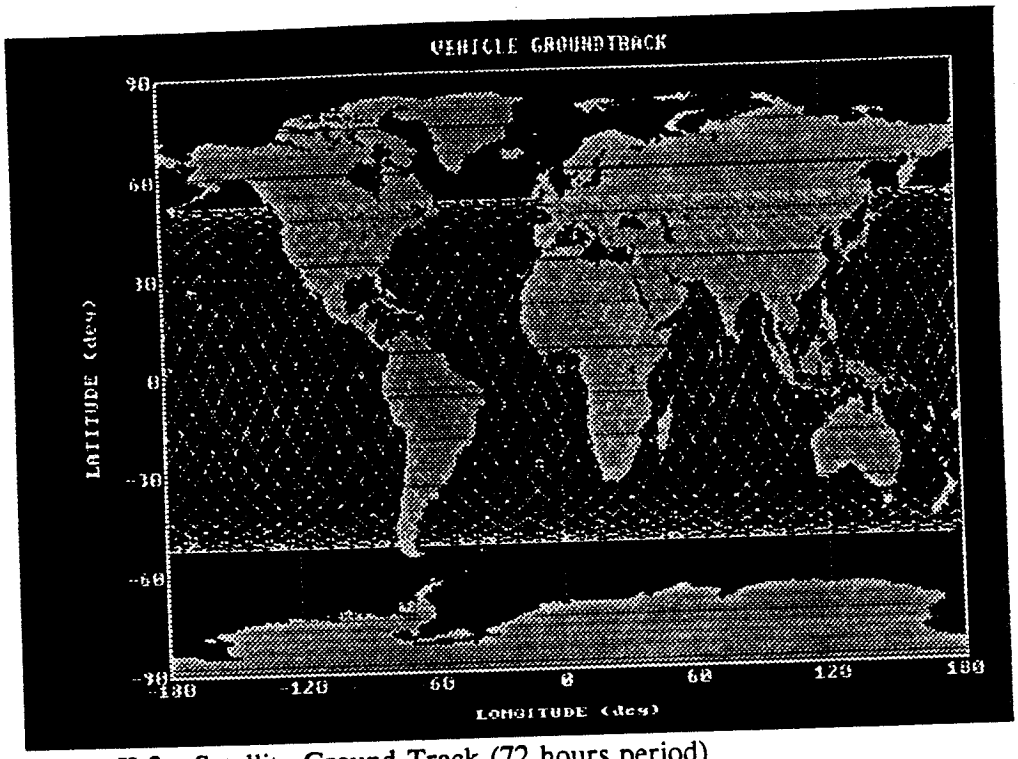

Figure II-2. Satellite Ground Track (72 hours period)

1. Number of Satellites in View

The constellation provides for a minimum of two satellites in view at any one time. Up to four satellites may be within a user's field of view at once, depending upon the latitude of the user. Three satellites are within the field of view of any user in the continental United States at all times since coverage circles will overlap more at higher latitudes than at the equator. For a representative instant in their orbits, coverage circles of all 48 satellites are depicted in Figure II-3.

2. Highest Power Demand Ground Track

The satellite ground track producing the highest power requirements is shown in Figure II-4. Although multiple satellites are able to distribute the incoming communications circuit loads, the track which proceeds north along the east coast of the

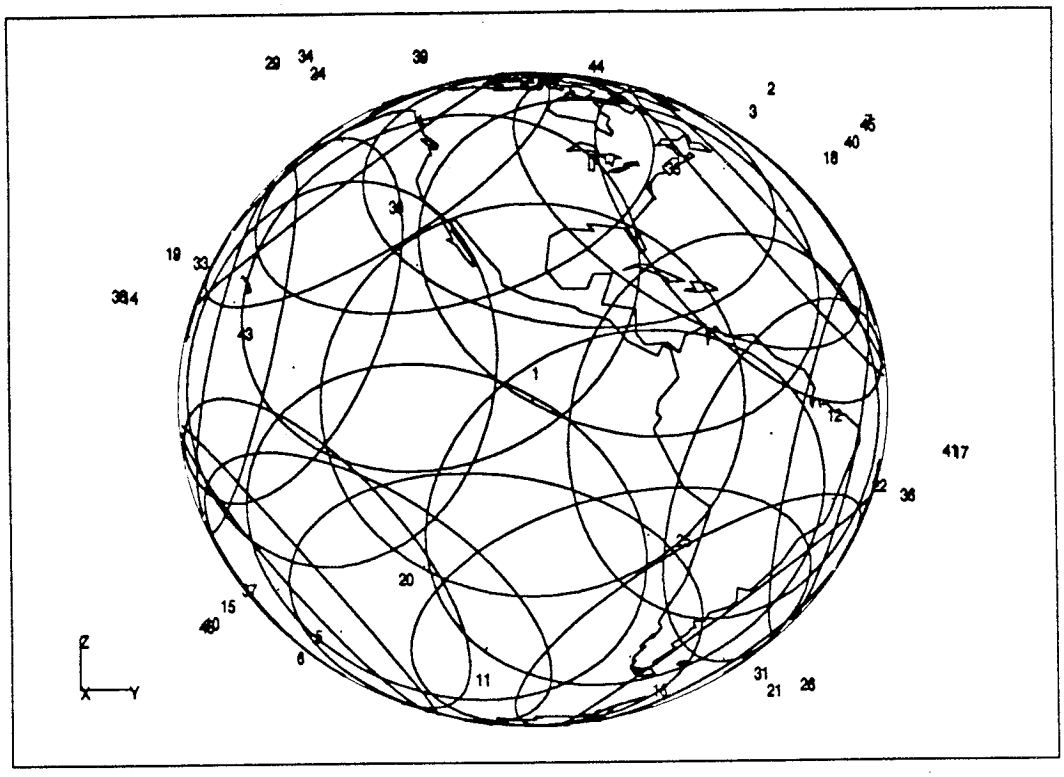

Figure II-3. Coverage Circles for Entire Constellation.

United States requires maximum power consumption and is immediately followed by a southerly course across western Europe, which also requires significant power. This track drives the thermal and electrical system designs of the spacecraft. Satellite useage and hence electrical power generation and thermal heat dissipation requirements are maximum when satellites are overhead these high population areas while mobile users are commuting to and from the workplace.

3. Locations of Ground Sites

Two ground stations will be used for Telemetry, Tracking and Control (TT&C). One will be placed on the west coast of the United States and the other on the east coast.

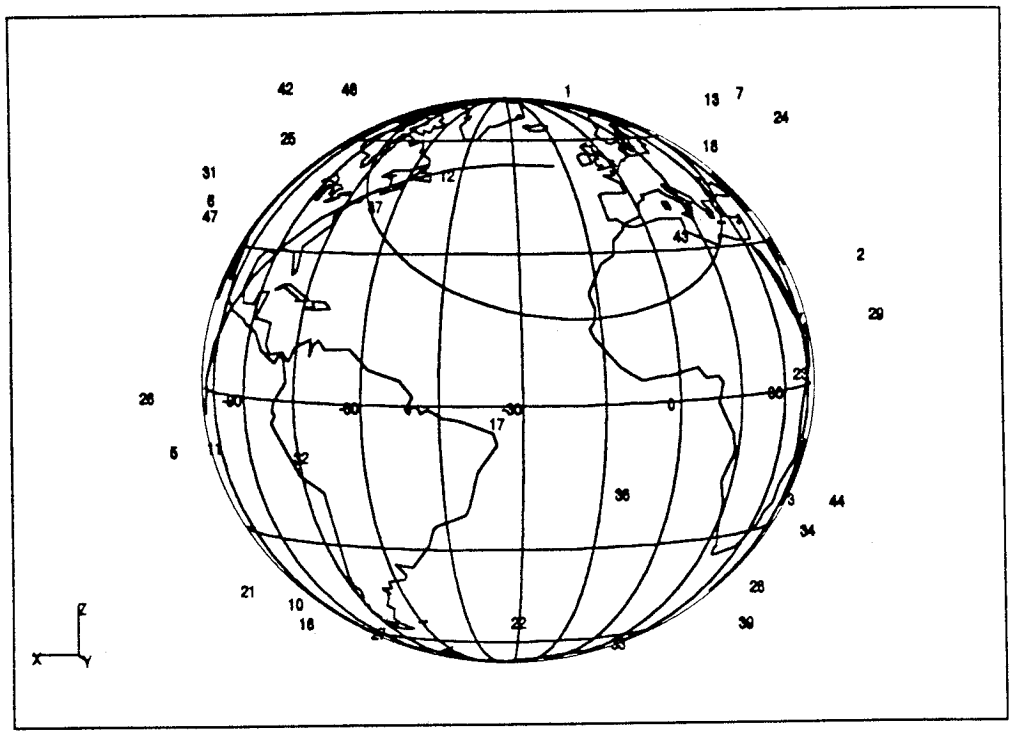

Figure II-4. Worst Case Orbit.

These two locations provide sufficient updates to the satellites. The west coast ground station is planned to be in the Los Angeles area and the east coast station is planned to be on the coast of Virginia. Table II.3 lists relative rise and set times for one satellite as seen from each ground station over a 72 hour period.

Due to TT&C stations locations satellites can receive TT&C transmissions from the ground stations during about 51 out of every 72 hour ground track revisit period. For the remaining 21 hours (two continous 10.5 hour periods), the satellite is not in contact with either ground station. This occurs between the time the ascending node precesses such that the satellite passes west of Los Angeles until the time that the Virginia site can reacquire it.

Table II.3. Ground Station Contact

Va = Coastal Virginia
LA = Los Angeles

Time	GS	Event	Time	GS	Event	Time	GS	Event
00:06:00	Va	rise	24:39:00	LA	rise	49:11:00	LA	rise
00:23:00	Va	set	24:41:00	Va	rise	49:17:00	Va	rise
01:57:00	LA	rise	24:46:00	LA	set	49:24:00	LA	set
02:06:00	Va	rise	24:59:00	Va	set	49:34:00	Va	set
02:13:00	LA	set	26:32:00	LA	rise	51:07:00	LA	rise
02:22:00	Va	set	26:42:00	Va	rise	51:19:00	Va	rise
03:55:00	LA	rise	26:49:00	LA	set	51:24:00	LA	set
04:08:00	Va	rise	26:58:00	Va	set	51:34:00	Va	set
04:12:00	LA	set	28:32:00	LA	rise	53:08:00	LA	rise
04:22:00	Va	set	28:44:00	Va	rise	53:20:00	Va	rise
05:58:00	LA	rise	28:48:00	LA	set	53:23:00	LA	set
06:08:00	Va	rise	28:59:00	Va	set	53:35:00	Va	set
06:11:00	LA	set	30:35:00	LA	rise	55:11:00	LA	rise
06:24:00	Va	set	30:44:00	Va	rise	55:19:00	Va	rise
08:00:00	LA	rise	30:47:00	LA	set	55:24:00	LA	set
08:07:00	Va	rise	31:00:00	Va	set	55:37:00	Va	set
08:13:00	LA	set	32:35:00	LA	rise	57:11:00	LA	rise
08:24:00	Va	set	32:43:00	Va	rise	57:19:00	Va	rise
09:59:00	LA	rise	32:50:00	LA	set	57:27:00	LA	set
10:08:00	Va	rise	33:00:00	Va	set	57:34:00	Va	set
10:15:00	LA	set	34:34:00	LA	rise	59:10:00	LA	rise
10:19:00	Va	set	34:51:00	LA	set	59:27:00	LA	set
11:58:00	LA	rise	36:34:00	LA	rise	61:12:00	LA	rise
12:14:00	LA	set	36:48:00	LA	set	61:20:00	LA	set
22:45:00	Va	rise	47:19:00	Va	rise	70:00:00	Va	rise
22:58:00	Va	set	47:35:00	Va	set	70:09:00	Va	set
						71:54:00	Va	rise

Notes:

(1) Minimum of 10 degrees elevation angle from ground sight.
(2) Time scale is elapsed time, relative from the beginning of the simulation.

E. LAUNCH SEQUENCE

The launch sequence entails selection of the launch vehicle (which also sets the launch site) and determining launch windows and injection orbits. The satellites are configured to utilize both Delta and Ariane as launch vehicles.

1. Launch Windows

Actual launch windows are hard to determine since they depend upon which orbital plane is to be launched. The launch of the first plane of satellites will determine the launch windows for the following planes in order to provide minimum repositioning of the injection orbital plane for propellant and weight savings considerations. The first plane may be launched at any time since precession will occur; relative spacing between orbital planes is the important factor. Adjacent planes need not be launched consecutively, either. The plane most easily accessible may be launched next.

2. Injection Orbit

The launch vehicle will place the satellite stacks into an injection orbit which is slightly elliptic, but within the same plane as the operational orbit. The injection orbit was chosen to allow for one satellite to be transferred into its operational orbit for every three injection orbits. This requires minimum repositioning of the satellite to reach its operational station. The parameters for the transfer orbit are listed in Table II.4.

F. ON-ORBIT MANEUVERS

Satellites will be required to undergo a series of orbital adjustments over their lifetime. The propulsion system is designed to include these maneuvers.

Table II.4. Injection Orbit Parameters

Semi-major axis (km):	8052.22
Eccentricity:	0.035
Inclination (deg):	52.0
Radius at apogee (km):	8337.30
Radius at perigee (km):	7767.15
Period (min):	119.85

1. Operational Orbit Injection Sequence

The satellite will be required to perform a velocity change maneuver to enter a circular orbit from the injection orbit. The velocity increment required to circularize the orbit is 149.39 meters per second. All satellites will need to fine tune their positions within the orbital plane with respect to the first satellite injected.

2. Repositioning

Satellite repositioning will not be required. If one satellite fails, there is sufficient overlap to continue full service over most of the surface of the Earth. Remaining satellites will not be redistributed within the plane in order to maintain the required phasing to prevent collisions with satellites in the other planes.

3. Station Keeping

All perturbing forces are cyclic except for solar pressure forces. Out of plane station keeping is not required. Maintaining separation of the satellites within the plane is the only station keeping required. Less propellant is required for in plane station keeping

than for out of plane station keeping, decreasing the weight of the satellite and lowering the unit cost of placing it in orbit.

4. Deorbit

The satellites will be deorbited at the end of their useful life. Propellant for deorbiting the satellites is included in the propellant budget.

G. ON-ORBIT STORAGE AND REACTIVATION OF SPARES

One on-orbit spare per orbit was originally planned, but the size of the stowed configuration in the shroud limited the number of satellites per launch to six instead of seven. The spare satellite was to be stored within the same orbital plane as the ones it would replace. The spare would remain in a dormant mode, requiring only housekeeping power to monitor the ground stations and maintain its position, until it was needed. Reactivation would be accomplished using a TT&C transmission upon discovery of a failed satellite. This ensured minimal propellant on board for repositioning the spare to its operational station.

To minimize the amount of propellant in the satellites and to maintain identical designs for every spacecraft, all adjacent satellites between the spare and the failed satellite would have been shifted 60 degrees to fill the gap made by the nonfunctional satellite. For example, if satellite number 4 failed and the spare was located between satellites 1 and 2, satellite 3 would move into 4's position, 2 into 3's position, and the spare would move into 2's position. Enough propellant would have been added to each satellite to perform one 60 degree repositioning maneuver.

H. REFERENCES

1. Wertz, J. R. and W. J. Larson, *Space Mission Analysis And Design*, Kluwer Academic Publishers, 1991.

B. GENERAL DESCRIPTION

The satellite is built around three major component sections: the main body, the phased array antenna and the solar array. The main body is a rectangular parallelepiped measuring 1.14 x 0.98 x 0.60 meters, constructed of aluminum honeycomb. All subsystem components, with the exception of the phased array and solar panels, are housed in this structure. The phased array antenna is attached to the Earth face and the two solar array panels deploy from the + and - X faces. In its stowed configuration, the satellite measures 1.40 x 1.40 x 0.78 m. Launch mass for each satellite is 397 kg. SLD mass is 217.2 kg which yields a total launch vehicle payload mass of 2599.2 kg, well under the Delta II's 3300 kg limit for a 52 degree inclination, 1389 km altitude operational orbit. The main body shell surrounds a single spherical fuel tank and individual satellite components as displayed in figure III-1. Careful consideration was given to minimize center of mass (cm) offset while maintaining thermal heat balance. Appendix C contains a list of component masses and locations.

1. + Z (Earth) Panel

The size and orientation requirements of the payload antenna severely limit the amount of space available on the earth face. Only those systems that absolutely must be in view of the earth are allowed on the external side of the panel; therefore, only the TT&C and payload C-Band antennas are mounted at the center and both ends of the X axis, alternated with the two earth sensors. Internally, a 100 amp magnetic torque rod is centered on the -Y side of the panel, parallel to the X axis. Mounting and attaching

points for the fuel tank and other structural hardware are also located on the earth facing panel.

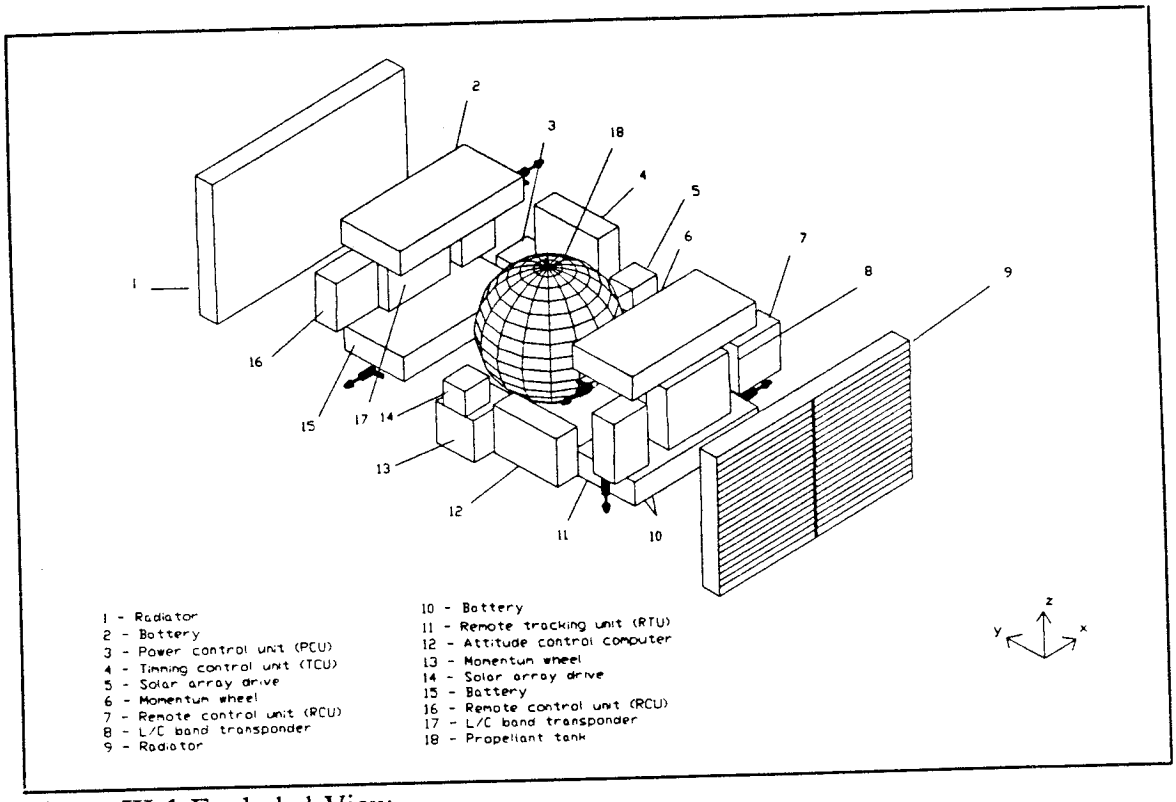

Figure III-1 Exploded View

2. - Z (Anit-Earth) Panel

Attached to the anti-earth face are two 2.2 N station keeping thrusters, mounted near the North-East and South-West corners. The sun sensor is also located near the Northwest corner.

3. +X (North) Panel

The +X panel, shown in figure III.2, supports systems and equipment which are not thermally critical and need not be installed on a thermal cold plate. Among the

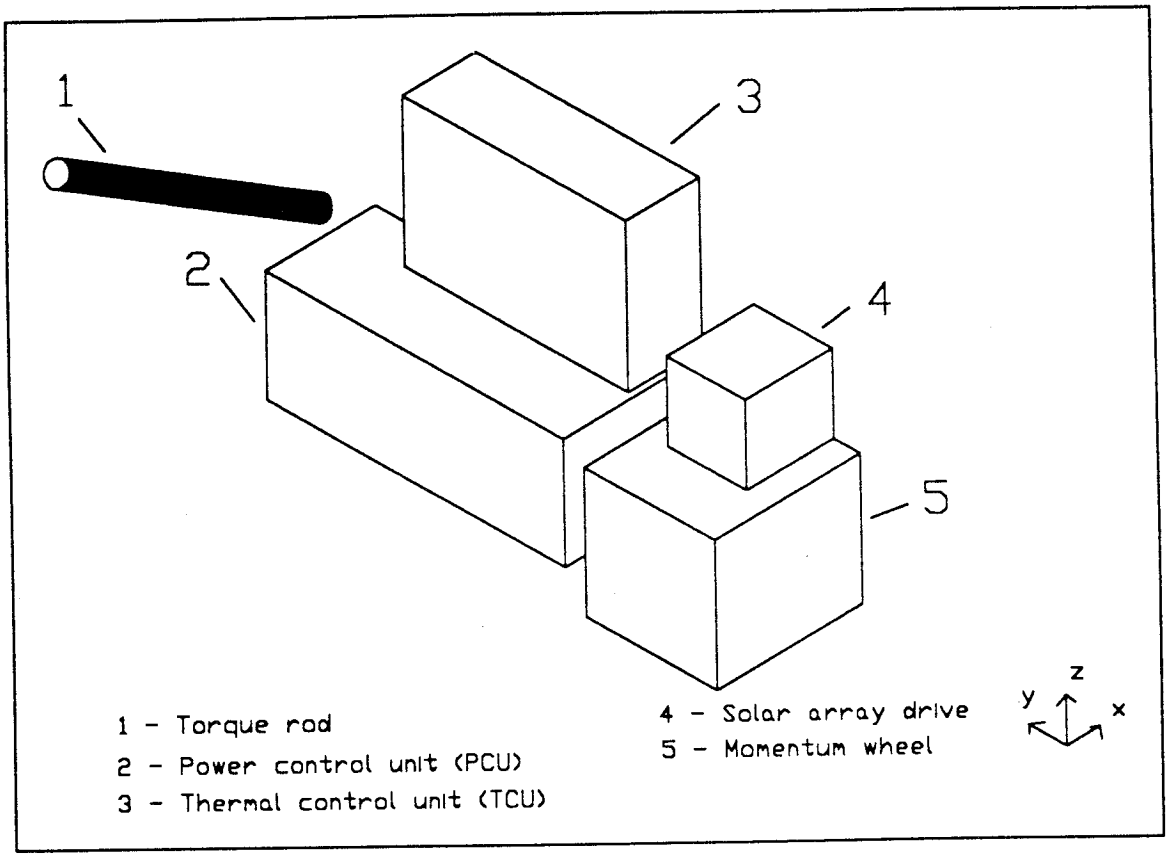

Figure III-2 Plus X Face

systems installed on this panel are one of two Solar Array Drives Assemblies (SADA's) and one of two bias momentum wheels, both located in the middle of the panel along the Z axis. The Timing Control Unit (TCU), which must be kept in close proximity to the phased array to reduce signal losses, is located on the western half of the panel, as is the Power Control Unit (PCU). Two 2.2 N thrusters are mounted in opposite corners of the +X panel.

4. -X (South) Panel

The second SADA and momentum wheel assemblies are located along the Z axis, directly opposite their counterparts as shown in figure III.3. The attitude control

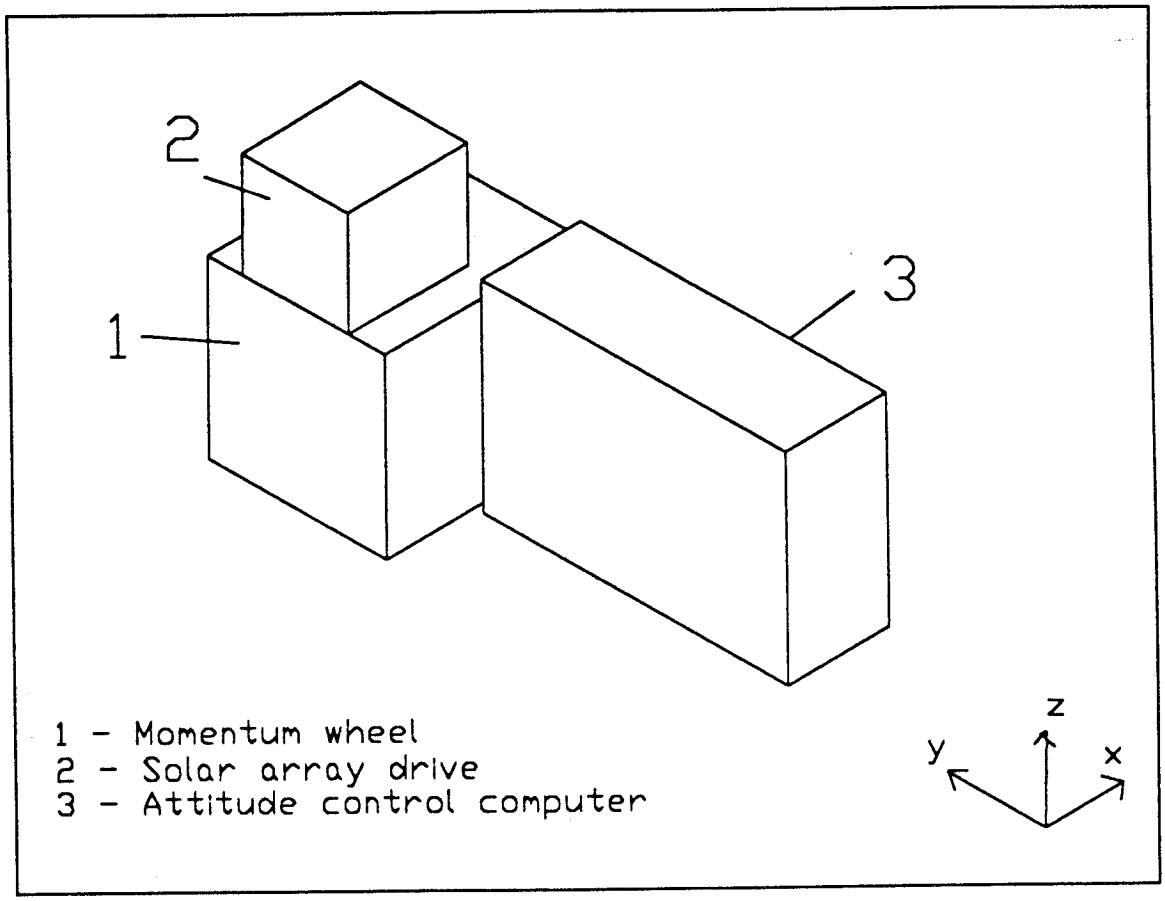

Figure III-3 Minus X Face

computer is east of centerline and a 100 amp magnetic torque rod is west of centerline parallel to the Z axis. Two 2.2 N station keeping thrusters are at opposite corners diagonally opposite their counterparts on the +X axis.

5. +Y (East) Panel

The +Y panel, illustrated in figure III-4, serves as the cold plate for the active thermal control system. Thermally activated louvers are mounted to a panel-size

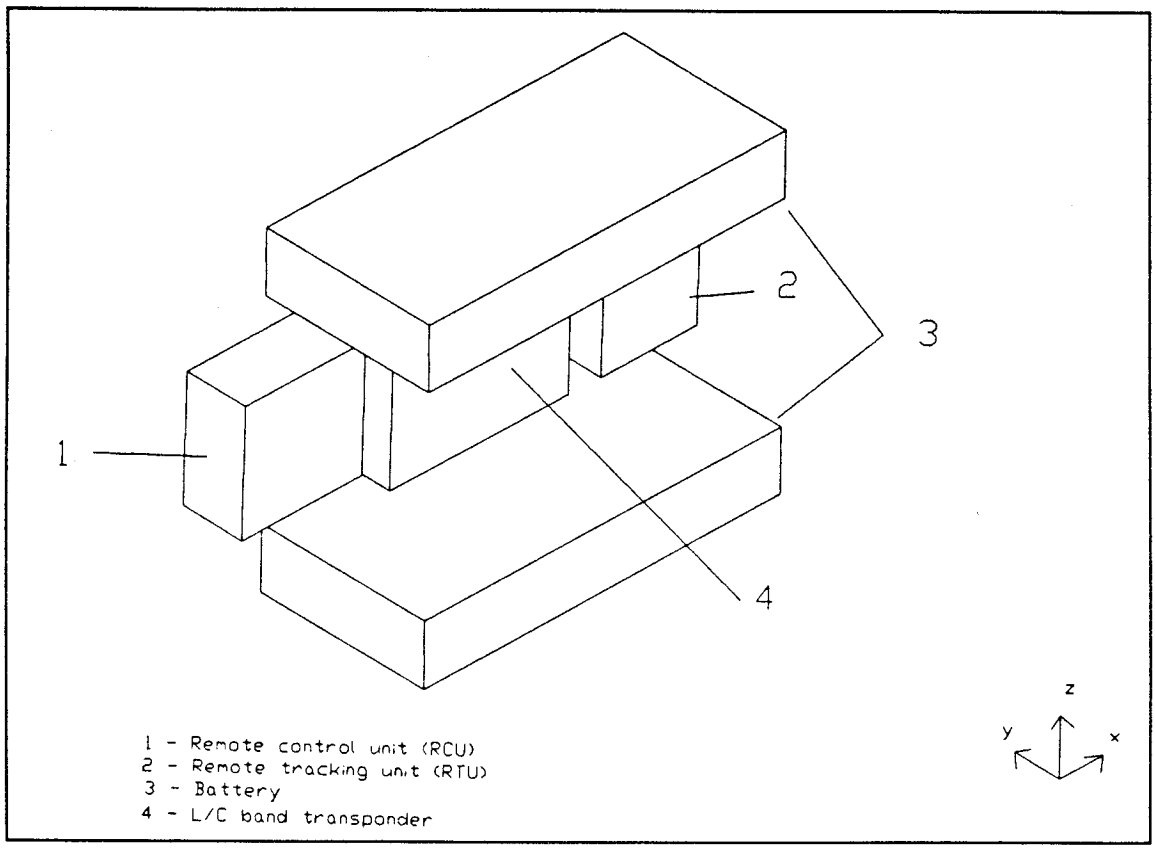

Figure III-4 Plus Y Face

radiator which is in turn mounted to the outboard side of the coldplate panel. A thermal capacitor covers the inboard face and serves to conduct heat away from the attached payload equipment. Structural and dynamic restrictions necessitate splitting the Ni-H_2 battery into four equal units. In this configuration the moments of inertia are more evenly distributed and also permitted the use of a single, standard sized fuel tank. One

six-cell battery is mounted along each of the earth and anti-earth edges. Between them, on opposite sides of the Z axis, are one of the two Remote Control Units (RCU's) and the L-to-C Transponder.

6. -Y (West) Panel

The -Y panel is identical to the +Y panel with the exception that its transponder is C-to-L as depicted in figure III-5.

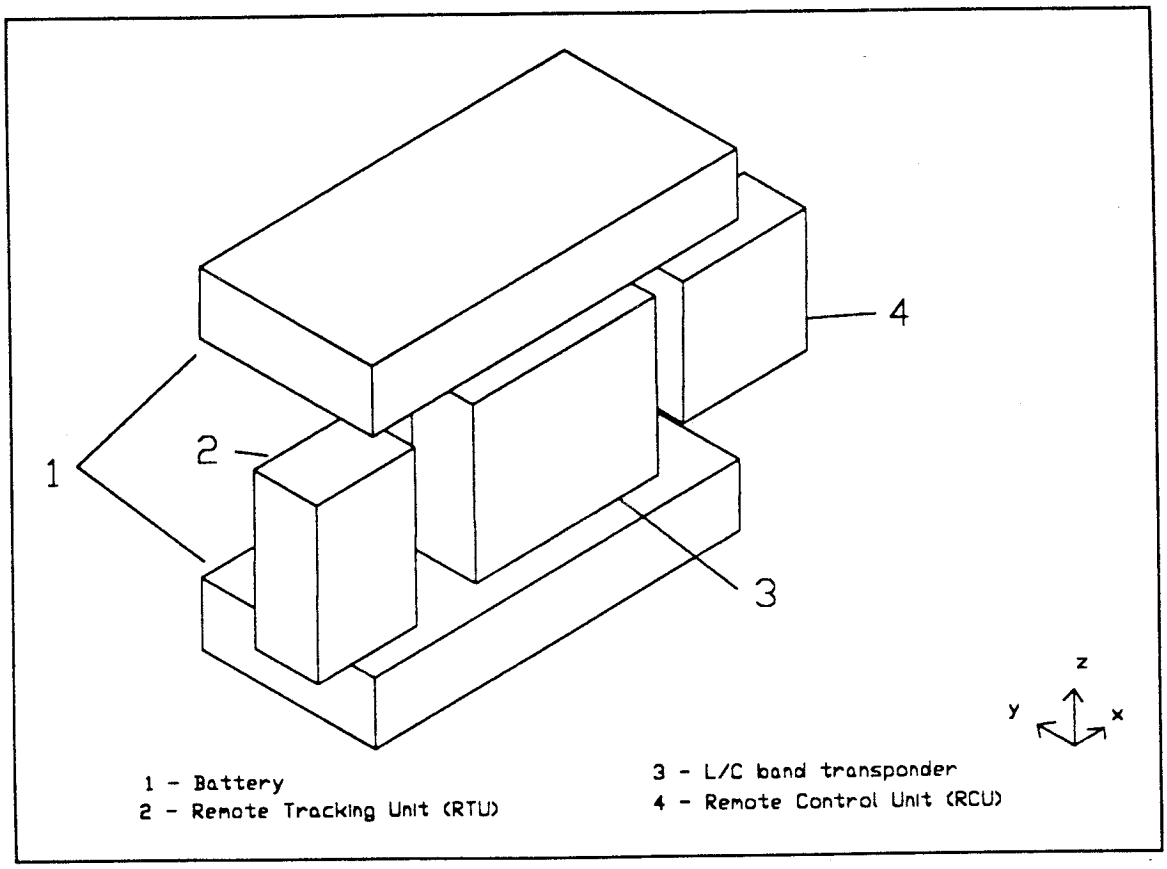

Figure III-5 Minus Y Face

7. Planar Array Antenna

The six panel antenna folds up across the outboard side of the +Z face. When deployed, the two center panels remain fixed while the remaining panels are hinged to deploy in the +X+Z and -X+Z directions.

8. Solar Arrays

The two solar array wings are connected to the satellite via the SADA's. Each wing is stowed as four deployable panels stacked parallel to their respective X panels. Once deployed, they provide 7.14 m^2 of surface area.

C. MASS SUMMARY

Table III-1 presents mass summaries for each spacecraft system.

D. POWER SUMMARY

Electric power requirements are summarized in Table III-2.

Table III-1 System Component Masses

Subsystem	Mass (kg)	
Attitude Control System		31.89
Electrical Power System		109.93
Propulsion System		19.39
Thermal Control System		27.70
Structure		42.51
Payload		60.00
TT&C		12.00
Dry Mass	303.42	
Propellant		57.17
Wet Mass	360.59	
10% Mass Margin		36.10
Total Mass	396.69	

Table III.2 System Power Requirements

System/Component	Nominal Power (W)
Communications	600
TT&C	12
Propulsion	18
Attitude Control	32
Electrical Power Control	40
Thermal	30
Wiring Harness	20
5 % Margin	40
Total	792

IV. LAUNCH VEHICLE INTEGRATION

A. INTRODUCTION

1. Scope

a. Operational Requirements

The launch vehicle integration effort must ensure compatibilty between the satellite launch package and the requirements imposed by the selected launch vehicle. In order to minimize program deployment costs, an entire operational orbit plane of the constellation will be placed on orbit using a single launch vehicle. To this end, the integration effort must allow for the dispensing of six satellites by the Delta II upper stage. To meet the operational requirement of a six satellite deployment per launch vehicle, a Satellite Launch Dispenser (SLD) design was incorporated into the program objectives.

b. Functional Requirements

The SLD must provide structural support to withstand the vibrational modes and acceleration loads imposed by the launch vehicle. SLD design must ensure that each satellite need only support its own mass during launch, and hence the SLD must support the loads placed on the combined satellite package. The SLD must additionally provide for the equipment support interface between the satellites and the launch vehicle prior to depoyment and for the proper dispensing of each satellite as appropriate.

Therefore, the SLD must be compatible with the respective launch vehicle adaptor ring and remain rigidly affixed to the upper stage of the vehicle throughout flight.

c. Restrictions

Although program objectives are to maintain scheduling flexibility by retaining the capability to use either the Delta II or the Ariane IV launch vehicles, the integration requirements imposed by the Delta II are significantly more restrictive than those imposed by the Ariane IV. Therefore, the launch vehicle integration effort is primarily concerned with ensuring design comaptability with the Delta II launch vehicle.

2. Method

a. Alternatives Explored

The decision to use a SLD assembly over simply stacking the spacecraft was based on several attractive design advantages. The primary benefit comes from simplification of the spacecraft body itself. Since the SLD is designed to withstand the composite system load, each individual spacecraft need only support its organic launch loads, simplifying the structure of each spacecraft and eliminating the need for the spacecraft structure to be capable of supporting the launch loads of the spacecraft stacked above it. Additionally the mounting and deployment mechanisms interference with other systems is minimized. A noteworthy benefit of the SLD is that a single malfunction in any one unit of the launch sequence in no way inhibits the deployment of the other spacecraft.

A rail system was also considered but was discarded for many of the same reasons as the stacking scheme. The attachment points were complicated and inevitably interfered with solar array and/or the thermal louvers. A single point launch failure would also debilitate the remaining spacecraft from deployment

b. Tradeoffs Performed

The SLD does however require sacrifices. The SLD structure occupies volume and mass that in no way contributes to the on orbit mission of the satellite. A scheme whereby the satellite bodies were stacked on each other would conceivable allow a larger and heavier spacecraft body; however, the added mass and size would contribute solely to the deployment and launch survival capability of the satellite stack, vice added payload capability.

Mounting the rails required that the exterior satellite faces be free of obstructions. This restriction significantly impacted the satellite design process.

B. LAUNCH VEHICLE

1. Delta Vehicle Description

Reference 1 contains a detailed description of the Delta II launch vehicle. The Delta II 7925, shown in Figure IV-1, is capable of putting a payload mass of 3300 kg into the required transfer orbit and subsequently into the operational orbit with a velocity change. This mass is based on a transfer orbit with a perigee velocity of 7.289 km/sec, a perigee altitude of 1389 km and an eccentricity of 0.035. Design launch mass in the Delta configuration is 2518.24 kg. The transfer and operational orbits are

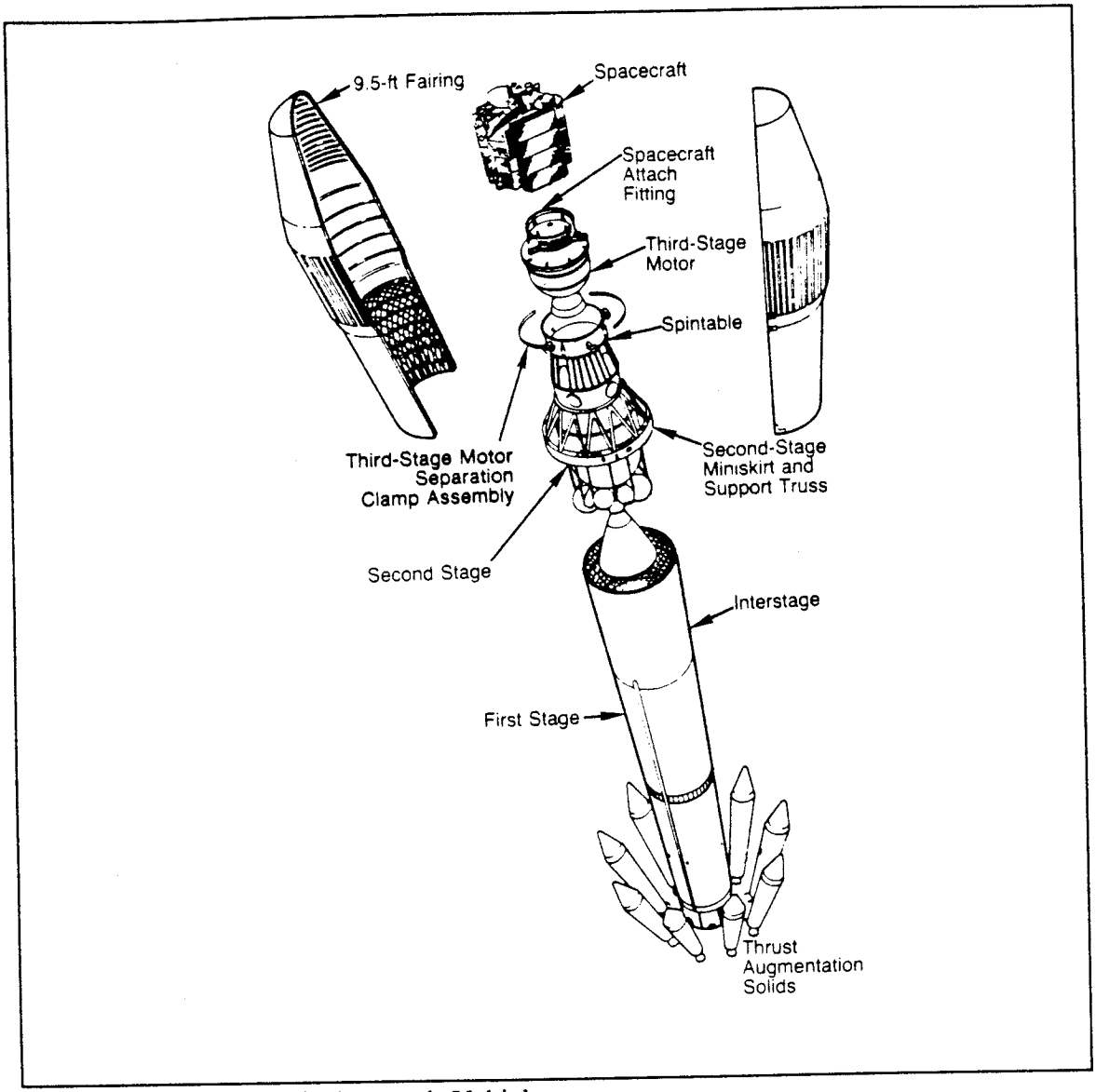

Figure IV-1 Delta II 7925 Launch Vehicle

presented in figure IV-2.

The Delta 7925 is a three stage launch vehicle. The SLD attaches to the launch vehicle via the manufacturers Payload Adaptor Fitting (PAF) 3172B. The SLD launch configuration, stowed within the Delta II long shroud, is shown in Figure IV-3.

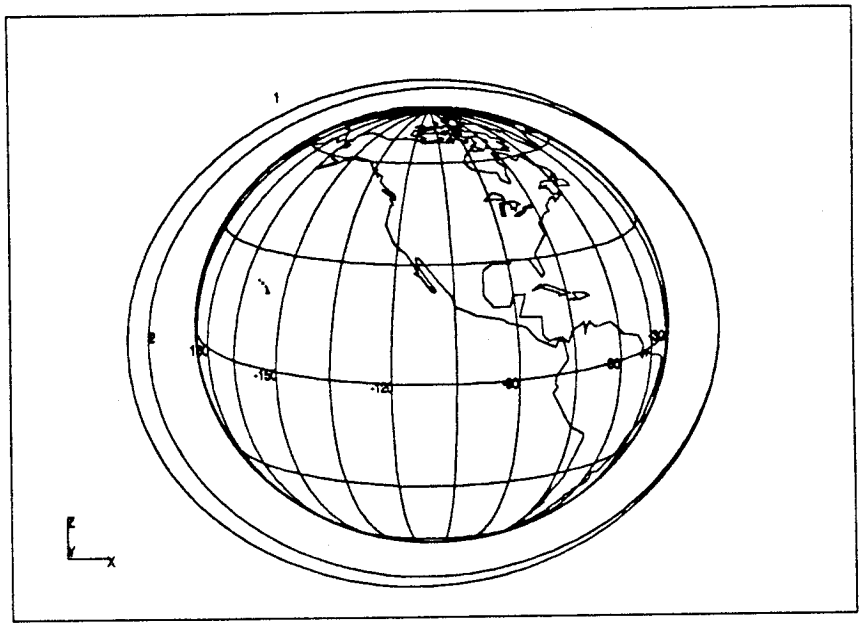

Figure IV-2 Transfer and Operational Orbits

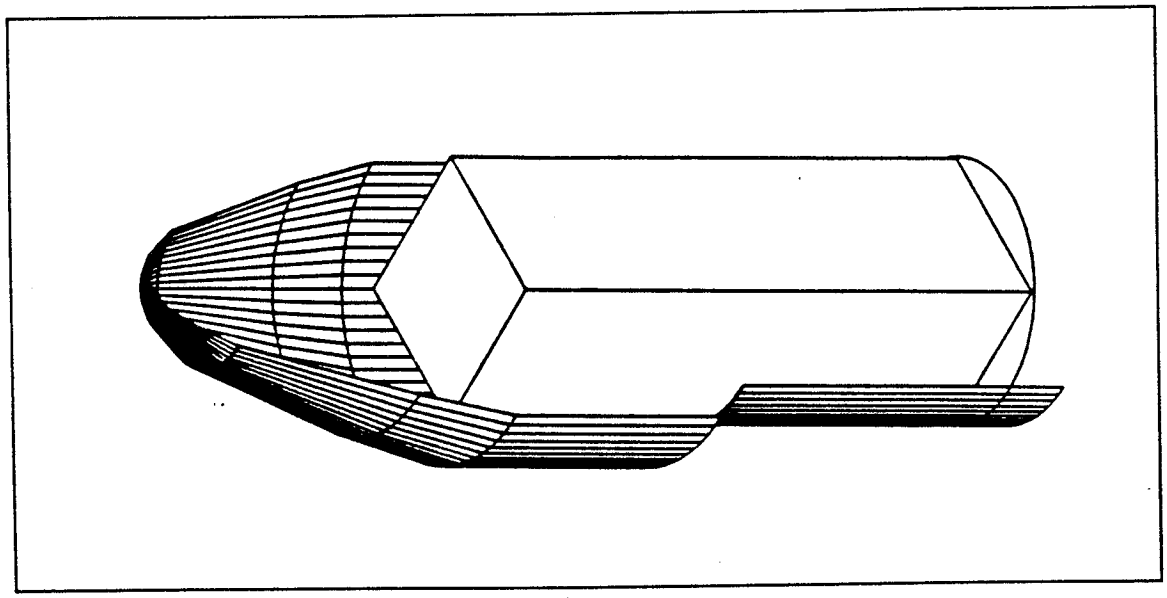

Figure IV-3 SLD in Delta II Long Shroud

a. First Stage

The first stage liquid-propellant booster is powered by a gimbaled main engine initially augmented by nine externally mounted solid motor cases. The solid propellant motor cases are jettisoned after motor burnout.

b. Second Stage

The second stage is powered by a pressure fed propulsion system. The thrust chamber is mounted on a gimbaled system for attitude control during powered flight. Roll, pitch an yaw are controlled by a second stage cold gas system. The second stage guidance compartment structure houses the flight control, inertial guidance, instrumentation, range safety, tracking and power systems.

c. Third Stage

The third stage propulsion system is a PAMSTAR 48 solid rocket motor. An attaching adapter is used to secure the dispensing unit to the third stage.

2. Launch and Orbit Injection

a. Sequence

A typical sequence of events for the Delta II three stage mission is in Table IV.1.

b. Stabilization

The launch vehicle third stage provides spin stabilization for the SLD during the transfer orbit. The third stage has an organic Nutation Control System (NCS) that is designed to maintain small cone angles of the combined upper stage and the

Table IV.1 Ignition Sequence

Event	Time (sec)
First Stage	
Main Engine Ignition	T+0
Solid Motor Ignition	T+0
Solid Motor Burnout	T+59
Solid Motor Ignition	T+64
Sold Motor Separation	T+65/66
Solid Motor Burnout	T+123
Sold Motor Separation	T+128
Main Engine Cutoff	T+265
Second Stage	
Blow Stage I/II Separation Bolts	M+8
Stage II Ignition	M+13
Faring Separation	M+40
Stage II Engine Cutoff (S1)	M+376
Stage II Engine Restart	S1+609
Stage II Engine Cutoff (S2)	S1+659
Third Stage	
Fire Spin Rockets Start Stage III Sequencer	S2+50
Separate Stage III	S2+52
Stage III Ignition	S2+90
Stage III Burnout	S2+177
Spacecraft	
Spacecraft Separation Begins	S2+290

spacecraft during thruster burn for transfer orbit injection. [Ref 1] Once the upper stage unit is in its proper transfer orbital plane, the body will de-spin prior to satellite dispensing.

c. Dispensing

The Delta third stage spins up to a 110 +/- 10% RPM aligning the spin axis with the velocity vector for orbital establishment. Once the orbit is established the Attitude Dynamics and Control System (ADCS) commences thruster firings for de-spin to a nominal 5 RPM. [Ref 2] The Delta ADCS logic interfaces with the SLD logic to deploy individual spacecraft, one at a time at every third return of the launch vehicle to the transfer orbit perigee. At commanded intervals, the logic signals the explosive bolts to release the spacecraft. As each satellite is dispensed the logic corrects the Delta ADCS for the mass and inertia changes. In the event of a deployment failure the Delta ADCS will be unaffected and a redundant cap will fire in the explosive bolt mechanism to release the satellite. Each satellite is passively stable when dispensed as it will be spinning about its own major axis. The remaining satellites continue to be stabilized by the third stage until they too are dispensed. As each satellite is dispensed its own three axis stabilization system will assume satellite control as described in the Attitude Dynamics and Control chapter.

C. GENERAL SLD DESCRIPTION

The SLD is the central controller of the satellite bodies throughout launch and operational orbit plane positioning. The SLD places all six spacecraft in the operational

orbital plane, dispensing a satellite every third time the launch vehicle returns to perigee. The SLD rigidly supports each spacecraft during launch and provides for their individual dispensing from their SLD housing, shown in Fig IV-4. SLD logic interfaces with the launch vehicle logics for individual spacecraft deployment. A single deployment canister for each launch vehicle is manufactured to specification. The SLD utilizes launch vehicle specific adapter rings for interface with the launch vehicle as applicable.

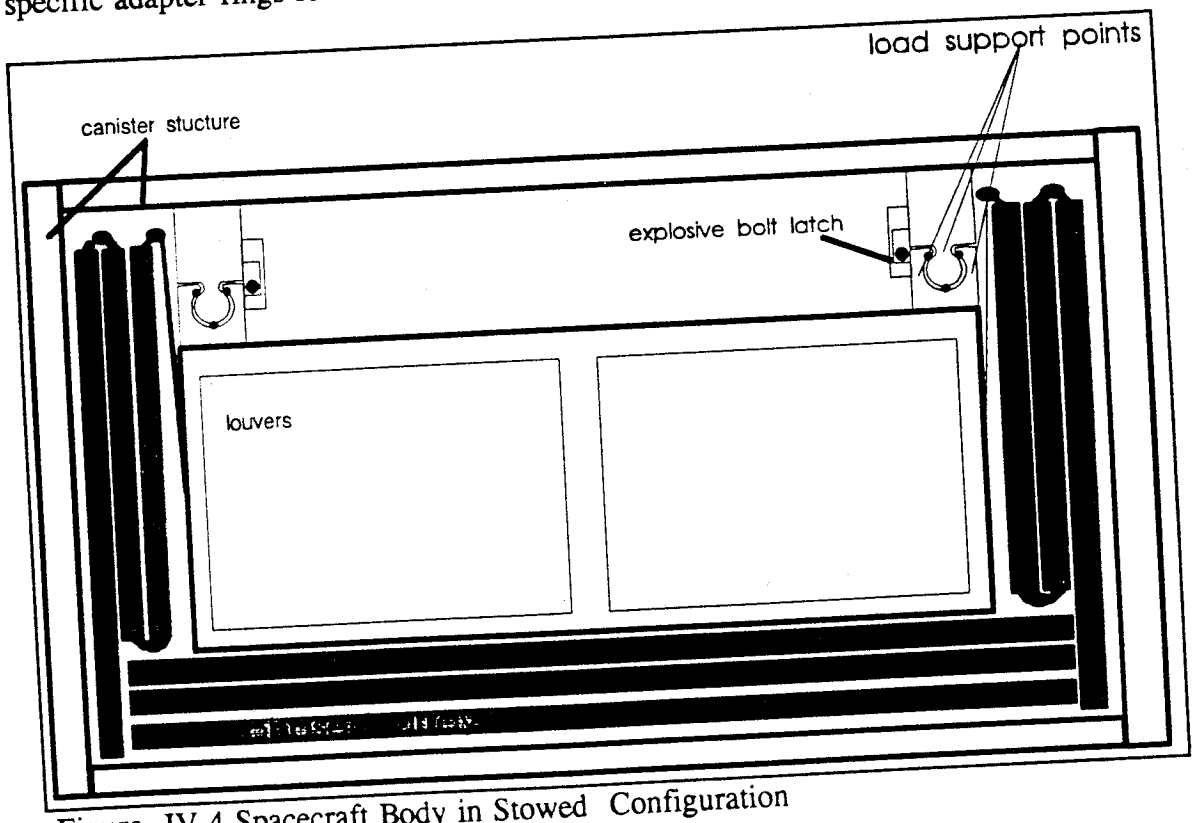

Figure IV-4 Spacecraft Body in Stowed Configuration

Vertical U-channel members provide stiffness and spacing to the entire structure. These members are fastened to honeycomb facing sheets and integrated into the box structure as shown in Figure IV-5. The honeycomb provides a mounting surface for the dispensing rails, and the strength to support the spacecraft during launch. Attached to

each rail is an explosive bolt latch and spring mechanism for release and deployment of the individual spacecraft. As the satellite leaves the SLD, an umbilical connection to the spacecraft separates indicating to the SLD/launch vehicle logics that the spacecraft has deployed. The physical characteristics of the SLD are given in Table IV.2.

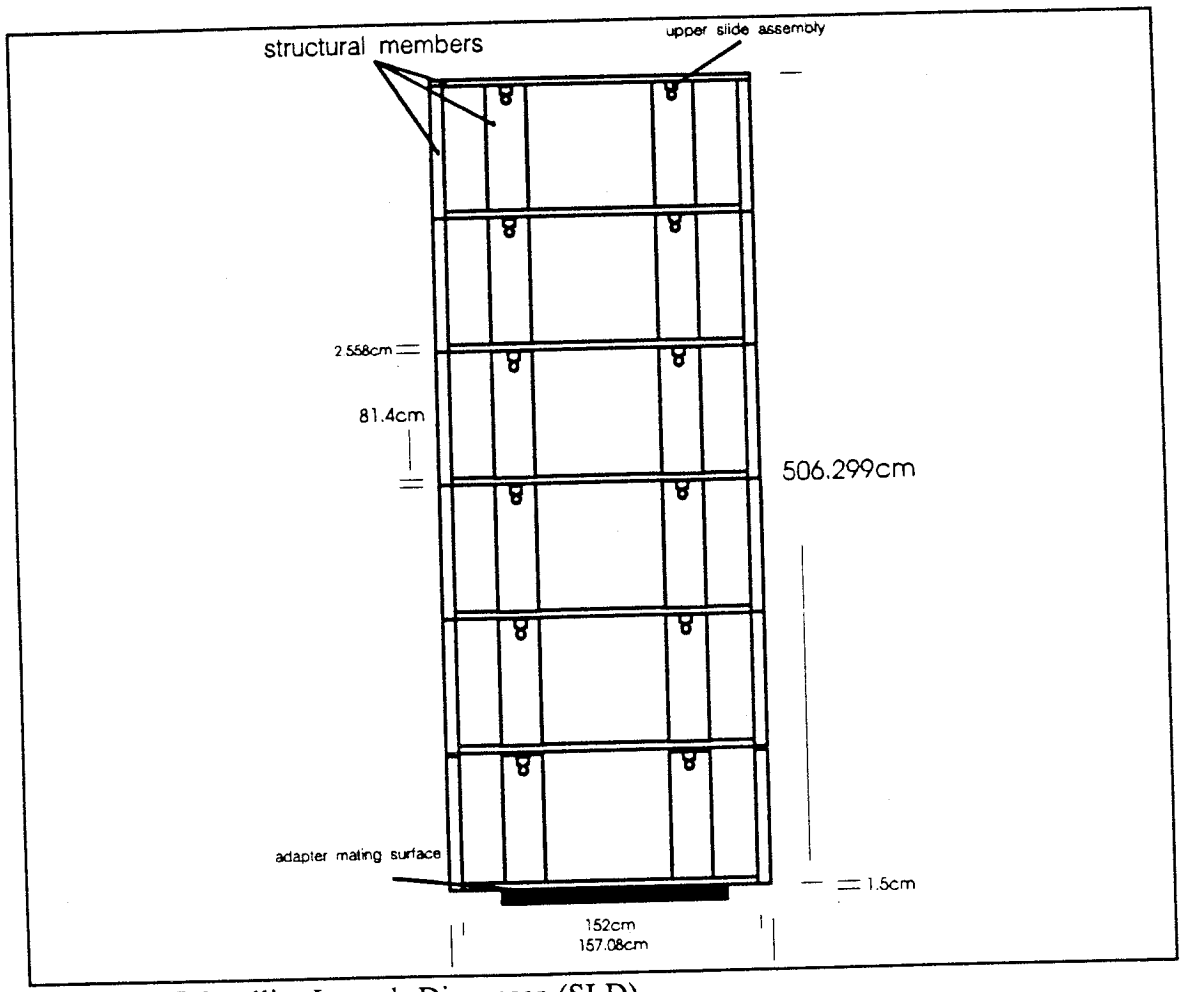

Figure IV-5 Satellite Launch Dispenser (SLD)

Table IV.2 SLD Characteristics

Mass	217.2 kg
I_{xx}	571.2 kg m^2
I_{yy}	657.7 kg m^2
I_{zz}	217.7 kg m^2

D. SLD COMPONENT DESCRIPTION

1. Dispensing Rails

a. Design

The upper slide rails are attached to the honeycomb facing sheets. The deployment rail system, as depicted in Figure IV-6, has its own bearing race that rigidly

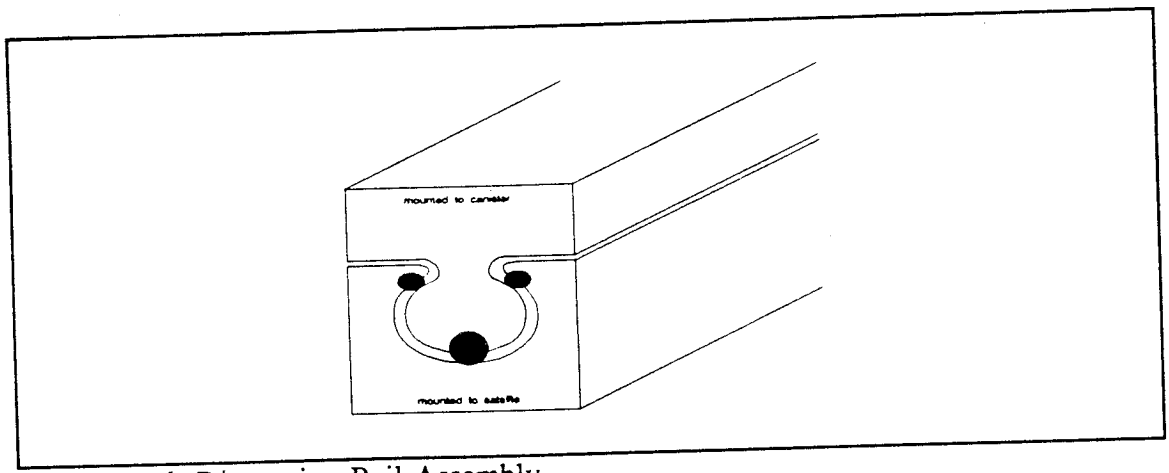

Figure IV-6 Dispensing Rail Assembly

supports the structure in any gravitational environment, as well as providing rotational stiffness during launch and vehicle spin up. Thus the rail design allows for motion in one direction only. Prior to separation, motion along the axis is constrained by the explosive bolt and latch mechanism. Table IV.3 presents dispensing rail physical characteristics.

Once fired the bolt releases from the nut and the spring forces the two rail halves apart, thus dispensing the satellite body. As the satellite leaves the SLD, the umbilical connection breaks indicating positive separation to the SLD logics.

Table IV.3 Rail Characteristics

m_{upper}	2.13 kg
m_{lower}	1.12 kg
$load_{upper}$	39.5 kg/cm^2
$load_{lower}$	39.5 kg/cm^2
I_{xx}	.0432 kg m^2
I_{yy}	1.273 kg m^2
I_{zz}	1.314 kg m^2
Factor of safety	80.3

2. Latch

The latch mechanism shown in Figure IV-7 is fully integrated into the deployment rail. The spring is preloaded as the satellite is loaded into the SLD prior to launch. The latch is an explosive bolt, that is command fired pyrotechnically. Each satellite requires two explosive bolts (one per rail system) and each bolt contains two electrically fired caps for redundancy.

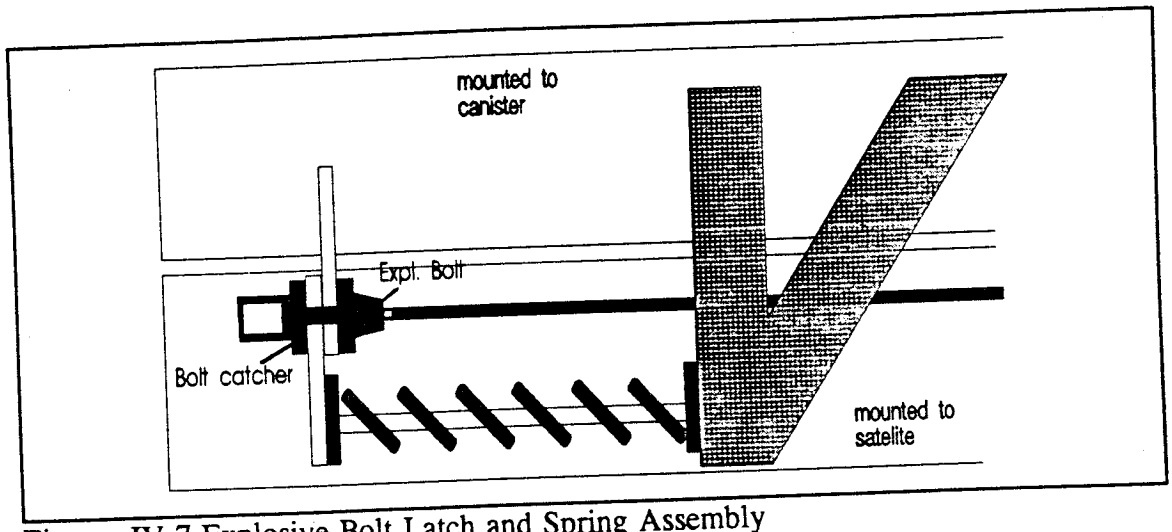

Figure IV-7 Explosive Bolt Latch and Spring Assembly

3. Honeycomb Panels

The honeycomb panel is 2.54 cm thick Titanium. Dimensions are shown in Figure IV-8. This panel configuration was chosen for its mass and shear properties. [Ref 6] An overview of the panel characteristics is given in Table IV.4.

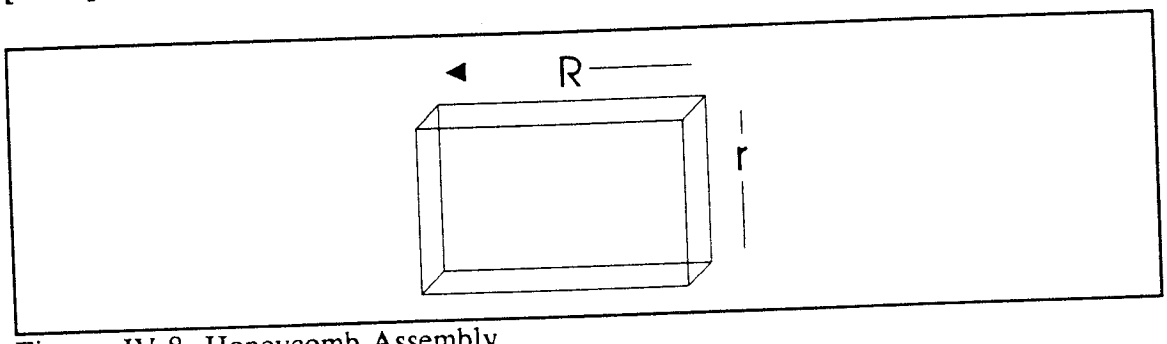

Figure IV-8 Honeycomb Assembly

4. Structural Members

The U-Channel members provide spacing and rigidity to the SLD. The U-Channels depicted in Figure IV-9 are positioned as shown in Fig IV-10 to allow clearance between the shroud and the SLD, while still giving the overall structure stiffness and a mounting surface for panel fastening brackets. Dimensions and characteristics are presented in Table IV.5.

Table IV.4 Panel Characteristics

R=length	1.52 m
r=width	1.00 m
t_{core}	2.54 cm
t_{skin}	.899 mm
t_{panel}	2.558 cm
mass	4.37 kg
I_{xx}	4.37 kg m^2
I_{yy}	10.1 kg m^2
I_{zz}	14.5 kg m^2
load	1547 kg
factor of safety	1.1

*note: a 10% margin of safety is required by Ariane Aerospace Corporation for all components flown in their Launch Vehicle.(Ref. 7)

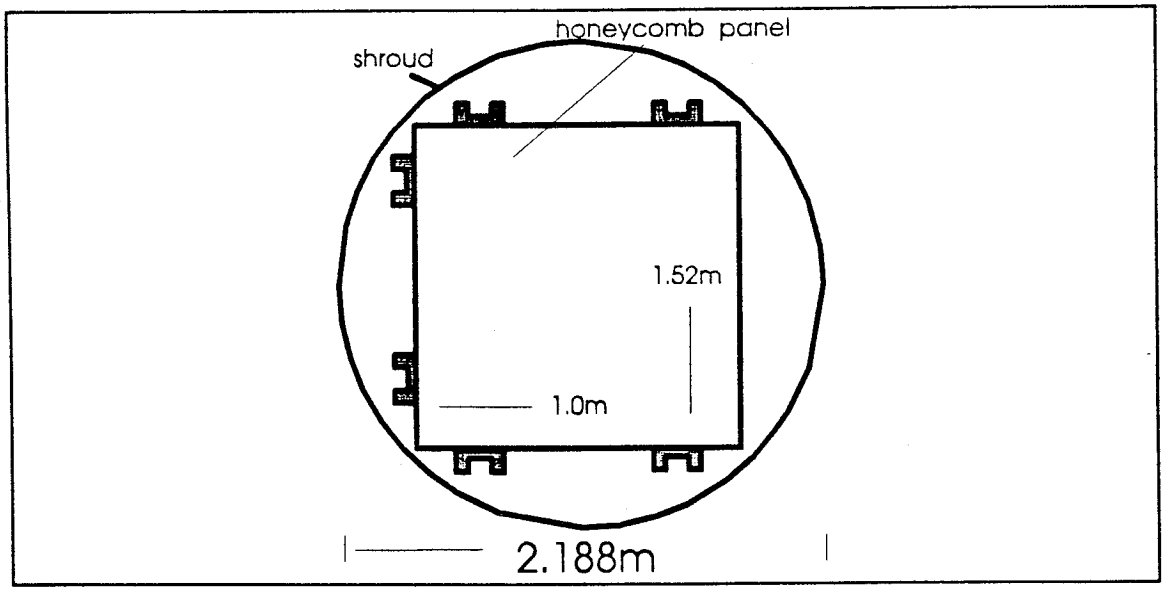

Figure IV-10 SLD Inside Delta II Shroud

Table IV.5 U-Channel Dimensions

h	6.15cm
H	8.23cm
b	1.27cm
B	2.54cm
L	5.08m
C	1.05cm
I_{xx}	38.7 kgm^2
I_{yy}	38.7 kgm^2
I_{zz}	.007 kgm^2

5. Adaptor Mating Surface

a. Dimensions

The adaptor mating surface, shown in Figure IV.11 is compatible with the adaptor rings for both Delta and Ariane launch vehicles. As such it has an inside diameter (ID) to match with the Delta 3172B PAF and an outside diameter (OD) to match the Ariane 1194A. Dimensions and characteristics are given in Table IV.6 and Table IV.7.

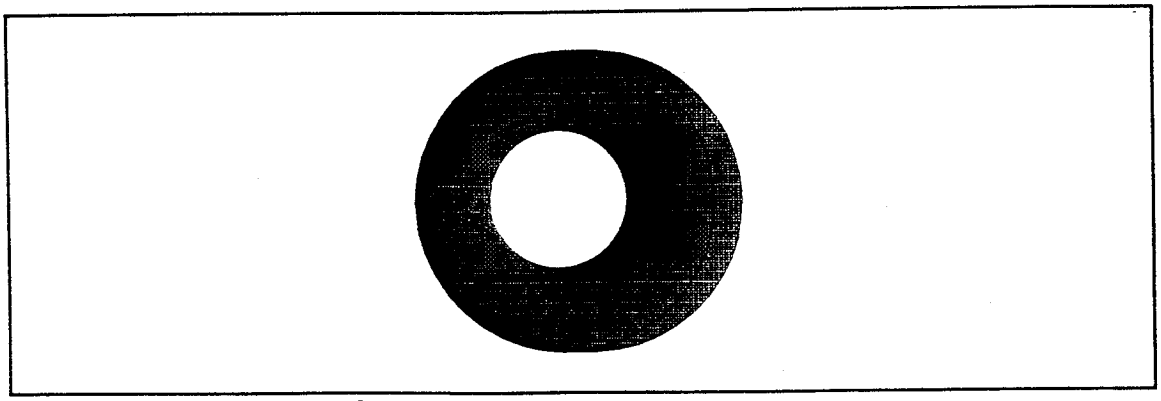

Figure IV-11 Mating Surface

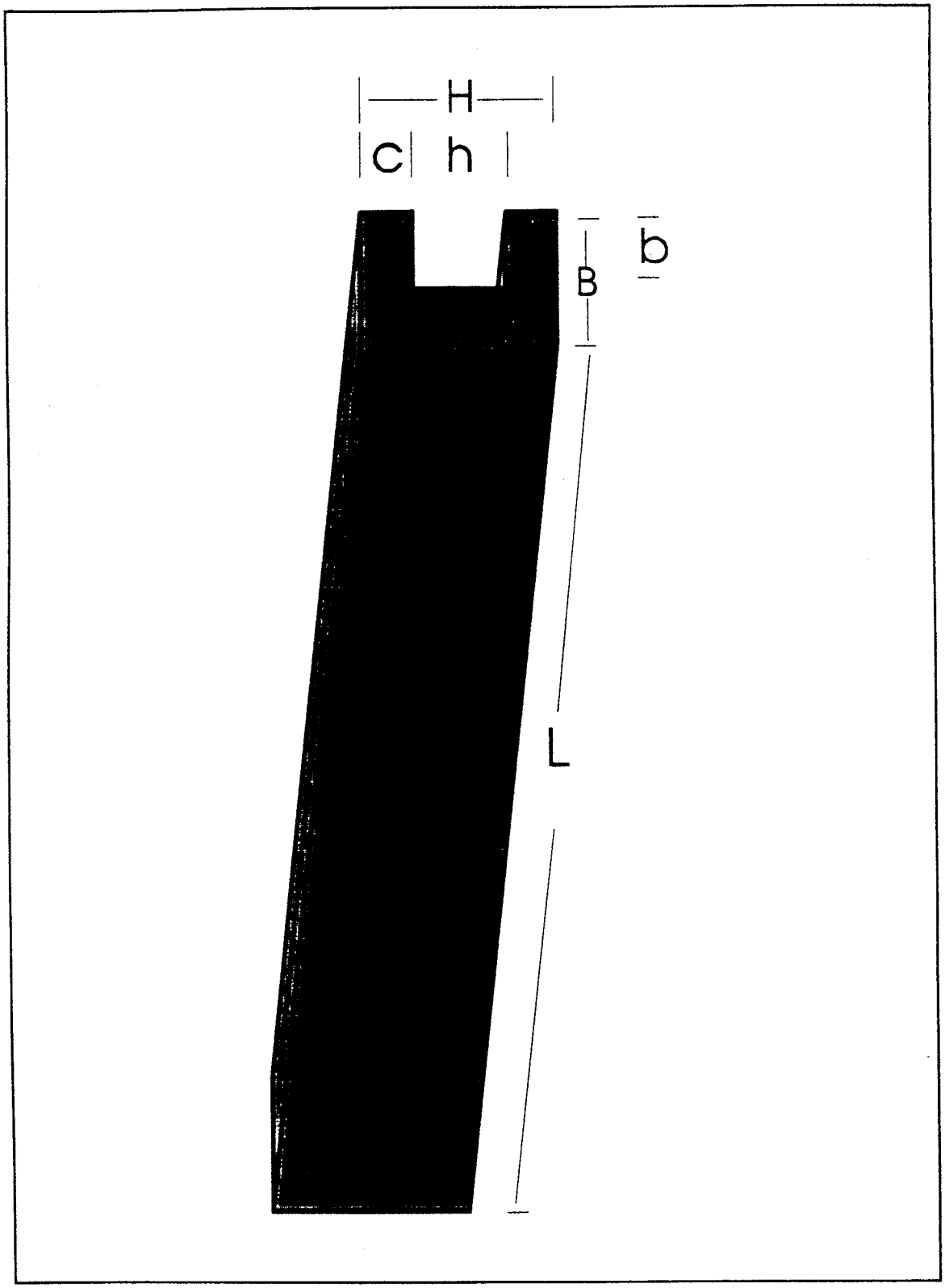

Figure IV-9 U-channel

Table IV.6 Adapter Specifications

Delta II		Ariane	
3172B PAF		1194A	
mass	57kg	mass	45kg
ID	876cm	ID	118.4cm
OD	958cm	OD	121.5cm
supports	3855kg	supports	3500kg
CG limit	**	CG limit	3500kg @ 2.5m

**note: CG limits not given for this adaptor. However limit for 2177kg adaptor is 2177kg @ 2.08m.

Table IV.7 Adaptor Mating Surface Dimensions

Inside Diameter	87.6 cm
Outside Diameter	121.5 cm
Thickness	1.5 cm
Mass	33.4 kg
Density	2.71 g/cm^3
I_{xx}	18.25 kg m^2
I_{yy}	18.25 kg m^2
I_{zz}	37.46 kg m^2

E. REFERENCES

1. McDonnell Douglas Astronautics Company. *Delta II commercial spacecraft users manual.* Huntington Beach CA. Jul 1987.

2. Naval Postgraduate School. *Spacecraft Design Project High Latitude Communications Satellite.* Monterey CA. Dec 1989.

3. Shames, Irving H. *Introduction to Solid Mechanics.*New Jersey: Prentice Hall, 1989.

4. Hodgman, Charles (ed.) *Handbook of Chemistry and Physics.* Cleveland Ohio, Chemical Rubber Publishing Co. 1958.

5. Baumeister, Theodore (ed.) *Mark's Mechanical Engineer's Handbook.* McGraw-Hill Book Company, New York. 1958.

6. Astech, *Astech Design Allowables Manual.* Santa Ana CA. May 1977 rev June 1985.

7. Arianespace, *Ariane 4 User's Manual Issue N1.* 1983

V. STRUCTURE

A. INTRODUCTION

1. Scope

a. Operational Requirements

The structural system is designed to provide mechanical support to all the spacecraft systems within the framework of the spacecraft configuration. It also provides alignments of actuators, sensors, antennas, and launch vehicle interface [Ref 1]. The structure must be able to survive launch loads and to isolate the other systems from the associated stresses. Orbital requirements dictate high stiffness to prevent deployed appendages from interacting with the spacecraft and causing attitude control disturbances. The design launch loads used were greater than the Delta II loads in order to counteract the large moments generated by the Spacecraft Launch Dispenser.

b. Functional Requirements

The structural configuration is designed to accommodate either a Delta launch or an Ariane launch using the spacecraft launch dispenser described in the launch integration section. The structural system is designed to support all of the spacecraft components in the smallest space possible due to the large number of spacecraft to be launched on one launch vehicle.

2. Method

a. Design, Model, and Software

Initial design of the structural system was performed using the estimation equations presented in Chapter 4 of Ref 1. After the configuration was finalized, Microsoft Excel 3.0 was used to calculate the spacecraft mass, moments of inertia,and center of mass offset. Calculations are presented in Appendix C. The GIFTS Finite Element Analysis Program was used to model the spacecraft in its final stowed configuration. For stiffness calculations, the spacecraft's panels were modeled as solid panels using an equivalent thickness calculated by setting the stiffness for an isotropic panel equal to the stiffness for a honeycomb panel.

b. Restrictions and Alternatives

The rectangular frame structure is used due to requirements for attaching the spacecraft to the Spacecraft Launch Dispenser (SLD). This allowed the launch loads to be distributed to the frame. A central tube structure was rejected because of space requirements, load distribution, and dispenser ejection requirements.

The cold plates are sized for both structural and thermal control requirements. These panels are fabricated from solid aluminum instead of honeycomb like the remainder of the other panels in order to meet both thermal control and structural requirements.

B. GENERAL SYSTEM DESCRIPTION

The structural system consists of a frame of rectangular tubing with panels attached to all sides. The pitch axis panels provide structural support for the majority of the equipment and the thermal control system. The roll axis panels support the minor heat generating equipment and the solar arrays. The earth panels are primarily designed to provide a mounting surface for the phased array antenna. The anti-earth panel is used as an access panel for construction and integration, and as an attachment face for the second TT&C antenna, which is incorporated for unusual attitude recovery.

The propellent tank supports consist of a ring around the diameter of the propellent tank with 2 inch outside diameter tubing attached to the bottom earth face rectangular frame.

C. INDIVIDUAL COMPONENT DESCRIPTION

The structural system is composed of an aluminum rectangular frame which serves as the primary load bearing structure, and attached aluminum honeycomb face panels and thermal control system cold plates which support the equipment components of other spacecraft systems.

1. Rectangular Frame

The rectangular frame consists of two sizes of rectangular cross-sectional tubing. The lateral tubing is 2.0 inch by 1.5 inch outside diameter 6061-T6 aluminum tubing with 1/8" wall thickness. The 2.0 inch face is aligned parallel with the Z axis to

absorb launch loads and maximize the area moment of inertia and to minimize the beam deflection. Figure V-1 depicts a cross-sectional view of the tubing.

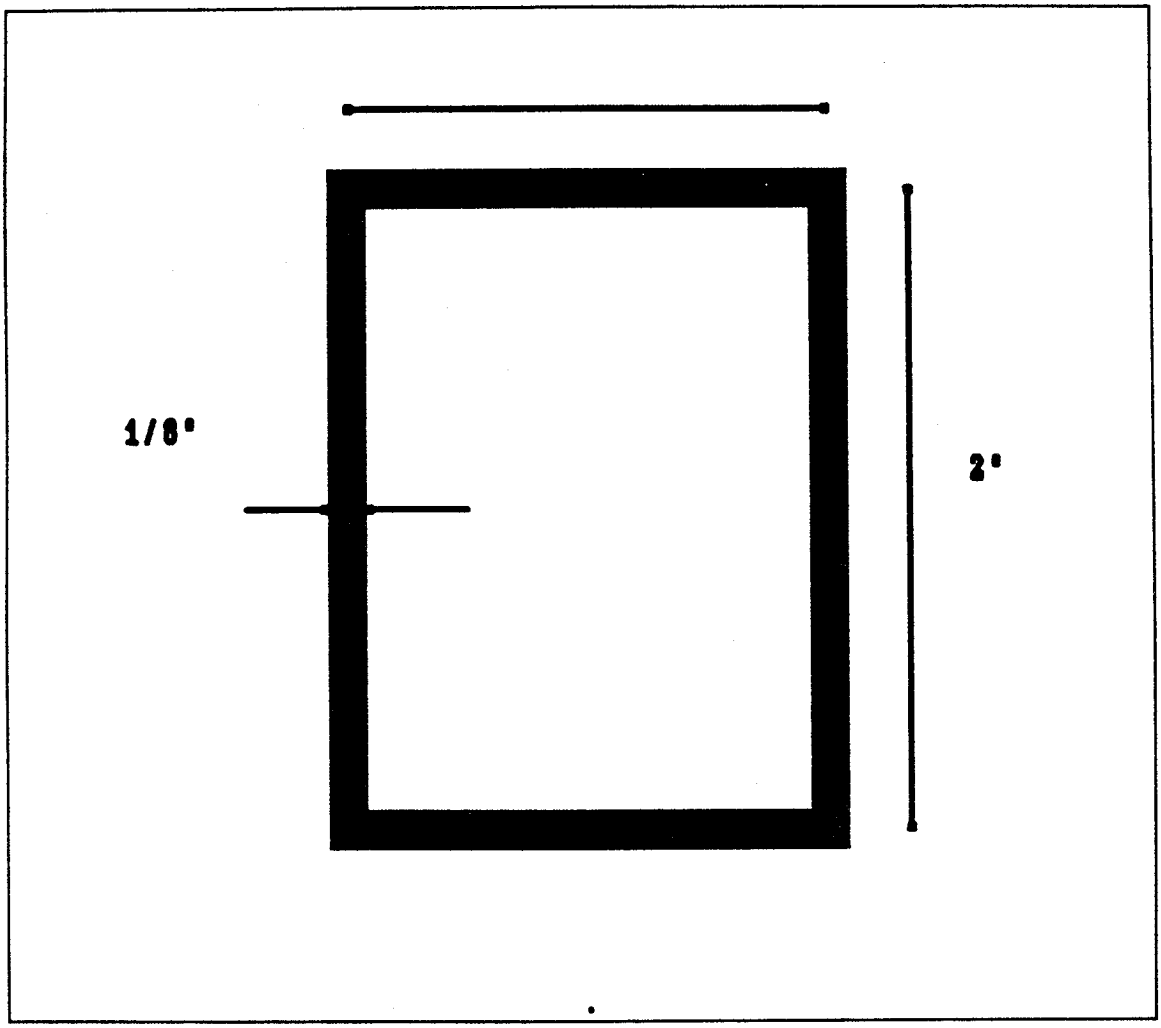

Figure V-1 Cross-sectional View of Lateral Tubing

The axial tubing consists of 1.5 inch by 1 inch outside diameter aluminum 6061-T6 tubing with 1/8" wall thickness. The large face is oriented towards the X axis. Figure V-2 depicts a cross-sectional view of the tubing.

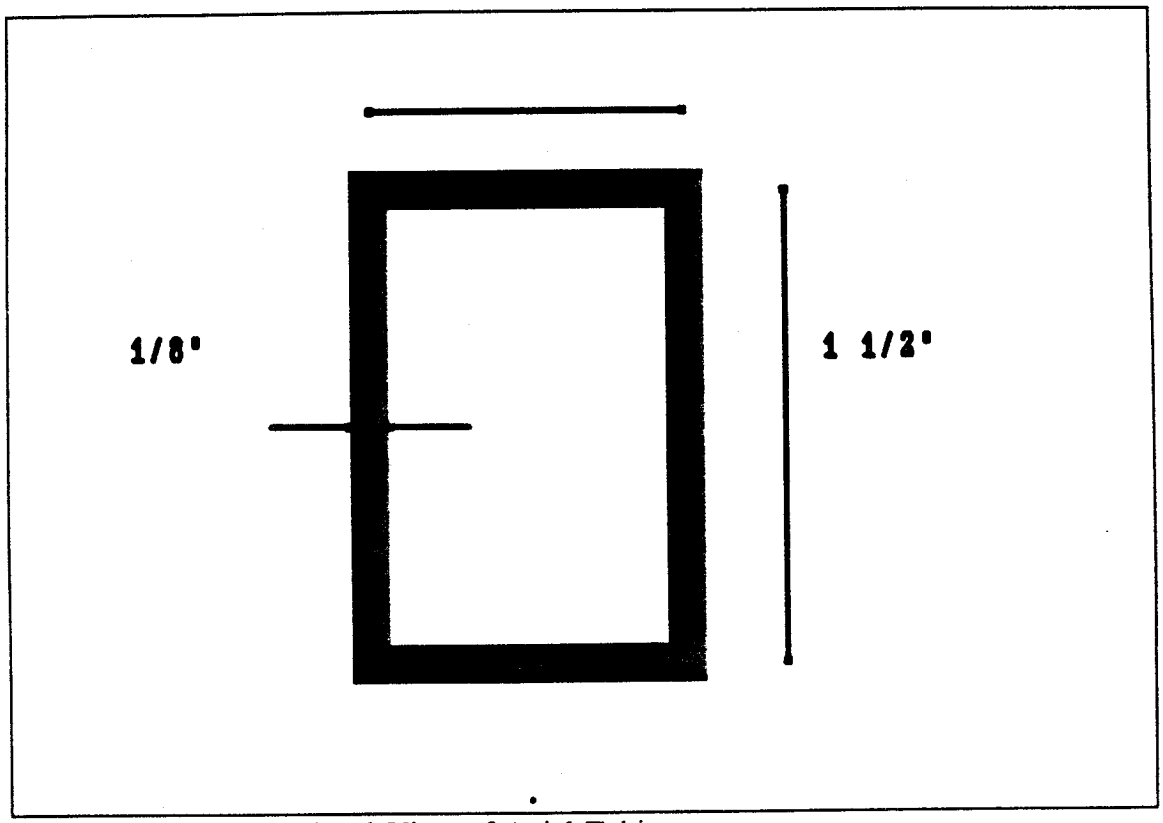

Figure V-2 Cross-sectional View of Axial Tubing

2. Equipment Panels

The honeycomb equipment panels are constructed of 6061- T6 aluminum, are designed to support 54 kilograms of component mass under 36 g's of dynamic loading and have a fundamental frequency above 30 Hz. The panels are not designed to absorb launch loads but simply to hold equipment in place and provide alignment for various

components. Initial design used the estimation equations from Ref 1. The calculations were performed with a spreadsheet and are summarized in Appendix C. Figure V-3 illustrates a typical panel.

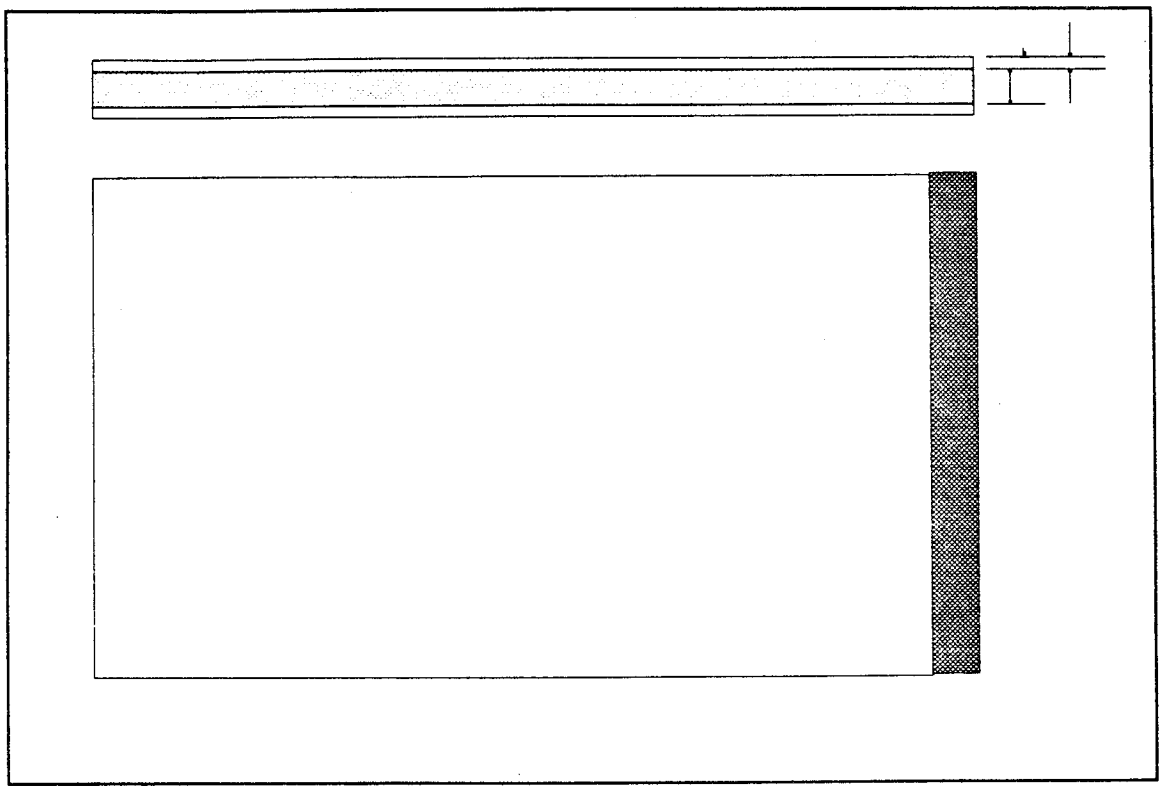

Figure V-3 Typical Honeycomb Panel

In addition to providing the spacecraft structure system mass budget, Table V.1 lists the values for the face skin thickness (t) and the core thickness (h). The $\pm$ Y panels act as the cold plate for the thermal control system and are solid aluminum 6061-T6 plate.

Table V.1 Spacecraft Structure Mass Summary

Component	Mass (kg)
± Z Honeycomb Panels (h=25.4 mm, t=.2mm)	3.60
± X Honeycomb Panels (h=25.4 mm, t=.2mm)	2.02
± Y Panels(Cold Plates) (t=3.5mm)	11.2
±X Lateral Tubing	3.368
± Y Lateral Tubing	2.896
Axial Tubing	1.248
Dispenser Rails	2.38
Misc.(Brackets & Struts)	15
Total	41.7

D. SYSTEM INTEGRATION

1. Spacecraft Properties

After the configuration was finalized, the spacecraft mass, center of mass offset, and total moments of inertia were calculated for various propellent loads and configurations. The results are summarized in Table V.2. Calculations are presented in Appendix C.

Static loads were applied to the model in the three coordinate directions. It should be noted that the model axes do not correspond to the actual spacecraft coordinate axes. The model axes are listed below:

- X axis: Corresponds to the spacecraft's pitch (y) axis. The model's X axis corresponds to the radiator side of the spacecraft.

- Y axis: Corresponds to the spacecraft's yaw (z) axis. This corresponds to the earth and anti-earth sides of the spacecraft.

- Z axis: Corresponds to the spacecraft's roll (x) axis. This corresponds to the spacecraft's side where the antenna and array are deployed.

The load cases are listed below:

- Load case 1: Corresponds to a 8.5 g load in the model's y axis.

- Load case 2: Corresponds to a 15 g load in the model's z axis.

- Load case 3: Corresponds to a 15 g load in the model's x axis.

The results of the three applied static load cases on the modeled structural members are depicted in figures V-4 through V-6. Table V.3 summarizes the static analysis. With a margin of safety of 1.1, the 15g static load produced the greatest structural deflections in the spacecraft +/- X axis panels, as shown in Von Mises plot in figure V-7. This of highest stress experienced a maximum loaded deflection of only 1.6 mm, thus providing more than adequate structural rigidity. Although the structural members are somewhat over designed in strength, a reduction in the size of the frame to optimize for static load strength would produce only a modest mass savings.

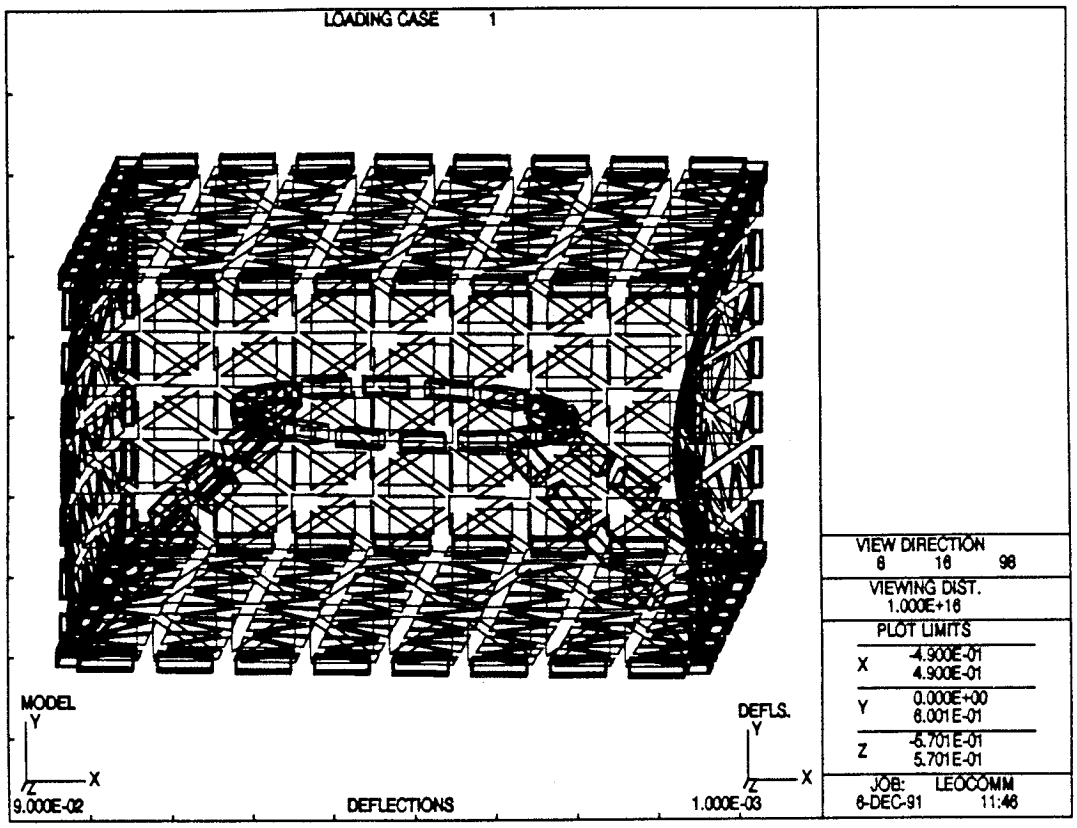

Figure V-4 Load Case 1 Static Plot

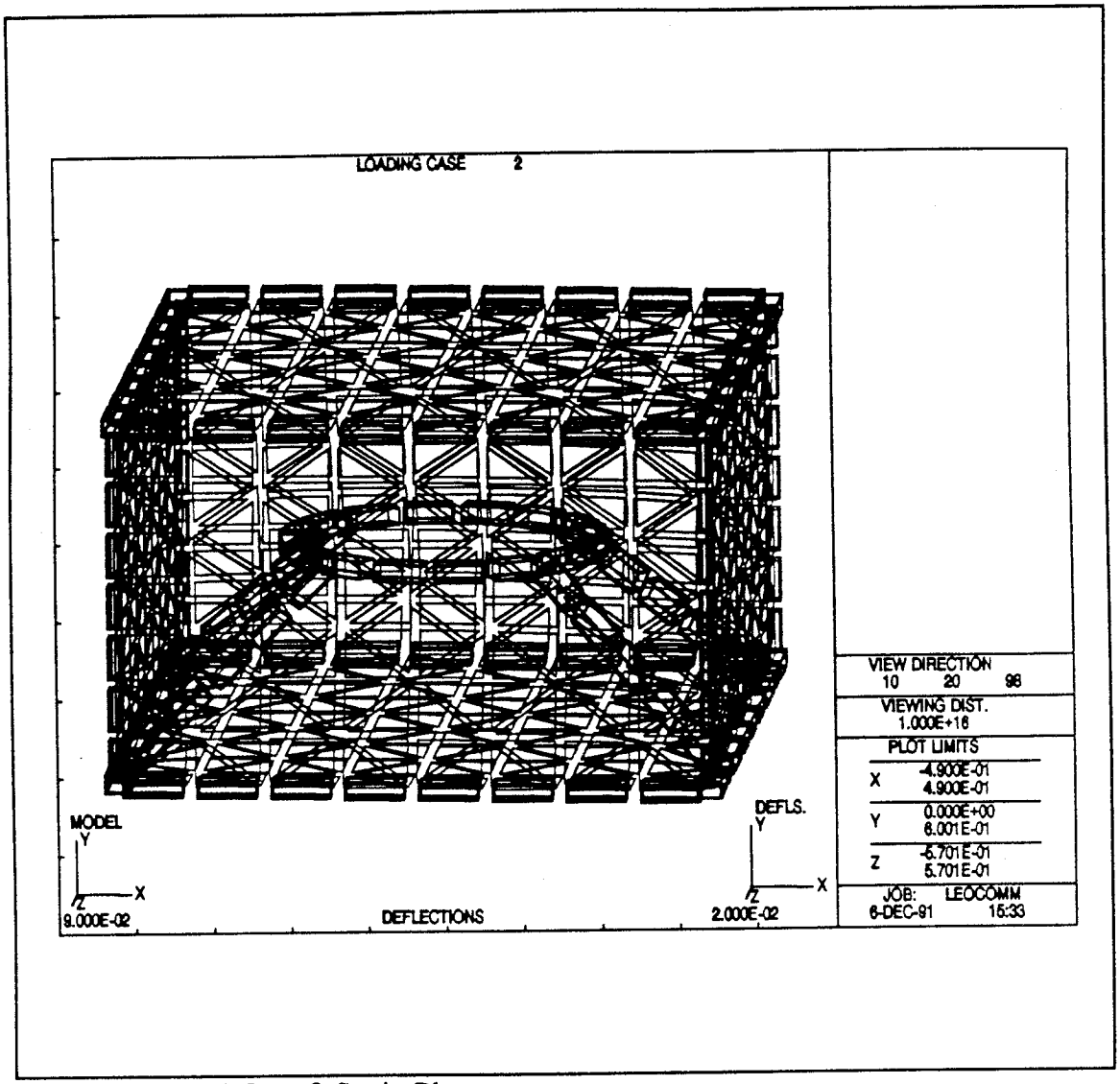

Figure V-5 Load Case 2 Static Plot

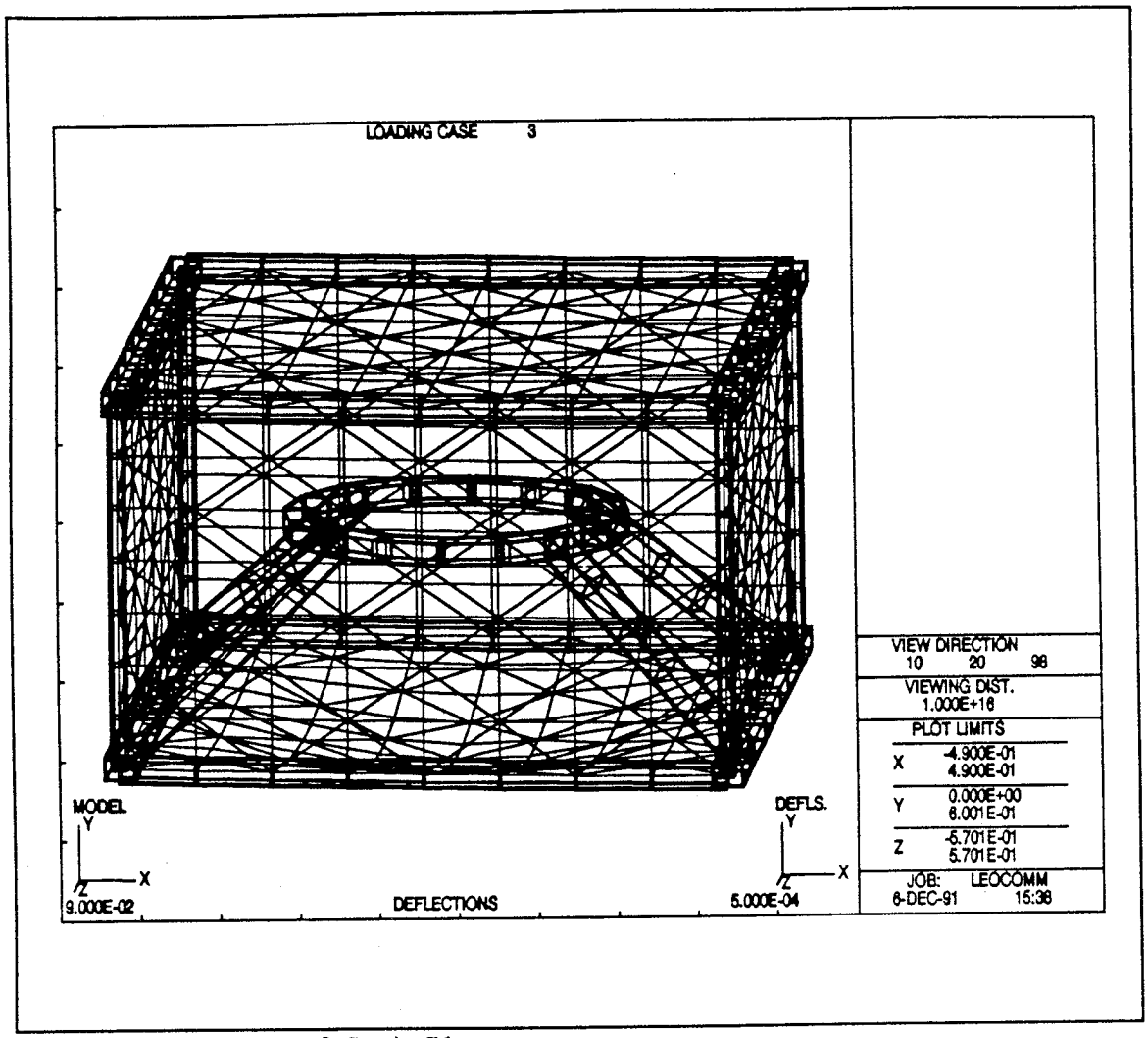

Figure V-6 Load Case 3 Static Plot

Table V.3 Structural Static Analysis Summary

Category	Load Case 1	Load Case 2	Load Case 3
Max Translationa l Deflection (mm)	1.03	1.6	.48
Max Rotational Deflection (radians)	4.8E-3	7.76E-3	1.38
Margin of Safety	12	1.1	76

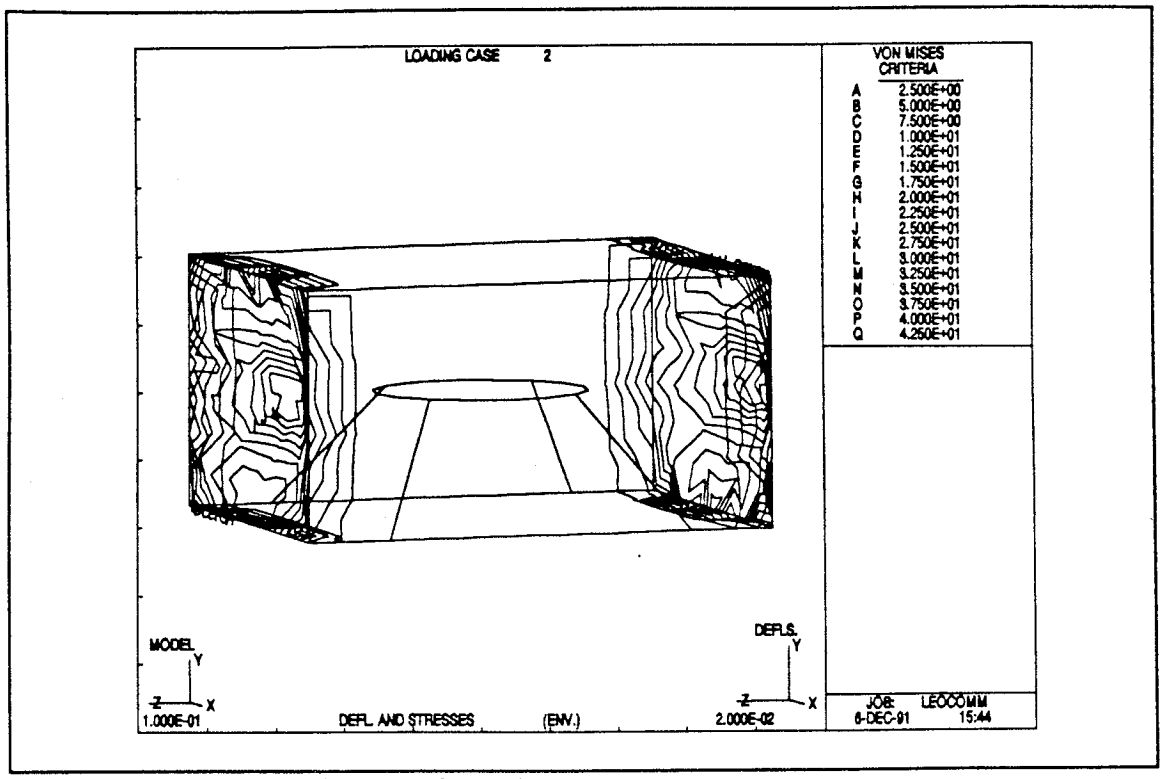

Figure V-7 Load Case 2 Von Mises Plot

3. Dynamic Analysis

The dynamic analysis was performed on the first six modes of the spacecraft. Table V.4 lists the first six modal frequencies and eigenvalues of the spacecraft. Figures V-8 through V-19 alternately present mode shape and mode vector plots for the first six dynamic modes of the spacecraft structure. With the exception of the +/- X face panels, the structure meets the Delta II fundamental frequency constraints of greater than 35 Hz axial and greater than 15 HZ lateral [Ref. 2]. While both forms of data plots depict structural deflection, the fundamental mode shape vector plots most clearly indicate the deflections of only the +/- X axis panels at the axial frequency of 19.18 HZ. An attempt to stiffen the affected panels by increasing their thickness resulted in an excessive

mass addition. A diagonal stiffener added to the +/- X panel exterior surfaces is believed to be a viable solution to the fundamental frequency problem with those panels. Time constraints and lack of computer resource availability precluded a thorough analysis of the proposed solution, which would require a modification to the finite elenent model. No modification is required to the +/- Y axis and +/- Z axis panels, or to the frame or propellant tank support structures. Further testing of a modified model is therefore recommended. Such a solution is not forseen to adversely impact integration efforts at the subsystem, system, spacecraft or SLD / launch vehicle level.

TableV.4 Dynamic Analysis Summary

Mode	Frequency (cps)	Eigenvalue
1	19.18	1.41123D+04
2	19.18	1.41198D+04
3	27.80	3.00984D+04
4	27.80	3.01006D+04
5	42.55	7.04571D+04
6	42.55	7.04681D+04

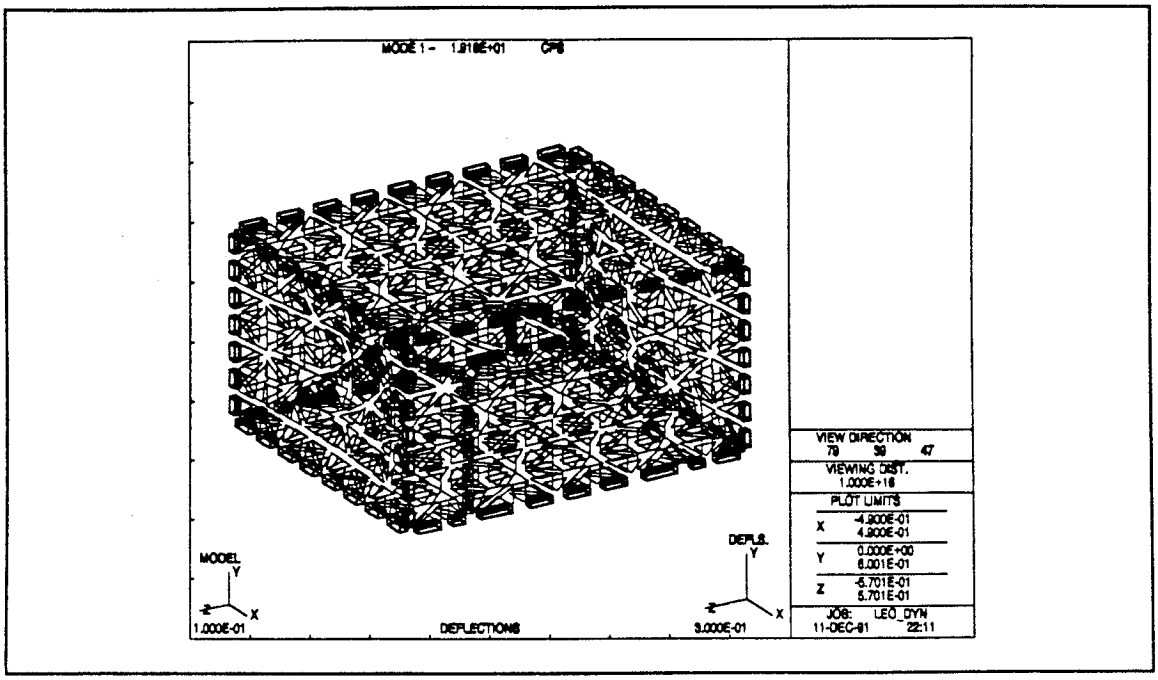

Figure V-8 Fundamental Mode Plot

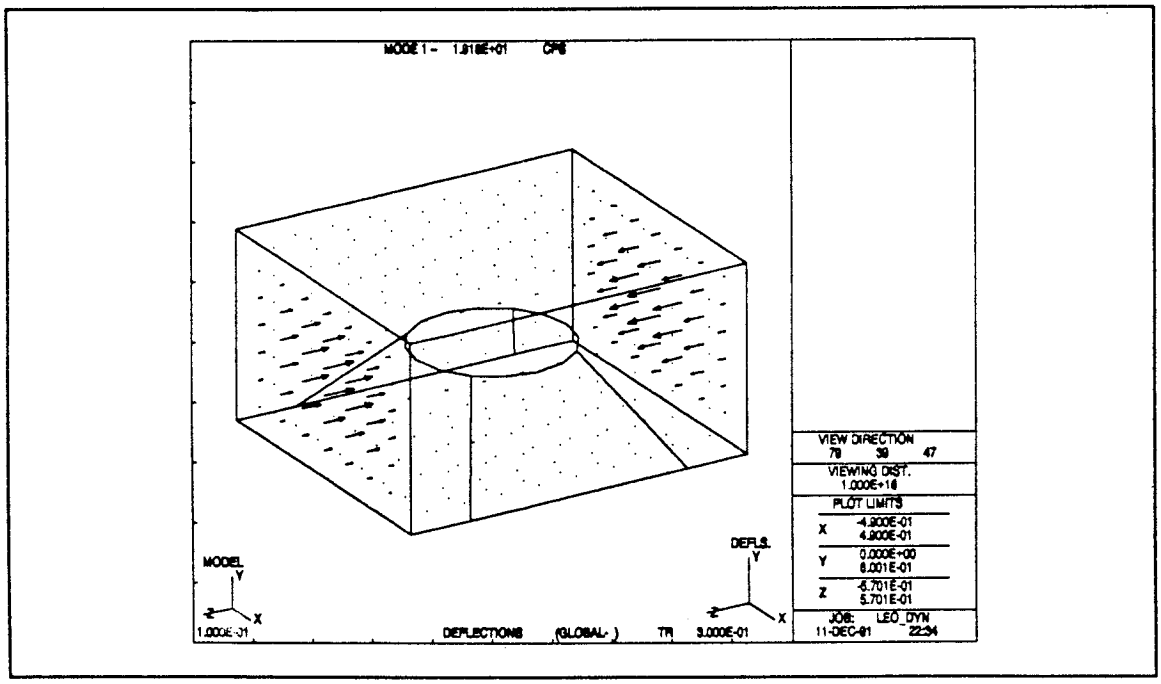

Figure V-9 Fundamental Mode Vector Plot

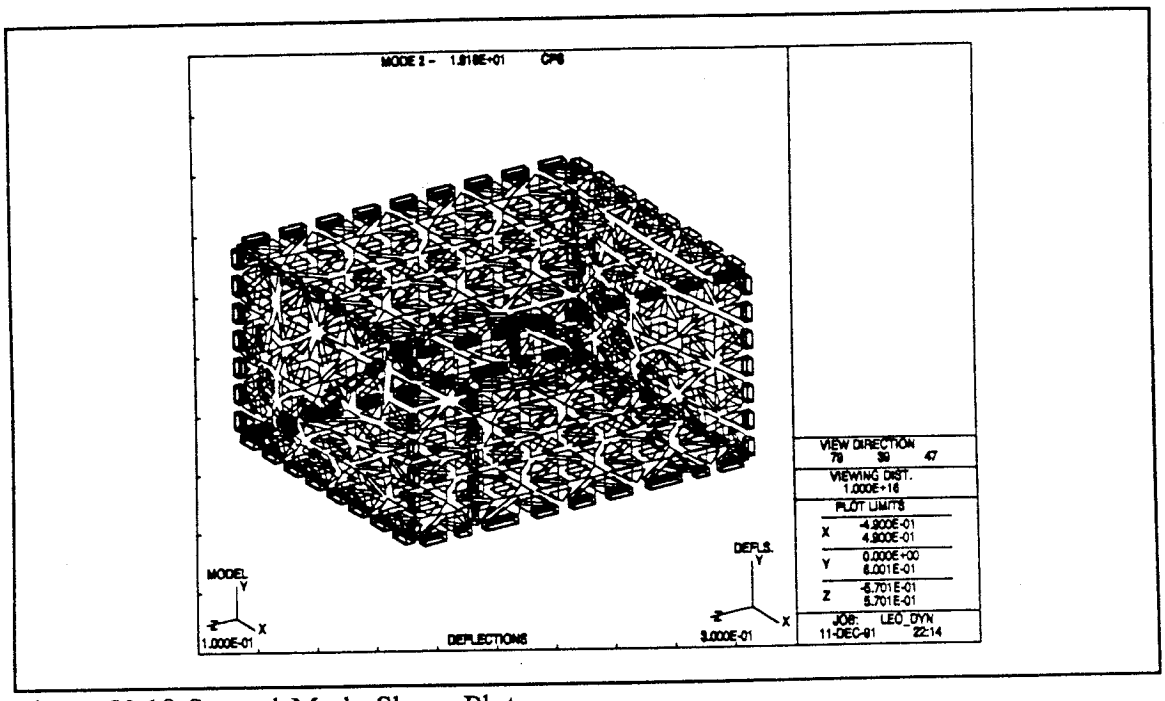

Figure V-10 Second Mode Shape Plot

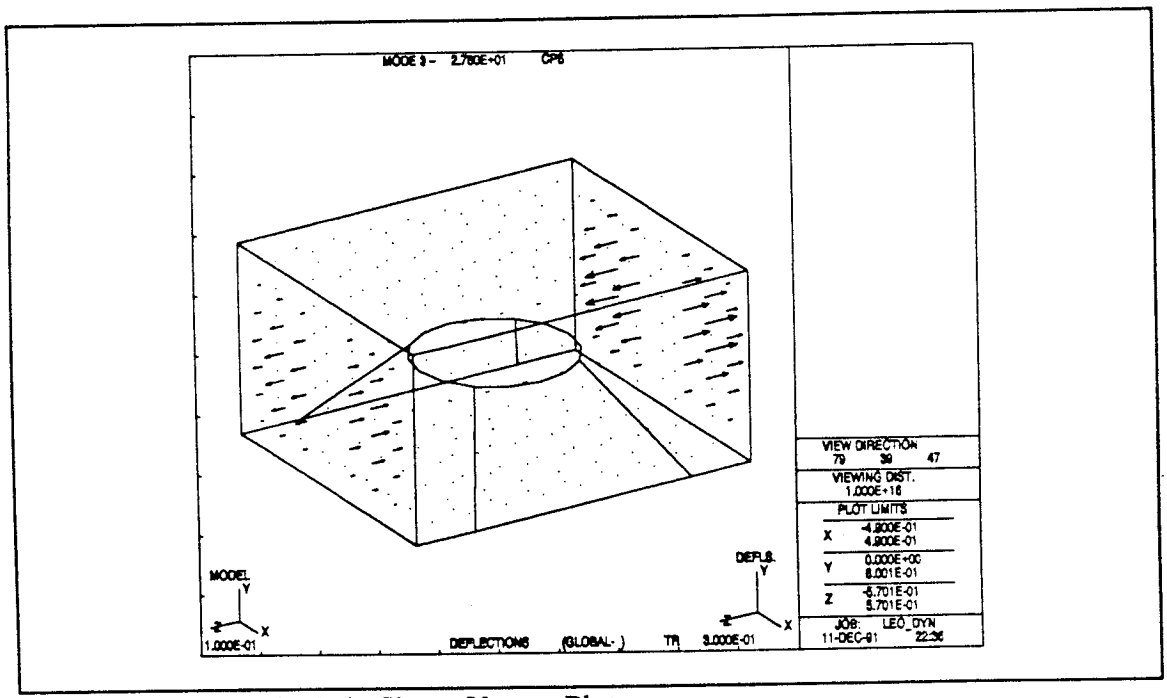

Figure V-11 Second Mode Shape Vector Plot

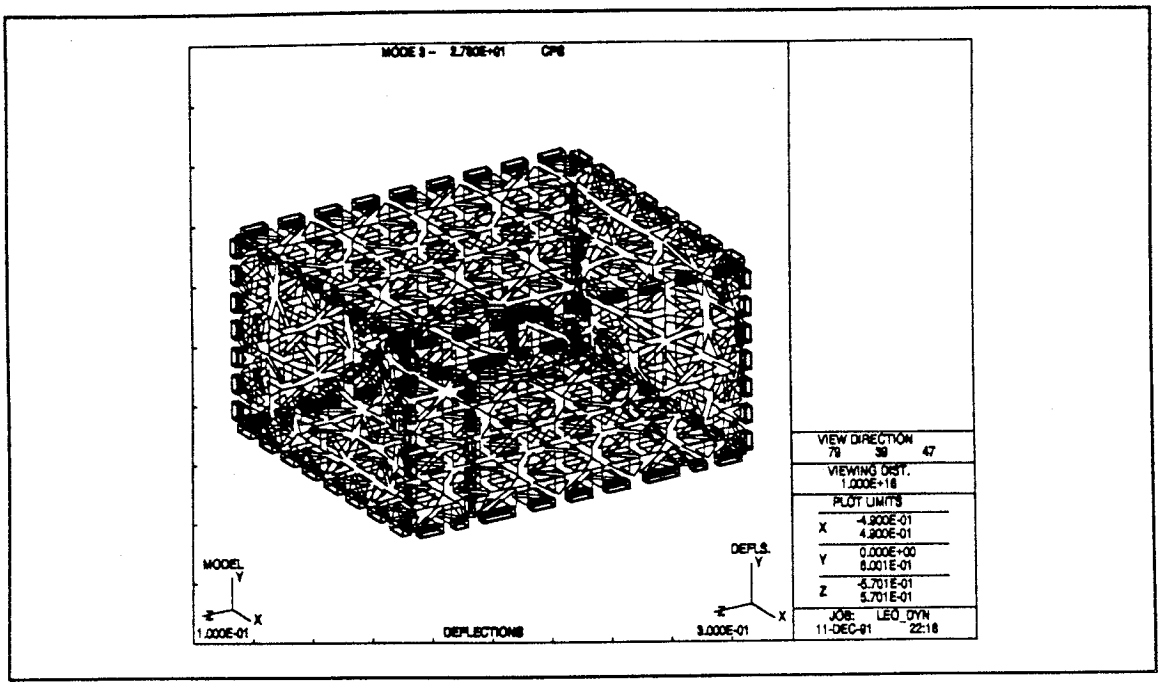

Figure V-12 Third Mode Shape Plot

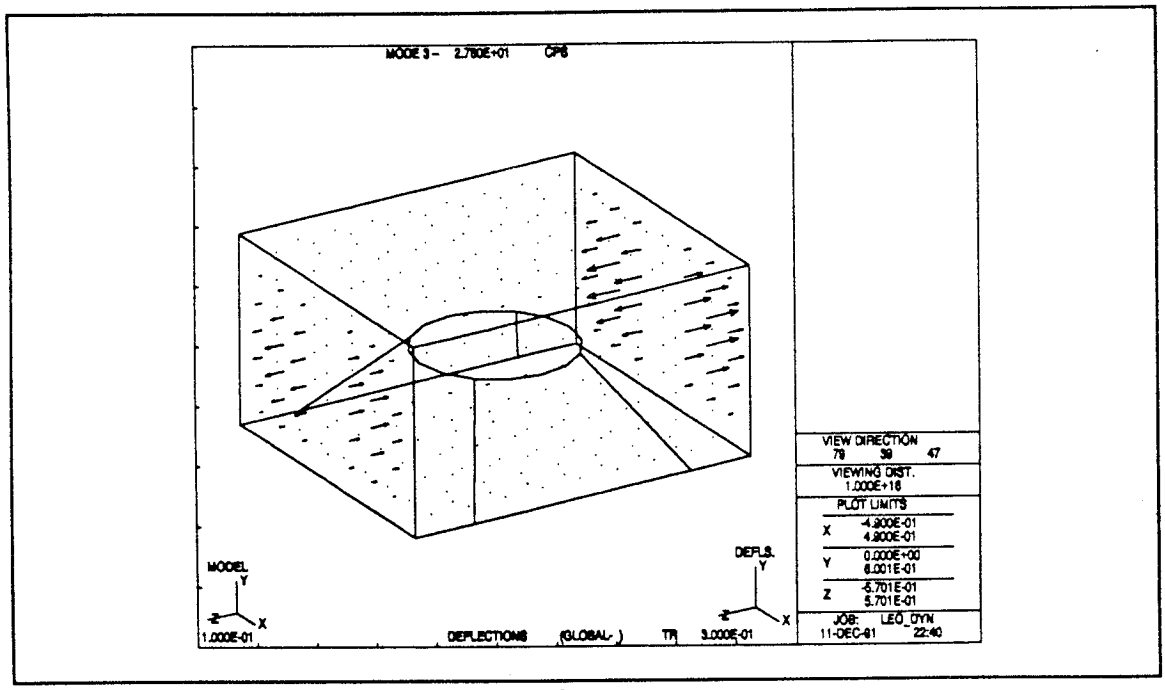

Figure V-13 Third Mode Shape Vector Plot

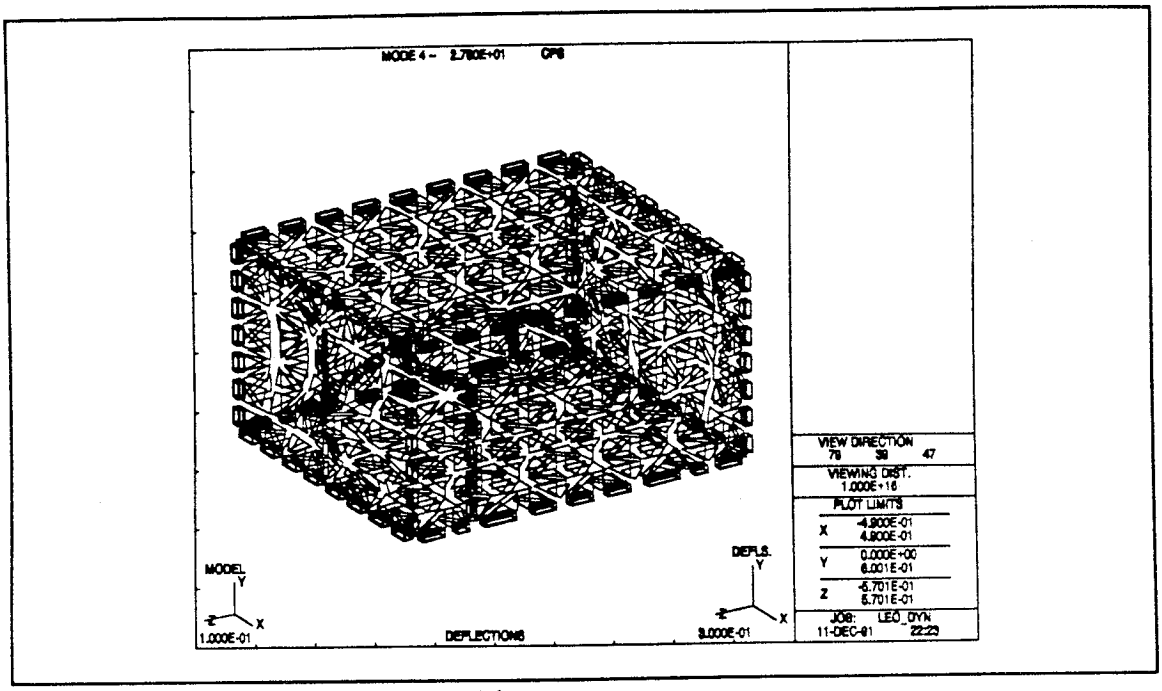

Figure V-14 Fourth Mode Shape Plot

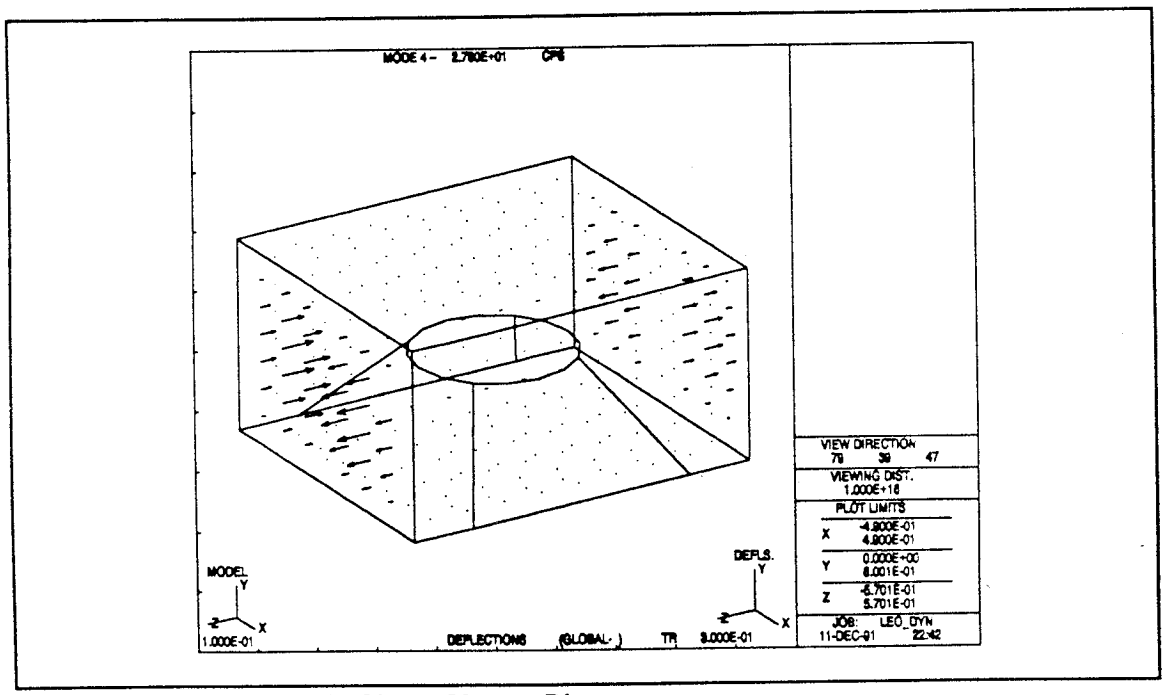

FigureV-15 Fourth Mode Shape Vector Plot

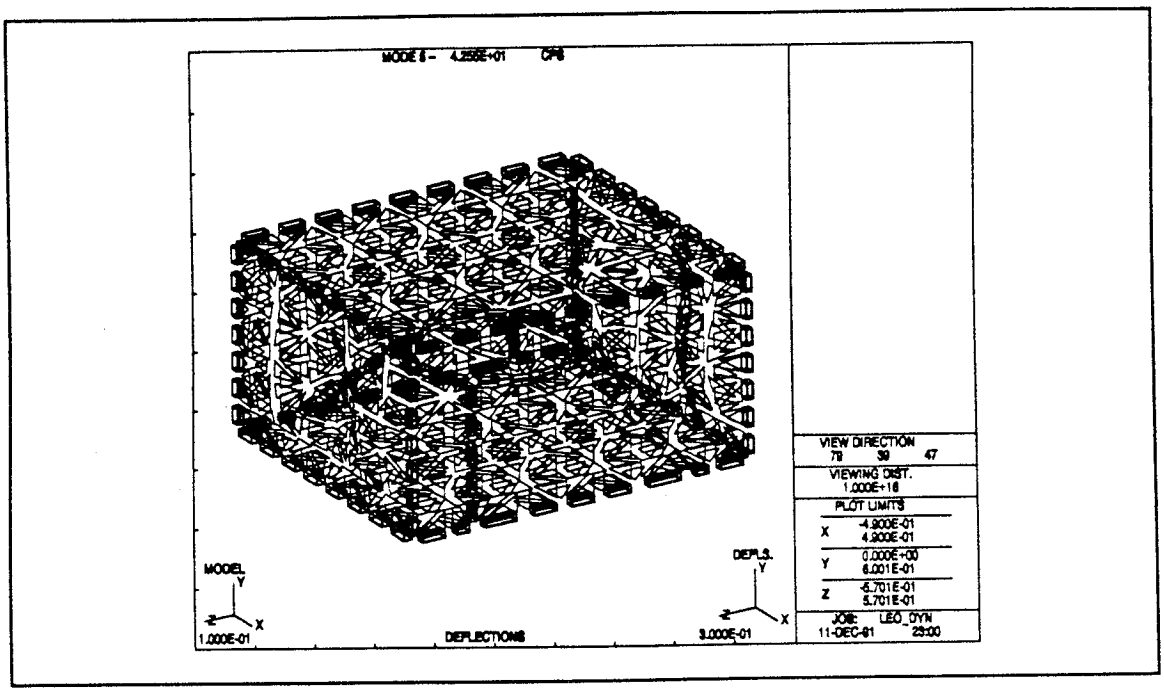

Figure V-16 Fifth Mode Shape Plot

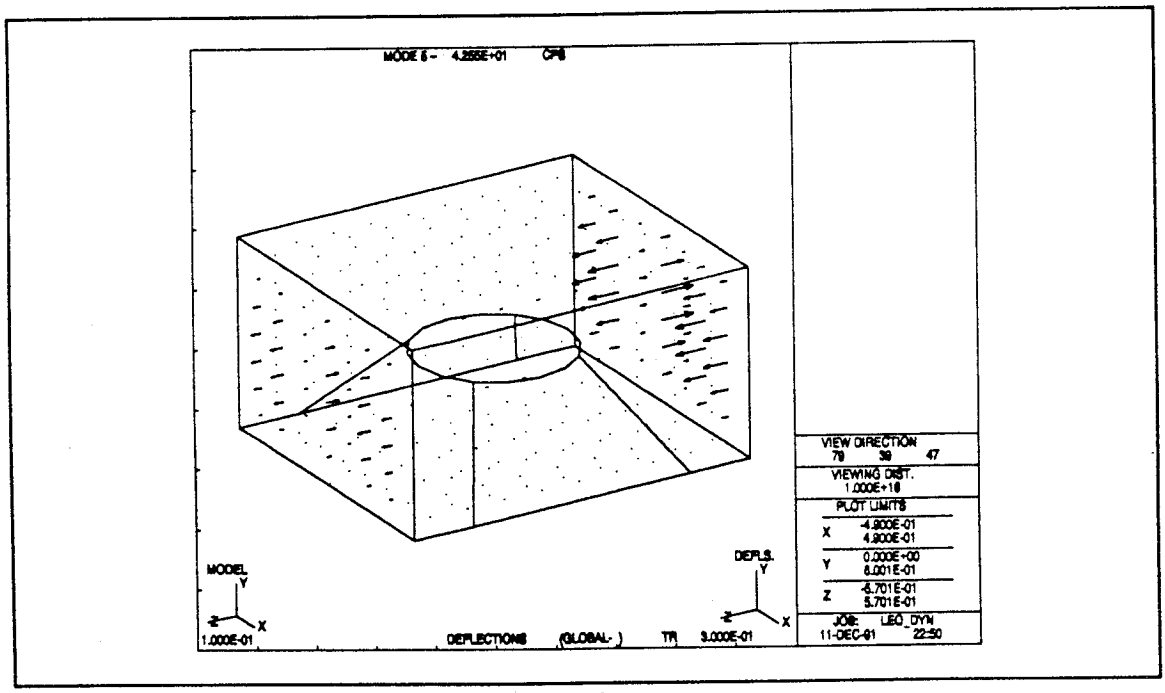

Figure V-17 Fifth Mode Shape Frequency Plot

C-2

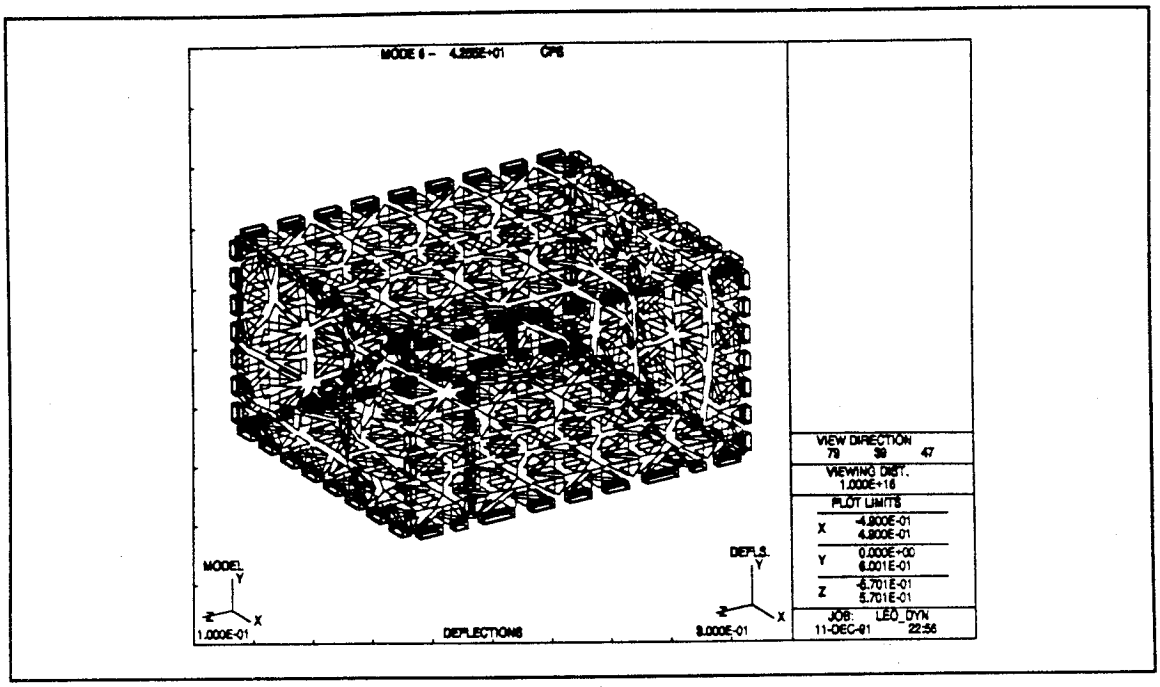

Figure V-18 Sixth Mode Shape Frequency Plot

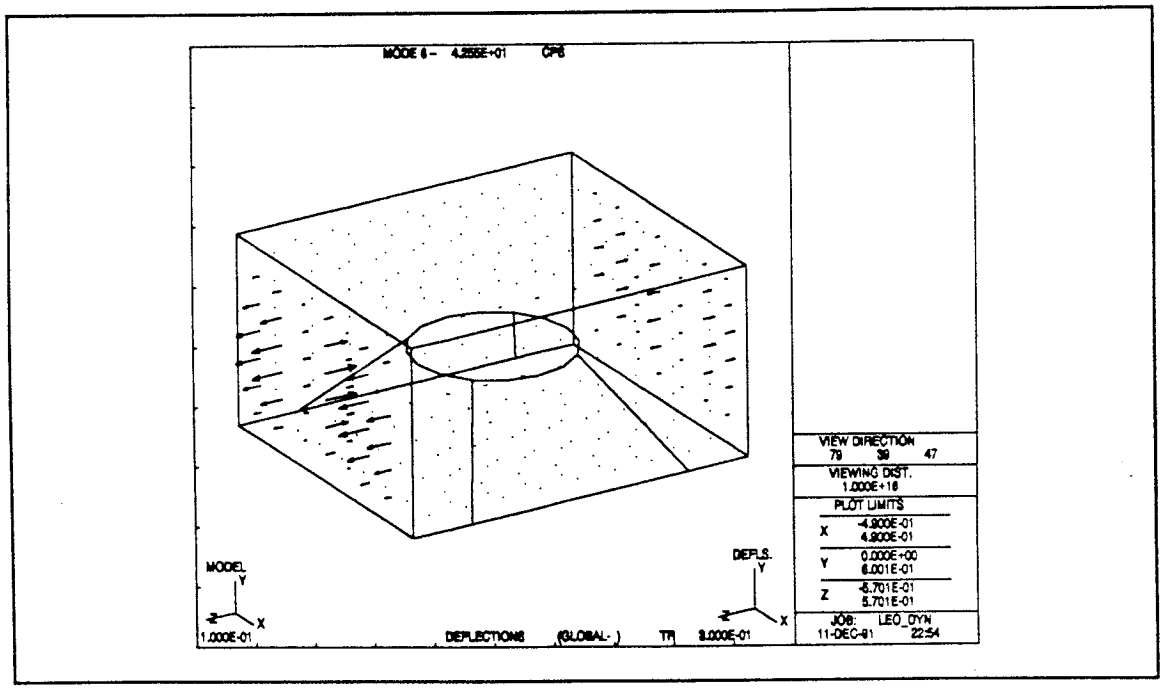

Figure V-19 Sixth Mode Vector Plot

E. REFERENCES

1. Agrawal, B. N., *Design of Geosynchronous Spacecraft*, Prentice Hall, Inc., Englewood Cliffs, NJ, 1986

2. Morgan, W. L., *Communication Satellite Handbook*, John Wiley & Sons, NY, NY, 1989

VI. PAYLOAD

A. INTRODUCTION

A detailed description of the payload is presented in the GLOBALSTAR FCC Licensing Request [Ref. 1].

1. Requirements

a. Mission

The mission of the satellite constellation is to provide a conduit for voice, data, messaging, and position location information for cellular telephone users when those users are not within range of a terrestrial cellular telephone network. Coverage extends from 75 degrees North to 75 degrees South latitude. To complete a communications link, both the user and a gateway must be in the field of view of at least one spacecraft. Contractor data indicates that the Radio Determination Satellite Service (RDSS) can provide position accuracies of approximately one mile for single satellite operations and approximately 200 meters when two satellites are in view.

b. Frequency and Data Rate

The uplink and downlink between users and the spacecraft are L-Band, from 1610.0 to 1626.5 MHz. Gateway to spacecraft links are C-Band, with the uplink from 6525.0 to 6541.5 MHz and the downlink from 5199.5 to 5216.0 MHz. User equipment provides voice and data encoding/decoding at a variable rate of 1.2 to 9.6

kilo-bits per second (KBPS). The carrier signal is burst transmitted to and from satellites at a bit rate of 28.8 KBPS. Encoding and decoding is accomplished on the ground to minimize spacecraft mass and cost, thus the spacecraft acts as a transponder only, with no on-board data processing.

2. Summary of System Operation

a. Operating Scheme

The GLOBALSTAR concept, which is presented in detail in Ref. 1, provides communications for a maximum number of users with a minimum of bandwidth by employing a combination of antenna beam separation, Frequency Division Multiple Access (FDMA), Code Division Multiple Access (CDMA), and Time Division Multiple Access (TDMA). Six elliptical spot beams provide coverage over the spacecraft footprint. At any one time, two of these elliptical beams are active and using the same frequency range, but are widely separated on the ground, providing frequency re-use of the full band. The L-Band is divided into 13 sub-bands of 1.25 MHz each to provide FDMA. Spread spectrum techniques (CDMA) are used for signal transmission within each sub-band. To provide TDMA, a system of beam hopping is used. During each 10 milliseconds (ms) of a 60 millisecond duty cycle, two antennas are enabled. Each uses the same spectrum band, so the transponder system relies on signal coding to properly direct the information flow. The first 30 ms of the duty cycle is allotted for transmission, and the second 30 ms is allotted for reception. This technique is illustrated

in Appendix D. The methodology above yields a total of 2626 full duplex channels per spacecraft.

b. Gateway Functions

The gateways are data encryption/ de-cryption facilities that link the spacecraft in view with the Public Service Telephone Network (PSTN). Each gateway contains four antennas. One antenna is dedicated for each of the nearest three spacecraft overhead and one remains ready for the next acquisition. Each antenna is two meters in diameter, has a transmit Effective Isotropic Radiator Power (EIRP) of 32.2 to 44.2 dBW per burst per 1.25 MHz, and a gain of 40.2 dBi (dB isoflux) at 6500 MHz. The antennas are parabolic and passively track the spacecraft using ground generated ephemeris data. The gateway provides for the handoff of communication links from one spacecraft to another as each passes out of view. When a gateway is receiving a single user's transmission from multiple spacecraft, the signal with the highest amplitude is chosen.

c. User Equipment Functions

When in range of a cellular telephone network, user equipment is designed to operate as a normal cellular telephone. When out of cell range, the user device links, via an overhead spacecraft, to a telecommunications gateway and, subsequently, to the PSTN. To the user, the user equipment is a cellular telephone with the added convenience of an RDSS position locator. The spacecraft communication link is a transparent function. When a cellular network carrier wave cannot be detected by

the unit, it broadcasts on the L-Band link to spacecraft overhead. Voice and data are encrypted/decrypted at a variable rate of 1.2 to 9.6 KBPS, and the carrier signal is transmitted and received at a bit rate of 28.8 KBPS during 10 millisecond bursts. A stand alone unit capable of position location only is also planned for production.

d. TT&C Station Functions

One TT&C station on each coast of the continental United States actively tracks each spacecraft as it passes overhead to maintain a central library of current ephemeris data for the constellation. These ephemeris data are sent to all of the gateways to allow for system-wide passive tracking. The TT&C stations also provide the commands to each spacecraft necessary for orbit corrections. The use of TT&C stations eliminates the need for autonomous spacecraft orbit corrections, thereby reducing spacecraft complexity and unit cost. TT&C operations are covered in more detail in chapter VII.

B. SYSTEM DESIGN AND HARDWARE DESCRIPTION

1. Link Parameters

The bandwidth of an individual channel is 1.25 MHz, providing 13 channels over the allotted L-Band frequency range. Link distances are different, depending on which spacecraft antenna is in use. For the two nadir pointing antennas, the nominal range is 1486 km. The mid-range antennas have a nominal range of 2108 km, and the far-range antennas have a nominal range of 2985 km. These ranges are the respective distances from the spacecraft to the centroid of each antenna pattern ellipse. Individual

antenna gains are varied to present the transponder with signal strengths that are largely independent of the user's distance from the spacecraft. A bit error rate of less than 10^{-6} is required for data transmission, and the signal to noise ratio is contractor specified at 15.0 dBW on the L-Band.

2. Equipment Parameters

a. Spacecraft Antenna Gains

The spacecraft L-Band antenna pattern consists of six isoflux (constant gain) ellipses which cover the footprint of the spacecraft as shown in figure VI-1. The pattern is physically symmetric with respect to the spacecraft's velocity vector. For beams 1 and 6, each antenna has a gain of 4.0 dB with a transmit power of 19 Watts (12.8 dBW). For beams 2 and 5, each antenna has a gain of 5.5 dB with a transmit power of 21 Watts (13.2 dBW). For beams 3 and 4, each antenna has a gain of 6.5 dB with a transmit power of 12 Watts (10.8 dBW). Beams 3 and 4 are nadir pointing, so there is no overlap of coverage with other satellites for these two antennas. The two C-Band antennas have a gain of 3.0 dB with a transmit power of 0.66 Watt (-1.8 dBW). Refer to Appendix D for more details.

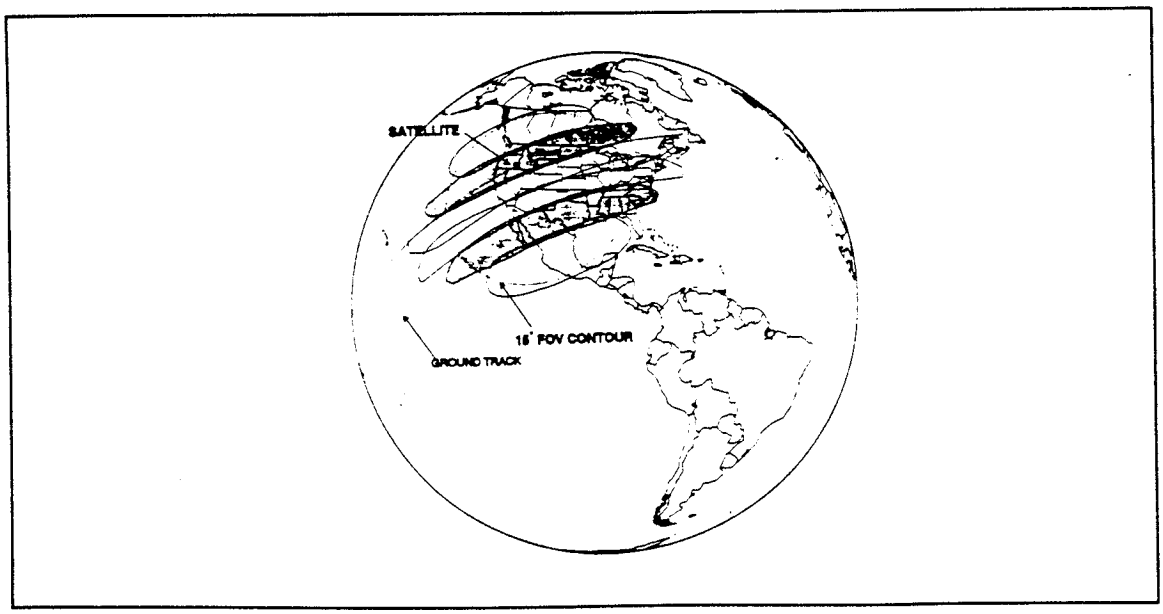

Figure VI-1 L-Band Antenna Spot Beams

b. Gateway Antenna Gains

Each ground station antenna is a parabolic dish with a diameter of two meters. Gain is 40.2 dB at 6.5 GHz. The transmitter EIRP per burst (10 ms) is 32.2 to 44.2 dBW (1660 to 26,300 Watts).

c. User Equipment

The user device employs a quadrifilar helix or patch type antenna. The RF power generated by a cellular-type device is 10 Watts peak and 0.67 Watts RMS. A nominal power of 6 Watts was used for calculation purposes. Gain is 3.0 dB.

d. Component Noise Temperatures

Noise temperatures for the L-Band Low Noise Amplifiers (LNAs) are 75°K for both the uplink and downlink. In the C-Band, the LNA noise temperatures are 170°K for the uplink and 65°K for the downlink. Ground-based antenna (gateways and user equipment) noise temperatures are taken to be 290°K. The spacecraft antenna noise temperatures are 150°K and 200°K for the C- and L-Band antennas, respectively. Composite or total thermal noise temperatures are 460°K and 365°K for the C- and L-Band uplinks, respectively, and 178.8°K and 264°K for the C- and L-Band downlinks, respectively.

e. Mass and Power Budgets

The electrical power and mass budgets for the payload are summarized in Tables VI.1 and VI.2.

Table VI.1 Payload Mass Budget

Component	Quantity	Mass (kg)
C-Band Antenna	2	1 (Each)
L-Band Antenna	6	10 (Total)
C-L Band Transponder	1	20
L-C Band Transponder	1	20
Timing and Control Unit	1	8
Total	11	60

Table VI.2 Payload Power Budget

Peak Load	827.6 Watts
Peak Transmitted Power	43.32 Watts
Peak Thermal Dissipation	784.28 Watts

3. Losses

a. Link Losses

The major contributor to link losses is free space propagation loss. This varies from a minimum of -159.5 dB between the user and a spacecraft directly overhead to -167.8 dB over the maximum link distance, 3461 km (for a minimum 10 degree elevation angle). Other losses include a -0.5 to -1.0 dB polarization loss, a 0.0 to -1.0 dB tracking misalignment loss, and typically a 0 dB (1 Watt) atmospheric attenuation loss.

b. Interference Effects

(1) Self Interference

Within each 1.25 MHz sub-band, multiple information signals overlap. However, the spread spectrum approach using chip-synchronized orthogonal codes minimizes interference between duplex channels.

(2) Fading

Multipath interference or fading is minimized since there is typically more than one spacecraft overhead the user. Terrain or man-made blockage is always a factor, though minimal at lower latitudes. Near the 75 degree latitude limit, however, the user must be aware that there must be a line of sight to spacecraft orbiting at a lower latitude. It was assumed by the contractor for link calculations that 30 percent of the user equipment will be vehicle-mounted and 70 percent will be hand-held. Of the vehicle-mounted equipment, 10 percent was assumed to be in the faded state, and of the hand-held equipment, 20 percent was assumed faded. Refer to Appendix D for tabulated results from the link calculations.

(3) Outside Interference

As with self interference, the use of spread spectrum techniques minimizes any interference from outside sources. This is referred to as the "anti-jam" capability inherent in CDMA technology.

4. Antenna Design

a. Requirements

(1) Design Criteria

To obtain the greatest amount of communications capacity, frequency re-use is essential. This dictates a spot beam antenna architecture. Strict beam shaping requirements and constraints of minimum mass and stowed volume within the launch vehicle result in the choice of a group of planar phased arrays. The use of elliptical spot beams distributed parallel to the spacecraft velocity vector eliminates the need for handoffs between beams as the spacecraft traverses overhead.

(2) Operating Bands

Permission for operation in the L-Band is contingent upon providing an RDSS position location service. If use of the L-Band is denied, a similar employment of spread spectrum techniques could be used elsewhere in the spectrum. C-Band operations are standard. Two C-Band antennas are used to eliminate the need for a diplexer, reducing system complexity, cost, and the possibility of signal crosstalk.

b. Description

The deployed payload antennas are composed of L-Band and C-Band planar arrays. Appendix D contains the calculations used to size the arrays.

(1) L-Band Planar Arrays

The construction of the planar array antennas is modeled after a European Space Agency (ESA) design [Ref. 2]. Each of the six planar array antennas

is composed of a Kevlar microsheet with rectangular copper patch radiating elements mounted on a NOMEX honeycomb substrate. NOMEX is used to provide structural rigidity and to minimize effects of thermal cycling. On the rear face of the substrate,

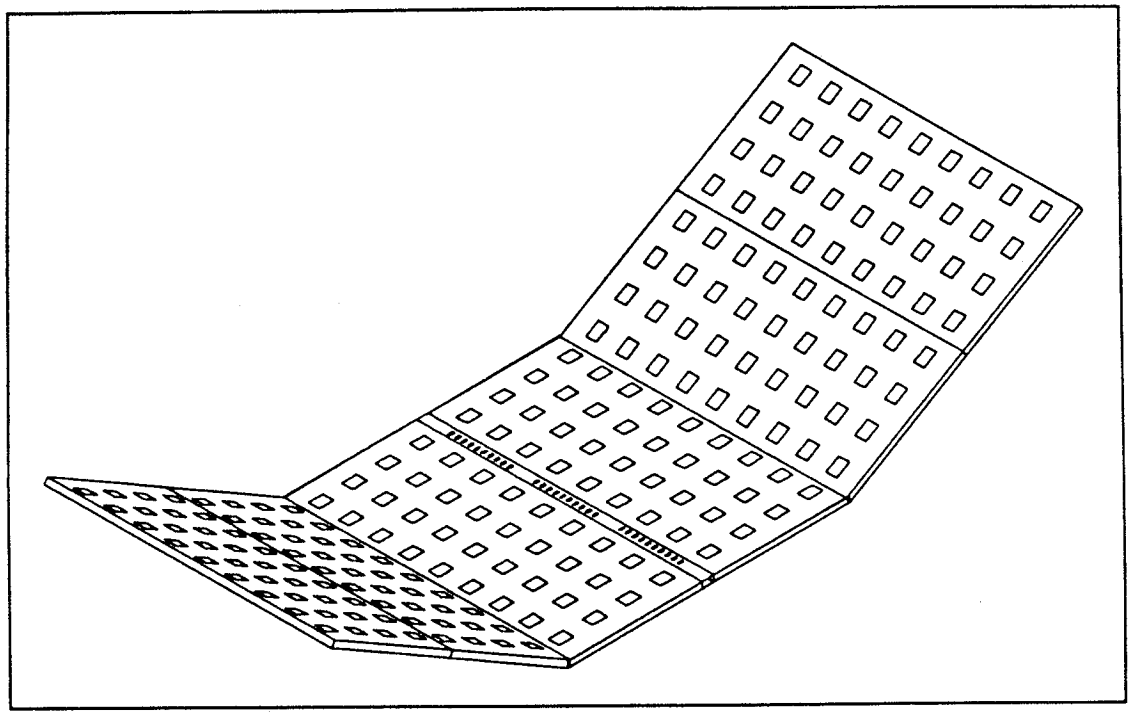

Figure VI-2 Phased Array Antenna

triplate striplines are run to connect the radiating patches to the associated Beam Forming Network (BFN). Each antenna is a 140 x 66.7 x 3.0 cm panel. Each radiating element measures 7.20 by 5.20 cm. The elements are spaced 0.55 wavelength or 10.20 cm apart. This produces a 9 x 4 matrix of copper antenna element patches for each panel, as shown in Figure VI-2. Each element radiates according to a prescribed phase distribution to both steer the elliptical beam and present a constant gain over the Earth's surface. The two center panels are fixed to the Earth face of the spacecraft, while the outer four panels deploy accordion style to an angle of 30 degrees from nadir to deconflict with the

solar arrays. The total planar array dimensions are 1.4 meters by 4.0 meters, and the long axis of the array is aligned with the spacecraft velocity vector. There is a gap of 6.6 cm between the two fixed panels to provide room for mounting the TT&C and C-Band antennas and the Earth horizon sensors. Electrical connections between antenna panels are made with coaxial conductors, as depicted in Figure VI-3.

(2) C-Band Planar Arrays

Planar array antennas were chosen over horns for the spacecraft to gateway link to achieve a greater beamwidth with less surface area. Two C-Band planar strip arrays are located on the centerline of the Earth face between the L-Band arrays.

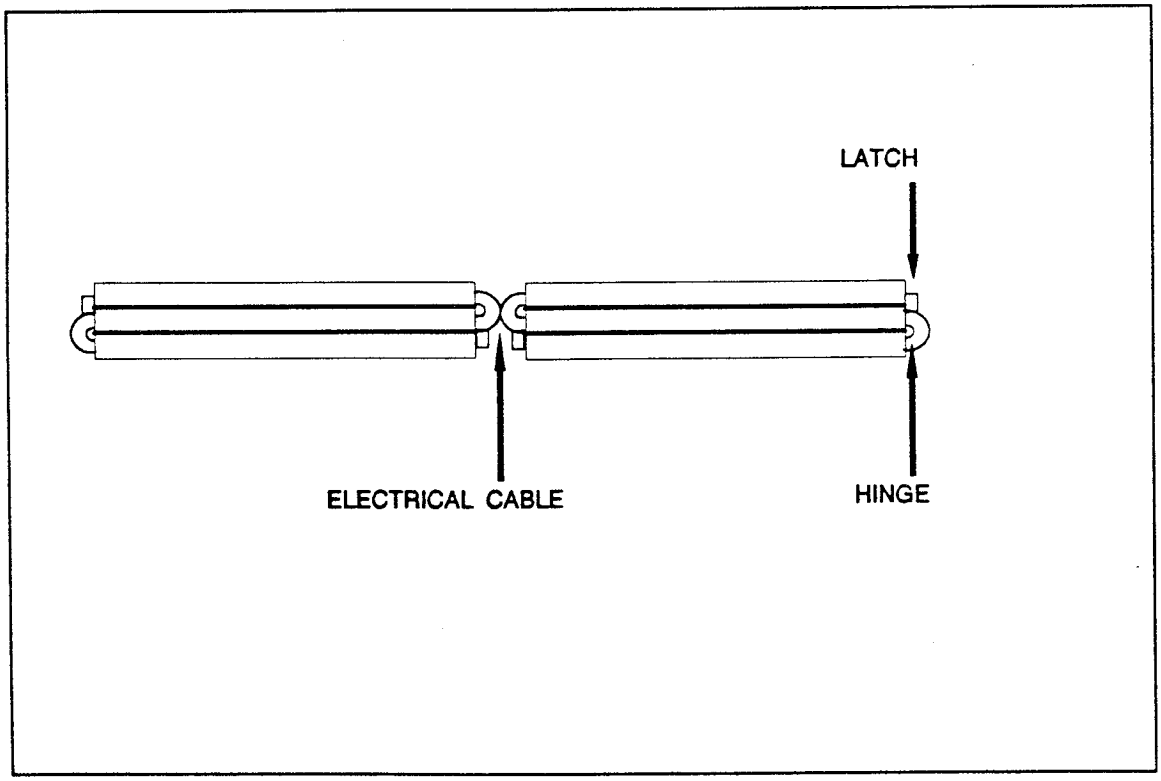

Figure VI-3 Phase Array Panel Layout

Each has ten patch elements sized for the respective midband wavelength. The distance between elements is 0.55 times the midband wavelength. The downlink antenna elements measure 2.20 cm by 1.00 cm and are separated by 3.20 cm. The uplink antenna elements measure 1.80 cm by 0.60 cm and are separated by 2.50 cm. Materials used in the C-Band arrays are the same as for the L-Band arrays.

5. Hardware Modules

a. L-C Band Transponder

The L-C Band Transponder receives signals sequentially from each of the L-Band antenna beams, filters and amplifies the signals, upconverts to the C-Band, then directs them to the C-Band transmit antenna. Synchronization is provided by the Timing and Control Unit.

b. C-L Band Transponder

The C-L Band Transponder receives signals from the C-Band receive antenna, filters and downconverts the signals to the L-Band, then amplifies the signals and routes them to the proper L-Band antenna beam. Synchronization is provided by the Timing and Control Unit.

c. Timing and Control Unit

The Timing and Control Unit is essentially a clock mechanism that provides synchronization pulses to the two transponders and to the L-Band and C-Band planar array beam forming networks. It can be reset from the ground through the TT&C system.

C. System Performance

1. Link Budget Calculations

a. Requirement

To minimize interference with other space and land based broadcasting systems, power flux-densities at the Earth's surface must be below certain thresholds. Within the C-Band, the payload power flux-density is -159 to -161 dBW/m^2 in any 4 kHz band at any angle of arrival. Within the L-Band, the power flux-density is less than -139 dBW/m^2 in any 4 kHz band for angles of arrival between 10 and 90 degrees. Links must provide the required margins for low power transmitters and receivers, namely mobile users and faded users. Minimum spacecraft elevation angle is considered 10 degrees for a successful link.

b. Description

Thorough link budget calculations have been performed by the contractor. Summary link budgets are presented in tables in Appendix D.

2. Margins

For the satellite to user link, a 1.3 dB interference margin has been budgeted. Thermal noise margins of 1.1, 2.7, and 1.2 dB are budgeted for beams 1 & 6, 2 & 5, and 3 & 4, respectively. For the satellite to gateway link, there is a 1.0 dB interference margin. Thermal noise margins are 1.0, 1.1, and 1.3 dB.

D. REFERENCES

1. Loral Cellular Systems Corporation, *GLOBALSTAR SYSTEM APPLICATION before the Federal Communications Commission*, June 3, 1991.

2. Alexander, M.J., Trumpess, C.J., Griffin, J.M., Newton, M.L., and Roederer, A., "Microstrip Patch Array For L-Band Satellite Communications," paper presented at the Fifth International Conference on Antennas and Propagation, 1987.

3. Bartolucci, G., Giannini, F., and Paoloni, C., "Beam Forming Networks for Active Antenna Systems, "*Space Communication and Broadcasting*, v. 6, 1989.

4. *The Handbook of Antenna Design*, v. 2, Peter Peregrinus Ltd., 1983.

5. Rulf, G., and Robertshaw, G.A., *Understanding Antennas for Radar, Communications, and Avionics*, Van Nostrand Reinhold Company, Inc., 1987.

6. Milligan, T.A., *Modern Antenna Design*, McGraw-Hill, Inc., 1985.

VII. TELEMETRY TRACKING AND CONTROL

A. INTRODUCTION

1. Scope

In order to maintain positive control of and monitor health and performance data from the spacecraft, a Telemetry Tracking and Control (TT&C) system is required. The TT&C system consists of two parts, a spacecraft portion and a ground portion.

a. Operational requirements

The TT&C system must be able to communicate both spacecraft commands and ephemeris data as well as telemeter subsystem health and performance data. In addition, the spacecraft portion must be capable of interpreting and processing the commands it receives on either a real time, or delayed basis. The ground based portion of the system must not only track and communicate with the spacecraft, but it must also provide ephemeris data to the gateway network via a Satellite Operation Control Center (SOCC).

b. Functional requirements

(1) Spacecraft

The spacecraft package must provide a means for polling individual spacecraft systems for health and performance data and storing that data until it can be encoded and transmitted to one of two ground based tracking stations. Received

command data must be decoded and processed by the TT&C system. In addition, the system must be able to store commands for execution at a later time in order to be able to provide for autonomous operation during those times when the spacecraft is out of the field of view of ground stations. In order to insure that valid data are passed between the spacecraft and ground stations, a low bit error rate (BER) must be maintained.

(2) TT&C stations

Tracking stations must be provided to facilitate communication to and from the spacecraft. In addition, the tracking stations will provide ephemeris data to the SOCC. Due to weight, size, and power constraints on the spacecraft, the tracking stations' equipment must provide most of the system gain required. The tracking station must also be able to track up to three spacecraft simultaneously.

c. Artificialities

Under normal circumstances, the thermal performance of the electrical components could be accurately modeled using sophisticated software. Due to lack of access to this type of software, the thermal performance could only be estimated. This was done by taking into account the operating temperature range of standard electronic devices such as transistors and integrated circuits. The low end operating temperature was set by considering that receivers are more adversely affected by extreme cold than by heat. This is due to the fact that while high temperatures degrade receiver noise performance, extreme cold causes physical damage to circuit boards and circuit connections. A typical receiver has a low end operating temperature of -40 degrees C.

The high end operating temperature is governed by transmitter and microprocessor characteristics. Typically, these devices generate a relatively large amount of heat. Typical high end operating temperatures are around 84 to 90 degrees C. The thermal radiation was estimated by extrapolating from similar designs.

The size and weight of the TT&C package were also estimated from similar system designs. Box sizes were picked which were not only reasonable but also that allowed for future growth and increased sophistication.

2. Method

The design for this relatively simple TT&C package was arrived at by extrapolating from similar spacecraft designs and incorporating the latest proven technology. The basic design is a near standard, proven, TT&C design.

a. Computer software and system models

The antenna design for the spacecraft antennas was arrived at using Mathcad 3.0 to evaluate the theoretical performance of various antenna configurations.

The antenna design was optimized in an iterative process of trial and error and the results are presented in Appendix E.

b. Alternatives

A design which incorporated the spacecraft transmit/receive functions into the payload's C-band feeder signal was considered. This approach was abandoned because it would reduce the volume of revenue generating traffic that the payload could handle.

A spread spectrum TT&C signal format was also considered. A spread spectrum signal would have not only reduced the probability of interference from other sources, but it would also have simplified signal encryption. The spread spectrum format was abandoned for two reasons. One, the bandwidth required far exceeds the bandwidth necessary for the low data rate signal and two, the bandwidth required exceeds the bandwidth of the microstrip antenna.

c. Tradeoffs

The antenna design for the spacecraft TT&C package could have been accomplished by using monopole antennas vice microstrip arrays. Characteristics of several different types of antennas, including microstrip antennas, are discussed in references 1 and 2. A monopole antenna itself is simpler than a microstrip array and due to the small size of the antennas, the lighter weight of the microstrip array was not a consideration. For this application, the monopole and microstrip antennas give similar performance. Figure VII-1 shows how a basic patch is configured into an array.

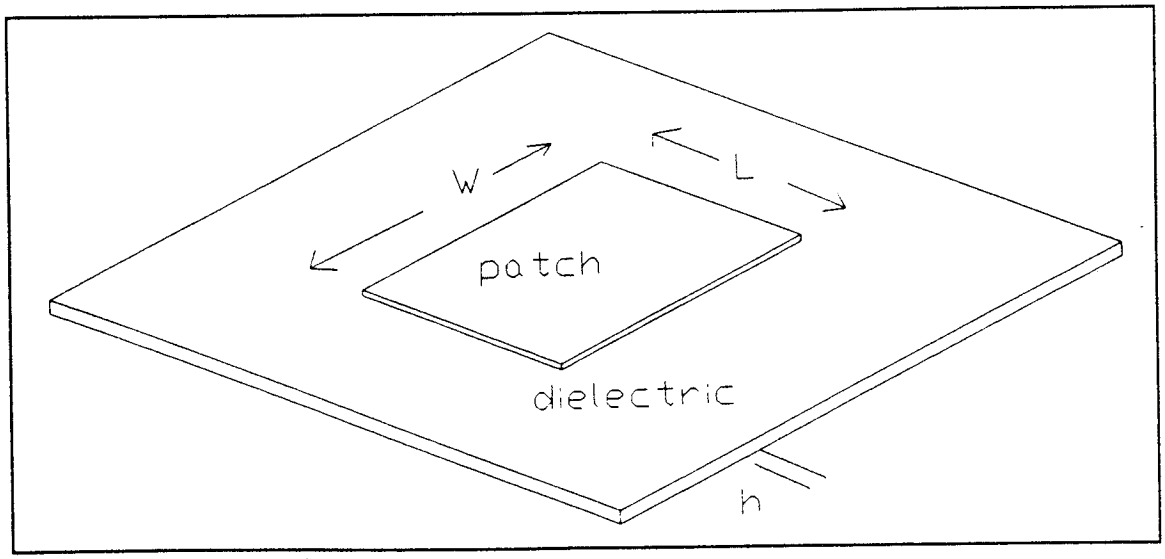

Figure VII-1 Microstrip Patch Array

A microstrip array was chosen over the monopole because the low profile microstrip adheres directly to the spacecraft skin and does not present an appendage that could be damaged during spacecraft handling and deployment. Additionally, due to the configuration of the payload antenna, a planar array, a microstrip TT&C antenna fits conveniently in the space available on the earth face of the spacecraft.

B. SYSTEM OVERVIEW

The spacecraft portion of the digital TT&C system receives and executes commands from the ground and downlinks telemetry data from spacecraft systems. System status information is obtained via a digital databus controlled by the system's command processor. In addition, the spacecraft package provides for limited autonomous operation by storing command data for execution at a specified time.

The ground based portion consists of two TT&C stations located in the continental United States that perform tracking and relay functions. The ground stations receive telemetry data from the spacecraft and relay it along with observed ephemeris data to the Satellite Operational Control Center (SOCC). The SOCC processes attitude control data and originates the appropriate attitude control and spacecraft system commands. The commands are then sent to the TT&C stations via land line to be transmitted to the spacecraft. In addition to issuing spacecraft commands, the SOCC also distributes ephemeris data to the gateway network.

In order to efficiently utilize the allocated frequencies, the command uplink signal and telemetry downlink signal are located at the edges of the C-band feeder frequency

band, at 6.5 GHz and 5.2 GHz respectively. Due to the low volume of data that needs to be exchanged, a data rate of 1 kbits/s for the telemetry link and 500 bits/s for the command link is sufficient. This requires a bandwidth of 500 Hz and 250 Hz respectively. The flow of information between the SOCC and a spacecraft is illustrated in figure VII-2.

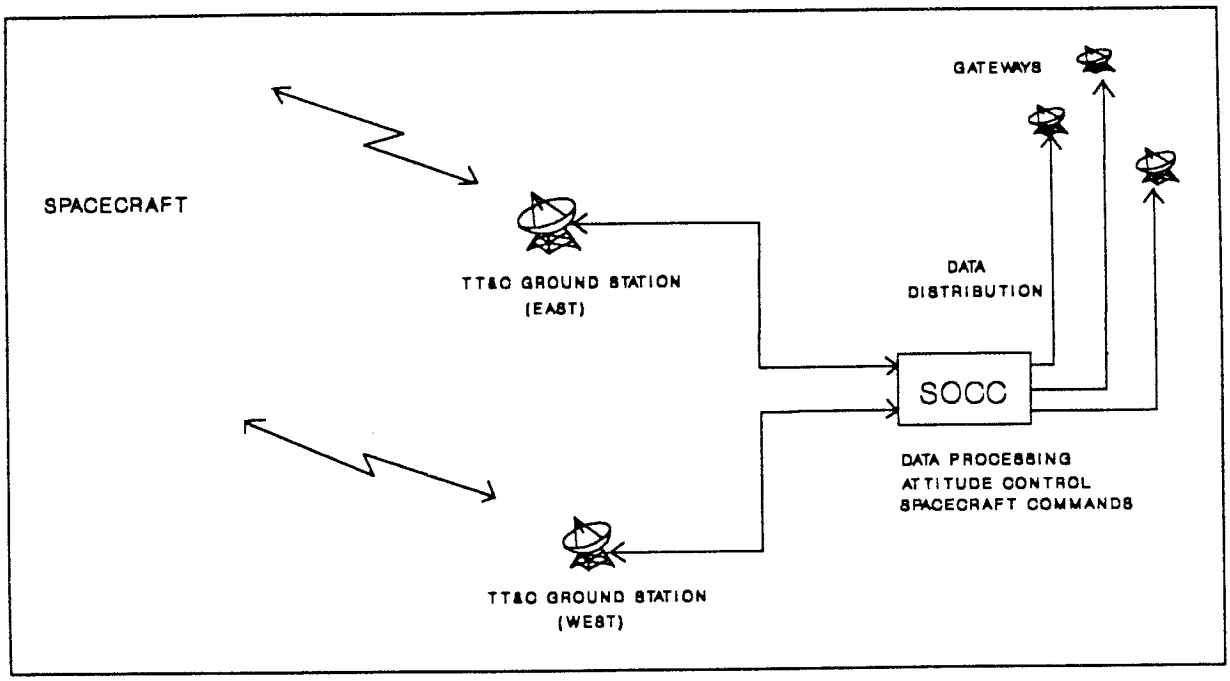

Figure VII-2 TT&C Connectivity

C. COMPONENT DESCRIPTION

The spacecraft portion of the TT&C package is completely independent of the payload. The spacecraft TT&C package consists of two separate Remote Tracking Units (RTU) and two Remote Command Units (RCU). This double redundancy design is

incorporated to enhance reliability. The RTUs provide encoding, decoding, modulation, demodulation, and transmit/receive functions. The RCU interprets and performs commands received via uplink , acts as the databus controller, and stores subsystem data for downlink.

The TT&C station equipment consists primarily of tracking antennas, transmitters and receivers.

1. Mass and power budgets.

The mass and power budgets for the TT&C system are shown in Table VII.1 along with size specifications and thermal radiation parameters.

Table VII.1 Mass and Power Budget

Subsystem	Mass (kg)	Power (Watts)	Thermal dissipation (Watts)	Size (cm)
RTU	7.4	7.2	25	45.7x45.7 x15.2
RCU	4.6	4.8	25	45.7x45.7 x15.2

2. Remote Tracking Unit (RTU)

Each RTU is composed of a receiver, a transmitter, a coding section, and antennas. Figure VII-3 shows a block diagram of a single RTU. There are two antenna

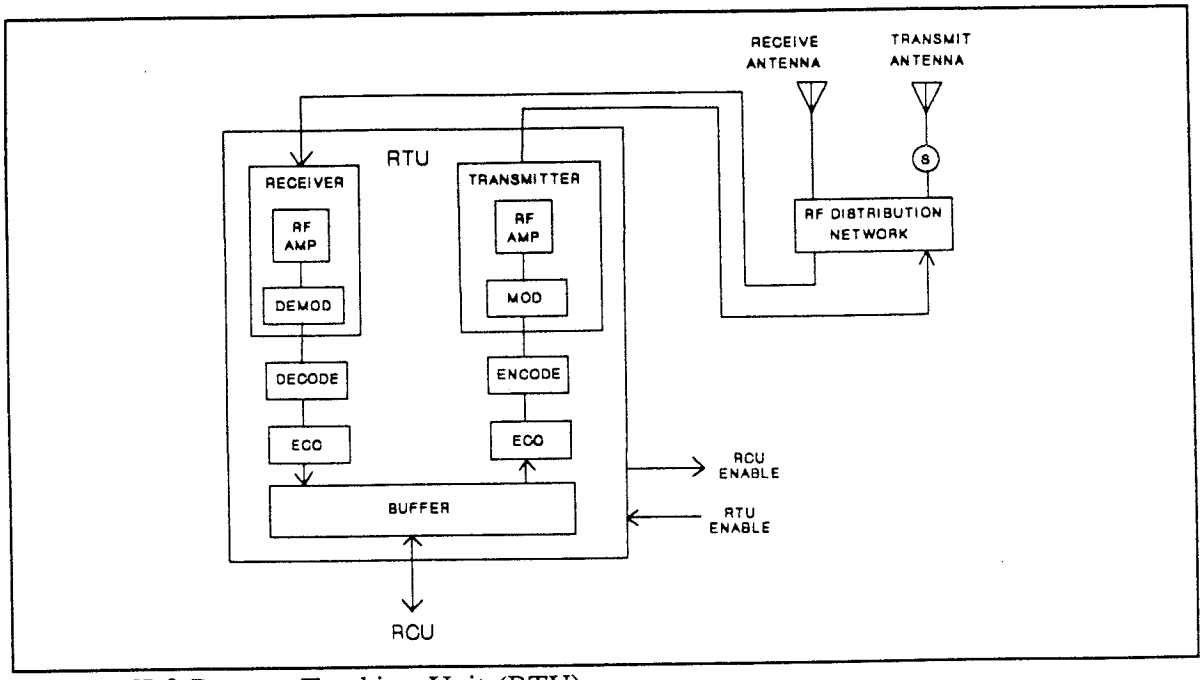

Figure VII-3 Remote Tracking Unit (RTU)

pairs which are connected to each RTU via an RF distribution network and a failsafe switch. The switch serves to allow only one transmit antenna to be active at a time.

During spacecraft deployment, TT&C is accomplished primarily via the anti-earth antenna pair. Successful deployment of the payload antenna completely unmasks the earth-face antenna pair giving them a clear field of view. Once a successful link has been established and the operation of each RTU has been verified, one RTU transmitter is placed in standby and the transmit antenna switch is positioned to enable the earth-face

transmit antenna. Both RTU receivers continue to function, the second one acting as a failsafe.

a. Transmitters and Receivers

The transmitters and receivers provide the modulation and demodulation for the data signal. Pulse Code Modulation (PCM) is used as it is particularly suited to digital communication. A link analysis for the TT&C system as well as a summary of system specifications are presented in Appendix E.

b. Data encryption

In addition to error correction coding, the data signal is encrypted just before modulation and deciphered just after demodulation by a separate coding section. This is to prevent unauthorized or inadvertent communication with the spacecraft. Error detection and correction is accomplished via Hamming code.

c. Antennas

The TT&C antennas are composed of microstrip antenna arrays. Due to the limited bandwidth of the microstrip antennas (12%-14% of band) and the wide separation between uplink and downlink frequencies (1.3 MHz), a separate array is required for the uplink and downlink signals. To ensure the ability to communicate with the spacecraft in unusual attitudes, there are two antenna pairs, one located on the earth face and on the anti-earth face. The antennas are fed by each RTU through an RF distribution network such that the antennas are effectively connected in parallel with the RTUs.

Microstrip antennas provide the advantages of low profile, ease of fabrication, and ease of installation. The low data rates of the telemetry and command signals are easily accommodated within the narrow bandwidth and low gain characteristics provided by the microstrip antennas. Microstrip antenna design is discussed in detail in reference 3. The required gain is achievable by using a linear array of microstrip patches. Reference 4 discusses array fabrication and contains performance comparisons of several microstrip array designs. The design details of the TT&C antennas are presented in Appendix E.

3. Remote Command Units (RCU)

The Remote Command Units consist of two independently addressable microprocessors along with associated memory and timing circuits. Figure VII-4 shows

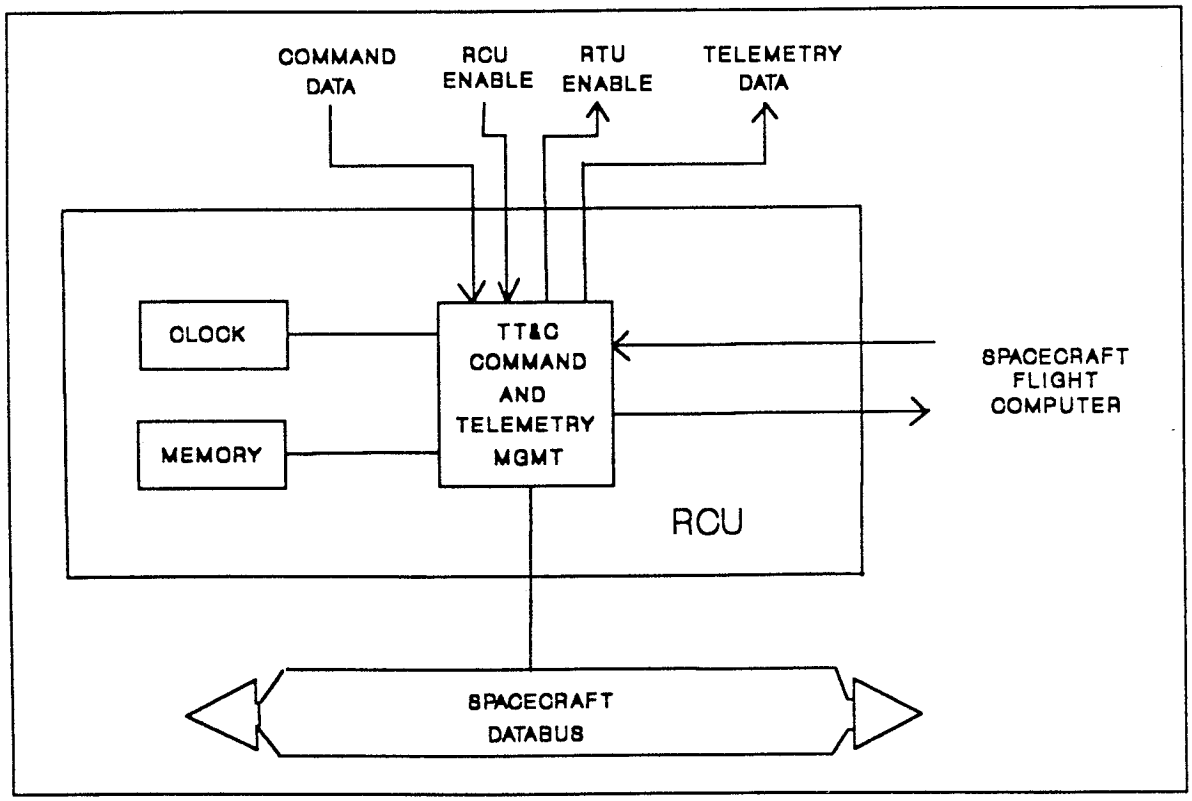

Figure VII-4 Remote Control Unit (RCU)

a block diagram of one RCU. The RCUs receive and interpret decoded commands from the RTUs. Only one RCU is on line at a time, the other remains in a monitor mode and performs as a failsafe system. The active RCU acts as the databus controller as it interacts with other systems, issuing commands and collecting data for downlink.

When command data is received via uplink, those commands not requiring immediate action are stored in a command buffer within each RCU. Each RCU has memory set aside for the storage of commands to be executed at a specified time. Commands are retrieved and executed by the active RCU from its command buffer until either it receives a command that requires immediate action or it receives a new list of commands. Health and performance data is collected by the RCUs by periodically polling the spacecraft systems. The data are then stored in RAM until they can be downlinked.

4. Ground equipment

The ground equipment consists of three tracking antennas and associated receiver/transmitters at each tracking station. This design allows each TT&C station to communicate with up to three spacecraft simultaneously (there will be a maximum of three satellites in view of a tracking station at any one time). Because the ground station must supply most of the system gain (approximately 40 dB), the tracking antennas are 2 meters in diameter. Figure VII-5 depicts ground equipment configuration.

Two ground stations, one located in southern California and one located on the mid Atlantic coast, are connected to the SOCC via direct land line. During any contiguous 72 hour period each spacecraft will be out of contact with ground station for two 10.5 hour periods. Except for these periods, the maximum time a spacecraft will be

out of view of a TT&C station is approximately 1.5 hours and it will remain in view for

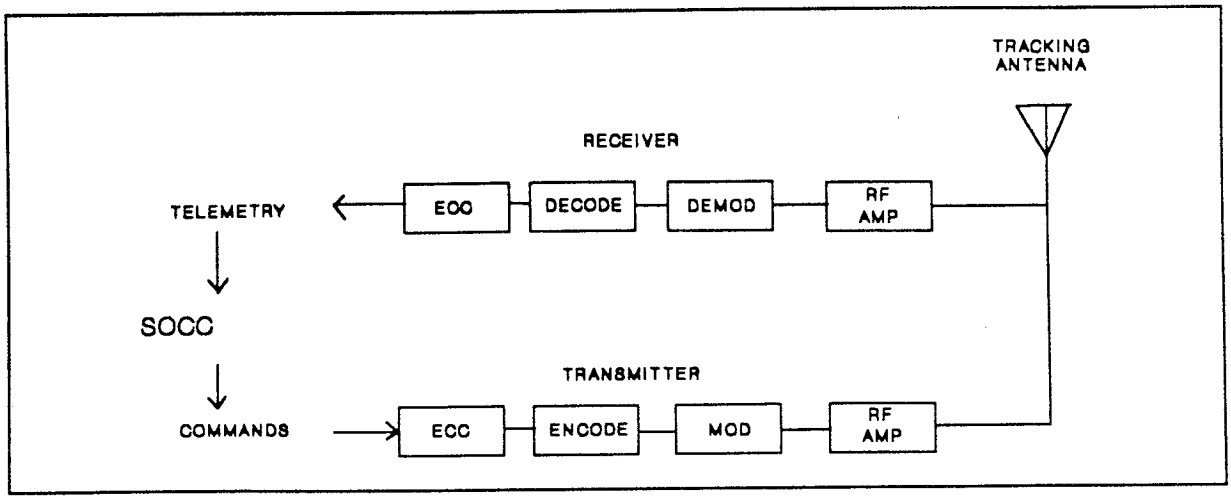

Figure VII-5 Ground Equipment

approximately 20 min. Table II.3 presented rise and set times for one spacecraft during a representative 72 hour orbital period, as seen by the two ground stations.

This TT&C system is similar to ones described in reference 5 in that the spacecraft must provide some degree of autonomous operation to avoid the high operating costs of maintaining 24 hour contact. Since the spacecraft TT&C package has the ability to store and execute a pre-loaded list of commands, continuous TT&C coverage for the spacecraft is not required. However, if it were desired, it could be attained by providing additional ground stations located through out the world.

5. Impact on other systems

a. Structures

In order to minimize line loss between the TT&C antennas and the RTU receivers, the RTUs are located within the spacecraft structure near the antennas.

The microstrip antennas are fabricated using standard printed circuit board etching techniques. The antenna arrays are mounted directly to the spacecraft skin with a through hull fitting to allow electrical connection with the RF distribution network.

b. Thermal and Electrical

The amount of heat radiated from and power consumed by the TT&C system remains relatively constant during all phases of the mission following spacecraft deployment. This is due to the fact that most of the TT&C activity is concerned with RCU functions which continue even when the spacecraft is not in view of a tracking station.

D. SUB-SYSTEM INTEGRATION

The TT&C RTUs are connected to the earth face and anti-earth face antennas via an RF distribution network and a transmitter antenna switch. The RTUs serve as the interface between the ground station and the RCUs. The RCUs communicate with and control the spacecraft systems via the spacecraft data bus.

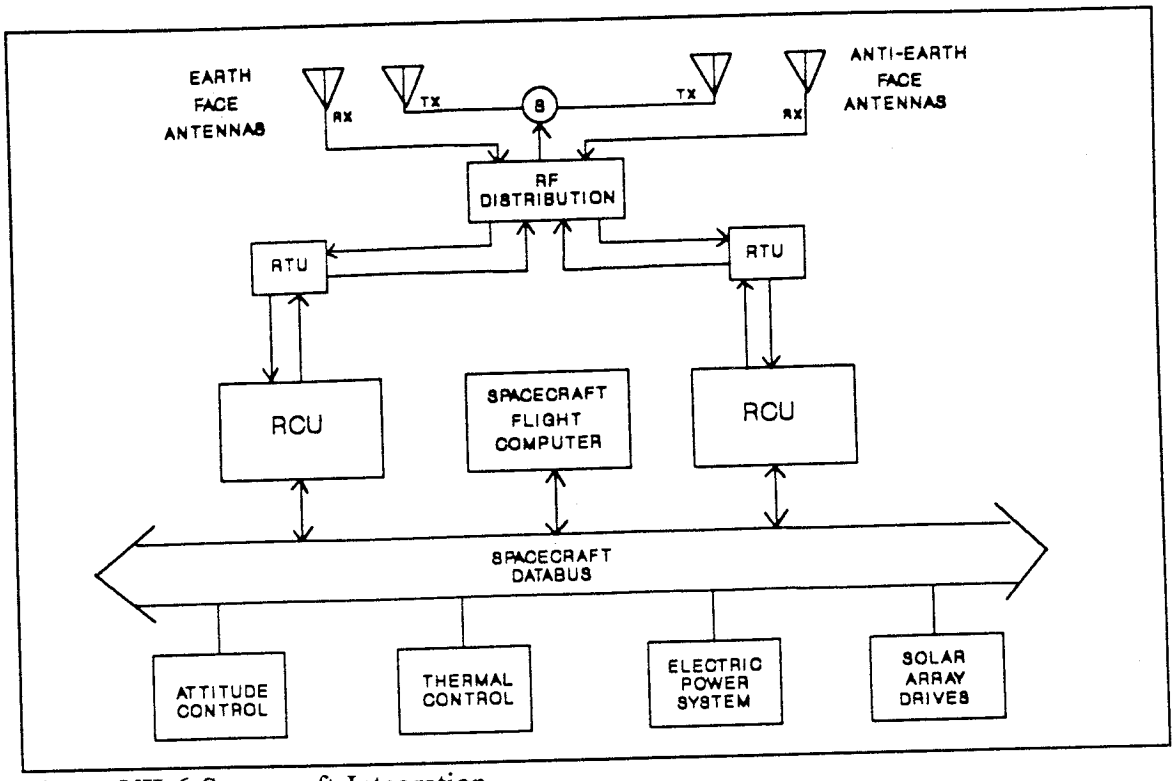

Figure VII-6 Spacecraft Integration

E. SYSTEM INTEGRATION

1. Spacecraft

The TT&C system interfaces with other systems via the spacecraft data bus. Inputs to the data bus are attitude control sensor information, electrical power system status, and thermal control sensor inputs. The RCUs and spacecraft databus were modeled after the standard digital satellite databus discussed in reference. Figure VII-6 diagrams the overall TT&C system configuration.

2. Ground Stations

The TT&C stations serve as the interface between the SOCC and the spacecraft. Attitude control sensor and spacecraft system status information is downlinked from the spacecraft to the TT&C station. These data are then relayed to the SOCC, via direct land line for processing. Attitude control and other system commands are generated at the SOCC and then transmitted to the TT&C stations where the information is uplinked to the spacecraft.

F. SPACECRAFT INTEGRATION

The TT&C system integrates the spacecraft subsystems with the ground based command and control facility. This allows complete control of the spacecraft from the ground yet at the same time, the spacecraft TT&C package allows a limited degree of autonomy for those times during which the vehicle is not in the field of view of a TT&C station.

G. REFERENCES

(1) C.A. Balanis, Antenna Theory, Analysis and Design, John Wiley & Sons, New York, 1982.

(2) John D. Kraus and Kieth R. Carver, Electromagnetics, McGraw Hill, New York, 1973.

(3) I.J. Bahi and P. Bhartia, Microstrip Antennas, Artech House, Inc., 1980.

(4) John Huang, Microstrip Antenna Developments at JPL, IEEE Antennas and Propagation Magazine, Vol. 33, No. 3, June 1991.

(5) Richard D. Carper and William H. Stallings III, CCSDS Telemetry Systems, Experience at the Goddard Space Flight Center, IEEE Network Magazine, Sept. 1990.

(6) T. Spinney, Y. Hassan, and M. Herte, Standard Satellite Databus Initiative, 1989 IEEE Aerospace Application Conference Digest.

VIII. ELECTRIC POWER SYSTEM DESIGN

A. INTRODUCTION

1. Operational Requirements

The satellite Electrical Power System (EPS) relies on photovoltaics for power generation and batteries for power storage. Space solar power systems using direct energy conversion must be capable of power generation, conditioning, distribution and storage. Communications payload power requirements will vary according to geographic population density, with user demand dictating peak power loading times. The following factors were considered in determining power requirements:

- 90% of the global population is in the Northern Hemisphere.
- China, India and the USSR have the largest populations but are not expected to provide significant customer market due to economic limitations.
- The United States, fourth largest country, has a population of 250 million. Distribution :
  - 42% in the Boston–N.Y.–Washington, DC triangle.
  - 10% on the west coast.
  - 10% in the midwest.
- 80% of Canada's population (27 million) lives within 100 miles of the U.S. border.
- Western Europe is expected to provide the bulk of the European customer market for the remainder of this century due to economic failures in Eastern Europe. Particularly: France (population 58 million), U.K. (58 million), "west"-Germany (61 million).
- Japan , 122 million, is considered the most significant Asian customer region.

For purposes of modeling payload power requirements, regions were considered as primary, secondary, or tertiary power demand areas according to their potential for customer marketing. Primary regions are the U.S.A., Japan, and western Europe. Secondary regions such as S.Korea, Hong Kong, U.A.E., etc. are expected to require a reduced, but measureable, power demand. Tertiary regions were modeled as having no population density, or no significant marketing potential.

Maximum payload power demand is expected over the northeastern U.S. seaboard at 1800 local time. This loading will experience seasonal variation, but is not expected to exceed 800 watts for 16 minutes. Additional spacecraft housekeeping of 200 watts indicated that the EPS must be capable of providing 850 watts for 20 minutes. This 255 W-hour requirement, illuminated or eclipse, dictated the actual EPS sizing. Satellite orbital pattern repeats a similar ground track once every 72 hours.

2. Functional Requirements

Spacecraft design life of 5 years at an altitude of 1389 km requires a power storage system capable of 24,000 charge/discharge cycles. Three-axis stabilization at an inclination of 52 degrees requires that the solar arrays be two-axis sun tracking. The arrays must withstand 5 years of degradation from radiation, thermal cycling, micrometeriods, and atomic oxygen (AO) attack. Variations in payload power will be experienced, parameters considered as worst case scenario for power demand were:

- peak loading occurs during eclipse;
- followed by minimal eclipse loading over Europe with insufficent time to fully recharge the battery before the next eclipse cycle.

3. Restrictions and Artificialities

The primary restriction in EPS design was the use of in-flight hardware. While this greatly simplified the choice of technologies to meet mission demands, it imposed some artificiality in excluding the following equipment:

- Ni/H2 common pressure vessel batteries have been extensively investigated for several years and would provide considerable mass savings for a LEO satellite.
- GaAs/Ge photovoltaics were considered based on 1991 costs for what would be a bulk buy in 3+ years. Adequately predicting future cost competetiveness of these cells is beyond the scope of this report, but it is expected that the economics of GaAs will continue to improve significantly for the remainder of this decade.

B. METHOD

1. Software / Method / Model Used

Modeling of solar array environmental degradation was conducted according to the procedures outlined in references 1–6. Results of array sizing calclations are presented in Appendix F. Battery sizing was modeled on the procedures of references 11–15. Solar array construction and specifications were modeled on the cells used on the EURECA satellite, as discusseed in references 10–14. Methods outlined in references 19–24 were used to model atomic oxygen attack. The solar array deployment mechanism design was modeled from references 24–28. Final array size and battery nameplate capacity were the result of iterative calculations to minimize final EPS mass and cost.

2. Alternatives Explored

a. Battery

Table VIII.1 lists the power to mass relationships of the five types of batteries investigated for this mission. The high number of charge/discharge cycles

Table VIII.1 Battery Power to Mass Ratios

System	EOD(V)	W-hr/kg
Ni-Cd	1.21	23-30
Ni-H2 (IPV)	1.25	25-40
Ni-H2 (CPV)	2.25	45-60
Ag-Zn	1.50	27-35
Na-S	1.75	140-210

required eliminated the sodium sulfur and silver/zinc batteries due an inherently short "wet" life, even with careful reconditioning. Nickle-cadmium was then considered for their proven reliability, low cost and minimum volume. As indicated in Table VIII.1, Ni/Cd depth of discharge for 24,000 cycle would be safely limited to 20%. This was then compared to the more expensive, and slighty larger, Ni/H2 at a DOD of 40% using Figure VIII-1. The reasons for choosing a Ni/H2 battery over Ni/Cd were:

- greater % DoD in LEO.
- less susceptible to memory effect.
- higher discharge voltage.
- higher charge voltage.
- requirement for occasional discharge to 60%.
- greater cell energy density.

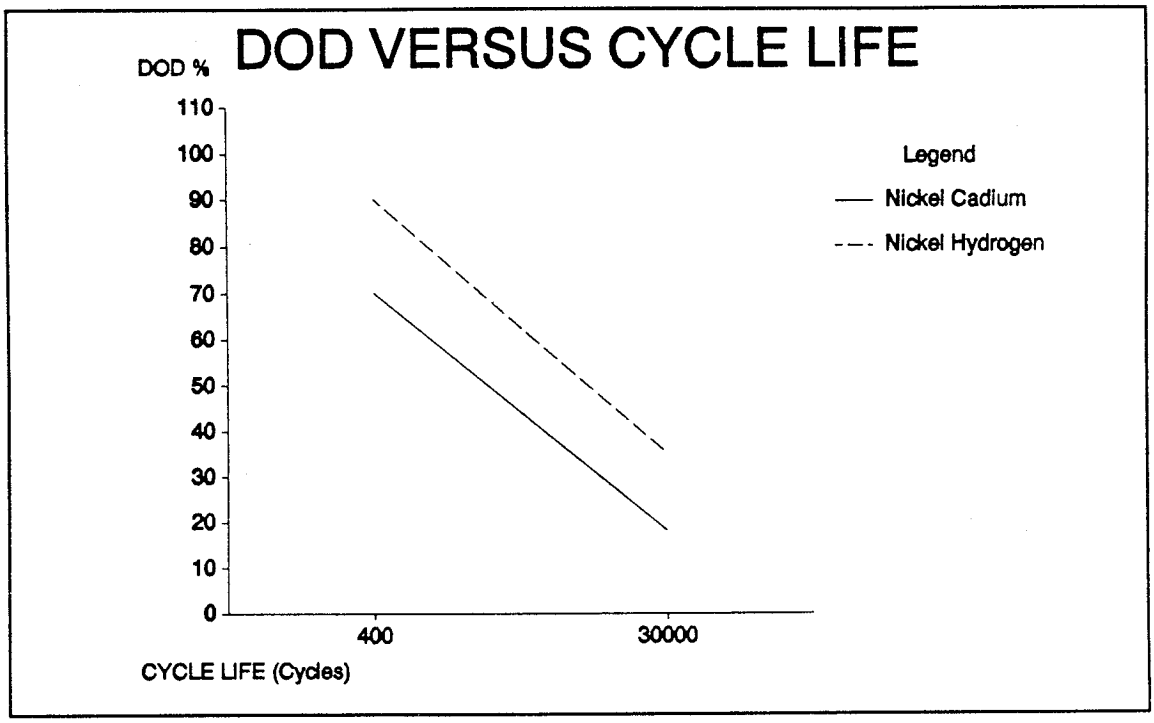

Figure VIII-1 DOD vs. Lifecycle

b. Solar Cells

Orbital inclination and altitude make cell resistance to radiation degradation a significant factor in array sizing. In/P cell technology is not viable due to lack of demonstrated performance and extremely high cost. GaAs/Ga was not considered due to high mechanical failure during array assembly. GaAs/Ge was seriously considered, but rejected. ASEC 24 Si BSF/R cells were selected for their low cost, demonstrated performance, efficiency and environmental degradation resistance.

c. Solar Array

The Lockheed flexible blanket array was first considered for its weight, stowed compactness, and cost. This design is not acceptable for this mission due to AO

degradation of the kapton substrate. While Lockheed has found a solution to this problem by incorporating a glass-fiber weave, use of the overall design has not yet been demonstrated in LEO. Also, the low frequency dynamics inherent to the flexible array are beyond the scope of this project.

Once a two-wing, rigid flat panel design was accepted, array sun tracking was investigated to minimize the complexity involved with the additional array drive and power transfer assembly that is required for each degree-of-freedom available to the arrays. An attempt was made to cant the arrays, 52 degrees, to compensate for the orbit inclination, and thus have only one axis tracking. This alernative is acceptable only in sun-synchronous orbits, or if the attitude is active-yaw controlled. The arrays must therefore be capable of two-axis sun tracking to compensate for spacecraft bus rotation during orbit since payload requirements restrict attitude rotation about the yaw axis. While no LEO spacecraft currently employs two-axis solar array sun-tracking, this configuration will soon be implemented on commercial LEO spacecraft (LMSC's F-SAT), and is considered feasible.

3. Tradeoffs Performed

Variation in power loading with ground track results in long periods of non-peak demand and allows great flexibility in EPS design. Since over-design of the EPS is a primary consideration, a careful balance between solar array sizing and battery size was sought in order to minimize cost and mass. The objective of minimizing solar array size is of foremost importance, since traditional procedures of designing for maximum

power required at end-of-life would lead to excessive overdesign in this case due to infrequent use.

C. GENERAL ELECTRIC POWER SYSTEM DESCRIPTION

The solar array was downsized to a minimum nominal power requirement at EOL of 600 watts. The battery was then sized to provide peak power during eclipse at a DoD of 60%, with a nominal DOD of 40%. This allows sufficient battery capacity to augment power from the arrays when loading exceeds photovoltaic power available. A nickel/hydrogen battery of 'nameplate' 40 A-hr cells was determined to be sufficient to meets these demands. A battery configuration of 22 cells would have met the requirement of a minimum bus discharge voltage of 28 volts. 23 cells were selected to take advantage of the higher charge voltage available from the arrays when over regions of tertiary loading.

D. INDIVIDUAL COMPONENT DESCRIPTION

1. Solar Array Design

Spacecraft End-Of-Life (EOL) power requirement of 600 watts resulted in 40 strings of 95 cells in series to provide power at 30 volts during any portion of sunlit phase. Five of the series strings are connected in parallel to form a redundant group. The array strings are routed to the panel connector and connected in parallel via connecting boards in order to generate the required, independent electrical connections.

Flat solar cell shunt diodes are provided for every 10 cells in series to prevent damage to the cells during shadowing or current generation mismatch.

Undefined shadowing can lead to unacceptable high hot spot temperatures due to electrical power consumption during shadowing when the solar cell has to absorb energy rather than produce it. The bypass diodes limit the power consumption in the shaded cells by reducing the maximum possible cell reverse operation voltage. The shunt diodes which protect each shunt interval of 3 rows of 12 cells are placed on the back of the panel in the unrestrictred areas to minimize the effect on the available sun irradiated area and thus optimize cell packing factor. Each diode is bonded to the Ag connector bars for heat dissipation when conductive. All exposed, silver contacts are coated with Kapton to minimize loss to AO. Kapton F layers are also bonded to the shunt diode matrices.

a. Solar Cell Coverglass

The main objective in coverglass selection was to minimize the mass to power ratio for the desired degree of cell environmental protection. The Connector Integrated solar Cell (CIC), a solar cell equipped with an interconnector and 100% covered by a coverglass, was selected. CMX coverglass of 150 micron thickness is used to optimize mass for this mission altitude and duration. The cerium doped microsheet limits the risk of damage of interconnector stress relief loop by handling and thus reduces assembly costs. Coverglass characteriastics are presented in Table VIII.2.

Table VIII.2 Solar Cell Coverglass

CMX borosilicate w/5% CeO2	150 microns
Adhesive DC-93500	75 microns
Anitreflective layer	MgF2
CIC absorbtivity (unloaded)	0.75
CIC emissivity (hemispher)	0.83

b. Solar Cells

Selection of 10 ohm-cm, BSFR silicon, 2 cm by 4 cm cells of 200 micron thickness was determined to optimize cost and mass to power ratio. Radiation degradation is the primary loss in cell efficiency. Thermal cycling fatigue is of significance, 24,000 eclipses for this mission, and has different effects on cell interconnections and welds.

Stress on solar cell interconnectors is imposed by the thermal movement of the panel structure leading to relative movement of adjacent cells, causing cell to cell gap variation and thus cyclic stressing of the interconnector stress relief loop. These gap variations can be tolerated by etching a mesh pattern into the stress relief loop, and increasing:

- the cell gap in series direction to 1.2 mm;
- the stress relief loop radii to 0.2 mm;
- interconnector loop beyond the coverglass to create large stress compensating legs.

The stress induced to welding joints on solar cell n- and p-contacts are volume stresses resulting varying material expansion coefficients within a weld. Stresses will be minimized by an adequate thermal match, and by minimizing mass in weld thickness and area. Solar cell construction, depicted in Figure VIII-2, is detailed in Table VIII.3. Solar cell degradation over the five year mission life is presented in Table VIII.4.

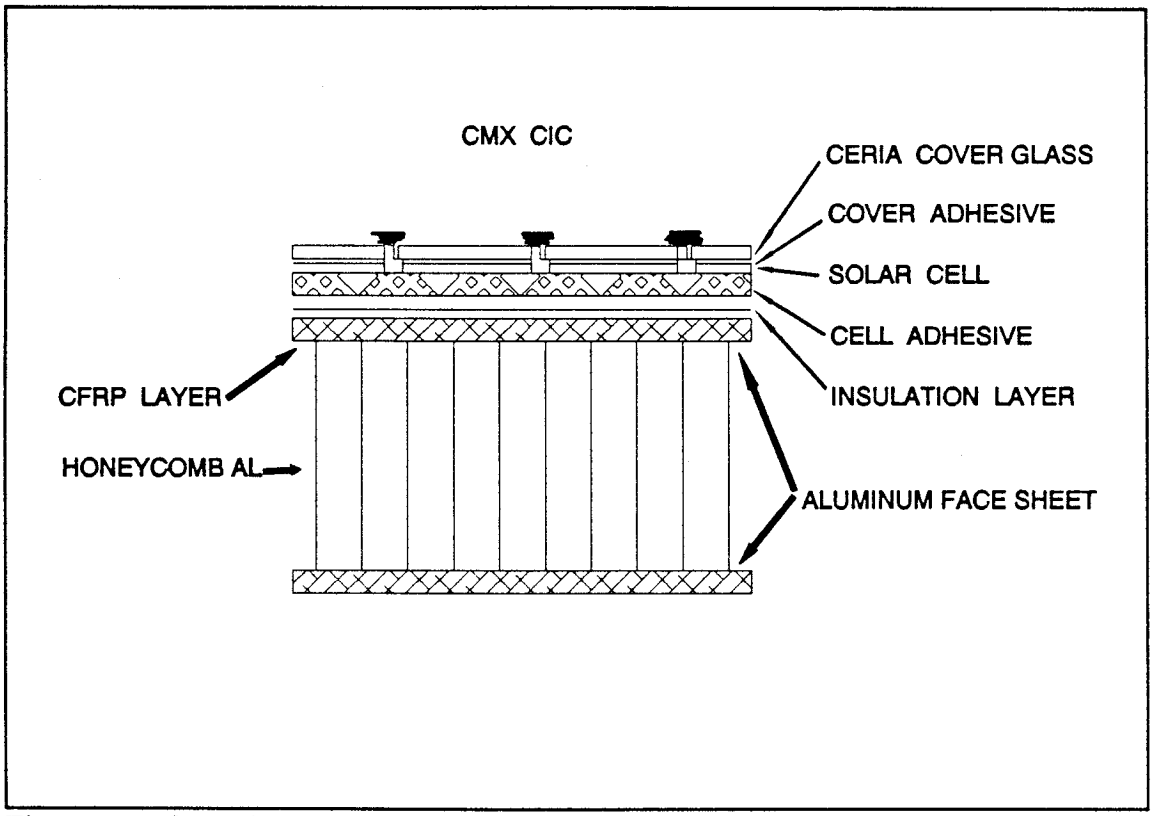

Figure VIII-2 Solar Cell

Temperature considerations for the solar arrays dictate that EOL performance be controlled by individual cell maximum power output at exposed temperature. Therefore, cell power is restricted to environmental operating temperatures. Thermal parameters are listed in Table VIII.5.

Table VIII.3 Solar Cell Structure

Cell: 200 micron Si (10 ohm-cm)
Contacts: Ti/ Pd/ Ag
Back surface reflector: Al
Back surface field: p+ boron
Dimensions: 2.00 x 4.00 cm
Adhesive: RTV-142 0.1 cm

Table VIII.4 Solar Cell Parameters

Solar Cell Parameters	BOL	EOL
Cell power (mW/cm^2)	19.2	13.0
Voc (V)	.610	.495
Vmp (V)	.500	.400
Isc (A)	.435	.350
Imp (A)	.400	.330
Pmax (mW)	160	104
Operating Temp (°C)	64.0	64.0
Radiation loss (%)	N/A	30
Transmission loss (%)	N/A	2.0
Environmental loss (%)	N/A	4.1

2. Solar Array Configuration

The solar array, as shown in figure VIII-3, consists of two fully interchangeable wings of four panels each that fold for stowage during launch phase. Each wing has three 120 x 80 cm panels and a fourth 120 x 140 cm panel totaling 3.57 square meters of solar array area. The rigid flat panels are mounted on honeycomb

Table VIII.5 Temperature Variation

Temperature variation	(%/°C)
Voc	-0.370
Isc	0.000
Vl	-0.443
Pmax	-0.460
Equivalent 1Mev fluence	(e-/cm^2)
5 years Imp, Isc	9.67 E14
5 years Vmp, Voc	1.475 E15

aluminum as specified in Table VIII.6. Panel thickness of 22 mm, with edges reinforced by aluminum square tubes, was chosen to provide adequate stiffness characteristics. On the panel backside a Kapton/ITO/silicon paint is bonded for protection against charging and atomic oxygen erosion.

Table VIII.6 Solar Array Components

Solar Array Component	Thickness
Insulation (Glasfibre/Teflon/Kapton/Tefl)	85 microns (35/12.5/25/12.5)
CFRP layer (2)	60 microns
Aluminum facesheets (2)	130 microns
Honeycomb Aluminum	2.20 cm
Kapton/ITO/Si base paint	0.10 cm

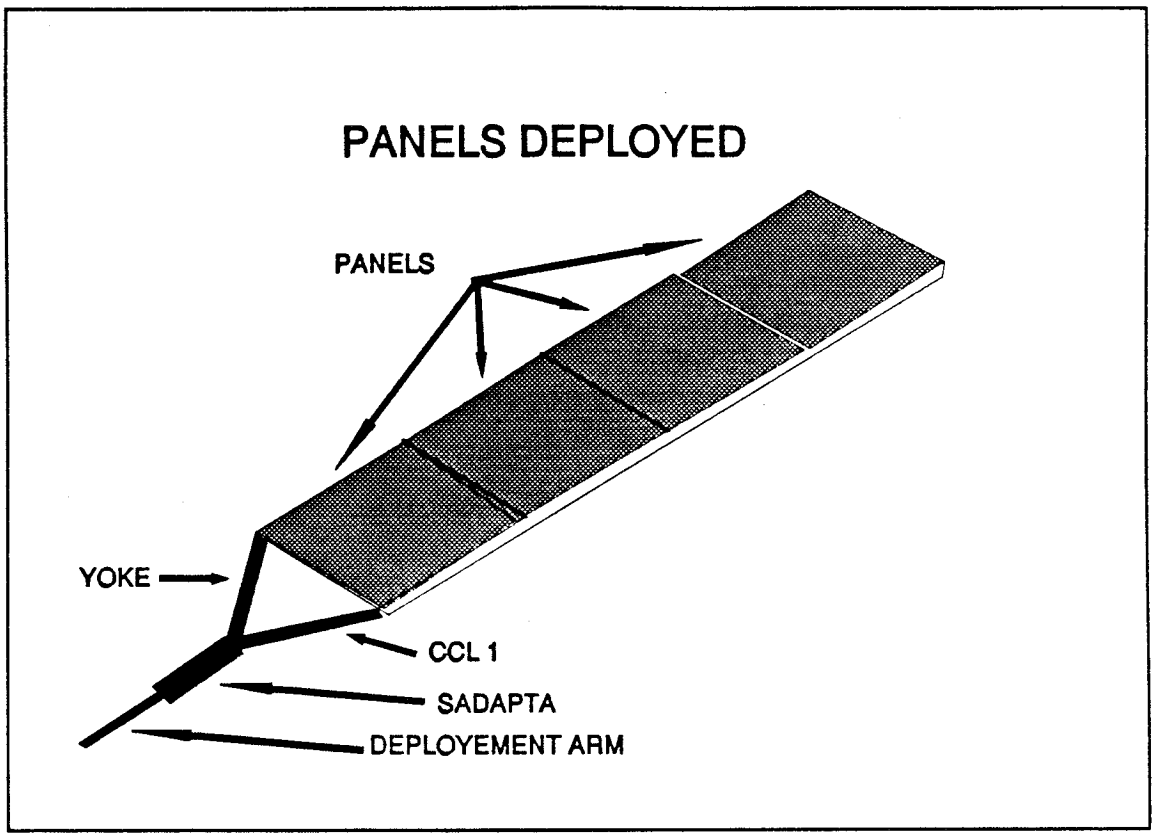

VIII-3 Solar Panels Deployed

3. Solar Array Deployment Mechanism

The four panels, deployment arm, outboard SADA, and yoke are to deploy together in accordion fashion. In the stowed configuration, depicted in figure VIII-4, the panels and arm assembly are held in place against deployment springs by four clampdown cables that resist out-of-plane vibration. In-plane vibration and panel spacing is provided by standoff snubbers that fit on the tensioning cable. For deployment release, the cable is severed at its base by redundant pyrotechnic guillotine cutters, allowing spring pressure to extend the arm and wing as a single degree-of-freedom system. The yoke is equipped with an eddy current damping system that limits wing extension

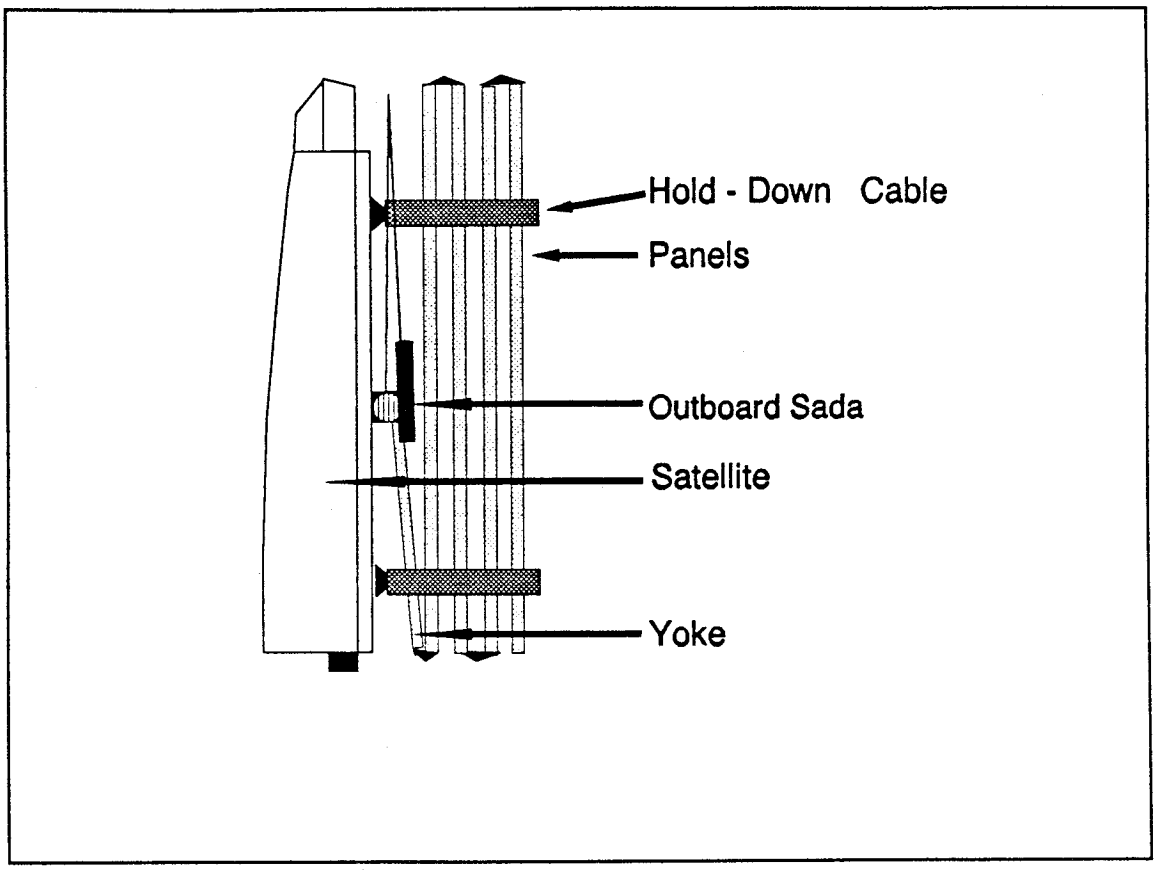

Figure VIII-4 Solar Panels Stowed

velocity and thus minimizes panel travel shocks. End of travel locking is provided by means of a cam and pawl device. The yoke and four panels are tensioned to full extension by a closed cable loop that provides redundancy for spring torque as shown in figure VIII-5. Panel hinges are provided with spherical self-alignment bearings to compensate for misalignments due to thermal deformations.

The deployment arm and yoke are constructed of rectangular aluminum tubing and hold the array away from the spacecraft a distance of 1.0 meter when the drive motor is extended. The deployment arm extends from the inboard drive motor to the yoke through the outboard motor and is hinged for stowage. The yoke structure ties the solar

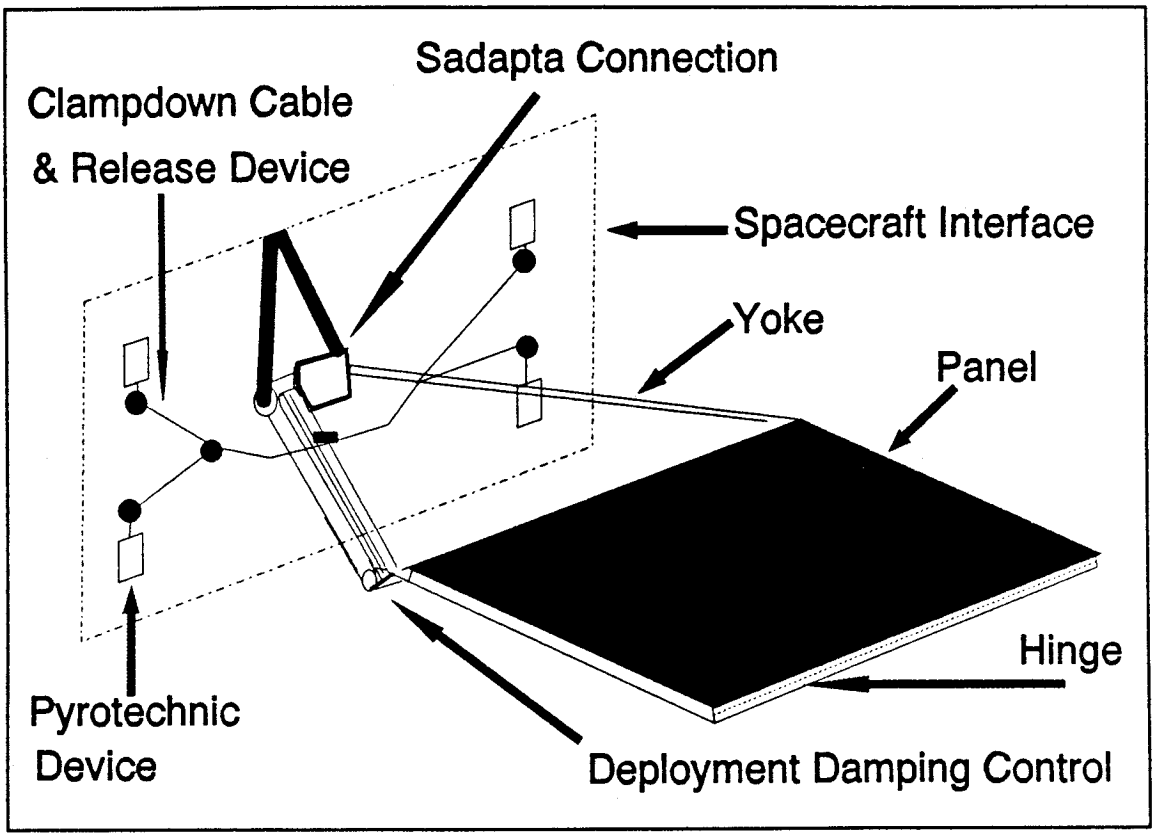

Figure VIII-5 Panels Deployer

array and associated cabling to the outboard power transfer assembly. The deployment arm, yoke, and harness are wrapped with reflective tape for expansion limitations and general reflective flux.

4. Solar Array Drive Assembly

Solar array sun tracking is provided by two solar array drive assemblies (SADA). The outboard drive motor provides array roll orientation about the deployment arm for orbit longitude variation. It connects the deployment arm to the yoke through a twist-flex power transfer assembly. The inboard drive mechanism provides array pointing by tilting the deployment arm at its base for variation in orbit inclination. The

inboard motor is a bearing assembly with harmonic motor drive inside the bus that transfers power into the craft through a roll-ring power transfer device. Actual array orientation is determined by using peak-power sun tracking. Tracking feedback loop sends drive signals to the motors until array output power is optimum.

5. Battery Design

Each of the 23 nickle-hydrogen cells is an individual pressure vessel housed in an insulated aluminum sleeve. Optimal monitoring requires that each cell have a pressure strain-gage, as well as voltage and temperature sensors. The sleeves are welded together and enclosed in an aluminum battery module. Battery specifications are listed in Table VIII.7.

Five year design life in this orbit will require 24,000 charge/discharge cycles. The EP NiH2 cells are considered safe for this cycle life to a nominal 40% depth of discharge, with the capability to discharge to 60% infrequently. The majority of the discharges is expected to be in the 30% range, providing a considerable power margin and avoiding any memory effect from constant cycle levels.

Battery charging power will vary seasonally. High battery capacity permits limiting discharging to C/2. EPS monitoring and predicting power loading will allow the initial charge/ discharge ratio to be maintained at an optimum 110%. Periodically thereafter, the charge current will be varied slightly in a goal to maintain end-of-charge-voltage (EOCV) of about 1.55. When fully charged, capacity will be maintained by trickle charging at C/100.

Table VIII.7 Battery Specifications

Eagle-Pitcher Ni/H2 RNH-40-7	23 cells
Rated cell capacity	40 A-hr
Nominal voltage	1.22 V
Cell mass	1.130 kg
Cell diameter	8.31 cm
Length	25.0 cm
Capacity (C/2 to 1.00 V @ 10°C)	47.0 A-hr
Specific energy	50.7 WH/kg
Energy density	36.7 WH/l
Minimum battery discharge voltage	28.0 V
Battery capacity @ 40% DoD	480 W-hr
Operating pressure (IPV safety margin= 3.5:1)	600 psig

6. Power Control Unit

The power control unit maintains spacecraft bus voltage level for distribution throughout the electric power system. The dual power bus is fully regulated to 28 volts.

a. Shunt Regulator

Each bus is independently regulated by a sequential linear shunt mounted on the corresponding solar array wing. The shunt dissipates excess power supplied by the array. This is especially important during BOL, when power generated by the solar cells greatly exceeds payload requirements during all phases of orbit. Series switch connection of the array to the shunt allows an entire wing to be taken "off-line" when power available from one wing is adequate to meet load demands. Later in life, when

environmental degradation makes a single array insufficient, the switch can be closed and power drawn from both wings simultaneously.

b. Battery Charge and Discharge Regulator

The battery charge regulator maintains proper charge on the battery and conditions battery discharge voltage to meet bus requirements. Variation in cell capacity will, at times, require voltage boosting during eclipse periods. For purposes of battery charging, a constant current must be supplied through a buck circuit when the required charge rate is below bus voltage. The regulator uses a common charge/discharge unit that shares an inductor for both the boost and buck operation in one design.

7. Mass Budget

The EPS mass budget is presented in Table VIII.8. Data include a 10% mass margin.

E. ELECTRIC POWER SUB-SYSTEM INTEGRATION

1. Thermal Control

Nickle-Hydrogen batteries suffer severe open circuit degradation when not operated within specified temperature parameters. The EPS design was calculated for NiH2 optimum behavior, and therefore requires that battery module temperature remain within specified 0 to 10 degrees centigrade.

Table VIII.8 EPS Subsystem Component

EPS Subsystem Component	Mass (kg)
Battery module	30.0
Solar Array Subassembly	16.0/wing
Wiring Harness	9.6
Deployment Mechanism	6.0/wing
Array Drive Assembly	16.0
Array Drive Electronics	2.5
Power Control Unit	5.6
Shunt Resistor Bank	2.23

2. Telemetry

In order to properly monitor EPS performance, and optimize component life, extensive EPS data is monitored by on-board sensors and down linked via telemetry. This data includes 23 cell pressures, 35 temperatures, 37 voltages, and 16 current sensor readings. While this level of monitoring may initially seem excessive, the 48 satellite constellation, and long mission expectancy, will benefit from careful EPS performance management.

F. REFERENCES

[1] "Solar Cell Radiation Handbook", Third Edition, NASA/JPL publication 82-69. Addendum 1988.

[2] "Solar Cell Array Design Handbook", vol 1 & 2, NASA/JPL

publication SP43-38.

[3] Applied Solar Energy Corporation, "ASEC Space Products Catalog 1991".

[4] AGRAWAL B.N.(1986) "Design of Geosynchronous Spacecraft".

[5] TRW SPACE TECHNOLOGY GROUP (1986) "Gamma Ray Observatory operations data book". Unpublished.

[6] FAHRENBRUCH A.L. & BUBE R.H. (1983) "Fundamentals of Solar Cells".

[7] HAFEN D.P., (1991) Lockheed Missle & Space Co, "Comparison of Nickel-Hydrogen and Nickel-Cadmium Reliability",Intersociety Energy Conversion Conference Session on Aerospace Batteries.

[8] GASTON S.J. & CHILELLI N.V.(1990) "Cell pressure as a state-of-charge indicator in IPV nickel-hydrogen batteries", Proceedings of the 26th Intersociety Energy Conversion Conference.pp 43-47.

[9] WHEELER J.R. & COATES D.K. (1986) "Nickel-hydrogen cell life test", Proceedings of the 21th Intersociety Energy Conversion Conference. pp1531-1536.

[10] SCHIFFER S.F. et al,(1990) "NiH2 battery cell life tests for low earth orbit applications", Proceedings of the 26th

Intersociety Energy Conversion Conference. pp55-60.

[11] PICKETT D.F.(1989) Advanced nickel-hydrogen batteries"Space Power Vol8, No4,1989. pp435-441.

[12] DONLEY S.W. & DALTON P.J.(1989) "Nickel-hydrogen cell low earth orbit life test at NWSC/Crane", Proceedings of the 25th Intersociety Energy Conversion Conference. pp1417-1422.

[13] MILLER L.(1988) "The NiH2 battery system: a space flight application summary", Proceedings of the 24th Intersociety Energy Conversion Conference. pp489-491

[14] OTZINGER B.M. & WHEELER J.R.(1989) "Common pressure vessel nickel-hydrogen battery development", Proceedings of the 24th Intersociety Energy Conversion Conference.pp1381-1386.

[15] BAKER et al,(1990) "The Hubble space telescope nickel-hydrogen battery design", Proceedings of the 26th Intersociety Energy Conversion Conference.pp1-6.

[16] BAGGETT R.M. & WHITT T.H.(1989) "Nickel-hydrogen battery testing for the Hubble space telescope", Proceedings of the 25th Intersociety Energy Conversion Conference.pp1411-1414.

[17] MILLER et al,(1989) "Multi-mission NiH2 battery cells for the 1990's", Proceedings of the 25th Intersociety Energy Conversion Conference.pp1387-1393.

[18] SCHULTZ N.R.(1989) "NASA flight cells and battery issues", Proceedings of the 25th Intersociety Energy Conversion Conference.pp1423-1428.

[19] BANKS B.A. et al,(1990) "LEO atomic oxygen,micrometeroid, and debris interactions with photovoltaic arrays", Proceedings of the 23rd IEEE Photovoltaic Specialists Conference.

[20] BILGER et al,(1989) "Photovoltaic array environmental protection program", Proceedings of the 22nd IEEE Photovoltaic Specialists Conference.pp361-369.

[21] SEVERNS J.G. et al,(1989)"Flight experience with LIPSIII" Proceedings of the 22nd IEEE Photovoltaic Specialist Conference.

[22] CHETTY P.R.K.(1988) "RADARSAT Electrical power system",Proceedings of the 24th Intersociety Energy Conversion Conference.pp775-783.

[23] DAS S. & SELVARAJ I.(1988) "Solar array mechanisms for Indian satellites, APPLE,IRS,and INSAT-IITS", Space Power, vol 7, No3, 1988. pp247-260.

[24] GERLACH L. & GORGENS B.(1985) "Advanced solar generator technology for the EURECA low Earth orbit", Proceedings of the 16th IEEE Photovoltaic Specialists Conference.

[25] RALPH E.L. & CHUNG M.A.(1990) "Retractable planar space photovoltaic array", Proceedings of the 23rd IEEE Photovoltaic Specialists Conference.pp1369-1373.

[26] MORGAN W.T. et al,(1989)"AXAF Electrical power system", Proceedings of the 22nd IEEE Photovoltaic Specialist Conference.

[27] JUILLET J.J. & PELENC L.(1986) "ARABSAT solar generator concept and in orbit performance"Proceedings of the 17th IEEE Photovoltaic Specialists Conference.pp1452-1457.

[28] GERLACH et al.(1990) "HST solar generator design for a decade in orbit", Proceedings of the 23rd IEEE Photovoltaic Specialists Conference.pp1308-1313.

[29] MORGAN W.T. et al,(1989)"AXAF Electrical power system", Proceedings of the 22nd IEEE Photovoltaic Specialist Conference.

THIS PAGE INTENTIONALLY LEFT BLANK

IX. THERMAL CONTROL SYSTEM

A. INTRODUCTION

1. Scope

a. Operational Requirements

The thermal control system is required to maintain spacecraft temperatures within the allowable range for components and subsystems. A listing of equipment temperature limits is provided in Table IX.1.

b. Functional Requirements

The spacecraft configuration allocates two sides of the spacecraft bus, measuring 0.98 m x 0.60 m each, for thermal control system exposure to the environment. The bus interior allows adequate space to wrap thermal blankets and insulation around equipment that requires it.

c. Restrictions/Constraints/Artificialities

Widely varying power requirements for the communications payload prompted a decision to use a psuedo-active control system. Thermal louvers were chosen both to meet this requirement and to ensure off-the-shelf availability. Louvers have been proven in space for the design lifetime.

Table IX.1 Thermal Requirements

Equipment	Temperature Limits (°C/°F)		
	Nominal	Minimum	Maximum
Payload:			
TCU	0 / 32	-40/ -40	90/ 119
Transmitters	0 / 32	-40/ -40	90/119
TT&C:			
PCU	0 / 32	-40/ -40	90/119
Power Subsystem:			
Solar Arrays	64/ 147	-160/ -256	80/ 176
Batteries	5/ 41	0 / 32	10/ 50
Shunt Assembly	64/ 147	-45/ -49	65/ 149
Propulsion:			
Propellent Tank	10/ 50	4 / 39	60/140
Propellent Lines	10/ 50	4 / 39	112/ 234
Thrusters	30/ 86	10/ 50	120/ 248
Mechanics:			
Pyrotechnics	NA	-170/ -274	55/ 131
Rail Bearings	NA	-40/ -40	40/ 104
Attitude Control:			
Earth/Sun Sensors	30/ 86	-20/ -4	60/ 140
Momentum Wheels	30/ 86	-15/ 5	55/130
Mag. Torque Rods	30/ 86	-30/ -22	70/ 158

By restricting the spacecraft size to fit either Delta or Ariane launch vehicle shrouds and stack size to ensure the launch of a full orbital plane at one time, close tolerances exist for structural attachment of the thermal control system components.

Finite element modeling of communications payload equipment has been limited to point heat sources, within boxes of the appropriate dimensions, for convenience of modeling. This model would require further refinement for completeness once the detailed heat dissipation characteristics were known for each individual circuit card assembly.

2. Method

a. Software/Method/Model Used

A finite-element approach was used to model the thermal characteristics of the spacecraft and its environment. The software used was the Integrated Thermal Analysis System for personal computers, version 7.3 (PC-ITAS), written and distributed by Analytix Corporation. PC-ITAS, while not user friendly in the common sense, provided a powerful tool to model the constantly shifting geometry of the orbit and to compute the transient and steady-state solutions to the finite-element models. Unfortunately, version 7.3 has numerous program errors which prevents complete modeling for this system. Errors in modeling or computing are discussed below within the discription of the appropriate model. Two models were built using primitive geometric shapes, heat-generating nodes and thermal parameters. One was developed

to design the required insulation, thermal blankets and heater sizes, and the other to validate the total thermal package following the stacked thermal package design.

The first model concentrated on the worst cold-case anticipated by the spacecraft in order to design required heating elements and insulation thicknesses. The spacecraft was modeled as a box of correct dimensions covered in thermal insulation. The thermal parameters entered into the model for the insulation corresponded to four layers of thin-film kapton. Radiation was the only method of heat transfer considered through the insulation. This assumption was justified by assuming that the kapton layers were physically seperated by a nylon mesh, as is a common practice at Lockheed Space and Missiles Company. The hydrazine fuel tank was modeled as a sphere within the box, and again the thermal parameters were adjusted to model multi-layered kapton insulation around them. Heat-source nodes inside the sphere were added to account for the heating elements. Several runs of the program were sufficient to determine that an average temperature of 22.5 °C (72.5 °F) could be maintained in the tank by an addition of 2.5 W. The insulation modeled was considered to be sufficient and the addition of a 5 W resistance heater was incorporated onto the surface of the propellent tank. The thermal mass of the hydrazine in the tank was not considered, but this is considered justified because any tendency to hold heat will tend to keep the tank warmer, as would waste heat radiating from the payload. A diagram of the model used for heater and insulation design is provided in Figure IX-1. Appendix G includes selected PC-ITAS results from this model, showing the transient and steady-state temperatures for the hydrazine tank are within thermal tolerance.

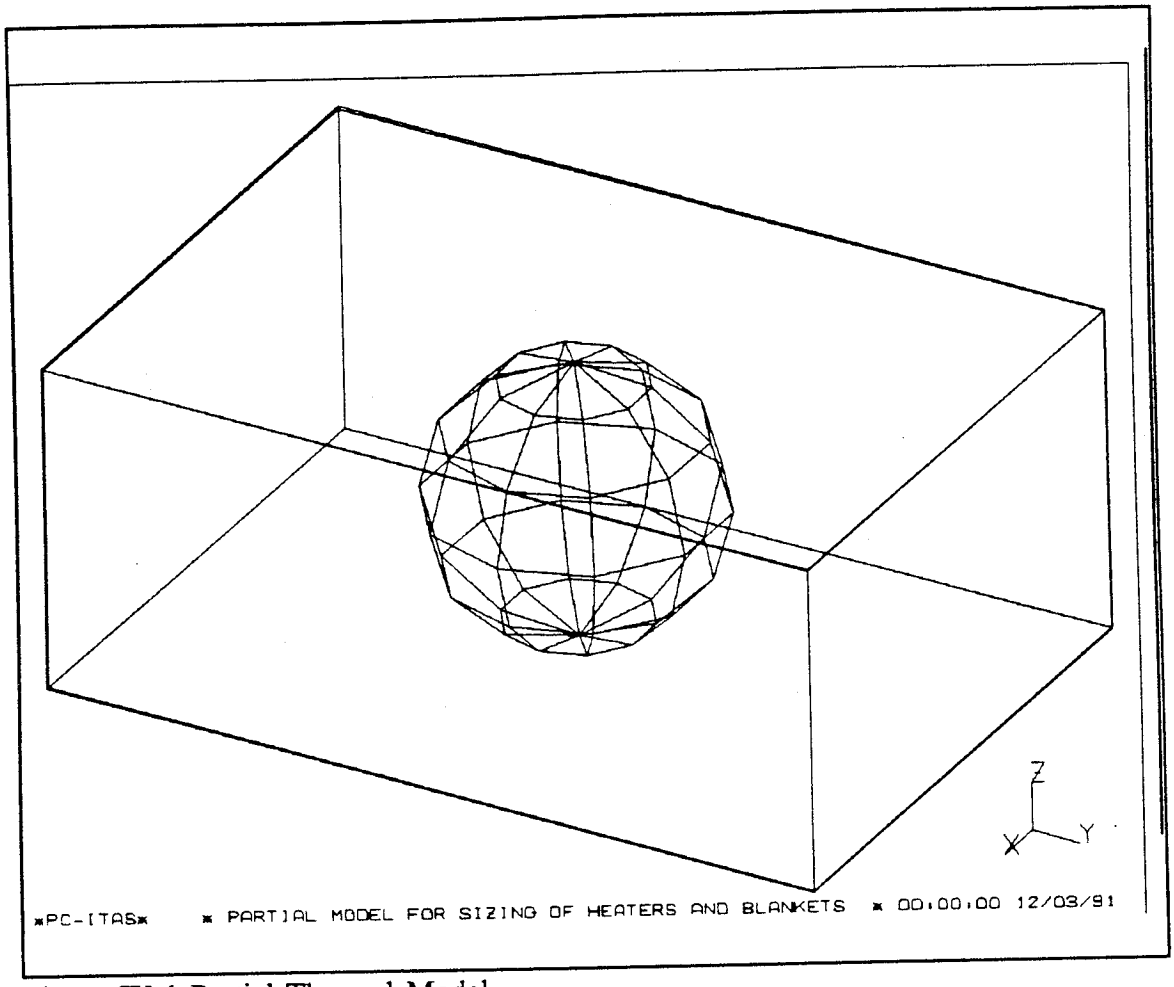

Figure IX-1 Partial Thermal Model

A complete thermal model was built to validate the thermal control system. The full thermal model is presented in Figure IX-2. All heat-generating pieces of equipment are included in this model. Results of the full thermal model, including individual node temperatures, steady-state and transient solutions, are presented in Appendix G. Due to PC-ITAS version 7.3 program errors, the temperature solutions presented are for a model which does not include the full thermal dissipation expected. The model results are therefore colder than those expected from a correct model. Specifically, it is believed that a 5 W heater, controlled by a thermostat, added to each

thruster location will bring the temperatures of those locations within limits. The batteries should not have a high-conductance path to the phase changers because they absorb an excessive amount of heat from the communications equipment. The batteries should be insulated from the phase changers and a conductance path provided to the sides of the spacecraft containing the solar arrays. If this design could be carried through to completion, a relocation of the batteries is preferred.

A diagram of the model used is provided in Figure IX-2. The results of transient and steady-state analyses, which show that all equipment, except the batteries and the thrusters, stay within allowable temperature limits, are presented in Appendix G. The batteries were found to be difficult to maintain within the required temperature limits.

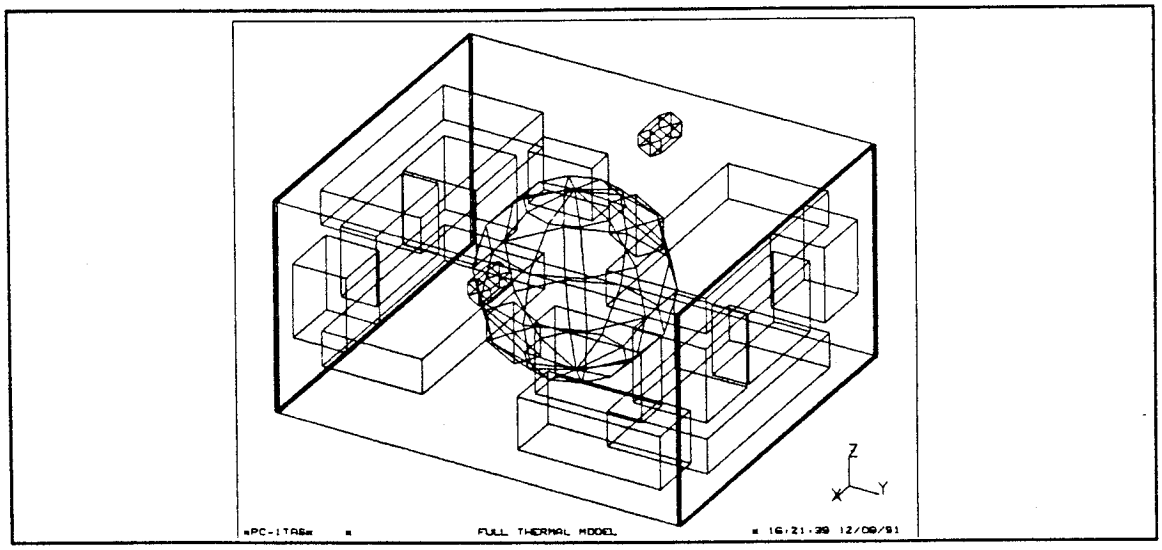

Figure IX-2 Full Thermal Model

b. Alternatives Explored

The widely varying heat dissipation levels due to the changing power requirements based on user tasking and the fact that the mission orbit allows sunlight on all sides of the spacecraft at some time necessitate the use of an active or psuedo-active thermal control system. All active or psuedo-active systems other than the one chosen had the distinct disadvantages of being unproven, unflown or propietary in nature. Some of the methods considered were:

(1) Cross-over or Diode Heat Pipes.

These systems are similar to standard heat pipes, but they transfer heat in only one direction. They have been proven in the laboratory, but as of November 1991 none have flown in space. They were considered too unreliable for a large constellation buy until a proof-of-concept satellite is flown successfully.

(2) Thermal Switches.

Thermal switches have flown on Lockheed LEO satellites in the 1980's. Use of these switches provides a means of disengaging the thermal path from a piece of equipment to a thermal radiator. They have not been flown in satellites with lifetimes of more than three years as of November 1991. Life testing and reliability questions led to the rejection of this concept for the mission.

c. *Tradeoffs Performed*

Since the orbital environment required for the mission ensures that all sides of the spacecraft receive equal amounts of sunlight over the mission life, the psuedo-East and -West faces were chosen for the thermal system. This was done to allow placement of the solar array drive assemblies along the velocity vector.

To ensure structural stability on the sides of the spacecraft covered by thermal control system components, the vertical structural beams comprising the spacecraft bus are bolted to the cold plates at the four corners of the bus. It is recognized that some heat transfer will take place through these structural elements from the phase changers to the cold plates.

B. GENERAL SYSTEM DESCRIPTION

1. Stacked Thermal Package

The design of the stacked thermal package is presented in Figure IX-3. Four of these packages, two per side, comprise the backbone of the thermal control system. Each package consists of a thermal louver box, thermal radiator, a cold plate and a phase changer. Since two of these packages sit side-by-side, the cold plates and phase changers are actually of double width and serve to connect the packages, as depicted in Figure IX-4.

The equipment to be cooled bolts to a cold plate through holes in the phase changer. The phase changers themselves are not strong enough to be weight bearing. Heat dissipates mostly in the phase changer, melting the parafin inside. Even if a power

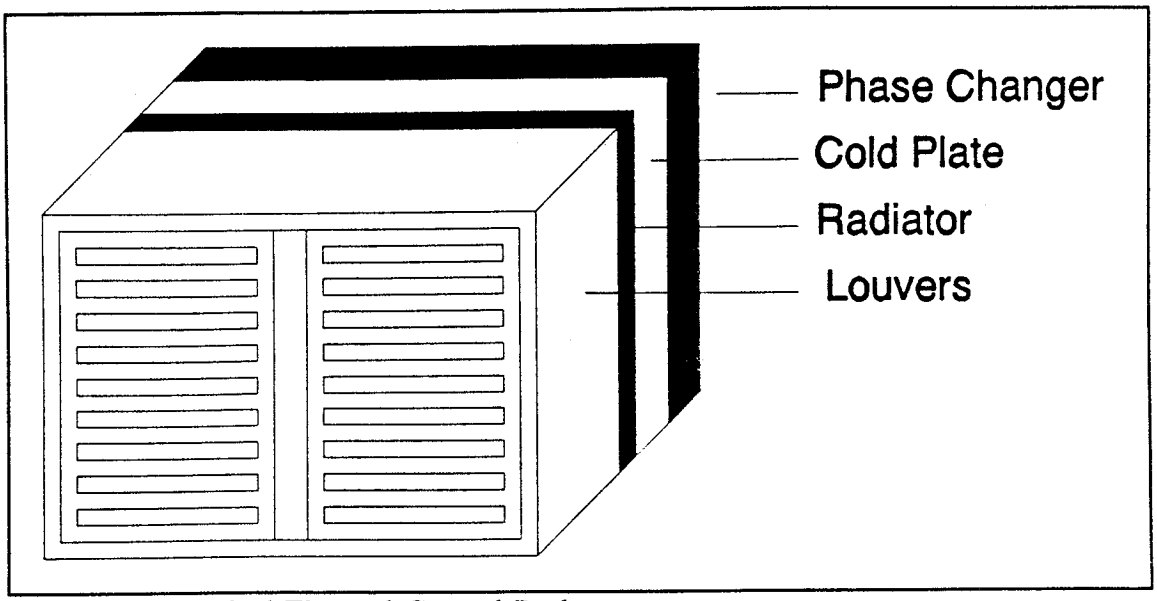

Figure IX-3 Stacked Thermal Control Package

spike is present, heat is conducted to the cold plate at a relatively uniform rate. The cold plate spreads the heat evenly across its surface, where conduction to the optical surface radiators (OSRs) takes place. The heat is then free to radiate to space. The efficiency of the radiative transfer is determined by the opening and closing of the thermal louvers.

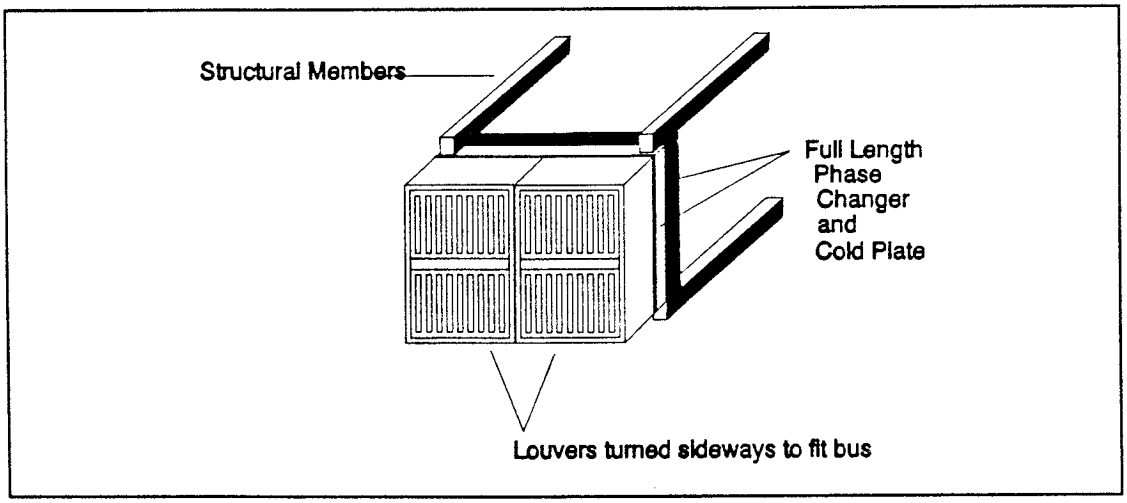

Figure IX-4 Integrated Thermal Control Package

2. Heaters

The results of thermal modeling indicate that heaters are required on the fuel tank, the six propellent lines to the thrusters and on the battery elements. Since the battery is seperated into four cells, located on either side of the spacecraft, heaters are required for each cell. Seven 5 W resistance heaters meet the requirements modeled. These heaters are turned on and off in response to a series of thermostats which were also modeled in the complete thermal model. Figure IX-5 depicts the type of heater used.

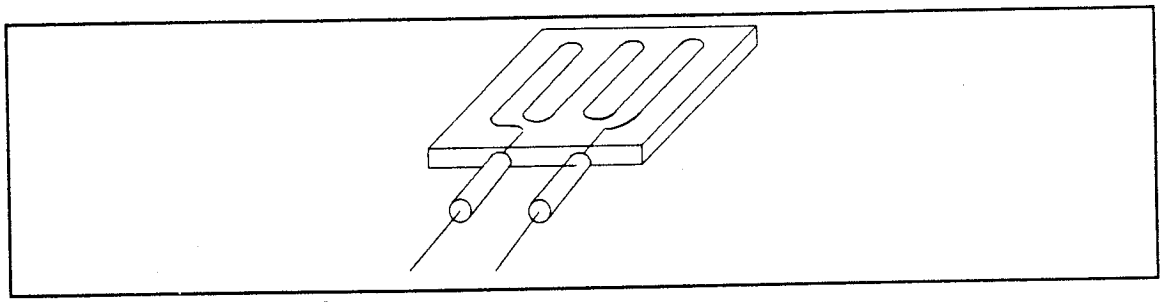

Figure IX-5 5 Watt Heater

3. Passive Means

Insulation surrounding batteries, the propellent tank, propellent lines and various other system equipment is necessary to reduce the power required to keep them within temperature limits. Any system or component that is artificially heated is also insulated to retain that heat.

A thermal blanket surrounds the spacecraft bus and antenna leads. Due to its small size, the entire spacecraft is insulated with a seperate thermal blanket. The material for both the insulation and the thermal blanket is multi-layered kapton seperated by a thin nylon mesh.

Paint has been budgeted for exposed surfaces of the spacecraft not covered by the thermal blanket. Testing of the optical properties of the surface will be required on the physical thermal model before type and amount can be determined.

C. INDIVIDUAL COMPONENT DESCRIPTION

1. Thermal Louvers

a. Description

Thermal louvers are shutter-type devices which act to change the optical properties and shadowing in front of a thermal radiator, thereby providing a method for controlling temperature. The louvers used in this design are Fairchild 18-blade louvers. They match the required surface area for the radiator design and volume requirements for the spacecraft configuration and provide linear temperature control over a 15 °C operating range. The specific temperature range was chosen for this design by adjusting the spring tension in the bimetallic control actuators.

Each blade is controlled by a seperate bimetallic actuator. This allows a temperature gradient to be handled across the radiator surface. Failure of conduction in the cold plate can therefore be partially handled automatically by the louvers. No power is consumed by the actuators as they react solely to temperature changes in the

base plate. In the case of this design, the base plate temperature is approximately the same as the radiator surface because they are conductively connected.

Counter rotating blades, with differing optical properties on opposite sides, allow the 10 °C operating range. Older louvers have a 18 °C range and rotate through only 180°. The lesser range can be used to provide more exact thermal control by more quickly reacting to changes in temperature.

Both the radiators and the thermal louvers were sized to ensure that adequate heat rejection could be accomplished in the case of catastrophic failure of all bimetallic actuators. Failure of the louvers will therefore effect the performance of the thermal control system only by requiring more heater power.

b. Budget

The thermal louver summary is presented in Table IX.2.

Table IX.2 Thermal Louver Summary

Equipment	Dimensions	Power Required	Mass
Thermal Louvers (4)	48.06 cm x 57.15 cm x 6.89 cm (each)	0 W	1.50 kg (each)

c. Margins

The louver surface area was chosen to match as exactly as possible the surface area of the radiator behind it. All margin for radiative transfer was applied to the radiator design.

d. Restrictions Imposed on Other Sub-System Components

The individual louver boxes are bolted to the cold plate behind them. The cold plate must take the loads imposed by these boxes.

2. Radiators

a. Description

Radiators consist of Flexible Optical Solar Reflector (FOSR) tape covering an aluminum substrate. The tape is a teflon material backed with adhesive. The aluminum substrate is integral with the cold plate described in the next section.

At the beginning of life, the emmissivity of the radiator surface is 0.8. This drops rapidly within the first year to about 0.72, then levels over the remainder of the design life. This equates to an nominal equipment temperature of 52 °C at BOL and 55 °C at EOL.

Calculations for the radiator sizing, nominal and worst-case power profiles are presented in Appendix G. MATHCAD version 2.4 was used to design the radiators due to the iterative nature of the problem.

b. Budget

Table IX.3 Radiator Summary

Equipment	Dimensions	Power Required	Mass
Radiators (4)	48.06 cm x 57.15 cm x 0.20 cm (each)	0 W	1.0 kg (total)

c. Margins

The radiator design incorporates average power assumptions higher than those actually expected, resulting in an intensional over-design of the radiators by approximately 10%. Earth's albedo, approximately 30% of solar irradiance, was also accounted for in the design.

d. Restrictions Imposed on Other Sub-System Components

During manufacture, attachment of the louver boxes will take place after radiator tiles are applied to the cold plate surface. Extreme care must be taken to avoid scratching or other damage to the radiators that would result in changes in their optical properties.

3. Cold Plates

a. Description

The cold plates are simply aluminum slabs of adequate thermal mass to conduct heat from equipment to the radiator surface. They perform the function of limiting the temperature gradient seen by the radiators. As heat leaves the equipment and phase changers, it is conducted to the cold plate. Heat spreads across the cold plate volume, limiting local hot spots, before conducting to the radiators.

b. Budget

The cold plate summary is presented in Table IX.4.

Table IX.4 Cold Plate Summary

Equipment	Dimensions	Power Required	Mass
Cold Plates (2)	96.12 cm x 57.15 cm x 0.35 cm (each)	0 W	5.19 kg (each)

c. Margins

No margin was taken in the cold plate design since they were sized to the radiator surface required.

d. Restrictions Imposed on Other Sub-System Components

The cold plates are joined to the equipment bolts and to the phase changer surface so as to have the best conductance possible. To this end, a thermal grease (RTV) is used. The grease fills the microscopic voids that are present in any metal-to-metal contact. This grease will outgas to space over time, but will not flow.

The cold plates also serve as the local structural member, with structural beams bolted to the short sides of the plates. Figure IX-6 depicts the cold plate-phase changer-equipment interfaces with RTV application points.

4. Phase Changers

a. Description

Phase changers are blocks of paraffin material that change phase from solid to liquid when heat is applied. Encased in an aluminum sheeting, the paraffin wax is a hydrocarbon polymer that may be chosen so as to have the desired melting

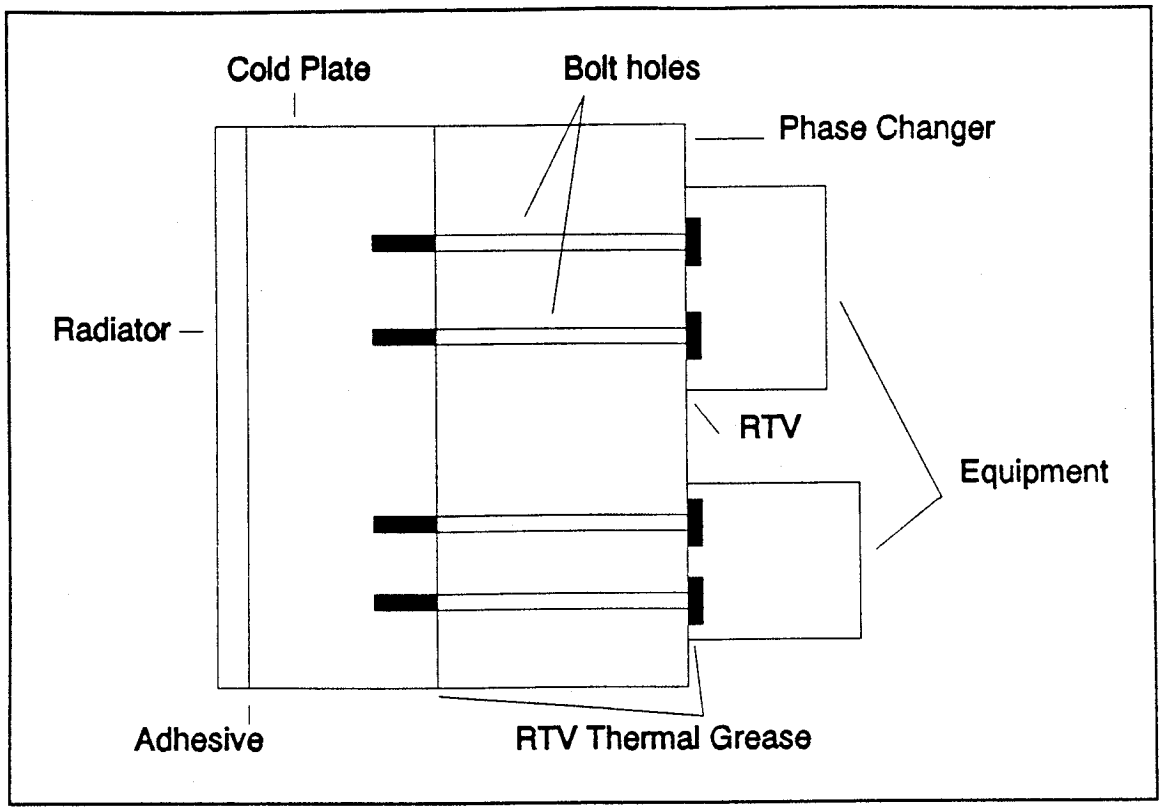

Figure IX-6 Equipment Mounting Characteristics

temperature. Figure IX-7, reproduced from Ref. 4, shows the relation between the hydrocarbon polymer and melting temperature. To maintain the payload electronics at a nominal 0 °C it is not possible to use a wax. However, if the radiators are designed to do this for normal operations, the phase changers absorb power spikes that significantly overload the radiative abilities in the short term. The hydrocarbon $C_{22}H_{46}$ has a melting temperature of approximately 28 °C (83 °F), 10 °C below the maximum allowable electronics temperature. This compound is commonly called Docosane, and is often written $CH_3(CH_2)_{20}CH_3$.

The thickness of the phase changer is a function of the thermal mass desired. For large power spikes in the 870 W range, this equates to a volume of 3571

cm^3, or a thickness of 0.65 cm by setting the surface area equal to that of the radiators. This assures that the largest power spike able to be generated by the communications payload, with all channels operating, will just melt all the available paraffin.

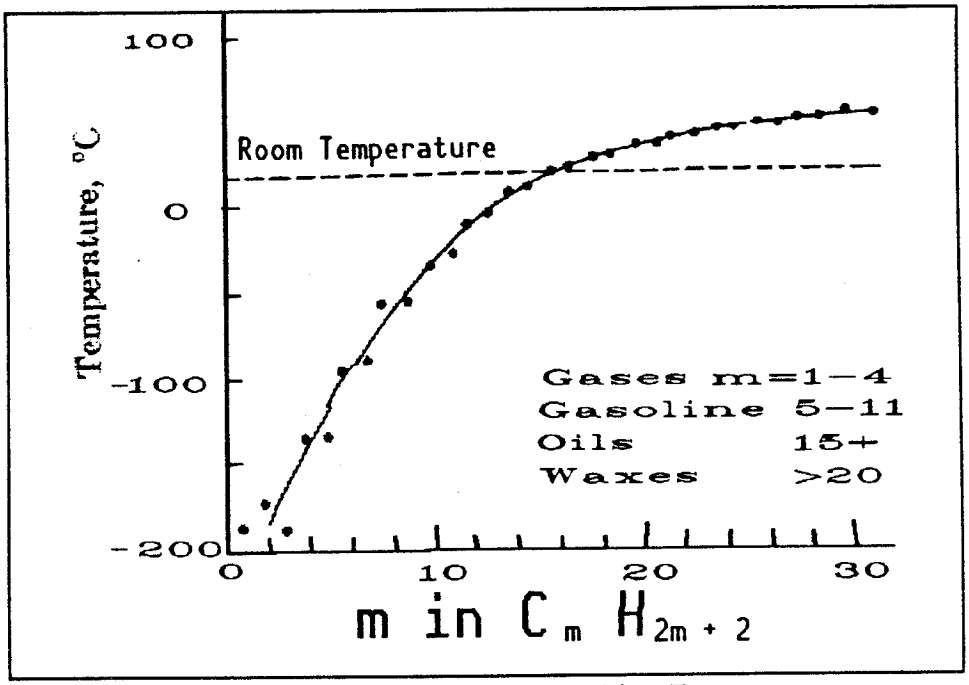

Figure IX-7 Hydrocarbon Structure vs. Melting Temperature

b. Budget

The phase changer summary is presented in Table IX.5.

Table IX.5 Phase Changer Summary

Equipment	Dimensions	Power Required	Mass
Phase Changers (2)	96.12 cm x 57.15 cm x 0.70 cm	0 W	2.85 kg (each)

c. Margins

Phase changers were sized to account for power spikes over the average, yet the melting temperature is higher than the average temperature of the electronics. This provides a high-temperature protection for power spikes of approximately 20%.

d. Restrictions Imposed on Other Sub-System Components

The phase changers cannot support the weight of equipment themselves. The mass of electronic equipment is supported by through-bolts to the cold plate. This is shown in Figure IX-6.

5. Heaters

a. Description

Eleven 5-Watt electrical resistance heaters were found to be adequate for all applications by PC-ITAS thermal modeling. Heaters are placed on the propellent tank under the insulation, on each battery cell and on each of the six thrusters. Thermostats are used to control the on-off switching of each individual heater, and are placed as close to the object being heated as possible.

b. Budget

The heater summary is provided in Table IX.6.

c. Margins

A 100% margin was designed for all heater requirements based on thermal modeling.

Table IX.6 Heater Summary

Equipment	Dimensions	Power Required	Mass
Heaters (11)	3 cm x 3 cm x 0.2 cm (each), 1 cm x 1 cm x 1 cm (Thermostats) (each)	5 W per heater	< 1.00 kg

d. Restrictions Imposed on Other Sub-System Components

Heaters must be placed under insulation in all cases. Wires and thermostatic control must likewise be placed under the insulation. Wherever possible, thermostats that control heater switching must be placed in close thermal contact with the device being controlled.

6. Thermal Blankets and Insulation

a. Description

Thin film kapton sheets, seperated by a fine nylon mesh is used for insulation. As has been discussed earlier, this method allows an accurate modeling to neglect conductive effects through the insulation. A diagram showing the kapton cross section is shown in Figure IX-8. A thermal blanket around the entire spacecraft is not necessary because of the high power dissipation rate.

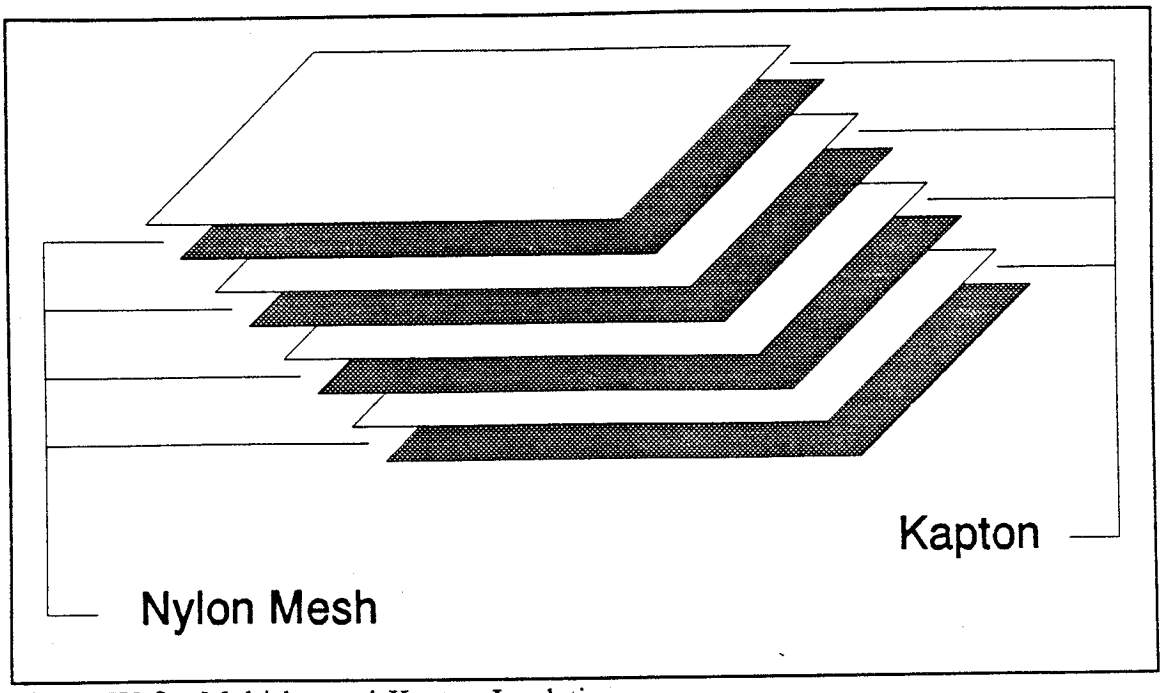

Figure IX-8 Multi-layered Kapton Insulation

b. Budget

The insulation summary is presented in Table IX.7.

Table IX.7 Insulation Summary

Equipment	Dimensions	Power Required	Mass
Battery Insulation	5120 cm^2	0 W	0.8 kg
ACC and TT&C Insulation	9694 cm^2	0 W	1 kg
Communications Payload Insulation	6600 cm^2	0 W	0.8 kg
Propellent Tank and Lines Insulation	8471 cm^2	0 W	1 kg

c. Margins

In keeping with current industry practice, the insulation was over-designed by approximately 50%. Most LEO satellites run warm because of this. Inherent inaccuracies in modeling make predicting the performance of insulation difficult.

d. Restrictions Imposed on Other Sub-System Components

The added bulk of insulation is accounted for in the spacecraft configuration.

D. SUB-SYSTEM INTEGRATION

1. Budgets

The total budget for the stacked thermal package is given in the System Integration section. Heaters and insulation do not require sub-system integration.

2. Margins

The stacked thermal package has been estimated to be 20% over-rated when assembled.

3. Restrictions Imposed on Other Sub-Systems

The heater package will require 30 W of power when fully active. The integration of the cold plates with the structure requires close coordination for assembly.

E. SYSTEM INTEGRATION

1. Budgets

The thermal system summary is presented in Table IX.8.

Table IX.8 Thermal System Summary

Equipment	Dimensions	Power Required	Mass
Stacked Themal Package	96.14 cm x 57.15 cm x 8.14 cm (each of 2)	0 W	21.6 kg
Heaters	30.8 cm^3	30 W	1 kg
Thermal Blankets and Insulation	30,000 cm^2	0 W	3.6 kg
Totals	Non-comparable dimer.sions	30 W	29.1 kg (with 10% margin)

F. SPACECRAFT INTEGRATION

The area in front of the louver boxes must be clear such that the radiators see free space. The solar array assemblies were placed on opposite sides to minimize shadowing. The radiators were designed with a full Earth albedo of 30% taken into account even though some shadowing is expected from the communications antenna. This ensures adequate radiation to space as indicated by the successful PC-ITAS model run.

G. REFERENCES

(1) Brij N. Agrawal, Design of Geosynchronous Spacecraft, Prentice-Hall, 1986.

(2) Halliday and Resnick, Fundamentals of Physics, 3rd ed., Wiley, 1988.

(3) Wertz and Larson (ed.), Space Mission Analysis and Design, Space Technology Library, 1991.

(4) L.H. Van Vlack, Elements of Materials Science and Engineering, Addison Wesley, 1980.

(5) J.P. Holman, Thermodynamics, 4th ed., McGraw Hill, 1988.

(6) J.P. Holman, Heat Transfer, McGraw Hill, 1981.

(7) R.C. West (ed.), Handbook of Chemistry and Physics, 62nd ed., Chemical Rubber Company, 1981.

THIS PAGE INTENTIONALLY LEFT BLANK

X. ATTITUDE CONTROL

A. INTRODUCTION

The successful completion of a communications satellite's mission is dependent upon its ability to meet precise antenna pointing requirements. The function of the Attitude Control System (ACS) is to maintain stability and spacecraft attitude within established limits. Antenna pointing accuracies provide the specifications around which the attitude control system is designed.

1. Operational Requirements

The attitude control requirements stem from specifications defined by the customer. These satellites are required to be Earth-pointing and utilize shaped antenna beam patterns, thereby restricting yaw requirements. Antenna specifications require pointing accuracies of $\pm$ 1 degree about any axis.

2. Functional Requirements

Functional requirements determine the range of duties to be performed by the attitude control system. Two ground stations (one on each coast of the United States) can accurately track the satellites and have the ability to uplink attitude correction and navigation data. Ground tracking stations will provide navigational control in the event that satellites must be repositioned.

The spacecraft has fixed yaw requirements due to the Earth-pointing planar antenna being fixed to the body of the spacecraft. This negates any slew requirements being imposed

on the attitude control system. ACS requirements for each satellite break out as follows: stability and control, and attitude determination.

B. METHOD OF ATTITUDE CONTROL SYSTEM SELECTION

Various attitude control systems were examined in order to select that system best able meet the stated requirements. For first order approximations, the satellites were modelled as rigid bodies with nonrotating, rigid solar arrays.

1. Alternative Designs and Tradeoffs

The desired spacecraft are low Earth-orbiting, Earth-pointing communications satellites requiring pointing accuracies of $\pm$ 1 degree. While these pointing accuracies are fairly loose, they nonetheless preclude gravity gradient or single-spin methods of attitude control. Dual-spin satellites are capable of attaining accuracies of $\pm$ 1 degree but this satellite design has the added restriction of high power requirements. Solar panels are the most cost effective means of meeting these requirements. Because these satellites must remain oriented toward the local vertical and require large solar arrays, a three axis stabilized attitude control system was chosen.

There are two types of three axis stabilized systems commonly in use today, zero-momentum or bias-momentum. Zero-momentum systems use three reaction wheels that are initially at rest. Disturbance torques cause these wheels to gain speed which must then be dumped. Bias-momentum systems utilize a single momentum wheel whose spin axis is aligned with the negative pitch axis. The momentum wheel spins continuously at a high speed providing gyroscopic stiffness which, in turn, provides coarse yaw control.

Bias-momentum systems have the advantage of being simpler than zero-momentum systems and are less expensive. The slight loss in accuracy that accompanies a bias-momentum system is well within design limits.

The orbital altitude chosen for this mission is such that aerodynamic effects such as drag, are negligible and the dominant disturbing force is provided by the magnetic field of the Earth. Therefore, fixed yaw requirements, medium accuracy antenna pointing requirements and orbital altitudes lead to a simple and cost effective attitude control system utilizing a bias-momentum wheel. Roll disturbance torques and momentum dumping are controlled through the use of magnetic torque rods.

C. GENERAL SYSTEM DESCRIPTION

The ACS provides autonomous attitude control through the use of a bias-momentum wheel to control pitch and damp disturbances in roll and yaw. Magnetic torque rods are used for roll control and momentum wheel desaturation. As stated previously, the momentum wheel is oriented so that its spin axis is aligned with the negative pitch axis, or, its angular momentum vector is aligned with the local vertical. The magnetic torque rod used to control roll is able to provide a 50 AMP-m^2 magnetic dipole and is offset by an angle of 71 degrees. This allows a single torque rod to counter errors in both roll and yaw. The torque rod used to desaturate the momentum wheel also provides a 50 AMP-m^2 magnetic dipole. Attitude sensors include a solar aspect sensor for initial orientation, a two-axis scanning Earth horizon sensor (EHS) for nadir angle determination and a two-

axis magnetometer to measure magnetic field strength. All signals relating to attitude control are processed through the attitude control computer.

Redundancy is provided for by the addition of an extra momentum wheel assembly. Onboard thrusters may be used for roll control and wheel desaturation in the event of magnetic torque rod failure. Of the sensors, only the EHS has been provided redundancy since the solar aspect sensor and magnetometer are not essential to the completion of the

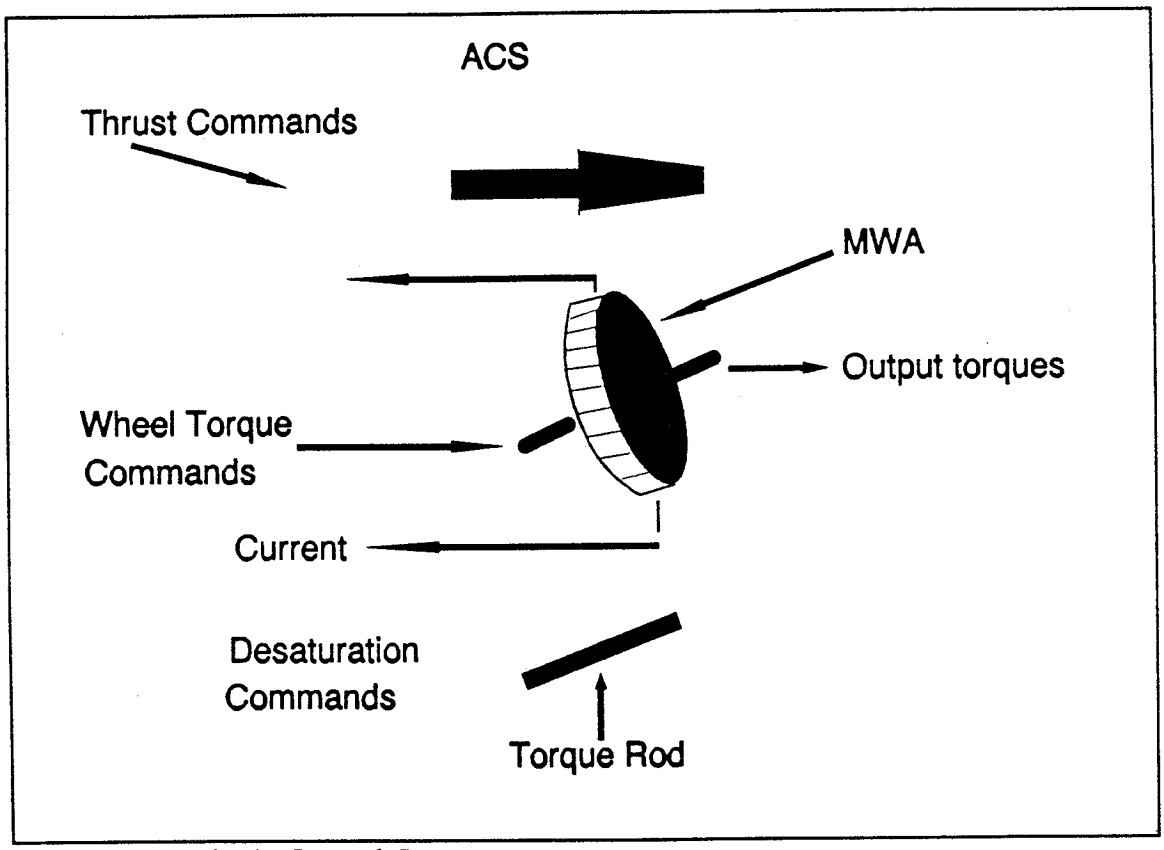

Figure X-1 Attitude Control System

mission. In the event of an attitude control computer failure, attitude control commands may be provided by ground control. Figure X-1 above, illustrates the system design.

saturation limit of 130 AMP-m^2. Torque rods have indefinite life requirements since they have no moving parts with the additional benefit of very high reliability.

4. Sensors

The solar aspect sensor and Earth horizon sensors are manufactured by Applied Research Corporation. The solar aspect sensor is accurate to within $\pm$ 0.1 degree and has a field of view of 32° x 32°. The Earth horizon sensor is accurate to within $\pm$ 0.5 degrees and scans from -5° to 5°. Manufacturer specifications are defined in Tables X.2 and X.3.

Table X.1 Attitude Control System Components

Component	Weight (kg)	Size	Power (W)	Manufacturer
Momentum Wheel	10.4	15.0	20.0	Honeywell
Desat Torque Rod	3.2	50 Am^2	1.5	Ithaco
Roll Torque Rod	3.2	50 Am^2	1.5	Ithaco
Earth Sensor	0.72	N/A	1.6	Applied Research Corp. (APR)
Sun Sensor	0.75	N/A	1.6	APR
Attitude Control Computer	2.5	N/A	6.0	Ithaco

Table X.2 Solar Aspect Ssensor (EHS) -- Typical Specifications

Accuracy		< 0.04^0 (12-bit mode) < 0.1^0 (8-bit mode)	
Field of View		32^0x 32^0 (8-bit mode) 64^0x 64^0(12-bit mode)	
Power Interface Voltage Current		 + 28V Continous (Normal Op) 58 mA (1.6 Watt)	
Physical Interface Size Mass Thermal		 53 x 104 x 109 mm 750 g - 20^0 to +60^0C	
Data Interface			
Clock		8320 Hz	
Enable		16 Clock Periods	
Vibration and Acceleration			
Frequency (Hz)	g / Hz	SLOPE	g (rms)
20	0.025	--	
20 - 50	--	+ 6 dB / octave	
50 - 600	0.150	--	12.9
600 - 2000	--	- 4.5 dB / octave	
2000	0.025	--	

Table X.3 Earth Horizon Sensor (EHS) -- Typical Specifications

Accuracy	< 0.5^0 noise equivalent angle < 0.1^0(rms)		
Scan Angle	- 5^0 to +5^0		
Instantaneous Field of View	-5^0 (horizontal) to x 2^0 (vertical)		
Power Interface Voltage Current	 + 28V + 4V Continous (Normal Op) +150V Continuous (Survive) 62 mA for 0.935 sec each sec 180 mA for 0.065 sec each sec 70 mA Average (2 Watt)		
Physical Interface Size Mass Thermal	 49 x 102 x 102 mm (Housing) 720 g 70 mA Average (2 Watts)		
Data Interface			
Vibration and Acceleration			
Frequency (Hz)	g / Hz	SLOPE	g (rms)
20	0.025	--	
20 - 50	--	+ 6 dB / octave	
50 - 600	0.150	--	12.9
600 - 2000	--	- 4.5 dB / octave	
2000	0.025	--	

E. SUB-SYSTEM INTEGRATION

The attitude control system operates at the command of the attitude control computer. The EHS determines satellite attitude by measuring the nadir angle. This information, along with momentum wheel speed is sent to the attitude control computer which then processes the information and determines what type of attitude control is required. In this manner, attitude control is accomplished autonomously. Redundancy is provided for by ground control.

F. SYSTEM INTEGRATION AND PERFORMANCE

Each time a motor operates onboard the satellite, a torque is imposed. The attitude control system "senses" these torques, and, through commands received from ground stations, reacts to damp the resulting adverse motions. Additionally, the satellite counters external torques described in the following section.

Of considerable importance is the initial orientation procedure through which the satellite becomes fully stabilized with the payload pointing in the proper direction. When released from the SLD, the satellites are passively stabilized by spinning about their major axis with an angular velocity imparted to them by the launch vehicle. Following solar array deployment, satellite thrusters are commanded to despin the satellite after which, the momentum wheel spins up to provide gyroscopic stabilization. The satellite slowly revolves about its major axis to acquire the sun. If unable to acquire the sun within approximately five revolutions, the satellite will rotate about its roll axis. Initial attitude determination data is provided by the solar aspect sensor. Once sun acquisition

has occured, the satellite will acquire the Earth with its Earth horizon sensor by rotating about its y-axis. Peak bus voltage is monitored to maintain optimal solar array pointing.

After the Earth has been acquired, the satellite will maintain its attitude within $\pm$ 1 degree through its primary attitude control system of MWA's and magnetic torque rods.

Magnetic disturbances provide the largest torques acting on the satellites and are on the order of 10^{-5} N-m. Gravity gradient and solar pressure disturbance torques are approximately two orders of magnitude smaller than magnetic disturbances. Aerodynamic disturbances are negligible due to the altitude of the orbit.

Magnetic disturbance torques are secular torques resulting from the Earth's magnetic field reacting with the satellites residual magnetic dipole. These torques are used to calculate system gains and time constants. All calculations are included in a Mathcad program included in Appendix H.

G. REFERENCES

Agrawal, B. N., *Design of Geosynchronous Spacecraft,* Prentice Hall, 1986

XI. PROPULSION

A. INTRODUCTION

1. Scope

The satellite mission necessitates accurate positioning of each satellite in a multiplane constellation. The propulsion system is designed to inject each satellite into its proper position in the orbital plane, maintain that position throughout the lifespan, and de-orbit at end-of-life.

a. Operational Requirements

The mission requires an 8-plane, 48-satellite constellation in a low earth orbit along a 52 degree inclination. Choice of launch vehicle, transfer orbit, operational orbit, and position accuracy all define propulsion system requirements. Early estimates of individual satellite mass allowed consideration of loading one plane per launch vehicle to minimize launch costs. The six satellites must be placed in the orbit at equal intervals. After injection from the SLD, each satellite must be despun, oriented and decelerated to enter operational orbit. Except for the lead satellite, each following satellite must overcome a greater delta-v to correct its argument of perigee and right ascension with respect to the lead satellite. During operational status, the propulsion system corrects for minor errors in the orbit. Orbital accuracies are set at 1 degree off of intended position. At end-of-life, the remaining propellant de-orbits the satellite into a higher drag orbit.

b. Functional Requirements

The major limiting factor for the propulsion system is the amount of propellant (mass and volume) that can be carried within the restricted box structure. Other limitations imposed on the system are thruster location and moment arm. Thruster location is preferably at the farthest point from the center of mass to maximize the moment arm. However, the SLD configuration requires the thrusters to be located flush to the deck. This, in addition to the limit imposed by location of the thermal gear, reduces the maximum moment arm for more efficient thruster operations during despin maneuvers. The position of the thrusters with respect to the solar arrays places a canting requirement which reduces thruster efficiency during delta-v maneuvers.

c. Artificialities

Timing of thrust operations is not included in the analysis and design.

2. Method

a. Software

The delta-v calculations are taken from Orbital Workbench version 1.01. The Orbital Transfer branch of the Orbital Workbench program was extremely helpful in calculating delta-v for the various maneuvers which included the design of the transfer orbit to minimize delta-v. The propellant budget was designed on Microsoft Excel 3.0.

b. Alternatives Explored

A positive expulsion elastometric diaphram tank was first considered in lieu of the tank design used in the final design. Consideration was given with regard to

cost verses the designed mission of the diaphragm tank. Positive expulsion tanks are primarily designed for missions which require high accelerations and, therefore, their use would be an overdesign for this mission. They were also deemed inefficient because of the decrease in useable volume to total volume ratio. Additional alternatives included the number of tanks. Choices ranged from one to four. More than one tank would increase volume and mass of propellant containment per mass of propellant. For this reason, as well as cost, one tank is selected.

c. Tradeoffs Performed

The injection orbit is specifically designed to minimize required delta-V for initial orbit positioning, which is the largest demand on propellant mass. This tradeoff investigation compared relative rotation of argument of perigee, relative recession of the nodes, and velocities at perigee between the circular operational orbit and injection orbits of various apogees. Careful attention was given to minimize the delta-v requirement for this maneuver and yet not require excessive time in the injection orbit. Choosing the injection orbit so that all satellites are ejected from the SLD within 16 orbits, minimizes the delta-v requirement to correct for the differences described above, and balances this requirement with minimizing the time elapsed between first and last injection.

B. GENERAL SYSTEM DESCRIPTION

The primary components include one 60 cdm tank, six 2.2 N thrusters, and associated plumbing. The thrusters operate on hydrazine propellant using Shell 405

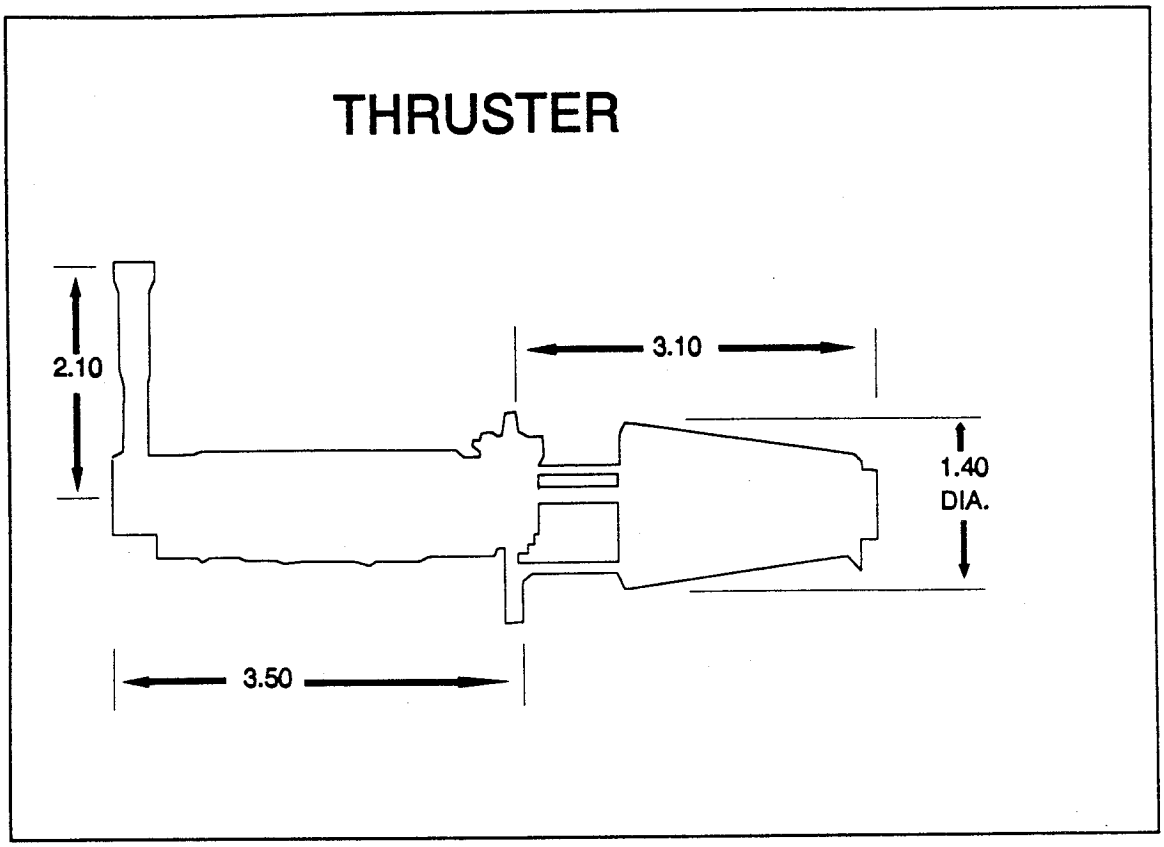

Figure XI-1 Thruster Outline

catalyst. Propulsion system mass and propellent budgets are presented in Table XI.1.

C. INDIVIDUAL COMPONENT DESCRIPTION

1. Thruster Description

Six identical thrusters are used for each satellite. Thruster characteristics are presented in Table XI.2. Each thruster (Rocket Research Company Model MR-11A) has been previously flight tested. Thruster design is presented in Figure XI-1.

The particular combination of thrusters required for specific maneuvers is listed in Table XI.3 for thruster operations. Thruster operations in the x-axis are inhibited by the solar arrays. Solar array deployment must occur before any thruster is

Table XI.1 Mass Budget

Maneuver	Delta V (m/s)	Isp (sec)	Mass Change (kg)	Final Mass (kg)
Launch Mass				374.00
Attitude Orientation	1.00	224.00	0.17	373.00
Orbit Injection	149.390	223.96	24.57	349.26
Orbit Maintenance	9.19	218.56	1.49	347.76
EOL Deorbit	146.00	218.23	22.93	324.84
Propellent Holdup			0.98	323.85
Margin			7.02	316.83
TOTAL			57.17	

COMPONENT	
Tank, pressurant, and propellant	70
Thrusters (ea)	.344
Piping	4.5

fired along the (plus or minus) x axis. For this reason, they are canted 5 degrees out to avoid solar array impingement by the exhaust. Even so, coordination between solar array positioning and thruster firing must occur. Normal on-orbit maneuvering is not expected to be required on short notice so that this coordination can be planned out in advance.

Thruster locations are depicted in Table XI.4. Thruster location is limited by equipment location for other systems, especially thermal control. The antenna payload also limits positioning of any thruster along the negative z axis. Furthermore, integration into the SLD requires that thrusters be flush with the satellite faces.

Table XI.2 Thruster Characteristics

Propellent	N2H4
Catalyst	Shell 405
Thrust	2.200 N (0.5 lbf)
Valve Power	9.000 W (28 vdc, 45 °F)
Isp (BOL)	224.000 sec
Isp (EOL)	213.000 sec
Mass	0.344 kg ea.
Number	12.000
Minimum Impulse Bt.	0.0431 Ns (25 ms)
Flown on	ERBS
Manufactured by	Rocket Research Corporation (ROCKOR)
Model	MR-11A

Table XI.3 Thruster Operations

Operations	Thrusters
Injection	5 and 6
Station-Keeping	(1 and 2) or (5 and 6)
Positive Roll (+x)	5
Negative Roll (-x)	6
Positive Pitch (+y)	1 or 4 or 6
Negative Pitch (-y)	2 or 3 or 5
Positive Yaw (+z)	1 or 3
Negative Yaw (-z)	2 or 4

Table XI.4 Thrusters Locations

Thruster Designation	Spacecraft Coordinates		
1	-41.5	-36.0	20.0
2	-41.5	36.0	-20.0
3	41.5	36.0	20.0
4	41.5	-36.0	-20.0
5	-41.5	36.0	-26.0
6	41.5	-36.0	-26.0

2. Propellant Tank

The one propellant tank is a center-mounted spherical tank filled to 83% capacity with monopropellant hydrazine. It is a 49.3 cm outer diameter tank with a mass of 5.126 kg capable of holding 61.9 kg of hydrazine. Nitrogen pressurant is used to expel the hydrazine with no mechanical means of separating the pressurant and propellant. Surface tension devices (baffles and sponges) are designed in the tank to ensure liquid availability to the thrusters. Tank characteristics are listed in Table XI.5. Tank size is limited by the height of each satellite, thus the desire to launch one plane per launch vehicle is the primary imposition on tank size and therefore propellant capacity. Figure XI-2 depicts the tank outline.

3. Other

Welded titanium tubing interconnects the tank, thruster, and nitrogen bottle. Manual fill and drain valves on the tank assist in testing, loading, unloading, and

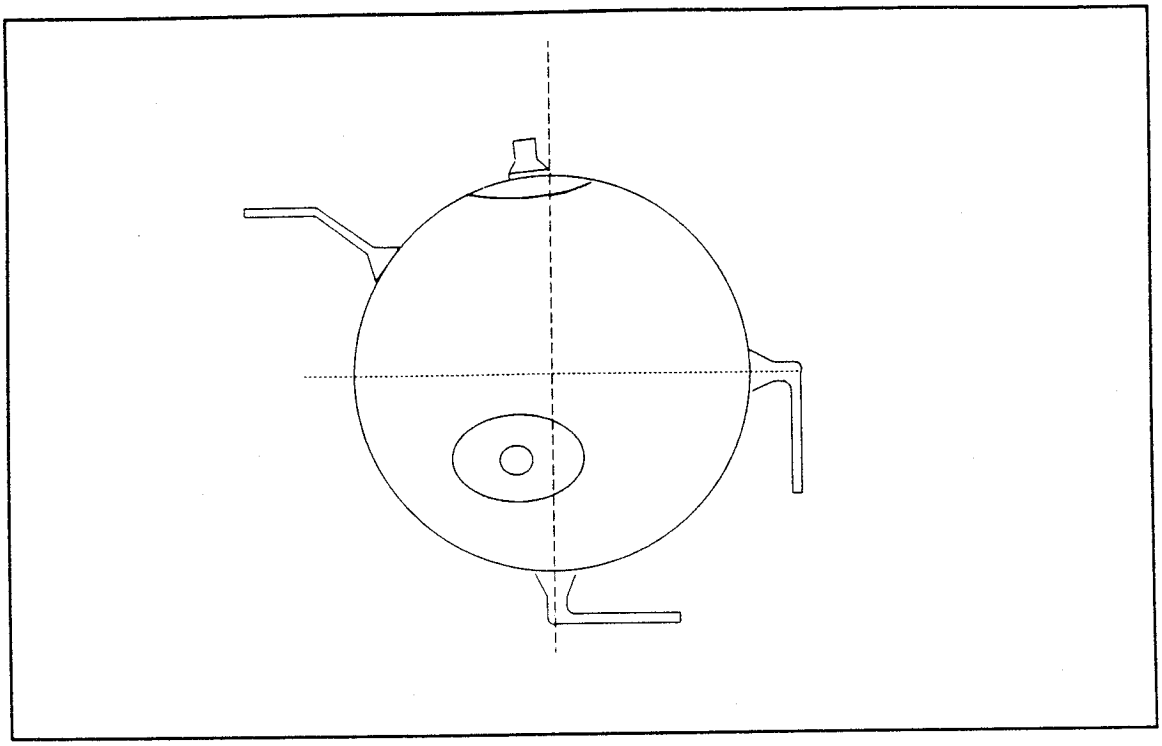

Table XI-2 Tank Outline

Table XI.5 Tank Characteristics

Number	1.000
Pressurant	N2
Radius	49.070 cm (ID) 49.260 cm (OD)
Wall Thickness	0.091 cm
Mass	5.216 kg each
Operating Pressure	2.340 MPa
Maximum Propellent Mass	61.867 kg each
Actual Propellent Mass	61.867 kg each
Manufactured by	TRW
Model	#80182-1

prelaunch operations. A filter is placed at the tank outlet to prevent thruster clogging or valve malfunction. The 6.35 mm interconnecting lines are made of titanium tubing and are welded to all fittings. Heaters are integrated in the tank and thrusters to prevent freezing of the hydrazine.

D. SUBSYSTEM INTEGRATION

The tank is initially pressurized at 300 psi. A command to fire a thruster opens the thruster valve for that particular thruster and propellant flows through the catalyst due to a pressure difference across the catalyst bed. The catalyst and hydrazene exothermally react and propellant flows out of the nozzle. The valve closes when the open signal ceases. A decrease in tank pressure is detected by a pressure transducer using strain gauges. The transducer sends a signal to the pressure regulator which passes nitrogen to the propellant tank until operating pressure is again achieved.

E. SYSTEM INTEGRATION

Figure XI-3 depicts the integration of propulsion system components.

F. SPACECRAFT INTEGRATION

The propulsion system integrates with the thermal control system in that the hydrazine must be maintained at greater than 50 degrees F to prevent freezing. This is accomplished by thermal blankets and a heater installed on the tank.

C-3

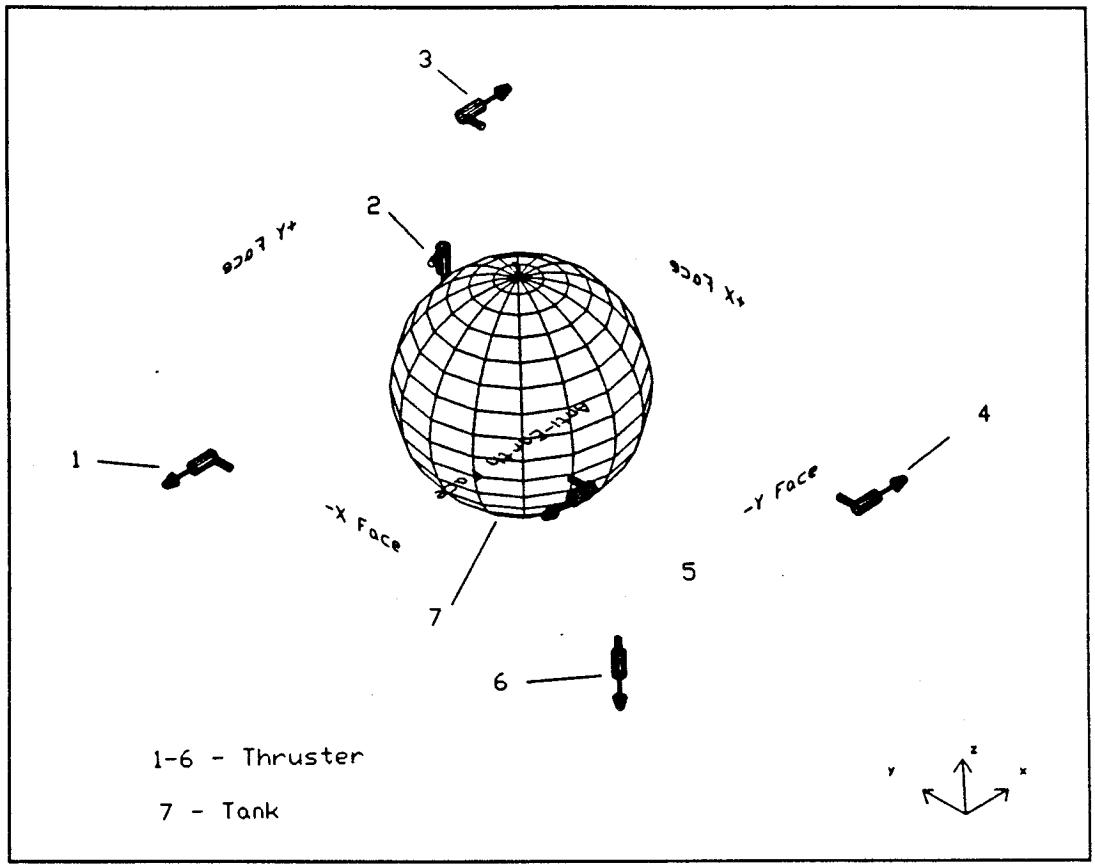

Figure XI-3 Propulsion System Components

G. REFERENCES

1. TRW Pressure Systems, Inc., *Aerospace and Hydrospace Tanks,* 18 December 1986

2. Rocket Research Company, *Product Information* folder of thruster information, 16 March 1987

XII. TEST

A. INTRODUCTION

1. Objectives

The objectives of the satellite test plan are to:

- Perform development testing of qualification and prototype hardware and computer program design concepts as early as possible to ensure early detection and resolution of design, fabrication, compatibility, performance, reliability, and life expectancy problems.

- Perform qualification testing of units and assemblies at presystem or system level to assure specification requirements have been met prior to initiation of flight hardware acceptance testing.

- Perform acceptance tests on all units before installation on the spacecraft to demonstrate flight-worthiness.

- Perform prelaunch validation tests to demonstrate that the space vehicle and the launch vehicle have been successfully integrated.

- Perform on-orbit performance tests to verify full operational capability to feedback into acceptance test planning system.

2. General Test Requirements

Figure XII-1 depicts an overview of the spacecraft test plan. A description of the general test plan requirements follows.

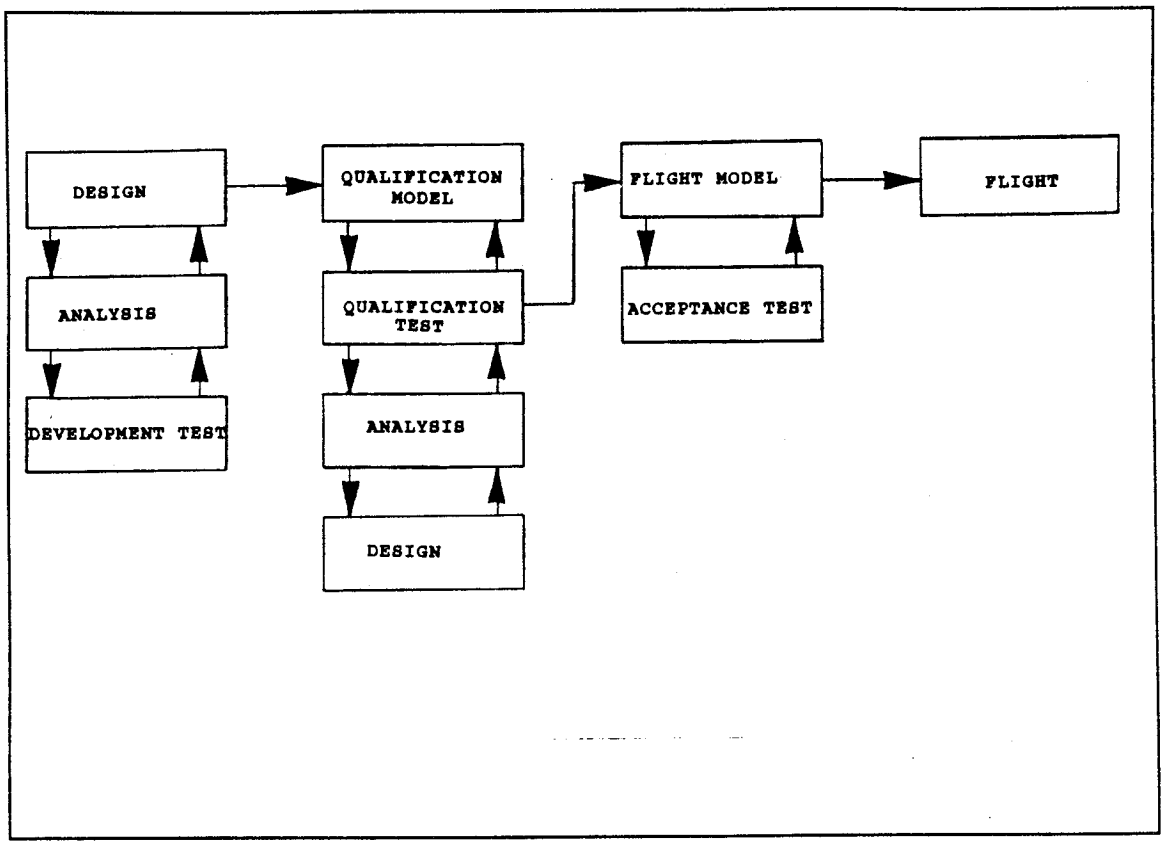

Figure XII-1 Satellite Test Plan

a. Development Testing

Development Tests are conducted to obtain information to aid in spacecraft design and manufacturing processes. These tests will generate the design parameters, validate design concepts, verify design criteria. determine design margins, identify failure modes, and to verify manufacturing processes. [MIL-STD p. 7]

b. Qualification Testing

Qualification Tests are conducted to demonstrate that the design specification requirements are met. The qualification test levels are the design levels which exceed the range of environments and stresses expected throughout the spacecraft's

mission. The qualification tests validate the acceptance test program's techniques, test procedures, test environments, test equipment, and test software. [MIL-STD p. 20]

c. Acceptance Testing

The acceptance test plan demonstrates the flight-worthiness of each spacecraft component and subassembly. The acceptance tests reveal manufacturing and/or workmanship inadequacies. Test levels for validation are based on ascent and on-orbit operational environments and stresses.[MIL-STD p. 20]

d. Prelaunch Validation Testing

Prelaunch validation testing is conducted once the spacecraft has been delivered to the launch site. The test objective is to assure the space vehicle survived transportation and is ready to be integrated with the launch vehicle. The space vehicle is retested following integration to demonstrate operational compatability between the launch system and spacecraft. [Ref. MIL-STD: p. 20]

e. On-Orbit Testing

The on-orbit test plan is an important consideration in the design of the remaining space vehicles. The specific requirements are not addressed in this document.

B. DEVELOPMENT TESTS

1. Development Test Vehicles

A development test vehicle is fabricated to provide engineering, design, and test information concerning the validity of analytical techniques and assumed design parameters, to uncover unexpected system response characteristics, to evaluate design

changes, to determine interface compatibility, to prove test procedures and techniques, and to determine if the equipment meets its performance specification. [MIL-STD p. 7]

2. Satellite Launch Dispenser Model

a. Ground Test Considerations

The large size of the Satellite Launch Dispenser (SLD) combined with loading due to gravity makes ground testing of the complete structure difficult. Gravitational stiffening, suspension effects, virtual air mass, preloads and air damping will alter dynamic characteristics. Other testing difficulties encountered are low resonant frequencies and high modal densities within the frequency range of interest which combine with small motions and accelerations. The complexity of the mechanisms and their associated nonlinearities cause structural complexities. From these considerations, The ground testing of the complete SLD will be difficult if not impossible.[ATLSS p. 114]

b. Ground Testing Approaches

Several ground testing approaches have been considered to overcome difficulties in testing the SLD. Scale model testing was considered since this would overcome size and gravity effects, but does not assure the detail representation required. Element tests provide a means of supplementing the model tests and will be effective in the testing of joints. The substructure testing method appears to be the most promising. Substructure testing enables the dynamic behavior of the actual structure to be measured while overcoming some of the concerns with respect to size, gravity, and modal density.

The tests will be directed toward the verification of analysis using either models of partial structures.[ATLSS p. 115]

c. Design, Development, and Verification

Ground tests of the SLD are used primarily to verify analysis. The use of a prototype structure for the ground test verification is supplemented by analysis with the major emphasis placed on the development of accurate analytical methods.

3. Component Development Tests

The majority of the development tests are conducted on breadboard and prototype hardware at the subsystem and component level. Since many of the spacecraft components have been previously flight proven, their are only a few items of interest which will require the earliest possible verification of critical design concepts to reduce the risk of involved in committing the design to qualification and flight hardware. The emphasis of the testing is on electrical and mechanical performance and the ability to withstand the environmental stress of ascent. Functional testing is conducted in simulated thermal and vibration environments.[MIL-STD p. 25]

4. Space Vehicle and Subsystem Development Tests

a. Modal Survey

The modal survey defines and verifies analytically derived dynamic model of the space vehicle for use in launch vehicle loading event simulations and for use in examinations of post-boost configuration elastic effects upon control precision and stability. The test is conducted on a flight quality structural subsystem augmented by

mass simulated components. The data obtained should be adequate to define orthogonal mode shapes, mode frequencies, and mode damping ratios of all modes which occur within the frequency range of interest.[MIL-STD p. 25]

b. Structural Development Test

The structural development tests verify the stiffness properties of the space vehicle and measure the member load and stress distributions.[MIL STD p. 26] Structural tests may be done in conjunction with the modal survey.

c. Acoustic and Shock Development Test

The acoustic test exposes the space vehicle to the qualification environment in an acoustic chamber.

d. Thermal Balance Development Test

The thermal balance development test verifies the analytical modeling of the space vehicle and component thermal design criteria. The thermal model consists of a thermally equivalent structure with the addition of equipment panels, thermal control insulation, finishes, and thermally equivalent models of electronic, pneumatic, and mechanical components. The thermal balance test is conducted in a space environments simulation test chamber capable of simulating the ascent, transfer orbit, and orbital thermal vacuum conditions.[MIL STD p. 28]

e. Transport Development Test

The dynamic environment experienced by the satellite during road or air transportation is normally controlled to levels less than the max levels predicted for

launch or flight. Since road surface conditions are subject to change, an analysis of space vehicle response to the transportation environment may be necessary to verify that the spacecraft will not be damaged during transport. A spacecraft development model or simulator which has the space vehicle mass properties are used with instrumentation to measure both space vehicle and transporter dynamic responses. [MIL STD p. 28]

C. QUALIFICATION TESTS

1. Component Qualification Tests

The component qualification tests are conducted entirely on the component level either inplant or by the manufacturer. The exceptions to this testing are items which may only be tested at the subsystem level. Some of these are the wiring harnesses, interconnecting tubing, and radio frequency ciruits. [Ref. MILSTD: p. 43]

2. Qualification Test Vehicles

Two qualification test vehicles are required for this project. These are the spacecraft and the satellite launch dispenser, which are qualified as individual units and will require separate test plans. The spacecraft and satellite launch dispenser qualification vehicles are produced from the same drawings, materials, equipment, and manufacturing processes as the flight vehicle. The spacecraft and the satellite launch dispenser are qualified at the design level as opposed to acceptance test levels.

3. Vehicle Qualification Tests

The space vehicle qualification tests consist of functional, electromagnetic compatability, acoustic, vibration, pyro shock, pressure, thermal vacuum, thermal

balance, and thermal cycling. Figure XII-2 depicts the test sequence. Special test such as alignments, calibrations, antenna patterns, and mass properties are conducted at the acceptance test level for flight vehicles, and are also conducted on the qualification vehicle.[Ref. MILSTD: p. 29] The acceptance level tests are discussed in detail in the Acceptance Test Plan in the next section.

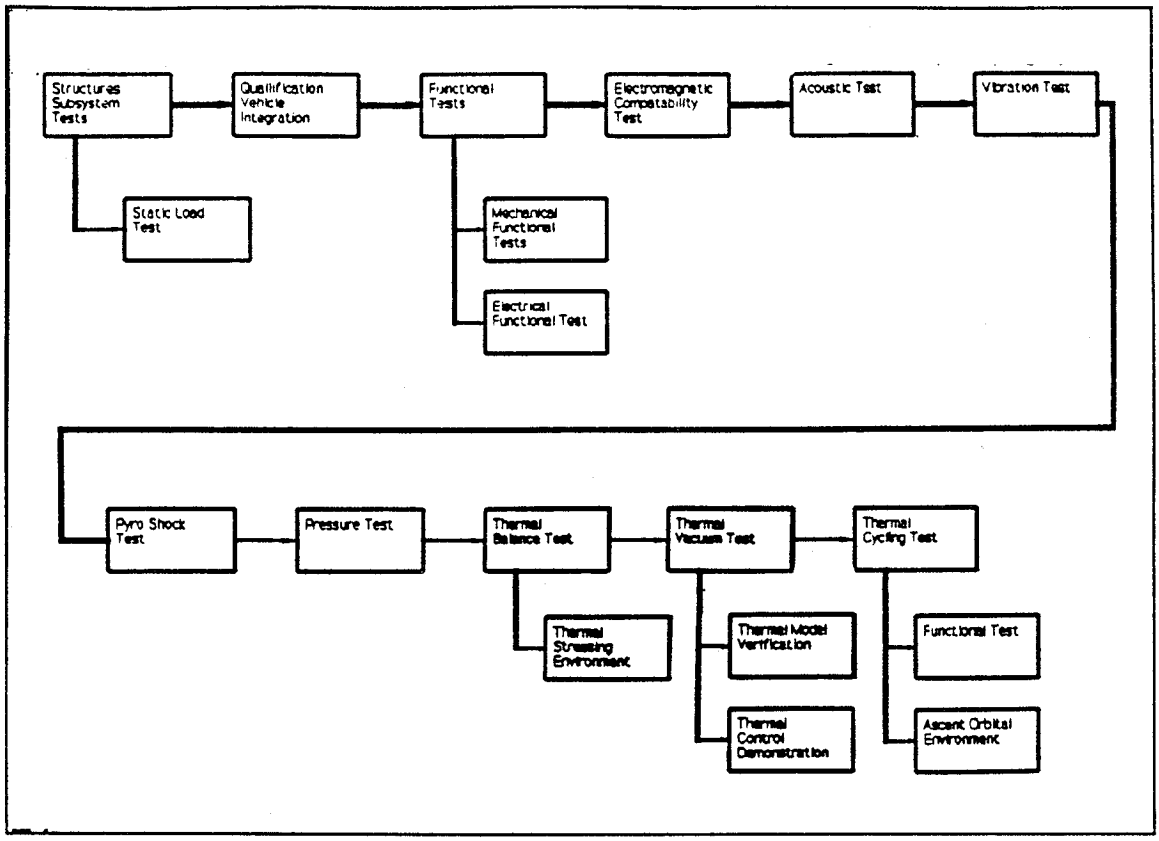

Figure XII-2 Satellite and Launch Dispenser Qualification Flow Diagram

a. Satellite Launch Dispenser Qualification Test Plan

The SLD test plan includes the mechanical and electrical functional, electromagnetic compatability, acoustic, vibration, pyro shock, pressure, thermal

vacuum, thermal balance, and thermal cycling qualification tests. Special tests include low level sine vibration tests, alignment checks, and satellite dispensing tests. All tests requiring mass property or thermal simulation are conducted with mass and/or thermal models of the spacecraft installed in the SLD.

b. Spacecraft Qualification Test Plan

The spacecraft qualification test plan includes the mechanical and electrical functional, electromagnetic compatability, acoustic, vibration, pyro shock, pressure, thermal vacuum, thermal balance, and thermal cycling qualification tests. Special tests include are include to test the Reaction Control Subsystem, the Solar Arrays, antennas and are as described in the Acceptance Test portion of the chapter.

D. ENVIRONMENTAL ACCEPTANCE TESTS

1. Component Environmental Acceptance Test Requirements

All components are subjected to the testing in this section.

a. Thermal Vacuum

The thermal vacuum test are conducted in accordance with component specifications, except that the hot and cold environments will be 20°F higher and lower, respectively, than the maximum and minimum expected orbital temperatures.[TRW p. 2-3]

b. Vibration

To simulate the spacecraft launch environment, while the equipment is mechanically and electrically energized, the equipment is subjected to the random

vibration acceptance environment shown in Figure XII-3. Vibration is applied consecutively in each of three orthogonal axes, for a period of 1.0 minute in each axis. The vibration is applied and measured at the launch vehicle interface or mounting points.[TRW p. 2-3]

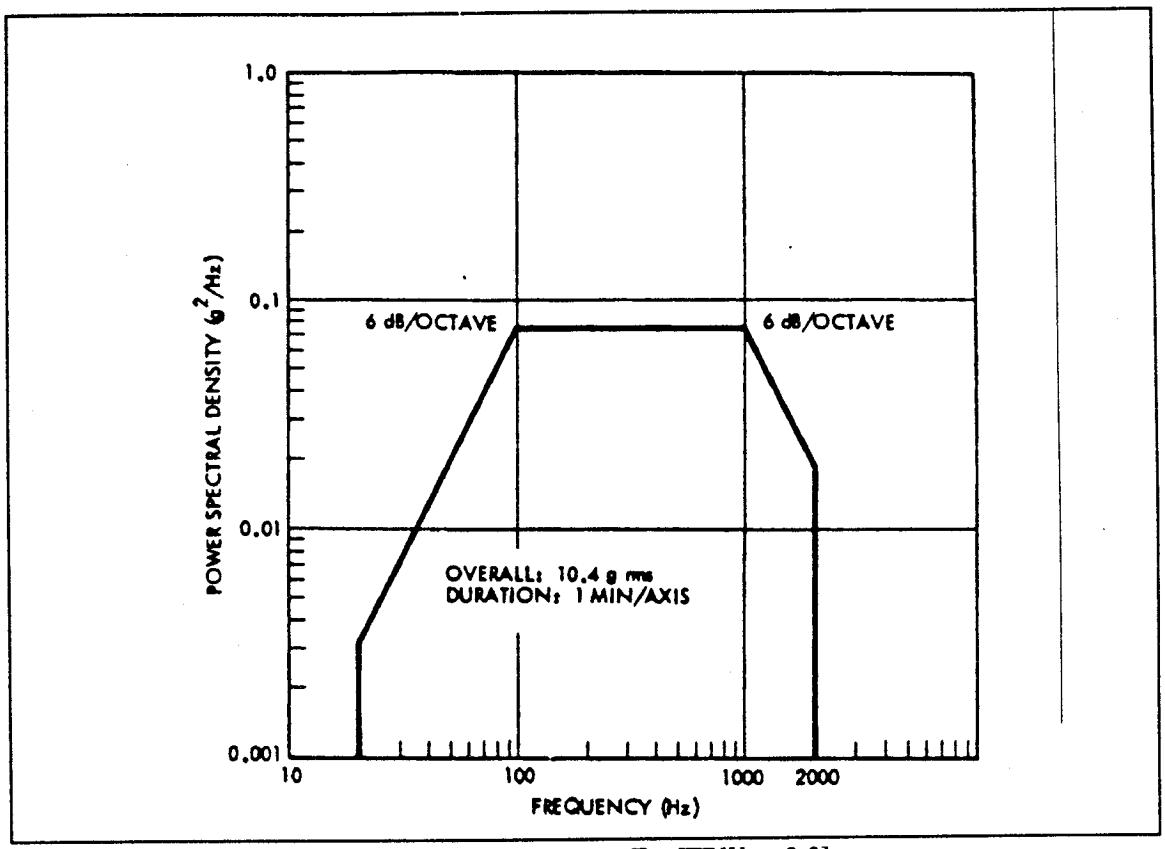

Figure XII-3 Spacecraft Random Vibration Acceptance Test[TRW p. 2-3]

2. Spacecraft Environmental Acceptance Test Requirements

All flight vehicles are subjected to the environmental tests described in this section.

a. Acoustics

The spacecraft in launch configuration, receives an incident broadband random sound field for a period of 1 minute.

b. Space Environment Simulation

The thermal vacuum space environment simulation exposes the spacecraft to worst case, high and low temperature conditions. Heat flux sources are used to simulate solar energy.

c. Low-Level Sine Vibration

The spacecraft is subjected to sine vibrations along the londitudinal principal axes perpendicular to the launch vehicle/spacecraft interface plane. The amplitude of the low-level sine vibration test is established using predicted spacecraft dynamic responses to transient boost events. The test level so that the spacecraft primary structure does not exceed 95 percent of the design limit load.[TRW p. 2-4]

E. COMPONENT ACCEPTANCE TESTS

Component Acceptance Tests are conducted to demonstrate that the equipment meets the required standards for workmanship and the performance requirements stated in the satellite specification. All components/subassemblies have been successfully acceptance tested and have been flight certified prior to installation on a flight spacecraft.

The structure subsystem components are subjected to physical inspections and dimensional checks to verify compliance with workmanship standards at the component

level. Environmental acceptance tests are conducted at the higher subassembly level as part of the spacecraft environmental acceptance test.

F. SPACECRAFT ACCEPTANCE TESTS

All flight spacecraft are subjected to the tests described in this section. The acceptance test flow annotated to show the status and activity of each major subsystem on a test-by-test basis is shown in Figure XII-4.

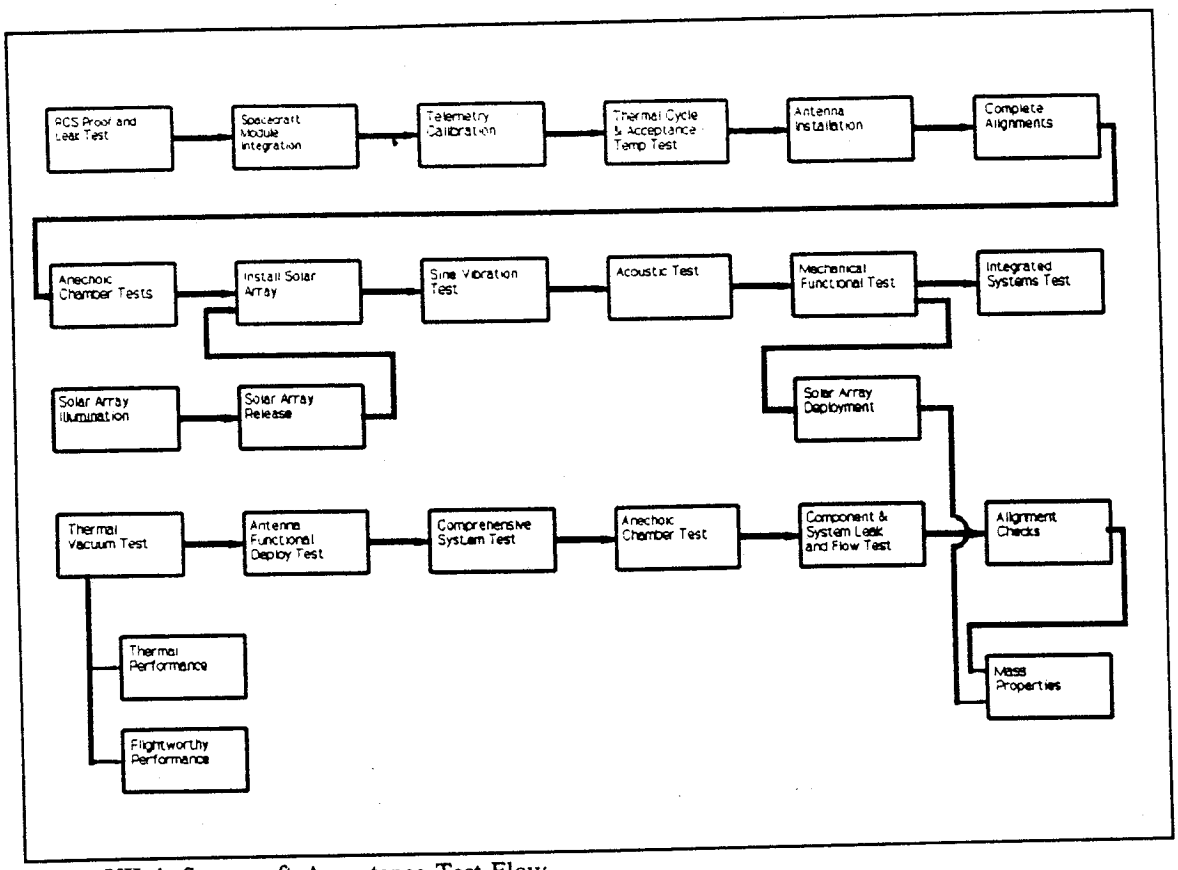

Figure XII-4 Spacecraft Acceptance Test Flow

1. Reaction Control System Proof Leak and Flow Tests

The objectives of the Reaction Control System (RCS) leak and flow tests are to verify RCS integrity at a pressure which is 1.67 times work pressure, to verify

RCS integrity at a working pressure within acceptable external leak rate, to verify the RCS components have acceptably low leak rates, to verify that thrusters are free of obstructions and that the gas flow impedance is acceptable low, and to verify proper valve operation.[TRW p. 303] The tests are performed on a fully configured RCS that has been assembled on the spacecraft module structure. A post-environmental exposure flow and leak tests are performed on a fully configured spacecraft, usually done prior to solar array installation as shown in Figure XII-4.[TRW p.315]

2. Telemetry Calibration

Telemetry calibrations are conducted to calibrate the analog telemetry parameters required for the full range of telemetry signals. The raw voltage data is sampled at points before signal conditioning, and the corresponding downlink before computer conversion.[TRW p. 320] Telemetered data are examined to substantiate the analytical verification of the required accuracy of the signals.

3. Spacecraft Subsystem Tests

Spacecraft subsystem tests are conducted to demonstrate the full operating characteristics of the spacecraft system and includes performance measurements to substantiate compliance with specifications. This test is conducted after the thermal vacuum chamber test and provides the primary post-environmental performance verification for the TT&C, ACS, and communications subsystems. The spacecraft is fully configured without solar array and batteries and with the antennas stowed. The ACS will be externally stimulated by simulated sensor and command inputs. [TRW p. 321]

4. Power Subsystem

Operational verification of the power subsystem is accomplished using simulated battery power to simulate launch and ascent. Subsequently, simulated solar array power is applied to simulate array deployment. A brief eclipse period is simulated by removing the test power source and the simulated batteries are discharged. Ordinance control and firing testing is performed as part of the electric power test sequence. Ordinance test point monitors are connected to the spacecraft at the pyrotechnic device interfaces. [TRW p. 336]

5. TT&C Subsystem

Simulated TT&C signals are sent by the PC computer to verify the command and telemetry responses. The command and telemetry verifications are based on telemetry response voltage changes, power changes. frequency changes, etc. as a result of a command specified. [TRW p. 338] TT&C is systematically operated in clear and encrypted modes to verify their operation.

6. Attitude Control Subsystem

The ACS is tested by simulation of the full range of ascent and on-orbit operations. Each sun and earth sensor is stimulated with a variety of error outputs. End-to-end control loop verification compares thruster, solar array drive, and reaction wheel responses to simulated error inputs to the sensor and(or) electronics. Successful completion of this test requires that the ACS demonstrate the appropriate response to ACS commands, that telemetered parameters and status information be verified via

telemetry, and that proper functional operation and logical performance on the AVCS control loops be demonstrated.

7. Communications Subsystem

The communications subsystem tests measure the input and output power of a particular channel under test over the dynamic range of interest, verifies the output power of each channel and demonstrates the channel power distribution capability, provides a test of the frequency generators, measure the end-to-end frequency response on the communication transponder and the carrier power-to-noise power ratio. Measurements of adjacent channel interference, bit error probability of the command channel, and phase linearity of the communications transponders are performed. The phase of the output signals is determined as a function of the input power. The spurious outputs and transmitter harmonics tests measure the unwanted signals outside the overall transmit band.

8. System Thermal Test

The objective of the system thermal test is to demonstrate acceptable system performance during conditions of thermal stress and provide performance baseline data for subsequent testing. The test is performed on the spacecraft with thermal instrumentation and mounted on a pedestal within the thermal chamber. The spacecraft is subjected to a series of seven thermal cycles with detailed performance measurements at the temperature extremes of the final cycle, as shown in Figure XII-5. During the thermal cycling, the spacecraft telemetry and selected performance parameters are monitored to detect status or anomalies. After the initial six thermal cycles, the chamber

temperature is reduced and stabilized at maximum low and the performance measurements are repeated. The chamber temperature is increase to the hot acceptance temperature limit, stabilized and the performance measurements taken. [TRW p. 365]

9. Integrated System Test

The integrated system test is a downscaled version of the spacecraft system test which is conducted within the series of environmental exposures to detect gross

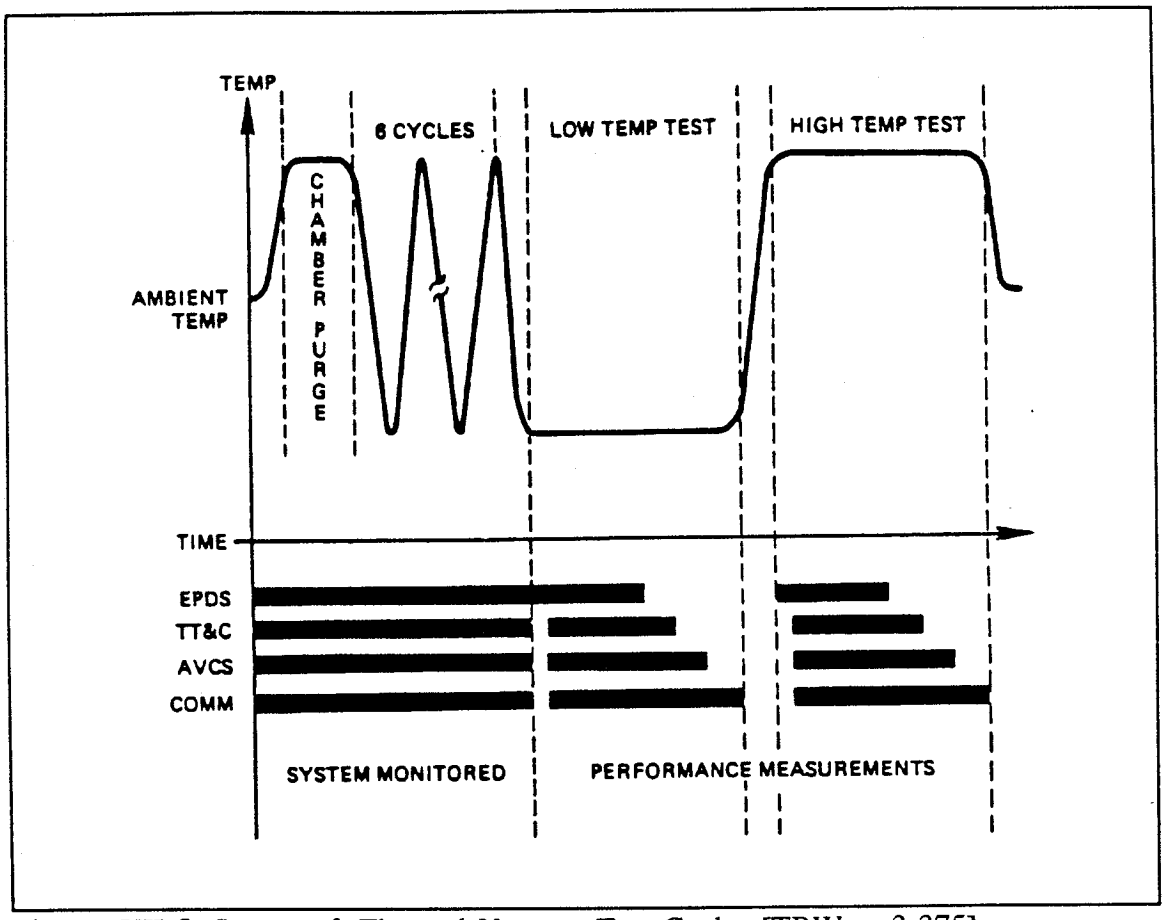

Figure XII-5 Spacecraft Thermal Vacuum Test Cycles [TRW p. 3-375]

functional failures which may occur as a result of these environments. The test is performed immediately preceding the thermal vacuum test with the spacecraft mounted

inside the chamber. All systems are activated in their normal operating modes.[TRW p. 376]

10. Communications Intermodulation Anechoic Test

The objectives of the anechoic chamber intermodulation test are to verify that the integrated spacecraft system meets performance requirements with respect to generated IM interference appearing in the payload receive band, and to provide baseline IM and antenna performance data before and after environmental exposures to verify that performance has not been affected. The test is conducted in an anechoic chamber with the spacecraft modules integrated without the solar arrays and with the antenna installed in the deployed configuration. Facility test probe antennas are placed in the near-field of the spacecraft antenna to provide the radiated uplinks and downlink.

11. System Alignment

System alignments, depicted in Figure XII-6, are performed at the spacecraft level to establish primary spacecraft coordinates and to ensure attitude and velocity control subsystem efficiency in minimizing pointing error and on orbit injection error. Final system alignments are performed after environmental exposure to compensate for structural relaxation during handling, environmental exposure, and/or component replacement. Primary spacecraft reference points are targeted and alignment of the thrusters, sensors, and antennas is accomplished during spacecraft module, payload module, and spacecraft integration. Alignments should be performed with an accuracy of 0.01 degree and 0.02 cm.[TRW p. 3-387]

12. Solar Array Illumination

The solar array performance characteristics are initially determined by the solar array illumination test. Subsequent illumination tests are accomplished in conjunction with visual inspections to monitor aliveness and physical integrity throughout the assembly process. The performance test is performed on each solar panel in a xenon flash test facility. Subsequent illumination tests are performed periodically after the solar panels have been assembled into solar arrays (sets of panels).[TRW p. 390]

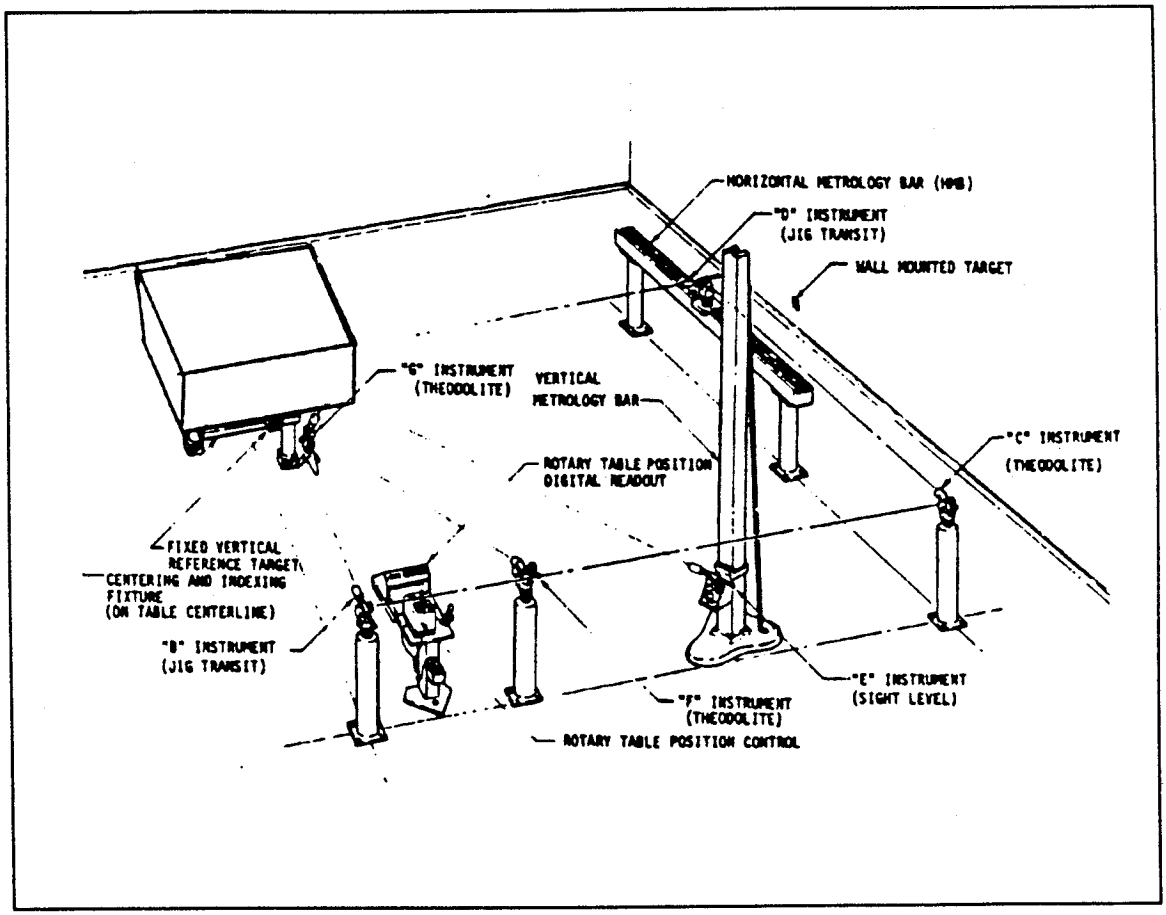

Figure XII-6 Spacecraft Alignment Test [TRW p. 3-387]

13. Solar Array Deployment

The objective of the solar array deployment test is to verify the functional adequacy of deployment hardware latches, and to verify unrestrained release in the flight configuration after dynamic test exposure. Outer panel deployment tests are performed with the solar arrays mounted on a fixture simulating the spacecraft/solar panel interface before being integrated to the spacecraft and on the fully configured spacecraft after environmental exposure. The panel motion is restrained with a variable speed motor, and deployment angle is measured with a potentiometer. Boom deployment tests are performed before and after dynamic test exposure with the boom mounted in a test setup that has a fixed simulated solar array drive and a movable mass simulated solar array that utilizes an air bearing table to simulate zero gravity as shown in Figure XII-7.[TRW 3-392]

14. Low-Level Sine Vibration

The objectives of the low-level sine vibration test are to demonstrate electrical integrity of all elements and the structural capability of those elements that are susceptible to sine vibration. The test serves as a demonstration of confidence in overall workmanship prior to committing the spacecraft to the series of functional environment tests and eventual flight. [TRW 3-394] The flight spacecraft is mounted on a shaker with the vibration input along the Z-axis at the adapter section. The spacecraft is in the flight configuration with solar array and antenna in the stowed configuration. The spacecraft functions are verified using telemetry during this test which all spacecraft elements are observed for workmanship within the limitations of the telemetry sampling rate during

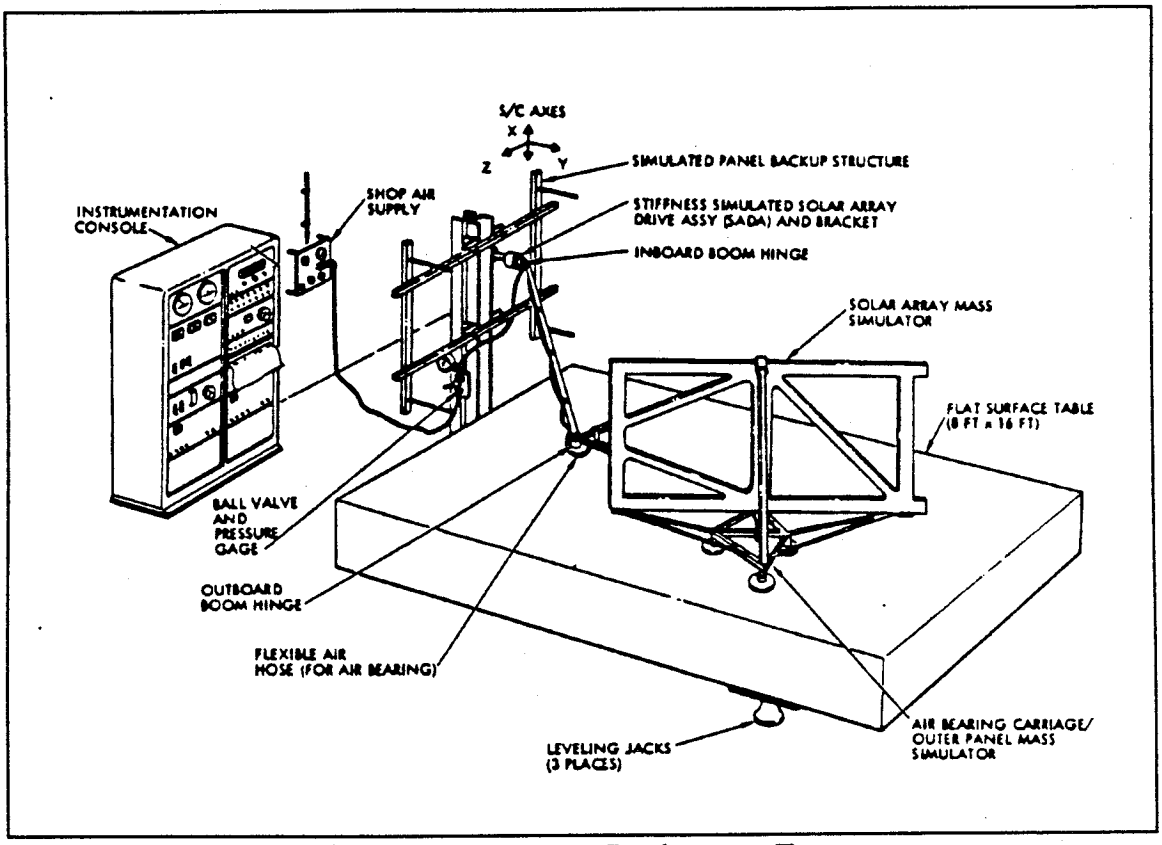

Figure XII-7 Spacecraft Solar Array Boom Deployment Test

vibration excitation. [TRW 3-396]

15. Acoustic Test

The acoustic test is performed to demonstrate that the spacecraft can withstand the acceptance acoustic environment without degradation of performance and without structural deformation. The spacecraft is in the electrical launch configuration and is on battery power with solar array and antenna in the stowed configuration. The spacecraft is placed in the acoustic chamber, the spacecraft is exposed to acceptance levels for 1 minute and the electrical status is verified via telemetry.[TRW 3-399]

16. Mechanical Inspection

Mechanical inspections are performed after dynamic environmental exposure to determine if any degradation of the solar array, antenna, thermal insulation, heat shields, and sensors has occurred. [TRW 3-401]

17. Thermal Vacuum Test

The thermal vacuum test has two prime objectives. The first objective is to verify through thermal performance, the integrity of the spacecraft thermal subsystem, in an induced thermal-vacuum environment of heat fluxes obtained during the qualification solar simulation test. Secondly, the thermal vacuum test verifies the integrity of the spacecraft by demonstrating flightworthy performance in a acceptance thermal-vacuum environment.

The performance tests to include will be ambient spacecraft functional test, thermal vacuum functional test, and spacecraft heater circuits functional test. Upon completion of the functional test, the thermal-vacuum chamber, depicted in Figure XII-8, is pumped down to 10^{-5} torr. During chamber transition, the spacecraft power and heat flux adjustments will be made to achieve orbital thermal equilibrium for the equinox condition. The heat flux sources will be set to simulate solar energy so that the resulting orbital average absorbed energy is equivalent to that experienced by the spacecraft during the equinox conditions resulting form the qualification solar simualtion test. This condition is maintained until thermal equilibrium is reached and includes up to three eclipses. Spacecraft equipment is powered on and the selected operational mode to

support the thermal objectives of interest and is continuously monitored for abnormal telemetry readings.

The next configuration is the summer solstice configuration where the average orbital heat fluxes obtained from qualification solar simulation test are simulated so that the resulting absorbed energy is equivalent to that experienced when the spacecraft is at summer solstice orientation.

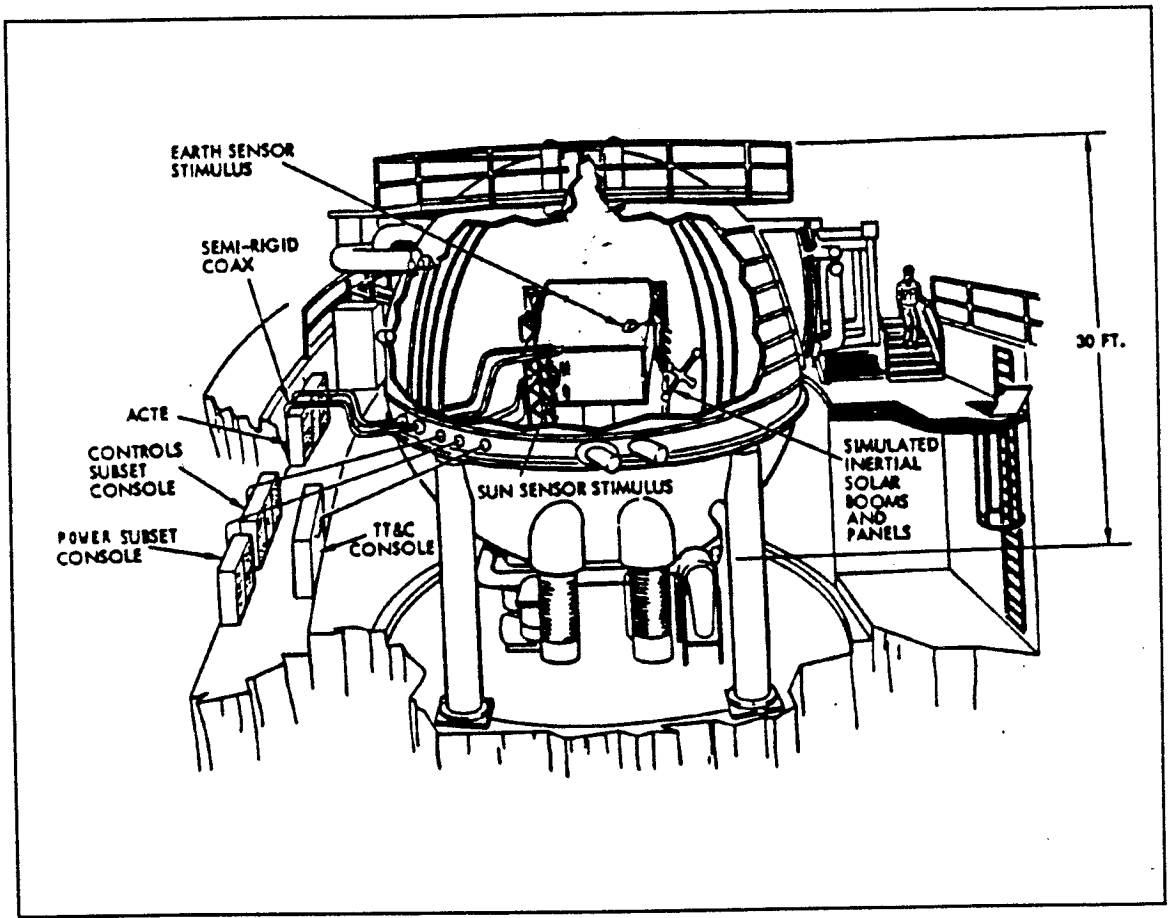

Figure XII-8 Spacecraft Thermal Vacuum Chamber Test

For the third thermal condition which is summer solstice diurnal extremes configuration, the diurnal extreme fluxes are simulated such that the resulting absorbed

energy approaches the diurnal extremes of an end-of-life summers solstice condition. The configuration results in the -Y side of the spacecraft is hot and the +Y side is cold.[TRW 3-404]

18. Phased Array Deployment Functional Test

The objective of the solar array deployment test is to verify the functional adequacy of deployment hardware latches, and to verify unrestrained release in the flight configuration after dynamic test exposure. Outer panel deployment tests are performed with the solar arrays mounted on a fixture simulating the spacecraft/solar panel interface before being integrated to the spacecraft and on the fully configured spacecraft after environmental exposure. The panel motion is restrained with a variable speed motor, and deployment angle is measured with a potentiometer.

19. Mass Properties

The mass property test objectives are to balance the spacecraft to reduce static and dynamic inbalance to within allowable flight tolerances. soacecraft weight is determined and is used at a later time with the apogee kick motor, propellant, and pressurant weights to determine spacecraft launch weight. Spacecraft mass properties are measured with the spacecraft fully integrated, less the apogee kick motor, propellant and with a minimum orf pressurant. [TRW 3-411] Spacecraft static and dynamic unbalance measurements about the spin axis are performed with the spacecraft mounted to a spin balance machine. Balanced weights are attached to the spacecraft to align the mass principal axis with the geometric Z-axis.[TRW p. 3-413]

THIS PAGE INTENTIONALLY LEFT BLANK

XIII. COST ANALYSIS

A. INTRODUCTION

This cost analysis is performed in order to determine the viability of the satellite program. Additionally, it provides an initial overall projected cost by segment (i.e., ground, space, user) and an expected revenue plan to recover costs.

1. Scope

The cost analysis encompasses three segments defined, in Ref. 1 as, the ground, space and user segments. Note that the space segment cost includes development, testing and launch of 48 satellites.

a. Operational Requirements

The costs incurred during the development, testing, launch and maintenance of the satellites over their life span are to be recovered with an appropriate profit margin.

b. Functional Requirements

In order to reduce launch costs, six satellites are packaged together for orbit insertion on the Delta II launch vehicle. When feasible, off the shelf components are chosen, and are to be procured in bulk quantities sufficient to meet the needs of the entire satellite building program. Costs for storage of the satellites are minimal, and

account for time between the build up of the first of the stack of six to the earliest possible launch date of the stack.

c. Restrictions/Constraints/Artificialities

Restrictions on a complete cost analysis model are primarily due to the scarcity of data for comparison. Historically, no space programs of the same class (i.e., small commercial satellites), have been built in such large quantities. Therefore, there are no appropriate cost models which provide accurate costs analysis across the board.

Not all components are individually accounted for in this cost analysis. Hence, individual components not accounted for are grouped according to classification (i.e., structure, payload, thermal, etc.) and are estimated as a percentage of the total known costs [Ref. 2]. Note that these costs also include integration factors, such as wiring harnesses.

Transportation to and from testing facilities and to the launch site are not included in the overall satellite costs, as these are not well defined parameters at this time.

As noted in Ref. 1, a proper cost analysis is performed utilizing the work breakdown structure as a costing framework. In this case, where the satellite buying program is so large and represents a historical landmark, the work packages are considered to offer the best alternative in arriving at the costs. Therefore this cost analysis should not be considered for use beyond Milestone 0, the feasibility study.

2. METHOD

a. Model Development

Various methods were employed for this cost analysis. Where component costs were available the bottom-up method of costing was utilized [Ref. 1]. As previously mentioned, some components were not individually priced and were grouped into categories based on their function. Costs for such components were formulated by use of Cost Equivalent Relationships (CER) obtained from Refs. 1 and 2. CER's are parametric equations based on historical cost data and rationalized to cost versus mass of the subsystem. Each parametric equation is limited in application by a range of applicable masses. Therefore even though components may have been identified, the parametric equations required that they be lumped together to form one total mass. Finally in formulating the model, costs of components which were not off-the-shelf, such as the payload antenna, overall structure and the SLD, reflect the additional cost of RDT&E amortized over the entire buy. As in the previous utilization of the CER's mass of the component was key in determining costs. By combining these two methods the first unit cost was established.

Finally, costs for testing of the satellites was formulated based on specific costs to test the entire satellite separately and as a stacked unit. Component level costs were not formulated since most components chosen were already flight qualified. Costs of testing the payload antenna are included in the costs of systems testing as a whole. These costs were formulated by use of CER's developed for testing. The total cost of testing was then amortized over the 48 satellites and applied to the first unit cost.

In determining the final cost of the program, a learning curve of 95% [Ref. 1], was assumed in determining the cost to produce each satellite (Appendix A). However, this may have led to a cost error of as much as 7%, since components costs which were quoted by the manufacturer or the Lockheed representative [Ref. 4], already are compensated for by that manufacturers learning rate.

b. Alternatives

The Unmanned Spacecraft Cost Model [Ref. 3] developed by the Air Force's Space Division in Los Angeles California was not utilized in the formulation of this analysis for numerous reasons.

Firstly, the model was developed as a cost estimating tool for Department Of Defense satellite acquisition programs. Several space component suppliers [Refs. 4, 5 and 6], state that a substantial savings in total costs are afforded if the buy is of a commercial nature. Secondly, the data base for the derivation of the parametric equations used in obtaining the CER's is not applicable to large procurement programs. Suppliers indicate that the large procurement quantities, if purchased at the most economic manufacturing rate, are significant drivers in providing the component at substantial savings.

c. Tradeoffs

(1) Formulation of The Model

In choosing not to utilize the Air Force's cost model the ability to price some of the components individually was diminished. However, by applying the

bottom-up approach for those components that can be identified, taking into account the size of the buy and the fact that it is commercial, and applying CER's [Ref. 1] to other groups more representative costs were obtained.

Since the expertise and resources for the formulation of a projected revenue generation scheme were not available, the decision was made to use Ref. 3 as a sole source for this information.

(2) Design Versus Cost Considerations

Whenever possible off-the-shelf flight qualified components were selected, as long as technological improvements for state of the art component, were not significant so as to degrade performance to unacceptable levels. This procurement policy leads to significant savings in manufacturing and testing. Further savings are realized if the purchase of the component can be scheduled so as to coincide with a buy from another ongoing program. However, this factor was not incorporated when determining component costs due to the uncertainty of the future market place and was only mentioned, so as to facilitate this sort of thinking in future more refined cost analysis of this program.

The optimum number of 6 satellites was in part driven by high launch costs. At a rate of $57.4 million per launch it was determined that the optimum size would allow stacking of enough satellites to fill an orbital plane.

In order to take advantage of volume buying discounts the decision was made to design for a single configuration, where all satellites can assume any

position in the stack. Testing costs were found to be less for a single configuration even though all satellites would need to meet the most rigorous launch conditions.

Weight of the torque rods was not a driving design constraint. This fact was important in Ithaco's cost estimate, where the more stringent the weight requirement the more costly the materials and manufacturing. The relation between weight and cost of manufacture was stated by Ithaco [Ref. 4], to be exponential in nature. This allowed some flexibility when determining the best cost versus weight design.

The size of the solar array was fixed using the less efficient silicon solar cell since, the cost of utilizing gallium arsenide cells doubled the cost of the array. Silicon cells, it was determined, would meet the specifications for power and weight hence, cost was the deciding factor.

An unexpected cost of $4 million per satellite to provide two axis solar array drive motors was allowed as this design was considered to be the only alternative available to keep from having to slew the satellite and payload antenna while tracking the sun for optimum solar array performance.

B. SEGMENT COSTS

Sections B.1 thru B.3 contain the estimated costs for ground, space and user segments respectively.

1. Ground Segment Costs

The ground segment costs consist of recurring and non-recurring costs associated with the development of two satellite control centers and six gateways as proposed in the GLOBALSTAR program by Loral [Ref. 3]. The projected cost of $31 million is $2 million more than Loral's estimate to account for the additional control center.

2. Space Segment Costs

Table XIII.1 below shows the launch cost, and component cost. Although Honeywell's reaction wheel assembly is more expensive than other manufacturers, their record of zero in flight failures is not matched in the industry. All other components were chosen by costs to procure.

3. User Segment Costs

User Segment costs are not included in this report as the specifications were not defined. This is unfortunate, since historically, the user segment costs can dwarf the space and ground segment costs, as for example in the GPS program.

C. TESTING COSTS

The cost of testing includes only the use of the testing facilities and the manhours to operate them. It does not include transportation cost to and from the test facility or, storage of the spacecraft awaiting tests. Table XIII.2 presents the cost of performing various test, based on a phone conversation with Joe Howser of the NRL [Ref. 7]. The test are broken down into qualification tests (performed on only the first six satellites)

Table XIII.1 Space Segment Costs

Component	First Unit Cost	Qty.	Total Cost	Manufacturer
Launch Vehicle				
Delta II	57.4	8	459.2	McDonald
Attitude Control				
RWA	0.250	96	12.00	Honeywell
Torque Rods	0.030	96	1.440	Ithaco
Magnometers	0.005	48	0.240	Ithaco
Safemode Sys.	0.750	48	36.000	Ithaco
ACC	1.200	48	57.600	Ithaco
Horizon Sensor	0.500	96	24.000	Applied Research Corp.
Sun Sensors	0.030	48	1.440	"
System Total Cost	2.824	48	135.552	
Electric Power				
Solar Panel	0.514	96	24.672	ASEC
Battery Ni-H_2	0.050	48	2.400	Eagle-Pitcher
Array Tracking Motors	0.800	192	38.400	Honeywell
System Total Cost	1.364	48	65.472	
Propulsion				
Thrusters	0.120	288	5.76	Rocor
Propellant Tank (includes plumbing and heating)	0.175	48	8.4	TRW
System Total Cost	0.295	48	14.160	
Thermal				
Louvers	0.654	96	31.392	Fairchild
Heater blankets, Radiators,Insulation	1.321	48	63.408	N/A
Subtotal	1.975	48	94.800	

1. Costs in millions of 1990 dollars.

and acceptance tests (performed on all satellites). Concurrent thermal vacuum and thermal balance testing is assumed.

Table XIII.1 Space Segment Costs (Continued)

Payload				
Antenna	1.231	48	59.124	Antennas Of America
Comm. Elect. Pkg.	3.820	48	183.36	N/A
System Total Cost	5.051	48	242.448	
TT&C				
RTU and RCU	1.309	48	62.848	N/A
Structure				
Spacecraft	1.056	48	50.688	N/A
SLD	3.435	6	27.485	N/A
System Total Cost	4.491		78.173	
G&A Satellite Program	2.89	48	138.72	
Insurance (Launch/ On-orbit)	2.313	48	111.0	
Total Including Component Level Testing	19.654	48	680.89	

D. LAUNCH AND IN ORBIT INSURANCE COSTS

According to Ref. 2, insurance costs are about 16% of the total cost of the program. Therefore insurance will cost $111.552 million.

E. SUMMARY OF COSTS

Theoretical First Unit Cost (TFUC), including the amortized system test costs, launch and orbit insurance is $21.728 million dollars. The total cost of the procurement of 48 satellites is $753.231 million dollars, which reflects a learning curve of 95% applied over the entire buy [Ref. 2].

Table XIII.2 Testing Costs

Test Type	Cost ($M)
Qualification Testing	
Acoustic/Vibration	0.06
Pyrotechnic	0.005
Thermal Vacuum	0.316
Thermal Balance	N/A
Thermal Cycling	N/A
Static	0.0133
Acceptance Testing	
Acoustic/Vibration	0.639
Thermal Vacuum/Balance	2.532
Total Cost Of Testing	3.553
Planning Test Formulation	2.000
Cost Of Testing Amortized Over 48 Satellites	2.074

1. Costs in millions of 1990 dollars.

F. REVENUE GENERATION

Revenue generated from this program is broken down by year for RDSS service. Table XIII.3 presents the revenue schedules for RDSS services [Ref. 3]. This estimate is based on achieving a 40% share of the US market by the year 2006. The incorporation of international markets is expected to significantly increase this revenue base. It is interesting to note that viability of the system is achieved by accounting for only the US market.

Revenues from mobile voice and data service are expected to ramp up from $77 million in 1997 to $574 million in 2006 and will level off after this [Ref. 4]. Therefore it is estimated that within 5 years the revenue generated from this program will $986.80 million dollars, yielding a profit margin of 26.40%.

Table XIII.3 Revenue From RDSS Service [Ref. 3]

Year	RDSS Customers ($x10^3$)	Total Annual Revenue ($x10^6$ Dollars)
1997	212	64.3
1998	271	76.3
1999	338	88.9
2000	412	102.1
2001	416	98.2
2002	419	94.3
2003	422	94.9
2004	424	95.5
2005	427	96.0
2006	441	99.2

G. REFERENCES

1. Wertz, J.R., and Larson, W.J., *Space Mission Analysis And Design*, Kluwer Academic Publishers, 1991.

2. Elbert, B.R., *Introduction To Satellite Communication*, Artech House,1987

3. Loral Cellular Space Division, *GLOBALSTAR Licensing Proposal*,1990

4. Interview between Kevin Vogler,Locheed,Missles&Space Company, Sunnyvale Ca.,October 1991.

5. Telephone conversation between J.C.Kinker,Honeywell Corp., and the author,3december1991.

6. Telephone conversation between J. Krebs, Ithaco Corp., and the author,4December1991.

7. Phone conversation between J.Houser, NRL, and Lieutenant J. Racine,November1991.

APPENDIX A

THIS PAGE INTENTIONALLY LEFT BLANK

THIS PAGE INTENTIONALLY LEFT BLANK

APPENDIX A

STATEMENT OF WORK

SPECIFICATION DEFINITION

SIZE

The satellite shall be designed to fit within the envelope requirements of the Ariane and Delta launch vehicles in a multiple launch configuration such that an entire orbital plane shall be filled using a single launch vehicle.

MASS

The satellite mass prior to launch shall be compatible with the mission requirements and the designated launch configuration including the required adapters.

STABILIZATION

The satellite shall be stabilized during all phases of the mission. If the satellite is passively stabilized, the ratio of the spin axis moment of inertia to the maximum transverse moment of inertia shall be greater than 1.05 under all possible propellant loadings.

MISSION REQUIREMENTS

Orbits

The satellite shall be designed to operate in Low Earth Orbits (LEO) at any specified inclination and at altitudes of between 500 and 900 nmi. The design of the constellation orbits shall minimize the number of on-orbit satellites while achieving all mission requirements.

Orbit and Attitude Correction

The satellite shall be designed to provide a "delta velocity" capability to change or correct the appropriate orbit parameters up to 50 meters per second per year over the mission lifetime, including attitude orientation, orbit injection, orbit maintenance, and End of Life (EOL) deorbit. Attitude corrections needed to meet the performance requirements of the payload shall be minimized.

MISSION LIFE

The satellite shall be designed for an operational mission life of 5.0 years.

RELIABILITY

The satellite design shall be such that the probability of successfully arriving in the correct orbit oriented in the proper operational attitude (assuming successful launch and separation) shall be 0.99; assuming initial correct

functioning in the required operational attitude the on-station reliability shall be estimated by the contractor.

ENVIRONMENT

Launch Environment

The satellite shall be designed to meet all performance requirements specified after exposure to the launch environments of the specified launch vehicles.

On-Orbit Environment

The design and application of satellite parts and materials shall be such as to ensure all performance specifications are met throughout the mission life of the satellite when operated in all expected environments. The satellite shall be designed to minimize energy storage due to differential charging and shall not be effected by uniform charging.

Unattended Operation

The satellite shall survive without degradation for periods of up to 10 hours without any RF command uplink.

COMMUNICATIONS SUBSYSTEM

The satellite communications subsystem comprises L and C band transponders capable of supporting a variety of communication signals between fixed ground stations and/or mobile units over a portion of the visible earth's surface.

The payload mass and d.c. power requirements of the payload range around 60 kg and 800 watts peak for 20 minutes, with a maximum antenna size of 5.6 square meters. The antenna pointing accuracy target is +/- 1° (1 σ).

TELEMETRY, TRACKING AND CONTROL (TT&C)

The TT&C system shall provide the necessary monitoring and control of the satellite throughout all mission phases including ground system testing, injection into orbit, and operation. The system shall be designed to permit the detection of satellite degradation and anomalous performance during all phases of the mission.

It shall be possible to operate the TT&C system in any mode without degradation of, or interference to, any sub-system. The TT&C system shall retain maximum operational capability under abnormal or emergency conditions including any anomalous attitude. It is envisaged that for the latter mode of operation that the TT&C system shall be accessed via a wide coverage antenna which shall be permanently connected.

Frequencies

The frequencies for the TT&C system shall be within the payload frequencies. The design of the command system shall minimize the effects of adjacent RF carriers.

TELECOMMAND AND TELEMETRY FORMAT AND QUALITY

The telecommand format shall provide a means of uniquely addressing each spacecraft of a series so that the probability of commanding another satellite of the same series when illuminated by equivalent RF flux density is less than 1 part in 10^9. The decoded bit error rate for both Telemetry and Telecommand services shall be superior to 1 part in 10^7 over the nominal range of RF flux densities to be specified.

HAZARDOUS TELECOMMANDS

A hazardous telecommand is defined as that which, if executed, could cause the specified mission life of the satellite to be reduced or jeopardized or constitute a safety hazard.

The design of the satellite shall preclude the accidental execution of any hazardous command. Initiation of one shot operations involving hazardous commands shall require at least two separate actions, command and execution, each being verification by telemetry.

ATTITUDE CONTROL SYSTEM (ACS)

The Attitude Control System shall sense the satellite orientation for attitude determination and shall provide attitude control to ensure that the satellite meets all attitude and orbit performance requirements throughout the mission. Performance shall be maintained during periods of attitude sensor interference by the sun or the moon. The ACS must provide the following functions:

- Provide attitude sensor data via the telemetry system for ground processing to determine the satellite orientation about all three axes;

- Provide orientation control and stabilization during transition from the pre-operational to the operational configuration including acquisition of the operational attitude;

- Deployment of appendages, and antenna earth capture;

- Maintain accurate antenna pointing with reference to the earth's disc;

- Provide recovery from predictable failure modes.

ACS Failure Modes

The overall design objectives regarding failure modes shall be to maintain the mission performance required by the communications sub-system. This may

be accomplished by means of either automatic detection and reconfiguration or by ground based failure identification and recovery.

Transition from Post Launch to Operational Configuration

The transition from the pre-operational configuration shall be initiated and controlled by either:

a) ground command, or
b) automatic control of the satellite attitude which shall be maintained throughout the duration of the transition.

Antenna earth capture shall be performed automatically on board the satellite with ground participation normally restricted to telecommand initialization of the capture sequence.

Sensors and Actuators

There shall be no obstruction in the field of view of the attitude sensors. There shall exist the capability of detecting the sun and moon interference and providing interference rejection. Sensor performance shall not be permanently degraded after exposure to sun or moon illumination.

All actuators shall be capable of providing a minimum torque factor of two under the worst case conditions.

Power System Interface

The ACS shall remain operational and shall maintain satellite stability during power bus fault clearance (i.e. fuse blowing or circuit breaker operation). Battery power shall be sufficient to operate the ACS and RCS in the event that the satellite is in eclipse.

REACTION CONTROL SYSTEM (RCS)

The RCS shall be capable of providing the velocity increments and control torques required during all phases of the mission.

The RCS shall, in conjunction with the ACS, provide for control of the satellite attitude stability and orbit adjustment during all phases of the mission.

POWER SYSTEM

The Power System will generate, store, condition, and distribute the electrical power required to ensure that the satellite meets all performance requirements during all phases of the mission. The design shall include an array of solar cells to provide electrical power during operation in sunlight and a battery sub-system to provide all electrical power required during operation in eclipse. A battery charge system shall be provided to supply suitable charge currents based on the characteristics of the selected battery

type and shall be capable of continuously trickle-charging the battery sub-system between eclipse periods. The Power System shall be stable under all predictable mission conditions and shall incorporate appropriate under and over-voltage protection.

Electromagnetic Interference (EMI)

Electrical or magnetic interference including switching transients shall not affect the performance of the Power System or any other satellite system throughout the mission.

THERMAL SYSTEM

The satellite design shall be such that satisfactory temperature environments shall be maintained for all components during pre-launch operation, launch, separation sequences, pre-operational and operational stages of the mission including eclipse periods plus on-orbit storage. Thermal control shall, as a goal, be achieved, to the maximum extent possible, by passive means (i.e. excluding moving parts, but may include heaters with automatic control with ground command override capability).

The thermal system shall be designed to maintain all equipments within operating on-orbit temperature units with a design margin of 15 C between these ranges and those over which the equipments are to be qualified.

STRUCTURAL SYSTEM

The Structural System shall provide a stable mechanical support for the satellite systems under all expected environments over the life of the satellite. The structure shall have, and maintain, the necessary dimensional stability through all phases of the mission including the launch phase.

THIS PAGE INTENTIONALLY LEFT BLANK

APPENDIX B

THIS PAGE INTENTIONALLY LEFT BLANK

THIS PAGE INTENTIONALLY LEFT BLANK

APPENDIX B

Moments of Inertia:

All moments for the SLD assembly are calculated via spreadsheet using Microsoft Excel. The upper rail has been modeled in two pieces, the square box and the supporting cylinder.

Strength Calculations:

The deployment canister will be designed to withstand an 8.5g axial load and a 15g lateral load. The material properties for each component are listed in the table below

Deployment Rails:

for the upper rail (attached to canister)

w=width	2.54	cm
h=height	2.54	cm
l=length	98	cm
r=radius	1/3h	cm
density	2.71	g/cm^3
t_{wall}	.2	cm
t_{slide}	.4	cm
yield	3170.5	kg/cm^2

mass = density * volume = 2.18kg

load=(s/c mass*8.5g)/(2_{walls}*t_{wall}*2_{rails})=39.73 kg/cm^3

this load is well below the allowable yield strength for aluminum.

Honeycomb Panels:

The strength of a panel is geometry dependant. Using the dimensions below and formula for a panel simply supported on the edges (note: English units are used to conform with reference material.)

R=length	1.52	m
r=width	1.0	m
k=const	1.15	cm
p=load	1609	kg
p^1=1.1xp	1770	kg
t_p=thick	2.557	cm
S_m	calc	lb/in

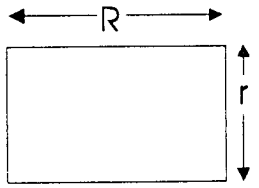

R/r=1.5 k=.454 arguments of ref 5.

$S_m = k * p^1/t^2 = 315.7 lb\backslash in^2$

S_m is the entering argument for the chart in the Astech Manual of honeycomb panel sheer strengths. Using Fig 2.3.2.1 from the Astech design manual; A 1in thick, 1/4in B cell, titanium core panel with a titanium face sheet thickness of .0035in is required to

support the launch loads. The resulting core density is 6.5 lb/ft^3.(ref 6).

panel mass=density * volume = 4.37 kg

U-Channel Members:

The maximum moment occurs at the lowest point that the U-Channel attaches to the SLD. Here the moment is due to all six spacecraft and the SLD itself above that point.

$M=S*I/C \qquad I/C=(BH^3-bh^3)/6H$

Moment on each U-Channel = 3024.7 ft lbs

GSL = 626.23 ft lbs

From reference 5 the Greatest Safe Load (GSL) in a channel beam is found by modifying the moment by a geometry dependant factor S (=4.83)

GSL = (3050*Area*H)/l

Where l is length between supports. To find the proper dimensions for the channel: multiply GSL by a 10% margin of safety. Use L as length between supports enter a beam width "H" and solve for area. The results of these iterations gave the dimensions below.

H	8.23cm
h	6.15cm
B	2.54cm
b	1.27cm
C	1.05cm

	MOMENTS OF INERTIA OF SLD WITHOUT SPACECRAFT					
ITEM			ITEM DIMENSIONS (CM)			MASS(KG)
		radius(x,y)	x	y	z	
rail body box			90	2.54	2.54	1.57
rail body box			90	2.54	2.54	1.57
rail body box			90	2.54	2.54	1.57
rail body box			90	2.54	2.54	1.57
rail body box			90	2.54	2.54	1.57
rail body box			90	2.54	2.54	1.57
rail body box			90	2.54	2.54	1.57
rail body box			90	2.54	2.54	1.57
rail body box			90	2.54	2.54	1.57
rail body box			90	2.54	2.54	1.57
rail body box			90	2.54	2.54	1.57
rail body box			90	2.54	2.54	1.57
rail body cylinder		0.89	90			0.61
rail body cylinder		0.89	90			0.61
rail body cylinder		0.89	90			0.61
rail body cylinder		0.89	90			0.61
rail body cylinder		0.89	90			0.61
rail body cylinder		0.89	90			0.61
rail body cylinder		0.89	90			0.61
rail body cylinder		0.89	90			0.61
rail body cylinder		0.89	90			0.61
rail body cylinder		0.89	90			0.61
rail body cylinder		0.89	90			0.61
rail body cylinder		0.89	90			0.61
panel 1			152	100	2.558	4.37
panel 2			152	100	2.558	4.37
panel 3			152	100	2.558	4.37
panel 4			152	100	2.558	4.37
panel 5			152	100	2.558	4.37
panel 6			152	100	2.558	4.37
			H	B		
frame member 1			8.23	2.54	506.3	18.119
frame member 2			8.23	2.54	506.3	18.119
frame member 3			2.54	8.23	506.3	18.119
frame member 4			2.54	8.23	506.3	18.119
frame member 5			8.23	2.54	506.3	18.119
frame member 6			8.23	2.54	506.3	18.119
			ID	OD	thickness	
adaptor mating surface			87.6	121.5	1.5	33.4
					system total	194.494
wiring and fasteners						3
				SUBTOTAL MASS		197.494
				10% MASS MARGIN		19.7494
				TOTAL MASS		217.2434

ITEM MOMENTS (KG*M^2)					ITEM POSITION (CM)	
Ix	Iy	Iz		x	y	z
0.002025802	1.272712901	1.272712901		-47.73	0	250.04
0.002025802	1.272712901	1.272712901		47.73	0	250.04
0.002025802	1.272712901	1.272712901		-47.73	0	166.08
0.002025802	1.272712901	1.272712901		47.73	0	166.08
0.002025802	1.272712901	1.272712901		-47.73	0	82.12
0.002025802	1.272712901	1.272712901		47.73	0	82.12
0.002025802	1.272712901	1.272712901		-47.73	0	-1.83
0.002025802	1.272712901	1.272712901		47.73	0	-1.83
0.002025802	1.272712901	1.272712901		-47.73	0	-85.79
0.002025802	1.272712901	1.272712901		47.73	0	-85.79
0.002025802	1.272712901	1.272712901		-47.73	0	-169.75
0.002025802	1.272712901	1.272712901		47.73	0	-169.75
0.04118708	2.41591E-05	0.04118708		47.73	0	247.88
0.04118708	2.41591E-05	0.04118708		-47.73	0	247.88
0.04118708	2.41591E-05	0.04118708		47.73	0	163.92
0.04118708	2.41591E-05	0.04118708		-47.73	0	163.92
0.04118708	2.41591E-05	0.04118708		-47.73	0	79.96
0.04118708	2.41591E-05	0.04118708		47.73	0	79.96
0.04118708	2.41591E-05	0.04118708		-47.73	0	-3.99
0.04118708	2.41591E-05	0.04118708		47.73	0	-3.99
0.04118708	2.41591E-05	0.04118708		-47.73	0	-87.95
0.04118708	2.41591E-05	0.04118708		47.73	0	-87.95
0.04118708	2.41591E-05	0.04118708		-47.73	0	-171.91
0.04118708	2.41591E-05	0.04118708		47.73	0	-171.91
4.37285945	10.09930745	14.466448		0	0	252.62
4.37285945	10.09930745	14.466448		0	0	168.66
4.37285945	10.09930745	14.466448		0	0	84.7
4.37285945	10.09930745	14.466448		0	0	0.75
4.37285945	10.09930745	14.466448		0	0	-83.21
4.37285945	10.09930745	14.466448		0	0	-167.17
38.70613116	38.71538413	0.006872843		-77.3	-41.27	0.75
38.70613116	38.71538413	0.006872843		-77.3	41.27	0.75
38.71538413	38.70613116	0.006872843		-47.73	51.3	0.75
38.71538413	38.70613116	0.006872843		47.73	51.3	0.75
38.70613116	38.71538413	0.006872843		77.3	41.27	0.75
38.70613116	38.71538413	0.006872843		77.3	-41.27	0.75
18.25489943	18.25489943	37.4681367		0	0	254.15

	CENTER OF MASS CONTRIBUTION				DISTANCE FROM CENTER (cm)		
	Cx	Cy	Cz		Dx	Dy	Dz
	-74.9361	0	392.5628		47.73	8.55726526	200.672438
	74.9361	0	392.5628		47.73	8.55726526	200.672438
	-74.9361	0	260.7456		47.73	8.55726526	116.712438
	74.9361	0	260.7456		47.73	8.55726526	116.712438
	-74.9361	0	128.9284		47.73	8.55726526	32.7524381
	74.9361	0	128.9284		47.73	8.55726526	32.7524381
	-74.9361	0	-2.8731		47.73	8.55726526	51.1975619
	74.9361	0	-2.8731		47.73	8.55726526	51.1975619
	-74.9361	0	-134.6903		47.73	8.55726526	135.157562
	74.9361	0	-134.6903		47.73	8.55726526	135.157562
	-74.9361	0	-266.5075		47.73	8.55726526	219.117562
	74.9361	0	-266.5075		47.73	8.55726526	219.117562
	29.1153	0	151.2068		47.73	8.55726526	198.512438
	-29.1153	0	151.2068		47.73	8.55726526	198.512438
	29.1153	0	99.9912		47.73	8.55726526	114.552438
	-29.1153	0	99.9912		47.73	8.55726526	114.552438
	-29.1153	0	48.7756		47.73	8.55726526	30.5924381
	29.1153	0	48.7756		47.73	8.55726526	30.5924381
	-29.1153	0	-2.4339		47.73	8.55726526	53.3575619
	29.1153	0	-2.4339		47.73	8.55726526	53.3575619
	-29.1153	0	-53.6495		47.73	8.55726526	137.317562
	29.1153	0	-53.6495		47.73	8.55726526	137.317562
	-29.1153	0	-104.8651		47.73	8.55726526	221.277562
	29.1153	0	-104.8651		47.73	8.55726526	221.277562
	0	0	1103.9494		0	8.55726526	203.252438
	0	0	737.0442		0	8.55726526	119.292438
	0	0	370.139		0	8.55726526	35.3324381
	0	0	3.2775		0	8.55726526	48.6175619
	0	0	-363.6277		0	8.55726526	132.577562
	0	0	-730.5329		0	8.55726526	216.537562
	-1400.5987	-747.77113	13.58925		77.3	49.8272653	48.6175619
	-1400.5987	747.77113	13.58925		77.3	32.7127347	48.6175619
	-864.81987	929.5047	13.58925		47.73	42.7427347	48.6175619
	864.81987	929.5047	13.58925		47.73	42.7427347	48.6175619
	1400.5987	747.77113	13.58925		77.3	32.7127347	48.6175619
	1400.5987	-747.77113	13.58925		77.3	49.8272653	48.6175619
	0	0	8488.61		0	8.55726526	204.782438
		CENTER OF MASS OFFSET(cm)					
	0	8.55726526	49.36756191				

	TOTAL MOMENT OF INERTIA (KG*M^2)					
	Ixx	Iyy	Izz	Ixy	Ixz	Iyz
	6.33582251	7.95268301	1.64187951	0.06412481	-1.50376099	-0.26960154
	6.33582251	7.95268301	1.64187951	-0.06412481	1.50376099	-0.26960154
	2.15214394	3.76900444	1.64187951	0.06412481	-0.87459749	-0.15680207
	2.15214394	3.76900444	1.64187951	-0.06412481	0.87459749	-0.15680207
	0.18193979	1.79880029	1.64187951	0.06412481	-0.245434	-0.04400259
	0.18193979	1.79880029	1.64187951	-0.06412481	0.245434	-0.04400259
	0.42504929	2.04190979	1.64187951	0.06412481	0.38365456	0.06878345
	0.42504929	2.04190979	1.64187951	-0.06412481	-0.38365456	0.06878345
	2.88153036	4.49839085	1.64187951	0.06412481	1.01281806	0.18158292
	2.88153036	4.49839085	1.64187951	-0.06412481	-1.01281806	0.18158292
	7.55148584	9.16834634	1.64187951	0.06412481	1.64198155	0.29438239
	7.55148584	9.16834634	1.64187951	-0.06412481	-1.64198155	0.29438239
	2.44949239	2.54282996	0.18462124	-0.02491473	0.57797492	-0.10362214
	2.44949239	2.54282996	0.18462124	0.02491473	-0.57797492	-0.10362214
	0.84611184	0.93944941	0.18462124	-0.02491473	0.33352286	-0.05979559
	0.84611184	0.93944941	0.18462124	0.02491473	-0.33352286	-0.05979559
	0.10274365	0.19608122	0.18462124	0.02491473	-0.0890708	-0.01596904
	0.10274365	0.19608122	0.18462124	-0.02491473	0.0890708	-0.01596904
	0.21932271	0.31266028	0.18462124	0.02491473	0.15535214	0.02785228
	0.21932271	0.31266028	0.18462124	-0.02491473	-0.15535214	0.02785228
	1.1958768	1.28921437	0.18462124	0.02491473	0.3998042	0.07167883
	1.1958768	1.28921437	0.18462124	-0.02491473	-0.3998042	0.07167883
	3.03244324	3.12578081	0.18462124	0.02491473	0.64425626	0.11550538
	3.03244324	3.12578081	0.18462124	-0.02491473	-0.64425626	0.11550538
	22.4580085	28.1524564	14.4984481	0	0	-0.76006756
	10.6236692	16.3181171	14.4984481	0	0	-0.44609704
	4.95040213	10.64485	14.4984481	0	0	-0.13212653
	5.43778218	11.1322301	14.4984481	0	0	0.18180658
	12.0859255	17.7803734	14.4984481	0	0	0.4957771
	24.8951409	30.5895888	14.4984481	0	0	0.80974761
	47.4873662	53.8247409	15.332007	6.97880029	6.8093694	4.38929179
	44.9278159	53.8247409	12.7724567	-4.58174137	6.8093694	-2.88167005
	46.308348	47.1166452	7.44489316	-3.69647663	4.20454336	-3.76521436
	46.308348	47.1166452	7.44489316	3.69647663	-4.20454336	-3.76521436
	44.9278159	53.8247409	12.7724567	4.58174137	-6.8093694	-2.88167005
	47.4873662	53.8247409	15.332007	-6.97880029	-6.8093694	4.38929179
	158.565206	158.320628	37.7127142	0	0	-5.85294133
		TOTAL SLD MOMENTS				
	571.211119	657.7408	217.720126	0	1.7764E-15	-9.99910187

THIS PAGE INTENTIONALLY LEFT BLANK

APPENDIX C

THIS PAGE INTENTIONALLY LEFT BLANK

THIS PAGE INTENTIONALLY LEFT BLANK

PANEL DESIGN WORKSHEET			
ANTIEARTH PANEL (+Z)			
OBJECTS MOUNTED:		MASS (KG)	
MULTILAYER INSULATION		1	
EARTH PANEL (-Z)			
OBJECTS MOUNTED:		MASS(KG)	
MULTILAYER INSULATION		1	
TORQUE ROD		2	
ANTENNA		10	
	TOTAL	13	
X PANEL			
OBJECTS MOUNTED:		MASS(KG)	
MULTILAYER INSULATION		1	
MOMENTUM WHEEL		6.8	
TIMING CONTROL UNIT		20	
POWER CONTROL UNIT		6	
SOLAR ARRAY DRIVE		2	
SOALR PANELS		16	
2 THRUSTERS		0.638	
	TOTAL	52.438	
(-X) PANEL			
OBJECTS MOUNTED:		MASS(KG)	
MULTILAYER INSULATION		1	
FLIGHT COMPUTER		3	
SOLAR ARRAY DRIVE		2	
SOLAR ARRAY PANELS		16	
MOMENTUM WHEEL		6.8	
2 THRUSTERS		0.638	
TORQUE ROD		1	
	TOTAL	30.438	
(+Y) PANEL			
OBJECTS MOUNTED:		MASS	
2 BATTERIES		15	
REMOTE COMMAND UNIT		6	
REMOTE TELEMETRY UNIT		8	
C/L BAND TRANSPONDER		10	
THERMAL CONTROL		10	
	TOTAL	49	

(-Y) PANEL			
OBJECTS MOUNTED:		MASS	
2 BATTERIES		15	
REMOTE COMMAND UNIT		6	
REMOTE TELEMETRY UNIT		8	
L/C TRANSPONDER		10	
THERMAL CONTROL		10	
	TOTAL	49	
ANTIEARTH PANEL			
LENGTH OF PANEL (b) (M)			1.14
WIDTH OF PANEL (a) (M)			0.98
THICKNESS OF PANEL (t) (M)			0.0001
VOLUME OF MATERIAL(M^3)			0.000112
APPROXIMATE MASS OF PANEL (KG)			1.5
GAMMA (MASS PER UNIT AREA)			1.342642
YOUNG'S MODULUS (PSI)			9.90E+06
YOUNG'S MODULUS (SI UNITS)			6.83E+10
POISSON'S RATIO			0.33
FUND. NATURAL FREQUENCY (HZ)			30
BETA			18.47
ASPECT RATIO			1.163265
HONEYCOMB HEIGHT (M)			0.0254
PANEL STIFFNESS FACTOR			3.83E+10
APPROX. FACE THICKNESS (mm)			0.00522
EARTH PANEL			
LENGTH OF PANEL (b) (M)			1.14
WIDTH OF PANEL (a) (M)			0.98
THICKNESS OF PANEL (t) (M)			0.0001
VOLUME OF MATERIAL(M^3)			0.000112
APPROXIMATE MASS OF PANEL (KG)			13
GAMMA (MASS PER UNIT AREA)			11.63623
YOUNG'S MODULUS (PSI)			9.90E+06
YOUNG'S MODULUS (SI UNITS)			6.83E+10
POISSON'S RATIO			0.33
FUND. NATURAL FREQUENCY (HZ)			30
BETA			18.47
ASPECT RATIO			1.163265
HONEYCOMB HEIGHT (M)			0.0254
PANEL STIFFNESS FACTOR			3.83E+10
APPROX. FACE THICKNESS (mm)			0.04524

X PANEL	
LENGTH OF PANEL (b) (M)	1.14
WIDTH OF PANEL (a) (M)	0.6
THICKNESS OF PANEL (t) (M)	0.0001
VOLUME OF MATERIAL(M^3)	6.84E-05
APPROXIMATE MASS OF PANEL (KG)	52.438
GAMMA (MASS PER UNIT AREA)	76.66374
YOUNG'S MODULUS (PSI)	9.90E+06
YOUNG'S MODULUS (SI UNITS)	6.83E+10
POISSON'S RATIO	0.33
FUND. NATURAL FREQUENCY (HZ)	30
BETA	12.72
ASPECT RATIO	1.9
HONEYCOMB HEIGHT (M)	0.0254
PANEL STIFFNESS FACTOR	3.83E+10
APPROX. FACE THICKNESS (mm)	0.088299
(-X) PANEL	
LENGTH OF PANEL (b) (M)	1.14
WIDTH OF PANEL (a) (M)	0.6
THICKNESS OF PANEL (t) (M)	0.0001
VOLUME OF MATERIAL(M^3)	6.84E-05
APPROXIMATE MASS OF PANEL (KG)	30.438
GAMMA (MASS PER UNIT AREA)	44.5
YOUNG'S MODULUS (PSI)	9.90E+06
YOUNG'S MODULUS (SI UNITS)	6.83E+10
POISSON'S RATIO	0.33
FUND. NATURAL FREQUENCY (HZ)	30
BETA	12.72
ASPECT RATIO	1.9
HONEYCOMB HEIGHT (M)	0.0254
PANEL STIFFNESS FACTOR	3.83E+10
APPROX. FACE THICKNESS (mm)	0.051254

YPANEL	
LENGTH OF PANEL (b) (M)	0.98
WIDTH OF PANEL (a) (M)	0.6
THICKNESS OF PANEL (t) (M)	0.0009
VOLUME OF MATERIAL(M^3)	0.000529
APPROXIMATE MASS OF PANEL (KG)	49
GAMMA (MASS PER UNIT AREA)	83.33333
YOUNG'S MODULUS (PSI)	9.90E+06
YOUNG'S MODULUS (SI UNITS)	6.83E+10
POISSON'S RATIO	0.33
FUND. NATURAL FREQUENCY (HZ)	30
BETA	13.76
ASPECT RATIO	1.633333
HONEYCOMB HEIGHT (M)	0.0254
PANEL STIFFNESS FACTOR	3.83E+10
APPROX. FACE THICKNESS (mm)	0.082021
(-Y)PANEL	
LENGTH OF PANEL (b) (M)	0.98
WIDTH OF PANEL (a) (M)	0.6
THICKNESS OF PANEL (t) (M)	0.0001
VOLUME OF MATERIAL(M^3)	5.88E-05
APPROXIMATE MASS OF PANEL (KG)	49
GAMMA (MASS PER UNIT AREA)	83.33333
YOUNG'S MODULUS (PSI)	9.90E+06
YOUNG'S MODULUS (SI UNITS)	6.83E+10
POISSON'S RATIO	0.33
FUND. NATURAL FREQUENCY (HZ)	30
BETA	13.76
ASPECT RATIO	1.633333
HONEYCOMB HEIGHT (M)	0.0254
PANEL STIFFNESS FACTOR	3.83E+10
APPROX. FACE THICKNESS (mm)	0.082021

PANEL DESIGN WORKS			
ANTIEARTH PANEL (+			
OBJECTS MOUNTED:			MASS (KG)
MULTILAYER INSULATI			1
EARTH PANEL (-Z)			
OBJECTS MOUNTED:			MASS(KG)
MULTILAYER INSULATI			1
TORQUE ROD			2
ANTENNA			10
		TOTAL	=SUM(D10:D12)
X PANEL			
OBJECTS MOUNTED:			MASS(KG)
MULTILAYER INSULATI			1
MOMENTUM WHEEL			6.8
TIMING CONTROL UNI			20
POWER CONTROL UNI			6
SOLAR ARRAY DRIVE			2
SOALR PANELS			16
2 THRUSTERS			0.638
		TOTAL	=SUM(D17:D23)
(-X) PANEL			
OBJECTS MOUNTED:			MASS(KG)
MULTILAYER INSULATI			1
FLIGHT COMPUTER			3
SOLAR ARRAY DRIVE			2
SOLAR ARRAY PANEL			16
MOMENTUM WHEEL			6.8
2 THRUSTERS			0.638
TORQUE ROD			1
		TOTAL	=SUM(D28:D34)
(+ Y) PANEL			
OBJECTS MOUNTED:			MASS
2 BATTERIES			15
REMOTE COMMAND U			6
REMOTE TELEMETRY U			8
C/L BAND TRANSPOND			10
THERMAL CONTROL			10
		TOTAL	=SUM(D39:D43)

(-Y) PANEL				
OBJECTS MOUNTED:			MASS	
2 BATTERIES			15	
REMOTE COMMAND U			6	
REMOTE TELEMETRY U			8	
L/C TRANSPONDER			10	
THERMAL CONTROL			10	
		TOTAL	=SUM(D51:D55)	
ANTIEARTH PANEL				
LENGTH OF PANEL (b)				1.14
WIDTH OF PANEL (a) (				0.98
THICKNESS OF PANEL				0.0001
VOLUME OF MATERIA				=E82*E83*E84
APPROXIMATE MASS				1.5
GAMMA (MASS PER U				=E66/(E82*E83)
YOUNG'S MODULUS (P				9900000
YOUNG'S MODULUS (				=E69*8894.75729311699
POISSON'S RATIO				0.33
FUND. NATURAL FRE				30
BETA				18.47
ASPECT RATIO				=E82/E83
HONEYCOMB HEIGHT (				0.0254
PANEL STIFFNESS FAC				=E70/(2*(1-E71^2))
APPROX. FACE THICK				=(E72^2*39.478417*E68*E83^4*1000)/(E75^2*E76*E73^2)
EARTH PANEL				
LENGTH OF PANEL (b)				1.14
WIDTH OF PANEL (a) (				0.98
THICKNESS OF PANEL				0.0001
VOLUME OF MATERIA				=E81*E82*E83
APPROXIMATE MASS				13
GAMMA (MASS PER U				=E85/(E81*E82)
YOUNG'S MODULUS (P				9900000
YOUNG'S MODULUS (				=E88*8894.75729311699
POISSON'S RATIO				0.33
FUND. NATURAL FRE				30
BETA				18.47
ASPECT RATIO				=E81/E82
HONEYCOMB HEIGHT (				0.0254
PANEL STIFFNESS FAC				=E89/(2*(1-E90^2))
APPROX. FACE THICK				=(E91^2*39.478417*E87*E82^4*1000)/(E94^2*E95*E92^2)

X PANEL				
LENGTH OF PANEL (b)				1.14
WIDTH OF PANEL (a) (				0.6
THICKNESS OF PANEL				0.0001
VOLUME OF MATERIA				=E99*E100*E101
APPROXIMATE MASS				52.438
GAMMA (MASS PER UI				=E103/(E99*E100)
YOUNG'S MODULUS (PI				9900000
YOUNG'S MODULUS (				=E106*6894.75729311699
POISSON'S RATIO				0.33
FUND. NATURAL FRE				30
BETA				12.72
ASPECT RATIO				=E99/E100
HONEYCOMB HEIGHT (I				0.0254
PANEL STIFFNESS FAC				=E107/(2*(1-E108^2))
APPROX. FACE THICK				=(E109^2*39.478417*E105*E100^4*1000)/(E112^2*E113*E110^2)
(-X) PANEL				
LENGTH OF PANEL (b)				1.14
WIDTH OF PANEL (a) (				0.6
THICKNESS OF PANEL				0.0001
VOLUME OF MATERIA				=E129*E130*E131
APPROXIMATE MASS				30.438
GAMMA (MASS PER UI				=E133/(E129*E130)
YOUNG'S MODULUS (PI				9900000
YOUNG'S MODULUS (				=E136*6894.75729311699
POISSON'S RATIO				0.33
FUND. NATURAL FRE				30
BETA				12.72
ASPECT RATIO				=E129/E130
HONEYCOMB HEIGHT (I				0.0254
PANEL STIFFNESS FAC				=E137/(2*(1-E138^2))
APPROX. FACE THICK				=(E139^2*39.478417*E135*E130^4*1000)/(E142^2*E143*E140^2)

YPANEL				
LENGTH OF PANEL (b)				0.98
WIDTH OF PANEL (a) (				0.6
THICKNESS OF PANEL				0.0009
VOLUME OF MATERIA				=E149*E150*E151
APPROXIMATE MASS				49
GAMMA (MASS PER U				=E153/(E149*E150)
YOUNG'S MODULUS (P				9900000
YOUNG'S MODULUS (				=E156*8894.75729311699
POISSON'S RATIO				0.33
FUND. NATURAL FRE				30
BETA				13.78
ASPECT RATIO				=E149/E150
HONEYCOMB HEIGHT (				0.0254
PANEL STIFFNESS FAC				=E157/(2*(1-E158^2))
APPROX. FACE THICK				=(E159^2*39.478417*E155*E150^4*1000)/(E162^2*E163*E160^2)
(-Y)PANEL				
LENGTH OF PANEL (b)				0.98
WIDTH OF PANEL (a) (				0.6
THICKNESS OF PANEL				0.0001
VOLUME OF MATERIA				=E171*E172*E173
APPROXIMATE MASS				49
GAMMA (MASS PER U				=E175/(E171*E172)
YOUNG'S MODULUS (P				9900000
YOUNG'S MODULUS (				=E178*8894.75729311699
POISSON'S RATIO				0.33
FUND. NATURAL FRE				30
BETA				13.78
ASPECT RATIO				=E171/E172
HONEYCOMB HEIGHT (				0.0254
PANEL STIFFNESS FAC				=E179/(2*(1-E180^2))
APPROX. FACE THICK				=(E181^2*39.478417*E177*E172^4*1000)/(E184^2*E185*E182^2)

ITEM	MOMENTS OF INERTIA WITH SOLAR ARRAYS EXTENDED: ITEM DIMENSIONS (CM) a	b	c	MASS(KG)
TELEMETRY TRACKING & COMMAND				
REMOTE COMMAND UNIT 1 (RCU)	16	16	21	8
REMOTE TELEMETRY UNIT 1 (RTU)	20.32	20.4	21	8
REMOTE COMMAND UNIT 2 (RCU)	16	16	21	8
REMOTE TELEMETRY 2 UNIT (RTU)	20.32	20.4	21	8
		SUBSYS. TOTAL		32
ATTITUDE CONTROL SYSTEM				
ATTITUDE CONTROL COMPUTER	8	18	18	3
MOMENTUM WHEEL 1 (PITCH)	17.5	19.8		10.4
MOMENTUM WHEEL 2 (PITCH)	17.5	19.8		10.1
EARTH SENSOR 1 (+X)	9.2	16.3		3.8
EARTH SENSOR 2 (-X)	9.2	16.3		3.8
SUN SENSOR	3.5	3.5	3.5	0.4
TORQUE ROD 1 (-X) BAR	1	30		1.7
TORQUE ROD 2 (-Z) BAR	1	60		3.2
		SUBSYS. TOTAL		30.7
REACTION CONTROL SYSTEM				
PROPELLANT TANK 1 = PROP.	51			70
TUBING AND VALVES(MNF DIST.)	98	114	80	4.5
THRUSTER 1	16.76	3.5	3.5	0.319
THRUSTER 2	16.76	3.5	3.5	0.319
THRUSTER 3	16.76	3.5	3.5	0.319
THRUSTER 4	3.5	3.5	16.76	0.319
THRUSTER 5	3.5	3.5	16.76	0.319
THRUSTER 6		SUBSYS. TOTAL		76.776
STRUCTURAL SUBSYSTEM	98	114	2.54	1.8
PANEL #1 (EARTH FACE)	2.54	88	80	1.81
PANEL #2 (+X FACE)	2.54	88	80	1.81
PANEL # 3 (+Y FACE)	88	0.32	80	5.6
PANEL #4 (-Y FACE)	88	0.32	80	5.6
PANEL # 5 (-Z FACE)	98	114	2.54	1.8
PANEL #6 (ANTI-EARTH FACE)	3.81	114	5.08	2.842
FRAME MEMBER 1	3.81	114	5.08	2.842
FRAME MEMBER 2	3.81	114	5.08	2.842
FRAME MEMBER 3	3.81	114	5.08	2.842
FRAME MEMBER 4	98	3.81	5.08	0.724
FRAME MEMBER 5	98	3.81	5.08	0.724
FRAME MEMBER 6	98	3.81	5.08	0.724
FRAME MEMBER 7	98	3.81	5.08	0.724
FRAME MEMBER 8	3.81	2.54	80	0.312
FRAME MEMBER 9	3.81	2.54	80	0.312
FRAME MEMBER 10	3.81	2.54	80	0.312
FRAME MEMBER 11	3.81	2.54	80	0.312
FRAME MEMBER 12	3.81	2.54	140	1.19
RAIL # 1	2.54	2.54	140	1.19
RAIL # 2	2.54	2.54	140	1.19
MISC(BRACKETS&STRUTS)	88	114	80	15
		SUBSYS. TOTAL		41.712
ELECTRIC POWER SUBSYSTEM				
BATTERY1	80	28	10	7.5
BATTERY2	80	28	10	7.5
BATTERY3	80	28	10	7.5
BATTERY4	80	28	10	7.5
POWER CONTROL UNIT	10	40	10	6
SOLAR ARRAY DRIVE 1 -Y	10	7.5		3
SOLAR ARRAY DRIVE 2 -Y	10	7.5		3
SOLAR ARRAY WING 1(+Y)	288	140	2	18
SOLAR ARRAY WING 2 (-Y)	288	140	2	18
SHUNT RESISTOR BANK1	28	140	2	11
SHUNT RESISTOR BANK2	28	140	2	11
ELECTRICAL INT.(MNF DIST)	98	114	80	13
		SUBSYS. TOTAL		87
THERMAL CONTROL SUBSYSTEM				
LOUVERS1(+Y)	47	8.89	58	1.9
LOUVERS2(+Y)	47	8.89	58	1.9
LOUVERS3 (-Y)	47	8.89	58	1.9
LOUVERS4 (-Y)	47	8.89	58	1.9
PHASE CHANGER 1 (+Y)	98	9.7	58	2.85
PHASE CHANGER 2(-Y)	98	9.7	58	2.85
RADIATOR 1 (+Y)	98	9.2	58	2.5
RADIATOR 2 (-Y)	98	9.2	58	2.5
MULTILAYER INSULATION	98	114	80	5
MISCELAN.(DIST)	98	114	80	3
		SUBSYS. TOTAL		19.7
PAYLOAD	148	140	5.1	4
PHASED ARRAY PANEL	120	140	5.1	3
PHASED ARRAY WING 1(+ x)	120	140	5.1	3
PHASED ARRAY WING 2(-x)	30	10	20	10
C-L BAND TRANSPONDER	30	10	20	10
L-C BAND TRANSPONDER	10	30	20	20
THRING CONTROL UNIT		SUBSYS. TOTAL		50
		SUBTOTAL MASS		329.307
		10% MASS MARGIN		32.9307
		TOTAL MASS		372.1377

0 ANTENNA DEPLOYED(FLAT FACE IN -Z DIR.) ITEM MOMENTS (KG*M^2) Ix	Iy	Iz	ITEM POSITION (CM) x	y	z
0.0323	0.03485	0.02405	-35	47	0
0.057144	0.066855656	0.09500094	25	47	0
0.0323	0.03485	0.02405	35	-47	0
0.057144	0.05869856	0.06500064	-25	-47	0
0.0013725	0.007325	0.0097	-46	-26	0
0.15925	0.11380118	0.11380118	-42	0	-20
0.03397881	0.02954107	0.00401847	-42	0	-16
0.05048811	0.02909882	0.02909882	26	0	-30
0.05048811	0.02909882	0.02909882	-26	0	-30
4.1667E-05	4.1667E-05	4.1667E-05	-40	20	30
0.127925	0.07525	0.00045	-47.5	30	0
0.9808	0.07525	0.0018	0	30	-30
1.8207	1.8207	1.8207	0	0	0
0.82225	0.45515	0.8475	0	0	0
6.5129E-06	0.00077928	0.00077928	-41.5	-26	20
6.5129E-06	0.00077928	0.00077928	-41.5	26	-20
6.5129E-06	0.00077928	0.00077928	41.5	26	20
6.5129E-06	0.00077928	0.00077928	41.5	-26	20
0.00077928	0.00077928	6.5129E-06	-41.5	26	-20
0.00077928	0.00077928	6.5129E-06	41.5	-26	20
0.195036277	0.14439677	0.339	0	0	30
0.11113267	0.0303543	0.04068797	48	0	0
0.11113267	0.0303543	0.04068797	-48	0	0
0.168005673	0.81818667	0.44819238	0	57	0
0.168005673	0.81818667	0.44819238	0	-57	0
0.195036277	0.14415677	0.339	0	0	-30
0.183773935	0.00056586	0.18259091	48	0	28
0.183773935	0.00056586	0.18259091	-48	0	28
0.183773935	0.00056586	0.18259091	48	0	-28
0.183773935	0.00056586	0.18259091	-48	0	-28
0.000048656	0.11619866	0.11606343	0	56	28
0.000048656	0.11619866	0.11606343	0	56	-28
0.000048656	0.11619866	0.11606343	0	-56	28
0.000048656	0.11619866	0.11606343	0	-56	-28
0.018753295	0.01879548	0.00010903	48	57	0
0.018753295	0.01879548	0.00010903	-48	57	0
0.018753295	0.01879548	0.00010903	48	-57	0
0.018753295	0.01879548	0.00010903	-48	-57	0
0.194430685	0.19443068	0.00012798	0	57	30
0.194430685	0.19443068	0.00012798	0	-57	30
2.0745	1.6806	3.828	0	0	0
0.09525	0.32125	0.374	0	45	20
0.09525	0.32125	0.374	0	45	-20
0.09525	0.32125	0.374	0	-45	20
0.09525	0.32125	0.374	0	-45	-20
0.09125	0.0225	0.09125	42	30	15
0.00028125	0.0056525	0.00281125	42	0	30
0.00028125	0.0056525	0.00281125	-42	0	30
2.81338667	0.87083333	11.28333333	107.5	0	20
2.81338667	0.87083333	11.28333333	-107.5	0	20
0.163338667	0.00824167	0.16854167	102	0	20
0.163338667	0.00824167	0.16854167	-102	0	20
1.7979	1.43043333	2.44833333	0	0	0
0.0426434	0.0698625	0.0282059	23.5	62	0
0.0426434	0.0698625	0.0282059	-23.5	62	0
0.0426434	0.0698625	0.0282059	23.5	-62	0
0.0426434	0.0698625	0.0282059	-23.5	-62	0
0.078290664	0.2287775	0.21885184	0	56	0
0.078290664	0.2287775	0.21885184	0	-56	0
0.014016883	0.00241667	0.02840017	23.5	57	0
0.014016883	0.00241667	0.02840017	-23.5	-57	0
0.0915	0.59018667	0.68168667	0	0	0
0.2788	0.22006667	0.37666667	0	0	0
0.85420033	0.85420033	1.30666667	0	0	-32.5
0.490695025	0.38065075	0.85	91.4	0	-72.4
0.490695025	0.38065075	0.85	-91.4	0	-72.4
0.041666667	0.10833333	0.08333333	5	52	0
0.041666667	0.10833333	0.08333333	5	-52	0
0.21666667	0.08333333	0.18666667	40	20	18

CENTER OF MASS CONTRIBUTION Cx	Cy	Cz
-210	282	0
200	376	0
210	-282	0
-200	-376	0
-132	-78	0
416	0	-208
-436.8	0	-166.4
88.8	0	-114
-88.8	0	-114
-10	0	12
-80.75	51	0
0	98	-98
0	0	0
0	0	0
-13.2395	-11.484	8.36
-13.2395	11.484	-8.36
13.2395	11.484	8.36
13.2395	-11.484	-8.36
-13.2395	11.484	8.364
13.2395	-11.484	8.364
0	0	84
48.48	0	0
-48.48	0	0
0	319.2	0
0	-319.2	0
0	0	-84
40.416	0	-23.576
40.416	0	23.576
-40.416	0	23.576
-40.416	0	-23.576
0	40.544	-20.272
0	40.544	20.272
0	-40.544	-20.272
0	-40.544	20.272
14.976	-17.784	0
14.976	17.784	0
-14.976	17.784	0
14.976	-17.784	0
0	67.83	25.7
0	-67.83	25.7
0	0	0
0	337.5	-180
0	337.5	180
0	-337.5	180
0	-337.5	-180
252	180	-90
84	0	40
-84	0	40
2880	0	320
-2880	0	320
102	0	20
-102	0	20
0	0	0
35.25	93	0
-35.25	93	0
35.25	-93	0
-35.25	-93	0
0	159.6	0
0	-159.6	0
-11.75	28.5	0
-11.75	-28.5	0
0	0	0
0	0	0
0	0	-130
274.2	0	-217.2
-274.2	0	-217.2
-80	520	0
80	-520	0
800	800	300

CENTER OF MASS OFFSETS: 2.16789587, 3.3968008, -0.51674534

DISTANCE FROM CENTER Dx	Dy	Dz
37.16789587	44.79031992	0.51674534
33.83211041	44.79031992	0.51674534
33.83211041	49.2968008	0.51674534
37.16789959	49.2968008	0.51674534
46.16789959	39.2968008	0.51674534
37.83211041	39.2968008	19.48325467
46.16789959	39.2968008	19.48325467
42.16789958	17.79031992	30.51674533
46.66789958	27.79031992	0.51674534
46.66789958	27.79031992	39.48325467
2.16789587	2.2968008	0.51674534
2.16789587	2.2968008	0.51674534
2.16789587	2.2968008	0.51674534
43.66789959	39.2968008	20.51674533
43.66789959	33.79031992	19.48325467
39.33211041	33.79031992	20.51674533
39.33211041	33.79031992	20.51674533
43.66789959	39.2968008	20.51674533
39.33211041	39.2968008	20.51674533
2.16789587	2.2968008	30.51674533
45.83211041	2.2968008	0.51674534
90.16789959	2.2968008	0.51674534
48.83211041	2.2968008	20.51674533
90.16789959	2.2968008	20.51674533
2.16789587	93.79031992	27.48325467
2.16789587	93.79031992	20.51674533
2.16789587	98.2968008	27.48325467
2.16789587	98.2968008	20.51674533
2.16789587	2.2968008	0.51674534
2.16789587	42.79031992	19.48325467
2.16789587	42.79031992	20.51674533
2.16789587	47.2968008	19.48325467
2.16789587	47.2968008	20.51674533
39.83211041	27.79031992	19.48325467
39.83211041	2.2968008	20.51674533
44.16789959	2.2968008	20.51674533
169.3321041	2.2968008	20.51674533
169.3321041	2.2968008	20.51674533
169.8678996	2.2968008	20.51674533
99.83211041	2.2968008	20.51674533
104.167896	2.2968008	20.51674533
2.16789587	2.2968008	0.51674534
21.33211041	86.79031992	0.51674534
25.66789959	88.79031992	0.51674534
21.33211041	84.2968008	0.51674534
25.66789959	84.2968008	0.51674534
2.16789587	53.79031992	0.51674534
2.16789587	58.2968008	0.51674534
25.66789959	84.79031992	0.51674534
25.66789959	89.2968008	0.51674534
2.16789587	2.2968008	0.51674534
2.16789587	2.2968008	0.51674534
2.16789587	2.2968008	31.80325467
89.33211041	2.2968008	71.80325467
93.66789959	2.2968008	71.80325467
7.16789587	49.79031992	0.51674534
2.33210413	84.2968008	0.51674534
37.83211041	27.79031992	18.51674534

TOTAL SPACECRAFT MOMENTS

TOTAL MOMENT OF INERTIA(KG*M^2) Ixx	Ixy	Ixz	Iyy	Iyz	Izz	Iyz
3.0611971	1.08258299	2.05198471	-0.99881431	-0.0115238	0.0135901	
2.0728988	0.89074453	2.07974536	0.81853448	0.00943871	0.0184014	
2.13917298	1.32838647	2.13893298	-0.97111062	0.01017095	-0.0152843	
2.58175831	1.33780787	2.58981567	1.07143228	-0.0112311	-0.0203781	
0.893280006	1.13810977	0.88938504	0.98182113	-0.0071577	-0.0043987	
1.185155113	3.09063945	1.90760993	-0.99038463	-0.7065782	0.0448391	
2.06278825	1.04821196	2.06483092	0.10950289	0.71121729	0.03898443	
0.3683316	0.4577534	0.24392972	-0.02000029	-0.2870062	0.02872252	
0.35388925	0.8291038	0.32980498	0.0245845	0.31656287	0.0217732	
0.00370305	0.14228216	0.00670306	-0.02080027	-0.0014708	0.0211805	
0.07776741	0.01389598	0.05809241	-0.02281312	-0.0043681	0.0021263	
1.20789348	0.97828795	0.24888345	-0.01921848	0.02045337	-0.2813987	
1.890625648	1.88849851	1.89062546	0.03485457	-0.0078417	-0.0063803	
0.02683678	0.0992798	0.05198678	0.00234065	-0.0005411	-0.0063409	
0.10780074	0.12343898	0.10838468	0.05334747	-0.0287788	-0.0230445	
0.09713015	0.12343898	0.09764421	-0.04684675	0.02714028	-0.0206707	
0.04560328	0.0994788	0.04638943	0.04228731	0.02634224	0.0230521	
0.09130084	0.0994788	0.09661903	-0.04809077	-0.0264468	0.02380207	
0.09778431	0.13243898	0.09713018	-0.04984878	-0.0286378	0.026909	
0.09130084	0.0994788	0.09670068	-0.04809077	0.02337064	-0.0233984	
0.19883239	0.14584089	0.34079581	0.00068826	-0.0111908	-0.0128163	
0.32389523	0.45487182	0.25257752	-0.01063199	0.00239204	-0.0001196	
0.36585307	0.52075149	0.33561837	0.01163776	-0.0026193	-0.0001196	
1.28403299	0.82145041	1.12659066	-0.06641007	-0.0006273	0.01562987	
2.12965853	0.82145041	2.41984618	0.0719876	-0.0006273	-0.0171915	
0.19883229	0.14584089	0.34079581	0.00068826	0.01150489	0.01212908	
0.36005251	0.25430383	0.35899407	-0.0006826	-0.1060589	0.0033 15	
0.36005251	0.25430383	0.35899407	-0.0006826	0.11004783	-0.0055148	
0.39509958	0.42439787	0.38484118	0.0007703	-0.1204583	-0.0056148	
0.39509958	0.42439787	0.38484118	0.0007703	0.11909303	0.0053 15	
0.39509959	0.42439787	0.38484118	0.0007702	0.11909303	0.0053 15	
0.20983065	0.11688018	0.32530772	-0.00842902	0.00431388	-0.1088578	
0.20983065	0.11688018	0.32530772	-0.00842902	-0.00447586	0.11087829	
0.21678567	0.11688018	0.33245832	0.00915001	0.00431265	0.11899925	
0.21678567	0.11688018	0.33245832	0.00915001	-0.00447586	-0.1203803	
0.21678567	0.11688018	0.33245832	0.00915001	-0.00447586	0.11087829	
0.19399435	0.14987179	0.17534992	-0.00479218	0.00073893	-0.0008185	
0.17765582	0.14987179	0.15901131	0.07822348	0.00073893	0.00088195	
0.19064729	0.17564491	0.17198787	-0.06582355	-0.0006883	0.00088195	
0.19399435	0.14987179	0.17534983	-0.06479218	0.00073893	-0.0009501	
0.95109028	0.19954518	0.36478758	-0.0141231	-0.0076727	0.19885427	
0.81340706	0.19954518	0.41910428	0.01329737	-0.0076727	-0.2152359	
2.0844528	1.66499532	2.83996838	0.00746884	-0.0018908	-0.0017802	
1.42844725	0.23829866	1.64519725	-0.06943207	0.03187825	-0.0239979	
1.42844726	0.23829866	1.64519726	-0.06943207	-0.0333588	0.057098	
1.73951939	0.23829866	1.9952939	0.0769009	0.03187825	0.89112171	
1.73951939	0.23829866	1.9952939	0.0769009	-0.0333588	-0.7277231	
1.73951939	0.23829866	1.9952939	0.0769009	-0.0333588	-0.2407349	
1.90388828	1.29411582	1.90368876	0.06206803	-0.3481391	-0.2407349	
0.32118868	0.64026281	0.32118868	-0.01829728	0.10244503	-0.0094256	
0.32118868	0.64026281	0.32118868	-0.01829728	0.10244503	-0.0094256	
0.38403819	0.79854821	0.39402816	0.03023897	-0.1813826	-0.0094256	
48.35783246	86.1415883	85.8373012	-0.90767695	9.47332268	-0.0763966	
48.5618191	108.788557	57.3813886	0.02390637	-5.5895282	-0.0763966	
1.1805381	1.29853147	1.1807141	-0.02292849	0.20452293	-0.0047123	
1.24899529	2.17542177	1.29418425	0.02392529	-0.2137169	-0.0047123	
1.21060758	1.49258374	2.48139092	0.00647299	-0.0014563	-0.0019428	
0.8459573	0.2061801	0.6311288	0.10160232	0.00165249	0.0046377	
0.47614033	0.28731478	0.66170283	-0.23988633	-0.0019899	0.0046377	
0.73101389	0.2061801	0.71867648	-0.20573791	0.00165249	-0.0049637	
0.76158123	0.28731478	0.74714382	0.24785454	-0.0019899	-0.0049637	
0.90319545	0.30145387	1.04219085	-0.02311934	-0.0003193	0.007909	
1.04982141	0.30145387	1.18880641	0.02801187	-0.0003193	-0.0056851	
0.19686008	0.11920078	0.22996421	-0.0702058	-0.0009631	0.00141238	
0.19686008	0.11920078	0.24714774	0.07810121	-0.0009631	-0.0021207	
0.12279441	0.11920078	0.14714774	0.07810121	-0.0009631	-0.0021207	
0.09648783	0.05488644	0.0466543	0.00248981	-0.0001601	-0.0009563	
0.27852901	0.22194658	0.37866168	0.00089584	-0.0002249	-0.0002373	
0.95819038	0.65798015	1.31065809	0.00189169	0.02773485	0.02282367	
2.89094338	5.13907179	2.24023211	-0.00148451	-1.8342882	0.04953049	
3.11871818	5.61393092	2.47906783	0.00447205	2.01779847	0.04953049	
2.59245341	0.21110908	2.60912008	-0.35826736	-0.0037039	0.0258832	
1.39763008	0.12437498	3.03849672	-0.18377419	0.00146348	-0.0280578	
4.61413738	5.80560674	4.88413739	2.09814083	1.17406175	0.89872887	
181.473281	283.06705	182.883193	2.14328668	0.68644388	0.61427313	

MOMENTS OF INERTIA WITH SOLAR ARRAYS EXTENDED — O ANTENNA DEPLOYED(FLAT FACE IN +Z DIR.) AND 50% FUEL REMAINING

ITEM	ITEM DIMENSIONS (CM) a	b	c	MASS(KG)	ITEM MOMENTS (KG*M^2) Ix	Iy	Iz	ITEM POSITION (CM) x	y	z	CENTER OF MASS CONTRIBUTION Cx	Cy	Cz	DISTANCE FROM CENTER Dx	Dy	Dz	TOTAL MOMENT OF INERTIA(KG*M^2) Ixx	Iyy	Izz	Ixy	Ixz	Iyz
TELEMETRY TRACKING & COMMAND																						
REMOTE COMMAND UNIT 1 (RCU)	16	18	21	6	0.0333	0.03485	0.02405	-35	47	0	-210	282	0	37.3782303	44.4803581	0.5666812	2.05868061	1.71140652	2.04943061	-0.99755024	-0.01271341	0.01512906
REMOTE TELEMETRY UNIT 1 (RTU)	20.22	20.4	21	8	0.057144	0.05665656	0.05500058	25	47	0	200	376	0	22.6217697	44.4803581	0.5666812	2.04934136	0.8754477	2.04719794	0.80487963	0.01015908	0.02017206
REMOTE COMMAND UNIT 2 (RCU)	16	15	21	6	0.0333	0.03485	0.02405	35	-47	0	210	-282	0	32.6217697	49.5196419	0.5666812	2.14312487	1.31186683	2.13327487	-0.96925101	0.0110956	-0.01684305
REMOTE TELEMETRY 2 UNIT (RTU)	20.22	20.4	21	8	0.057144	0.05665656	0.05500058	-25	-47	0	-200	-376	0	27.3782303	49.5196419	0.5666812	2.61855394	1.25596455	2.6164106	1.08460813	-0.01241618	-0.0224574
		SUBSYS. TOTAL		28																		
ATTITUDE CONTROL SYSTEM																						
ATTITUDE CONTROL COMPUTER	8	18	18	3	0.013725	0.007225	0.0097	-44	-26	0	-132	-78	0	46.3782303	28.5196419	0.5666812	0.90301007	1.20778915	0.89909307	0.39660716	-0.00788728	-0.00455017
MOMENTUM WHEEL 1 (PITCH)	19	19.8		10.4	0.18772	0.1278368	0.1278368	40	0	-20	416	0	-208	37.6217697	2.51964189	19.4331188	1.666336	3.07166372	1.6664529	-0.09858612	-0.76035265	0.05082308
MOMENTUM WHEEL 2 (PITCH)	19	19.8		10.4	0.0329768	0.03128667	0.06526247	-42	0	-16	-436.8	0	-166.4	44.3782303	2.51964189	15.4331188	2.09870376	4.1276955	2.12007042	0.11628894	0.71229029	0.04044137
EARTH SENSOR 1 A/h	5.2	16.3		3.8	0.0504811	0.02809682	0.02809682	26	0	-30	98.8	0	-114	23.6217697	2.51964189	29.4331188	0.26482901	0.4901677	0.24054472	-0.02261669	-0.26419989	0.02818115
EARTH SENSOR 2 A/h	5.2	16.3		3.8	0.0504811	0.02809682	0.02809682	-26	0	-30	-98.8	0	-114	28.3782303	2.51964189	29.4331188	0.35891667	0.63814302	0.33453339	0.02717113	0.31739873	0.02818115
SUN SENSOR	2.5	2.5	2.5	0.4	4.1667E-05	4.1667E-05	4.1667E-05	-40	20	30	-16	8	12	42.3782303	17.4803581	30.5666812	0.09410078	0.14371463	0.08410078	-0.02963147	-0.05181481	0.0213728
TORQUE ROD (-X) R/H	1	30		1.7	0.127925	0.07525	0.00085	-47.5	30	0	-80.75	51	0	49.8782303	27.4803581	0.5666812	0.67913635	0.83111487	0.55218136	-0.23301418	-0.00480678	0.00264828
TORQUE ROD (-Z) R/H	1	80		3.2	0.3608	0.07525	0.0016	0	30	-30	0	96	-96	2.37823029	27.4803581	29.4331188	1.20426434	0.07668983	0.24906434	-0.02091348	0.0223996	-0.25882648
		SUBSYS. TOTAL		38.7																		
REACTION CONTROL SYSTEM																						
PROPELLANT TANK 1	51			10	0.4335	0.4335	0.4335	0	0	0	0	0	0	2.37823029	2.51964189	0.5666812	0.44020487	0.44481196	0.44090467	0.00599229	-0.00134817	-0.00142824
PROPELLANT	20.2			30	0.122412	0.122412	0.122412	0	0	0	0	0	0	2.37823029	2.51964189	0.5666812	0.15042572	0.15634796	0.15842572	0.01797687	-0.00404452	-0.00428901
TUBING AND VALVES(UNIF DIST.)	96	114	60	4.5	0.62238	0.49518	0.8478	0	0	0	0	0	0	2.37823029	2.51964189	0.5666812	0.627752	0.50034038	0.85190306	0.00269653	-0.00060668	-0.00064279
THRUSTER 1	16.76	3.5	3.5	0.319	8.5129E-05	0.00077928	0.00077928	-41.5	-36	20	-13.2385	-11.484	6.38	43.8782303	38.5196419	20.5666812	0.1068143	0.12361337	0.10682836	0.05391694	-0.02878778	-0.0252721
THRUSTER 2	16.76	3.5	3.5	0.319	8.5129E-05	0.00077928	0.00077928	-41.5	36	-20	-13.2385	11.484	-6.38	43.8782303	33.4803581	19.4331188	0.09723898	0.12361337	0.09785413	-0.04686296	0.02730064	-0.02075903
THRUSTER 3	16.76	3.5	3.5	0.319	8.5129E-05	0.00077928	0.00077928	41.5	36	20	13.2385	11.484	6.38	39.1217697	33.4803581	20.5666812	0.0848483	0.096428	0.08836046	0.04178297	0.02566715	0.02196991
THRUSTER 4	16.76	3.5	3.5	0.319	8.5129E-05	0.00077928	0.00077928	41.5	-36	-20	13.2385	-11.484	-6.38	39.1217697	38.5196419	19.4331188	0.09622052	0.096428	0.09693469	-0.04807191	-0.02425223	0.02387096
THRUSTER 5	3.5	3.5	16.76	0.319	0.00077928	0.00077928	8.5129E-05	-41.5	36	20	-13.2385	11.484	6.294	43.8782303	33.4803581	20.5666812	0.09785413	0.12361337	0.09723898	-0.04686296	-0.03715908	0.02627405
THRUSTER 6	3.5	3.5	16.76	0.319	0.00077928	0.00077928	8.5129E-05	41.5	-36	20	13.2385	-11.484	6.294	39.1217697	38.5196419	20.5666812	0.09693469	0.096428	0.09622052	-0.04807191	0.03315805	-0.03264476
		SUBSYS. TOTAL		45.776																		
STRUCTURAL SUBSYSTEM																						
PANEL #1 (EARTH FACE	96	114	2.54	1.01	0.1094373	0.08086797	0.19021667	0	0	30	0	0	30.3	2.37823029	2.51964189	30.5666812	0.11064078	0.08303046	0.19143913	0.00000532	-0.0073422	-0.00777878
PANEL #2 (+x FACE)	2.54	96	60	1.8	0.19806	0.05408677	0.14415677	48	0	0	86.4	0	0	45.6217697	2.51964189	0.5666812	0.573846	0.80336129	0.81094178	-0.02069109	0.00465815	-0.0002571
PANEL # 3 (-x FACE)	2.54	96	60	1.8	0.19806	0.05408677	0.14415677	-48	0	0	-86.4	0	0	50.3782303	2.51964189	0.5666812	0.65602664	0.96770487	0.89213342	0.02284632	-0.00514052	-0.0002571
PANEL #4 (+y FACE)	96	2.54	60	5.6	0.16830107	0.61616667	0.44848774	0	57	0	0	319.2	0	2.37823029	54.4803581	0.5666812	1.8336097	0.62292136	2.11379634	-0.07255743	-0.00075496	0.01729498
PANEL # 5 (-y FACE)	96	2.54	60	5.6	0.16830107	0.61616667	0.44848774	0	-57	0	0	-319.2	0	2.37823029	59.5196419	0.5666812	2.19531757	0.62292136	2.43590424	0.07926879	-0.00075496	-0.01869472
PANEL #6 (ANTI-EARTH FACE)	96	114	2.54	1.01	0.1094373	0.08086797	0.19021667	0	0	-30	0	0	-30.3	2.37823029	2.51964189	29.4331188	0.11064078	0.08303046	0.19143913	0.00000532	0.00700987	0.00749035
FRAME MEMBER 1	3.81	114	5.08	0.842	0.18273935	0.00056586	0.18258091	48	0	-28	40.416	0	-23.576	45.6217697	2.51964189	27.4331188	0.35853322	0.3610049	0.35836478	-0.00967883	-0.10538029	0.00582004
FRAME MEMBER 2	3.81	114	5.08	0.842	0.18273935	0.00056586	0.18258091	48	0	28	40.416	0	23.576	45.6217697	2.51964189	28.5666812	0.35853322	0.3610049	0.35836478	-0.00967883	0.10972848	-0.00606097
FRAME MEMBER 3	3.81	114	5.08	0.842	0.18273935	0.00056586	0.18258091	-48	0	28	-40.416	0	23.576	50.3782303	2.51964189	28.5666812	0.39607065	0.43799838	0.39681221	0.01008794	-0.12117834	-0.00606097
FRAME MEMBER 4	3.81	114	5.08	0.842	0.18273935	0.00056586	0.18258091	-48	0	-28	-40.416	0	-23.576	50.3782303	2.51964189	27.4331188	0.39607065	0.43799838	0.39681221	0.01008794	0.11636709	0.00582004
FRAME MEMBER 5	96	3.81	5.08	0.724	0.00048656	0.11619966	0.11606343	0	56	-28	0	40.544	-20.272	2.37823029	53.4803581	27.4331188	0.30797062	0.11701606	0.22294709	-0.00920646	0.00472354	-0.10622043
FRAME MEMBER 6	96	3.81	5.08	0.724	0.00048656	0.11619966	0.11606343	0	56	28	0	40.544	20.272	2.37823029	53.4803581	28.5666812	0.30797062	0.11701606	0.22294709	-0.00920646	-0.00491876	0.11091033
FRAME MEMBER 7	96	3.81	5.08	0.724	0.00048656	0.11619966	0.11606343	0	-56	-28	0	-40.544	-20.272	2.37823029	58.5196419	27.4331188	0.34083336	0.11701606	0.2644122	0.01007614	0.00472354	0.11622824
FRAME MEMBER 8	96	3.81	5.08	0.724	0.00048656	0.11619966	0.11606343	0	-56	28	0	-40.544	20.272	2.37823029	58.5196419	28.5666812	0.34083336	0.11701606	0.2644122	0.01007614	-0.00491876	-0.12103279
FRAME MEMBER 9	3.81	2.54	60	0.312	0.01875359	0.01879548	0.00010903	48	-57	0	14.976	-17.784	0	45.6217697	59.5196419	0.5666812	0.19422029	0.14867147	0.17697974	-0.00472021	0.0000069	-0.00101271
FRAME MEMBER 10	3.81	2.54	60	0.312	0.01875359	0.01879548	0.00010903	48	57	0	14.976	17.784	0	45.6217697	54.4803581	0.5666812	0.17629095	0.14867147	0.15708304	0.0779473	0.0000069	0.00096356
FRAME MEMBER 11	3.81	2.54	60	0.312	0.01875359	0.01879548	0.00010903	-48	57	0	-14.976	17.784	0	50.3782303	54.4803581	0.5666812	0.1909431	0.17719487	0.17159899	-0.00863227	-0.0000103	0.00096356
FRAME MEMBER 12	3.81	2.54	60	0.312	0.01875359	0.01879548	0.00010903	48	-57	0	14.976	-17.784	0	45.6217697	59.5196419	0.5666812	0.19422029	0.14867147	0.17697974	-0.00472021	0.0000069	-0.00101271
RAIL # 1	2.54	2.54	140	1.19	0.19443086	0.19443086	0.00012796	0	57	30	0	67.83	35.7	2.37823029	54.4803581	30.5666812	0.54830673	0.19677677	0.35400004	-0.01541848	-0.0000071	0.19017009
RAIL # 2	2.54	2.54	140	1.19	0.19443086	0.19443086	0.00012796	0	-57	30	0	-67.83	35.7	2.37823029	59.5196419	30.5666812	0.61667166	0.19677677	0.42236896	0.01684481	-0.0000071	-0.21690025
MISC(BRACKETS&STRUTS)	96	114	60	15	2.0745	1.6506	2.625	0	0	0	0	0	0	2.37823029	2.51964189	0.5666812	2.09180666	1.66746784	2.64300666	0.00086843	-0.00202226	-0.00114291
		SUBSYS. TOTAL		41.712																		
ELECTRIC POWER SUBSYSTEM																						
BATTERY1	60	28	10	7.5	0.05525	0.23125	0.274	0	45	-20	0	337.5	-150	2.37823029	42.4803581	19.4331188	1.41292761	0.22873397	1.6216770	-0.07577106	0.02400223	-0.61914429
BATTERY2	60	28	10	7.5	0.05525	0.23125	0.274	0	45	20	0	337.5	150	2.37823029	42.4803581	20.5666812	1.41292761	0.22873397	1.6216770	-0.07577106	-0.02400223	0.09520039
BATTERY3	60	28	10	7.5	0.05525	0.23125	0.274	0	-45	-20	0	-337.5	-150	2.37823029	47.5196419	19.4331188	1.75307938	0.22873397	1.87182939	0.00478649	0.02400223	0.00290113
BATTERY4	60	28	10	7.5	0.05525	0.23125	0.274	0	-45	20	0	-337.5	150	2.37823029	47.5196419	20.5666812	1.75307938	0.22873397	1.87182939	0.00478649	-0.02400223	-0.73290612
POWER CONTROL UNIT	15	40	15	6	0.09125	0.0225	0.09125	42	30	-15	252	180	-90	39.6217697	27.4803581	14.4331188	1.40522283	1.00026156	1.40038983	0.06322228	-0.34311943	-0.23797036
SOLAR ARRAY DRIVE 1 dy	10	7.5		2	0.00281125	0.005625	0.00281125	42	0	20	84	0	40	39.6217697	2.51964189	20.5666812	0.31899919	0.03357988	0.31899919	-0.01556683	0.16337929	-0.01039424
SOLAR ARRAY DRIVE2 dy	10	7.5		2	0.00281125	0.005625	0.00281125	-42	0	20	-84	0	40	44.3782303	2.51964189	20.5666812	0.39716789	0.79330883	0.39716789	0.02228146	-0.18254436	-0.01039424
SOLAR ARRAY WING 1(+Y)	255	140	2	16	2.81366667	8.67083333	11.2833333	167.5	0	20	2680	0	320	165.12177	2.51964189	20.5666812	48.2483431	95.8181866	54.8178882	-0.06547624	3.43200371	-0.06291396
SOLAR ARRAY WING 2 (-Y)	255	140	2	16	2.81366667	8.67083333	11.2833333	-167.5	0	20	-2680	0	320	169.87823	2.51964189	20.5666812	48.7370654	101.018009	57.4673721	0.06495186	-1.98018461	-0.06291396
SHUNT RESISTOR BANK1	25	140	2	1	0.16336667	0.00524167	0.16854167	102	0	20	102	0	20	99.6217697	2.51964189	20.5666812	1.15640122	1.99014107	1.18182033	-0.02510112	0.30480001	-0.00519212
SHUNT RESISTOR BANK2	25	140	2	1	0.16336667	0.00524167	0.16854167	-102	0	20	-102	0	20	104.37823	2.51964189	20.5666812	1.25346302	2.18420466	1.25889603	0.01620956	-0.21487347	-0.00518212
ELECTRICAL INT.(UNIF DIST)	96	114	60	13	1.7979	1.43043333	2.44833333	0	0	0	0	0	0	2.37823029	2.51964189	0.5666812	1.8135009	1.44613806	2.44393029	0.00779908	-0.00175263	-0.00189664
		SUBSYS. TOTAL		87																		
THERMAL CONTROL SUBSYSTEM																						
LOUVERS1(+Y)	47	6.89	58	1.5	0.0426434	0.0698625	0.0282059	23.5	62	0	35.25	93	0	21.1217697	59.4803581	0.5666812	0.84924073	0.20960125	0.63901232	0.10944099	0.00179093	0.00005774
LOUVERS2(+Y)	47	6.89	58	1.5	0.0426434	0.0698625	0.0282059	-23.5	62	0	-35.25	93	0	25.8782303	59.4803581	0.5666812	0.87173277	0.27950724	0.66934627	-0.22009909	-0.00220044	0.00005774
LOUVERS 3 (-Y)	47	6.89	58	1.5	0.0426434	0.0698625	0.0282059	23.5	-62	0	35.25	-93	0	21.1217697	64.5196419	0.5666812	0.7339094	0.20350125	0.7106429	-0.20441835	0.00179093	-0.00540039
LOUVERS4 (-Y)	47	6.89	58	1.5	0.0426434	0.0698625	0.0282059	-23.5	-62	0	-35.25	-93	0	25.8782303	64.5196419	0.5666812	0.70781346	0.27950724	0.75207695	0.20944612	-0.00220044	-0.00540039
PHASE CHANGER (+Y)	96	0.7	58	2.85	0.07990664	0.298779	0.21889184	0	56	0	0	159.6	0	2.37823029	53.4803581	0.5666812	0.99669007	0.30199901	1.03564007	-0.03024075	-0.00038423	0.00064039
PHASE CHANGER (-Y)	96	0.7	58	2.85	0.07990664	0.298779	0.21889184	0	-56	0	0	-159.6	0	2.37823029	58.5196419	0.5666812	1.09781401	0.30199901	1.15940991	0.03960439	-0.00038423	-0.0004946
RADIATOR (+Y)	96	0.2	58	0.5	0.01401683	0.05241667	0.03840017	-23.5	57	0	-11.75	28.5	0	25.8782303	54.4803581	0.5666812	0.19960644	0.11038405	0.23029078	-0.07040278	-0.00073349	0.00154419
RADIATOR (-Y)	96	0.2	58	0.5	0.01401683	0.05241667	0.03840017	-23.5	-57	0	-11.75	-28.5	0	25.8782303	59.5196419	0.5666812	0.22462036	0.11038405	0.2499137	0.07791318	-0.00073349	-0.00168703
MULTILAYER INSULATION	96	114	60	5	0.6915	0.55016667	0.94166667	0	0	0	0	0	0	2.37823029	2.51964189	0.5666812	0.69790129	0.55863209	0.94766668	0.00299614	-0.00007406	-0.00071417
MISC(UNIF DIST)	96	114	60	2	0.2766	0.22006667	0.37666667	0	0	0	0	0	0	2.37823029	2.51964189	0.5666812	0.27900001	0.22313906	0.37906738	0.00119846	-0.00029963	-0.00028567
		SUBSYS. TOTAL		19.7																		
PAYLOAD																						
PHASED ARRAY PANEL	140	140	5.1	4	0.65420033	0.65420033	1.30666667	0	0	-32.5	0	0	-130	2.37823029	2.51964189	31.9331188	0.66069216	0.66073512	1.3114469	0.02220002	0.00037772	0.02310401
PHASED ARRAY WING1(+Y)	140	120	5.1	3	0.36065025	0.49065025	0.85	91.4	0	-72.4	274.2	0	-217.2	89.0217697	2.51964189	71.8331188	1.74001747	3.24657884	3.22936721	-0.06720066	-1.91641341	0.05432612
PHASED ARRAY WING2(-Y)	140	120	5.1	3	0.36065025	0.49065025	0.85	-91.4	0	-72.4	-274.2	0	-217.2	93.7782303	2.51964189	71.8331188	2.00060177	3.78720414	3.40021182	0.07066027	2.03091452	0.05432612
C/L BAND TRANSPONDER	30	10	20	10	0.04166667	0.10833333	0.08333333	-5	52	0	-50	520	0	7.37823029	49.4803581	0.5666812	2.54441079	0.2173009	2.59007746	-0.36507746	-0.00418259	0.02804048
L/C BAND TRANSPONDER	30	10	20	10	0.04166667	0.10833333	0.08333333	5	-52	0	50	-520	0	2.62176971	54.5196419	0.5666812	3.02093189	0.12208066	3.06280638	-0.14293796	0.00149423	-0.03089416
TIMING CONTROL UNIT	10	30	20	20	0.21666667	0.08333333	0.16666667	40	30	15	800	600	300	37.6217697	27.4803581	15.5666812	4.55780194	3.74463356	4.90780194	1.06771841	1.17130724	0.65556694
		SUBSYS. TOTAL		50																		
		SUBTOTAL MASS		309.207																		
		10% MASS MARGIN		30.9207						CENTER OF MASS OFFSET		2.37823029	2.51964189	-0.5666812	TOTAL SPACECRAFT MOMENTS		160.30393	252.713093	181.861609	2.12279464	0.00066078	0.41995198
		TOTAL MASS		340.1277																		

A	E	F	G	H	K	L	M	N	O	P	Q	R
	MOMENTS OF INERTIA WITH											
ITEM	ITEM DIMENSIONS (CM)			MASS(KG)	ITEM MOMENTS (KG*M^2)			ITEM POSITION (CM)				CENTER OF MASS CONTRIB
	a	b	c		Ix	Iy	Iz	x	y	z		Cx
TELEMETRY TRACKING & C												
REMOTE COMMAND UNIT 1	10	15	21	6	=H7*(F7^2+G7^2)/12/10000	=H7*((E7^2+G7^2)/12/10000	=H7*((E7^2+F7^2)/12/10000	-35	47	0		=H7*N7
REMOTE TELEMETRY UNIT	20.32	20.4	21	8	=H8*(F8^2+G8^2)/12/10000	=H8*((E8^2+G8^2)/12/10000	=H8*((E8^2+F8^2)/12/10000	25	47	0		=H8*N8
REMOTE COMMAND UNIT 2	10	15	21	6	=H9*(F9^2+G9^2)/12/10000	=H9*((E9^2+G9^2)/12/10000	=H9*((E9^2+F9^2)/12/10000	35	-47	0		=H9*N9
REMOTE TELEMETRY 2 UNI	20.32	20.4	21	8	=H10*(F10^2+G10^2)/12/10000	=H10*((E10^2+G10^2)/12/10000	=H10*((E10^2+F10^2)/12/10000	-25	-47	0		=H10*N10
		SUBSYS. TOTAL		=SUM(H7:H10)								
ATTITUDE CONTROL SYSTE												
ATTITUDE CONTROL COMPU	8	19	18	3	=H12*(F12^2+G12^2)/12/10000	=H12*((E12^2+G12^2)/12/10000	=H12*((E12^2+F12^2)/12/10000	-44	-29	0		=H12*N12
MOMENTUM WHEEL PITCH 1	17.5	19.8		10.4	=H13*(E13^2+G13^2)/12/10000	=H13*((E13^2+G13^2)/12/10000	=H13*((E13^2+F13^2)/12/10000	-44	-29	0		=H13*N13
MOMENTUM WHEEL PITCH 2	17.5	19.8		10.4	=H14*(E14^2/240000+(F14^2)/12/10000	=H14*((E14^2/240000+(F14^2)/12/10000	=L14	40	0	-20		=H14*N14
EARTH SENSOR 1 /-N	5.2	16.3		3.8	=H15*(F15^2+G15^2)/12/10000	=H15*((E15^2+G15^2)/12/10000	=H15*((E15^2+F15^2)/12/10000	-43	0	-16		=H15*N15
EARTH SENSOR 2 /+N	5.2	16.3		3.8	=H16/2*(F16^2/10000)	=H16*((F16^2/400000+(E16^2/12/10000	=H16*((F16^2/400000+(E16^2/12/10000	28	0	-30		=H16*N16
SUN SENSOR	2.5	2.5	2.5	0.4	=H17/2*(F17^2/10000)	=H17*((F17^2/400000+(E17^2/12/10000	=H17*((F17^2/400000+(E17^2/12/10000	-28	0	-30		=H17*N17
TORQUE ROD (-X) R/H	1	45		1.7	=H18*(F18^2+G18^2)/12/10000	=H18*((E18^2+G18^2)/12/10000	=H18*((E18^2+F18^2)/12/10000	-40	20	30		=H18*N18
TORQUE ROD (-Z) R/H	1	80		3.2	=H19*(E19^2/4000+H19*(F19^2)/12/2000	0.07526	=H19*(E19^2)/2000	-47.9	30	0		=H19*N19
		SUBSYS. TOTAL		=SUM(H13:H20)	=H20*(E20^2/4000+H20*(F20^2)/12/2000	0.07526	=H20*(E20^2)/2000	0	30	-30		=H20*N20
REACTION CONTROL SYSTE												
PROPELLANT TANK 1 + PRO	81			79								
TUBING AND VALVES/JUMP	98	114	80	4.6	=J*(H23)*(22^2)/2000000	=K23	=K23	0	0	0		=H23*N23
THRUSTER 1	10.78	3.8	3.8	0.319	=H24*(F24^2+G24^2)/12/20000	=H24*((E24^2+G24^2)/12/20000	=H24*((E24^2+F24^2)/12/20000	0	0	0		=H24*N24
THRUSTER 2	10.78	3.8	3.8	0.319	=H25*(F25^2+G25^2)/12/20000	=H25*((E25^2+G25^2)/12/20000	=H25*((E25^2+F25^2)/12/20000	-41.8	-38	20		=H25*N25
THRUSTER 3	10.78	3.8	3.8	0.319	=H26*(F26^2+G26^2)/12/20000	=H26*((E26^2+G26^2)/12/20000	=H26*((E26^2+F26^2)/12/20000	-41.8	38	-20		=H26*N26
THRUSTER 4	10.78	3.8	3.8	0.319	=H27*(F27^2+G27^2)/12/20000	=H27*((E27^2+G27^2)/12/20000	=H27*((E27^2+F27^2)/12/20000	41.8	38	20		=H27*N27
THRUSTER 5	3.8	3.8	10.78	0.319	=H28*(F28^2+G28^2)/12/20000	=H28*((E28^2+G28^2)/12/20000	=H28*((E28^2+F28^2)/12/20000	41.8	-38	-20		=H28*N28
THRUSTER 6	3.8	3.8	10.78	0.319	=H29*(F29^2+G29^2)/12/20000	=H29*((E29^2+G29^2)/12/20000	=H29*((E29^2+F29^2)/12/20000	-41.8	38	20		=H29*N29
		SUBSYS. TOTAL		=SUM(H23:H29)	=H30*(E30^2+G30^2)/12/20000	=H30*((E30^2+G30^2)/12/20000	=H30*((E30^2+F30^2)/12/20000	41.8	-38	20		=H30*N30
STRUCTURAL SUBSYSTEM												
PANEL #1 (EARTH FACE	98	114	3.84	1.01								
PANEL #2 (+x FACE)	3.84	98	80	1.8	=H33*(F33^2+G33^2)/12/20000	=H33*((E33^2+G33^2)/12/20000	=H33*((E33^2+F33^2)/12/20000	0	0	38		=H33*N33
PANEL # 3 (-x FACE)	3.84	98	80	1.8	=H34*(F34^2+G34^2)/12/20000	=H34*((E34^2+G34^2)/12/20000	=H34*((E34^2+F34^2)/12/20000	48	0	0		=H34*N34
PANEL #4 (+y FACE)	98	0.38	80	5.8	=H35*(F35^2+G35^2)/12/20000	=H35*((E35^2+G35^2)/12/20000	=H35*((E35^2+F35^2)/12/20000	-48	0	0		=H35*N35
PANEL # 5 (-y FACE)	99	0.38	80	5.8	=H36*(F36^2+G36^2)/12/20000	=H36*((E36^2+G36^2)/12/20000	=H36*((E36^2+F36^2)/12/20000	0	57	0		=H36*N36
PANELS (ANTI-EARTH FACE	98	114	3.84	1.01	=H37*(F37^2+G37^2)/12/20000	=H37*((E37^2+G37^2)/12/20000	=H37*((E37^2+F37^2)/12/20000	0	-57	0		=H37*N37
FRAME MEMBER 1	3.81	114	5.08	0.842	=H38*(F38^2+G38^2)/12/20000	=H38*((E38^2+G38^2)/12/20000	=H38*((E38^2+F38^2)/12/20000	0	0	-30		=H38*N38
FRAME MEMBER 2	3.81	114	5.08	0.842	=H39*(F39^2+G39^2)/12/80000	=H39*((E39^2+G39^2)/12/80000	=H39*((E39^2+F39^2)/12/80000	48	0	-28		=H39*N39
FRAME MEMBER 3	3.81	114	5.08	0.842	=H40*(F40^2+G40^2)/12/80000	=H40*((E40^2+G40^2)/12/80000	=H40*((E40^2+F40^2)/12/80000	48	0	28		=H40*N40
FRAME MEMBER 4	3.81	114	5.08	0.842	=H41*(F41^2+G41^2)/12/80000	=H41*((E41^2+G41^2)/12/80000	=H41*((E41^2+F41^2)/12/80000	-48	0	28		=H41*N41
FRAME MEMBER 5	98	3.81	5.08	0.724	=H42*(F42^2+G42^2)/12/80000	=H42*((E42^2+G42^2)/12/80000	=H42*((E42^2+F42^2)/12/80000	-48	0	-28		=H42*N42
FRAME MEMBER 6	98	3.81	5.08	0.724	=H43*(F43^2+G43^2)/12/80000	=H43*((E43^2+G43^2)/12/80000	=H43*((E43^2+F43^2)/12/80000	0	58	-28		=H43*N43
FRAME MEMBER 7	98	3.81	5.08	0.724	=H44*(F44^2+G44^2)/12/80000	=H44*((E44^2+G44^2)/12/80000	=H44*((E44^2+F44^2)/12/80000	0	58	28		=H44*N44
FRAME MEMBER 8	98	3.81	5.08	0.724	=H45*(F45^2+G45^2)/12/80000	=H45*((E45^2+G45^2)/12/80000	=H45*((E45^2+F45^2)/12/80000	0	-58	-28		=H45*N45
FRAME MEMBER 9	3.81	2.54	80	0.312	=H46*(F46^2+G46^2)/12/80000	=H46*((E46^2+G46^2)/12/80000	=H46*((E46^2+F46^2)/12/80000	0	-58	28		=H46*N46
FRAME MEMBER 10	3.81	2.54	80	0.312	=H47*(F47^2+G47^2)/12/80000	=H47*((E47^2+G47^2)/12/80000	=H47*((E47^2+F47^2)/12/80000	48	-57	0		=H47*N47
FRAME MEMBER 11	3.81	2.54	80	0.312	=H48*(F48^2+G48^2)/12/80000	=H48*((E48^2+G48^2)/12/80000	=H48*((E48^2+F48^2)/12/80000	48	57	0		=H48*N48
FRAME MEMBER 12	3.81	2.54	80	0.311	=H49*(F49^2+G49^2)/12/80000	=H49*((E49^2+G49^2)/12/80000	=H49*((E49^2+F49^2)/12/80000	-48	57	0		=H49*N49
RAIL # 1	2.54	2.54	140	1.19	=H50*(F50^2+G50^2)/12/80000	=H50*((E50^2+G50^2)/12/80000	=H50*((E50^2+F50^2)/12/80000	48	-57	0		=H50*N50
RAIL # 2	2.54	2.54	140	1.19	=H51*(F51^2+G51^2)/12/20000	=H51*((E51^2+G51^2)/12/20000	=H51*((E51^2+F51^2)/12/20000	0	-57	30		=H51*N51
MISC(BRACKETS&STRUTS)	98	114	80	15	=H52*(F52^2+G52^2)/12/20000	=H52*((E52^2+G52^2)/12/20000	=H52*((E52^2+F52^2)/12/20000	0	57	30		=H52*N52
		SUBSYS. TOTAL		=SUM(H33:H52)	=H53*(F53^2+G53^2)/12/20000	=H53*((E53^2+G53^2)/12/20000	=H53*((E53^2+F53^2)/12/20000	0	0	0		=H53*N53
ELECTRIC POWER SUBSYSTE												
BATTERY1	80	28	10	7.5	=H56*(F56^2+G56^2)/12/20000	=H56*((E56^2+G56^2)/12/20000	=H56*((E56^2+F56^2)/12/20000	0	48	-30		=H56*N56
BATTERY2	80	28	10	7.5	=H57*(F57^2+G57^2)/12/20000	=H57*((E57^2+G57^2)/12/20000	=H57*((E57^2+F57^2)/12/20000	0	-48	30		=H57*N57
BATTERY3	80	28	10	7.5	=H58*(F58^2+G58^2)/12/20000	=H58*((E58^2+G58^2)/12/20000	=H58*((E58^2+F58^2)/12/20000	0	-48	-30		=H58*N58
BATTERY4	80	28	10	7.5	=H59*(F59^2+G59^2)/12/20000	=H59*((E59^2+G59^2)/12/20000	=H59*((E59^2+F59^2)/12/20000	0	-48	30		=H59*N59
POWER CONTROL UNIT	15	40	18	6	=H60*(F60^2+G60^2)/12/20000	=H60*((E60^2+G60^2)/12/20000	=H60*((E60^2+F60^2)/12/20000	43	30	-18		=H60*N60
SOLAR ARRAY DRIVE 1 dv	10	7.9		2	=H61*(F61^2)/40000+H61*(G61^2)/12/20000	=H61*((F61^2)/40000+H61*((G61^2)/12/20000	=K61	43	0	30		=H61*N61
SOLAR ARRAY DRIVE2 dv	10	7.9		2	=H62*(F62^2)/40000+H62*(G62^2)/12/20000	=H62*((F62^2)/40000+H62*((G62^2)/12/20000	=K62	-43	0	30		=H62*N62
SOLAR ARRAY PANEL 1A	2	140	80	4	=H63*(F63^2+G63^2)/12/20000	=H63*((E63^2+G63^2)/12/20000	=H63*((E63^2+F63^2)/12/20000	53	0	0		=H63*N63
SOLAR ARRAY PANEL 1B	2	140	80	4	=H64*(F64^2+G64^2)/12/20000	=H64*((E64^2+G64^2)/12/20000	=H64*((E64^2+F64^2)/12/20000	57	0	0		=H64*N64
SOLAR ARRAY PANEL 1C	2	140	80	4	=H65*(F65^2+G65^2)/12/20000	=H65*((E65^2+G65^2)/12/20000	=H65*((E65^2+F65^2)/12/20000	61	0	0		=H65*N65
SOLAR ARRAY PANEL 1D	2	140	80	4	=H66*(F66^2+G66^2)/12/20000	=H66*((E66^2+G66^2)/12/20000	=H66*((E66^2+F66^2)/12/20000	65	0	0		=H66*N66
SOLAR ARRAY PANEL 2A	2	140	80	4	=H67*(F67^2+G67^2)/12/20000	=H67*((E67^2+G67^2)/12/20000	=H67*((E67^2+F67^2)/12/20000	-53	0	0		=H67*N67
SOLAR ARRAY PANEL 2B	2	140	80	4	=H68*(F68^2+G68^2)/12/20000	=H68*((E68^2+G68^2)/12/20000	=H68*((E68^2+F68^2)/12/20000	-57	0	0		=H68*N68
SOLAR ARRAY PANEL 2C	2	140	80	4	=H69*(F69^2+G69^2)/12/20000	=H69*((E69^2+G69^2)/12/20000	=H69*((E69^2+F69^2)/12/20000	-61	0	0		=H69*N69
SOLAR ARRAY PANEL 2D	2	140	80	4	=H70*(F70^2+G70^2)/12/20000	=H70*((E70^2+G70^2)/12/20000	=H70*((E70^2+F70^2)/12/20000	-65	0	0		=H70*N70
SHUNT RESISTOR BANK1	1	140	25	1	=H71*(F71^2+G71^2)/12/20000	=H71*((E71^2+G71^2)/12/20000	=H71*((E71^2+F71^2)/12/20000	-50	0	-30		=H71*N71
SHUNT RESISTOR BANK2	1	140	25	1	=H72*(F72^2+G72^2)/12/20000	=H72*((E72^2+G72^2)/12/20000	=H72*((E72^2+F72^2)/12/20000	50	0	30		=H72*N72
ELECTRICAL UNT (UNIF DIST)	98	114	80	13	=H73*(F73^2+G73^2)/12/20000	=H73*((E73^2+G73^2)/12/20000	=H73*((E73^2+F73^2)/12/20000	0	0	0		=H73*N73
		SUBSYS. TOTAL		=SUM(H56:H73)								
THERMAL CONTROL SUBSY												
LOUVERS1 (+Y)	47	8.89	86	1.5								
LOUVERS 2 (+Y)	47	8.89	86	1.5	=H76*(F76^2+G76^2)/12/20000	=H76*((E76^2+G76^2)/12/20000	=H76*((E76^2+F76^2)/12/20000	33.8	82	0		=H76*N76
LOUVERS 3 (-Y)	47	8.89	86	1.9	=H77*(F77^2+G77^2)/12/20000	=H77*((E77^2+G77^2)/12/20000	=H77*((E77^2+F77^2)/12/20000	-33.8	82	0		=H77*N77
LOUVERS4 (-Y)	47	8.89	86	1.9	=H78*(F78^2+G78^2)/12/20000	=H78*((E78^2+G78^2)/12/20000	=H78*((E78^2+F78^2)/12/20000	33.8	-82	0		=H78*N78
PHASE CHANGER (+Y)	98	0.7	98	1.9	=H79*(F79^2+G79^2)/12/20000	=H79*((E79^2+G79^2)/12/20000	=H79*((E79^2+F79^2)/12/20000	-33.8	-82	0		=H79*N79
PHASE CHANGER (-Y)	98	0.7	98	2.86	=H80*(F80^2+G80^2)/12/20000	=H80*((E80^2+G80^2)/12/20000	=H80*((E80^2+F80^2)/12/20000	0	86	0		=H80*N80
RADIATOR (+Y)	98	0.2	98	0.5	=H81*(F81^2+G81^2)/12/20000	=H81*((E81^2+G81^2)/12/20000	=H81*((E81^2+F81^2)/12/20000	0	-86	0		=H81*N81
RADIATOR (-Y)	98	0.2	98	0.5	=H82*(F82^2+G82^2)/12/20000	=H82*((E82^2+G82^2)/12/20000	=H82*((E82^2+F82^2)/12/20000	-33.8	57	0		=H82*N82
MULTILAYER INSULATION	98	114	80	9	=H83*(F83^2+G83^2)/12/20000	=H83*((E83^2+G83^2)/12/20000	=H83*((E83^2+F83^2)/12/20000	-33.8	-57	0		=H83*N83
MISC(UNIF DIST)	98	114	80	3	=H84*(F84^2+G84^2)/12/20000	=H84*((E84^2+G84^2)/12/20000	=H84*((E84^2+F84^2)/12/20000	0	0	0		=H84*N84
		SUBSYS. TOTAL		=SUM(H76:H83)	=H85*(F85^2+G85^2)/12/20000	=H85*((E85^2+G85^2)/12/20000	=H85*((E85^2+F85^2)/12/20000	0	0	0		=H85*N85
PAYLOAD												
PHASED ARRAY PANEL	140	140	9.1	6								
PHASED ARRAY WING 1(+x)	80	140	10.2	3	=H88*(F88^2+G88^2)/12/20000	=H88*((E88^2+G88^2)/12/20000	=H88*((E88^2+F88^2)/12/20000	0	0	-33.8		=H88*N88
PHASED ARRAY WING2(-x)	80	140	10.2	3	=H89*(F89^2+G89^2)/12/20000	=H89*((E89^2+G89^2)/12/20000	=H89*((E89^2+F89^2)/12/20000	48	0	-46.2		=H89*N89
C-L BAND TRANSPONDER	30	10	20	10	=H90*(F90^2+G90^2)/12/20000	=H90*((E90^2+G90^2)/12/20000	=H90*((E90^2+F90^2)/12/20000	-48	0	-46.2		=H90*N90
S-C BAND TRANSPONDER	30	10	20	10	=H91*(F91^2+G91^2)/12/20000	=H91*((E91^2+G91^2)/12/20000	=H91*((E91^2+F91^2)/12/20000	-8	53	0		=H91*N91
TIMING CONTROL UNIT	10	30	20	20	=H92*(F92^2+G92^2)/12/20000	=H92*((E92^2+G92^2)/12/20000	=H92*((E92^2+F92^2)/12/20000	8	-53	0		=H92*N92
		SUBSYS. TOTAL		=SUM(H88:H92)	=H93*(F93^2+G93^2)/12/20000	=H93*((E93^2+G93^2)/12/20000	=H93*((E93^2+F93^2)/12/20000	48	30	15		=H93*N93
		SUBTOTAL MASS		=SUM(H7:H84)/2								
		10% MASS MARGIN		=0.1*H94					CENTER OF MASS OFFSET			=SUM(R7:R93)/94
		TOTAL MASS		=H94+H97								

S	T	U	V	W	X	Z	AA	AB	AC	AD	AE
				DISTANCE FROM CENTER		TOTAL MOMENT OF INERTIA(KG*M^2)					
Cy	Cz		Dx	Dy	Dz	Ixx	Iyy	Izz	Ixy	Ixz	Iyz
=M7*O7	=M7*P7		=ABS(SR$96-N7)	=ABS(SS$96-O7)	=ABS(ST$96-P7)	=K7+M7*(W7^2+V7^2)/10000	=L7+M7*(V7^2+V7^2)/10000	=M7+M7*(V7^2+W7^2)/10000	=M7*(N7-R$98)*(O7-S$98)/10000	=M7*(N7-R$98)*(P7-T$98)/10000	=M7*(O7-S$98)*(P7-T$98)/10000
=M8*O8	=M8*P8		=ABS(SR$96-N8)	=ABS(SS$96-O8)	=ABS(ST$96-P8)	=K8+M8*(W8^2+V8^2)/10000	=L8+M8*(V8^2+V8^2)/10000	=M8+M8*(V8^2+W8^2)/10000	=M8*(N8-R$98)*(O8-S$98)/10000	=M8*(N8-R$98)*(P8-T$98)/10000	=M8*(O8-S$98)*(P8-T$98)/10000
=M9*O9	=M9*P9		=ABS(SR$96-N9)	=ABS(SS$96-O9)	=ABS(ST$96-P9)	=K9+M9*(W9^2+V9^2)/10000	=L9+M9*(V9^2+V9^2)/10000	=M9+M9*(V9^2+W9^2)/10000	=M9*(N9-R$98)*(O9-S$98)/10000	=M9*(N9-R$98)*(P9-T$98)/10000	=M9*(O9-S$98)*(P9-T$98)/10000
=M10*O10	=M10*P10		=ABS(SR$96-N10)	=ABS(SS$96-O10)	=ABS(ST$96-P10)	=K10+M10*(W10^2+V10^2)/10000	=L10+M10*(V10^2+V10^2)/10000	=M10+M10*(V10^2+W10^2)/10000	=M10*(N10-R$98)*(O10-S$98)/10000	=M10*(N10-R$98)*(P10-T$98)/10000	=M10*(O10-S$98)*(P10-T$98)/10000
=M13*O13	=M13*P13		=ABS(SR$96-N13)	=ABS(SS$96-O13)	=ABS(ST$96-P13)	=K13+M13*(W13^2+V13^2)/10000	=L13+M13*(V13^2+V13^2)/10000	=M13+M13*(V13^2+W13^2)/10000	=M13*(N13-R$98)*(O13-S$98)/10000	=M13*(N13-R$98)*(P13-T$98)/10000	=M13*(O13-S$98)*(P13-T$98)/10000
=M14*O14	=M14*P14		=ABS(SR$96-N14)	=ABS(SS$96-O14)	=ABS(ST$96-P14)	=K14+M14*(W14^2+V14^2)/10000	=L14+M14*(V14^2+V14^2)/10000	=M14+M14*(V14^2+W14^2)/10000	=M14*(N14-R$98)*(O14-S$98)/10000	=M14*(N14-R$98)*(P14-T$98)/10000	=M14*(O14-S$98)*(P14-T$98)/10000
=M15*O15	=M15*P15		=ABS(SR$96-N15)	=ABS(SS$96-O15)	=ABS(ST$96-P15)	=K15+M15*(W15^2+V15^2)/10000	=L15+M15*(V15^2+V15^2)/10000	=M15+M15*(V15^2+W15^2)/10000	=M15*(N15-R$98)*(O15-S$98)/10000	=M15*(N15-R$98)*(P15-T$98)/10000	=M15*(O15-S$98)*(P15-T$98)/10000
=M16*O16	=M16*P16		=ABS(SR$96-N16)	=ABS(SS$96-O16)	=ABS(ST$96-P16)	=K16+M16*(W16^2+V16^2)/10000	=L16+M16*(V16^2+V16^2)/10000	=M16+M16*(V16^2+W16^2)/10000	=M16*(N16-R$98)*(O16-S$98)/10000	=M16*(N16-R$98)*(P16-T$98)/10000	=M16*(O16-S$98)*(P16-T$98)/10000
=M17*O17	=M17*P17		=ABS(SR$96-N17)	=ABS(SS$96-O17)	=ABS(ST$96-P17)	=K17+M17*(W17^2+V17^2)/10000	=L17+M17*(V17^2+V17^2)/10000	=M17+M17*(V17^2+W17^2)/10000	=M17*(N17-R$98)*(O17-S$98)/10000	=M17*(N17-R$98)*(P17-T$98)/10000	=M17*(O17-S$98)*(P17-T$98)/10000
=M18*O18	=M18*P18		=ABS(SR$96-N18)	=ABS(SS$96-O18)	=ABS(ST$96-P18)	=K18+M18*(W18^2+V18^2)/10000	=L18+M18*(V18^2+V18^2)/10000	=M18+M18*(V18^2+W18^2)/10000	=M18*(N18-R$98)*(O18-S$98)/10000	=M18*(N18-R$98)*(P18-T$98)/10000	=M18*(O18-S$98)*(P18-T$98)/10000
=M19*O19	=M19*P19		=ABS(SR$96-N19)	=ABS(SS$96-O19)	=ABS(ST$96-P19)	=K19+M19*(W19^2+V19^2)/10000	=L19+M19*(V19^2+V19^2)/10000	=M19+M19*(V19^2+W19^2)/10000	=M19*(N19-R$98)*(O19-S$98)/10000	=M19*(N19-R$98)*(P19-T$98)/10000	=M19*(O19-S$98)*(P19-T$98)/10000
=M20*O20	=M20*P20		=ABS(SR$96-N20)	=ABS(SS$96-O20)	=ABS(ST$96-P20)	=K20+M20*(W20^2+V20^2)/10000	=L20+M20*(V20^2+V20^2)/10000	=M20+M20*(V20^2+W20^2)/10000	=M20*(N20-R$98)*(O20-S$98)/10000	=M20*(N20-R$98)*(P20-T$98)/10000	=M20*(O20-S$98)*(P20-T$98)/10000
=M23*O23	=M23*P23		=ABS(SR$96-N23)	=ABS(SS$96-O23)	=ABS(ST$96-P23)	=K23+M23*(W23^2+V23^2)/10000	=L23+M23*(V23^2+V23^2)/10000	=M23+M23*(V23^2+W23^2)/10000	=M23*(N23-R$98)*(O23-S$98)/10000	=M23*(N23-R$98)*(P23-T$98)/10000	=M23*(O23-S$98)*(P23-T$98)/10000
=M24*O24	=M24*P24		=ABS(SR$96-N24)	=ABS(SS$96-O24)	=ABS(ST$96-P24)	=K24+M24*(W24^2+V24^2)/10000	=L24+M24*(V24^2+V24^2)/10000	=M24+M24*(V24^2+W24^2)/10000	=M24*(N24-R$98)*(O24-S$98)/10000	=M24*(N24-R$98)*(P24-T$98)/10000	=M24*(O24-S$98)*(P24-T$98)/10000
=M25*O25	=M25*P25		=ABS(SR$96-N25)	=ABS(SS$96-O25)	=ABS(ST$96-P25)	=K25+M25*(W25^2+V25^2)/10000	=L25+M25*(V25^2+V25^2)/10000	=M25+M25*(V25^2+W25^2)/10000	=M25*(N25-R$98)*(O25-S$98)/10000	=M25*(N25-R$98)*(P25-T$98)/10000	=M25*(O25-S$98)*(P25-T$98)/10000
=M26*O26	=M26*P26		=ABS(SR$96-N26)	=ABS(SS$96-O26)	=ABS(ST$96-P26)	=K26+M26*(W26^2+V26^2)/10000	=L26+M26*(V26^2+V26^2)/10000	=M26+M26*(V26^2+W26^2)/10000	=M26*(N26-R$98)*(O26-S$98)/10000	=M26*(N26-R$98)*(P26-T$98)/10000	=M26*(O26-S$98)*(P26-T$98)/10000
=M27*O27	=M27*P27		=ABS(SR$96-N27)	=ABS(SS$96-O27)	=ABS(ST$96-P27)	=K27+M27*(W27^2+V27^2)/10000	=L27+M27*(V27^2+V27^2)/10000	=M27+M27*(V27^2+W27^2)/10000	=M27*(N27-R$98)*(O27-S$98)/10000	=M27*(N27-R$98)*(P27-T$98)/10000	=M27*(O27-S$98)*(P27-T$98)/10000
=M28*O28	=M28*P28		=ABS(SR$96-N28)	=ABS(SS$96-O28)	=ABS(ST$96-P28)	=K28+M28*(W28^2+V28^2)/10000	=L28+M28*(V28^2+V28^2)/10000	=M28+M28*(V28^2+W28^2)/10000	=M28*(N28-R$98)*(O28-S$98)/10000	=M28*(N28-R$98)*(P28-T$98)/10000	=M28*(O28-S$98)*(P28-T$98)/10000
=M29*O29	=M29*P29		=ABS(SR$96-N29)	=ABS(SS$96-O29)	=ABS(ST$96-P29)	=K29+M29*(W29^2+V29^2)/10000	=L29+M29*(V29^2+V29^2)/10000	=M29+M29*(V29^2+W29^2)/10000	=M29*(N29-R$98)*(O29-S$98)/10000	=M29*(N29-R$98)*(P29-T$98)/10000	=M29*(O29-S$98)*(P29-T$98)/10000
=M30*O30	=M30*P30		=ABS(SR$96-N30)	=ABS(SS$96-O30)	=ABS(ST$96-P30)	=K30+M30*(W30^2+V30^2)/10000	=L30+M30*(V30^2+V30^2)/10000	=M30+M30*(V30^2+W30^2)/10000	=M30*(N30-R$98)*(O30-S$98)/10000	=M30*(N30-R$98)*(P30-T$98)/10000	=M30*(O30-S$98)*(P30-T$98)/10000
=M33*O33	=M33*P33		=ABS(SR$96-N33)	=ABS(SS$96-O33)	=ABS(ST$96-P33)	=K33+M33*(W33^2+V33^2)/10000	=L33+M33*(V33^2+V33^2)/10000	=M33+M33*(V33^2+W33^2)/10000	=M33*(N33-R$98)*(O33-S$98)/10000	=M33*(N33-R$98)*(P33-T$98)/10000	=M33*(O33-S$98)*(P33-T$98)/10000
=M34*O34	=M34*P34		=ABS(SR$96-N34)	=ABS(SS$96-O34)	=ABS(ST$96-P34)	=K34+M34*(W34^2+V34^2)/10000	=L34+M34*(V34^2+V34^2)/10000	=M34+M34*(V34^2+W34^2)/10000	=M34*(N34-R$98)*(O34-S$98)/10000	=M34*(N34-R$98)*(P34-T$98)/10000	=M34*(O34-S$98)*(P34-T$98)/10000
=M35*O35	=M35*P35		=ABS(SR$96-N35)	=ABS(SS$96-O35)	=ABS(ST$96-P35)	=K35+M35*(W35^2+V35^2)/10000	=L35+M35*(V35^2+V35^2)/10000	=M35+M35*(V35^2+W35^2)/10000	=M35*(N35-R$98)*(O35-S$98)/10000	=M35*(N35-R$98)*(P35-T$98)/10000	=M35*(O35-S$98)*(P35-T$98)/10000
=M36*O36	=M36*P36		=ABS(SR$96-N36)	=ABS(SS$96-O36)	=ABS(ST$96-P36)	=K36+M36*(W36^2+V36^2)/10000	=L36+M36*(V36^2+V36^2)/10000	=M36+M36*(V36^2+W36^2)/10000	=M36*(N36-R$98)*(O36-S$98)/10000	=M36*(N36-R$98)*(P36-T$98)/10000	=M36*(O36-S$98)*(P36-T$98)/10000
=M37*O37	=M37*P37		=ABS(SR$96-N37)	=ABS(SS$96-O37)	=ABS(ST$96-P37)	=K37+M37*(W37^2+V37^2)/10000	=L37+M37*(V37^2+V37^2)/10000	=M37+M37*(V37^2+W37^2)/10000	=M37*(N37-R$98)*(O37-S$98)/10000	=M37*(N37-R$98)*(P37-T$98)/10000	=M37*(O37-S$98)*(P37-T$98)/10000
=M38*O38	=M38*P38		=ABS(SR$96-N38)	=ABS(SS$96-O38)	=ABS(ST$96-P38)	=K38+M38*(W38^2+V38^2)/10000	=L38+M38*(V38^2+V38^2)/10000	=M38+M38*(V38^2+W38^2)/10000	=M38*(N38-R$98)*(O38-S$98)/10000	=M38*(N38-R$98)*(P38-T$98)/10000	=M38*(O38-S$98)*(P38-T$98)/10000
=M39*O39	=M29*P39		=ABS(SR$96-N39)	=ABS(SS$96-O39)	=ABS(ST$96-P39)	=K39+M39*(W39^2+V39^2)/10000	=L39+M39*(V39^2+V39^2)/10000	=M39+M39*(V39^2+W39^2)/10000	=M39*(N39-R$98)*(O39-S$98)/10000	=M39*(N39-R$98)*(P39-T$98)/10000	=M39*(O39-S$98)*(P39-T$98)/10000
=M40*O40	=M40*P40		=ABS(SR$96-N40)	=ABS(SS$96-O40)	=ABS(ST$96-P40)	=K40+M40*(W40^2+V40^2)/10000	=L40+M40*(V40^2+V40^2)/10000	=M40+M40*(V40^2+W40^2)/10000	=M40*(N40-R$98)*(O40-S$98)/10000	=M40*(N40-R$98)*(P40-T$98)/10000	=M40*(O40-S$98)*(P40-T$98)/10000
=M41*O41	=M41*P41		=ABS(SR$96-N41)	=ABS(SS$96-O41)	=ABS(ST$96-P41)	=K41+M41*(W41^2+V41^2)/10000	=L41+M41*(V41^2+V41^2)/10000	=M41+M41*(V41^2+W41^2)/10000	=M41*(N41-R$98)*(O41-S$98)/10000	=M41*(N41-R$98)*(P41-T$98)/10000	=M41*(O41-S$98)*(P41-T$98)/10000
=M42*O42	=M42*P42		=ABS(SR$96-N42)	=ABS(SS$96-O42)	=ABS(ST$96-P42)	=K42+M42*(W42^2+V42^2)/10000	=L42+M42*(V42^2+V42^2)/10000	=M42+M42*(V42^2+W42^2)/10000	=M42*(N42-R$98)*(O42-S$98)/10000	=M42*(N42-R$98)*(P42-T$98)/10000	=M42*(O42-S$98)*(P42-T$98)/10000
=M43*O43	=M43*P43		=ABS(SR$96-N43)	=ABS(SS$96-O43)	=ABS(ST$96-P43)	=K43+M43*(W43^2+V43^2)/10000	=L43+M43*(V43^2+V43^2)/10000	=M43+M43*(V43^2+W43^2)/10000	=M43*(N43-R$98)*(O43-S$98)/10000	=M43*(N43-R$98)*(P43-T$98)/10000	=M43*(O43-S$98)*(P43-T$98)/10000
=M44*O44	=M44*P44		=ABS(SR$96-N44)	=ABS(SS$96-O44)	=ABS(ST$96-P44)	=K44+M44*(W44^2+V44^2)/10000	=L44+M44*(V44^2+V44^2)/10000	=M44+M44*(V44^2+W44^2)/10000	=M44*(N44-R$98)*(O44-S$98)/10000	=M44*(N44-R$98)*(P44-T$98)/10000	=M44*(O44-S$98)*(P44-T$98)/10000
=M45*O45	=M45*P45		=ABS(SR$96-N45)	=ABS(SS$96-O45)	=ABS(ST$96-P45)	=K45+M45*(W45^2+V45^2)/10000	=L45+M45*(V45^2+V45^2)/10000	=M45+M45*(V45^2+W45^2)/10000	=M45*(N45-R$98)*(O45-S$98)/10000	=M45*(N45-R$98)*(P45-T$98)/10000	=M45*(O45-S$98)*(P45-T$98)/10000
=M46*O46	=M46*P46		=ABS(SR$96-N46)	=ABS(SS$96-O46)	=ABS(ST$96-P46)	=K46+M46*(W46^2+V46^2)/10000	=L46+M46*(V46^2+V46^2)/10000	=M46+M46*(V46^2+W46^2)/10000	=M46*(N46-R$98)*(O46-S$98)/10000	=M46*(N46-R$98)*(P46-T$98)/10000	=M46*(O46-S$98)*(P46-T$98)/10000
=M47*O47	=M47*P47		=ABS(SR$96-N47)	=ABS(SS$96-O47)	=ABS(ST$96-P47)	=K47+M47*(W47^2+V47^2)/10000	=L47+M47*(V47^2+V47^2)/10000	=M47+M47*(V47^2+W47^2)/10000	=M47*(N47-R$98)*(O47-S$98)/10000	=M47*(N47-R$98)*(P47-T$98)/10000	=M47*(O47-S$98)*(P47-T$98)/10000
=M48*O48	=M48*P48		=ABS(SR$96-N48)	=ABS(SS$96-O48)	=ABS(ST$96-P48)	=K48+M48*(W48^2+V48^2)/10000	=L48+M48*(V48^2+V48^2)/10000	=M48+M48*(V48^2+W48^2)/10000	=M48*(N48-R$98)*(O48-S$98)/10000	=M48*(N48-R$98)*(P48-T$98)/10000	=M48*(O48-S$98)*(P48-T$98)/10000
=M49*O49	=M49*P49		=ABS(SR$96-N49)	=ABS(SS$96-O49)	=ABS(ST$96-P49)	=K49+M49*(W49^2+V49^2)/10000	=L49+M49*(V49^2+V49^2)/10000	=M49+M49*(V49^2+W49^2)/10000	=M49*(N49-R$98)*(O49-S$98)/10000	=M49*(N49-R$98)*(P49-T$98)/10000	=M49*(O49-S$98)*(P49-T$98)/10000
=M50*O50	=M50*P50		=ABS(SR$96-N50)	=ABS(SS$96-O50)	=ABS(ST$96-P50)	=K50+M50*(W50^2+V50^2)/10000	=L50+M50*(V50^2+V50^2)/10000	=M50+M50*(V50^2+W50^2)/10000	=M50*(N50-R$98)*(O50-S$98)/10000	=M50*(N50-R$98)*(P50-T$98)/10000	=M50*(O50-S$98)*(P50-T$98)/10000
=M51*O51	=M51*P51		=ABS(SR$96-N51)	=ABS(SS$96-O51)	=ABS(ST$96-P51)	=K51+M51*(W51^2+V51^2)/10000	=L51+M51*(V51^2+V51^2)/10000	=M51+M51*(V51^2+W51^2)/10000	=M51*(N51-R$98)*(O51-S$98)/10000	=M51*(N51-R$98)*(P51-T$98)/10000	=M51*(O51-S$98)*(P51-T$98)/10000
=M52*O52	=M52*P52		=ABS(SR$96-N52)	=ABS(SS$96-O52)	=ABS(ST$96-P52)	=K52+M52*(W52^2+V52^2)/10000	=L52+M52*(V52^2+V52^2)/10000	=M52+M52*(V52^2+W52^2)/10000	=M52*(N52-R$98)*(O52-S$98)/10000	=M52*(N52-R$98)*(P52-T$98)/10000	=M52*(O52-S$98)*(P52-T$98)/10000
=M53*O53	=M53*P53		=ABS(SR$96-N53)	=ABS(SS$96-O53)	=ABS(ST$96-P53)	=K53+M53*(W53^2+V53^2)/10000	=L53+M53*(V53^2+V53^2)/10000	=M53+M53*(V53^2+W53^2)/10000	=M53*(N53-R$98)*(O53-S$98)/10000	=M53*(N53-R$98)*(P53-T$98)/10000	=M53*(O53-S$98)*(P53-T$98)/10000
=M56*O56	=M56*P56		=ABS(SR$96-N56)	=ABS(SS$96-O56)	=ABS(ST$96-P56)	=K56+M56*(W56^2+V56^2)/10000	=L56+M56*(V56^2+V56^2)/10000	=M56+M56*(V56^2+W56^2)/10000	=M56*(N56-R$98)*(O56-S$98)/10000	=M56*(N56-R$98)*(P56-T$98)/10000	=M56*(O56-S$98)*(P56-T$98)/10000
=M57*O57	=M57*P57		=ABS(SR$96-N57)	=ABS(SS$96-O57)	=ABS(ST$96-P57)	=K57+M57*(W57^2+V57^2)/10000	=L57+M57*(V57^2+V57^2)/10000	=M57+M57*(V57^2+W57^2)/10000	=M57*(N57-R$98)*(O57-S$98)/10000	=M57*(N57-R$98)*(P57-T$98)/10000	=M57*(O57-S$98)*(P57-T$98)/10000
=M58*O58	=M58*P58		=ABS(SR$96-N58)	=ABS(SS$96-O58)	=ABS(ST$96-P58)	=K58+M58*(W58^2+V58^2)/10000	=L58+M58*(V58^2+V58^2)/10000	=M58+M58*(V58^2+W58^2)/10000	=M58*(N58-R$98)*(O58-S$98)/10000	=M58*(N58-R$98)*(P58-T$98)/10000	=M58*(O58-S$98)*(P58-T$98)/10000
=M59*O59	=M59*P59		=ABS(SR$96-N59)	=ABS(SS$96-O59)	=ABS(ST$96-P59)	=K59+M59*(W59^2+V59^2)/10000	=L59+M59*(V59^2+V59^2)/10000	=M59+M59*(V59^2+W59^2)/10000	=M59*(N59-R$98)*(O59-S$98)/10000	=M59*(N59-R$98)*(P59-T$98)/10000	=M59*(O59-S$98)*(P59-T$98)/10000
=M60*O60	=M60*P60		=ABS(SR$96-N60)	=ABS(SS$96-O60)	=ABS(ST$96-P60)	=K60+M60*(W60^2+V60^2)/10000	=L60+M60*(V60^2+V60^2)/10000	=M60+M60*(V60^2+W60^2)/10000	=M60*(N60-R$98)*(O60-S$98)/10000	=M60*(N60-R$98)*(P60-T$98)/10000	=M60*(O60-S$98)*(P60-T$98)/10000
=M61*O61	=M61*P61		=ABS(SR$96-N61)	=ABS(SS$96-O61)	=ABS(ST$96-P61)	=K61+M61*(W61^2+V61^2)/10000	=L61+M61*(V61^2+V61^2)/10000	=M61+M61*(V61^2+W61^2)/10000	=M61*(N61-R$98)*(O61-S$98)/10000	=M61*(N61-R$98)*(P61-T$98)/10000	=M61*(O61-S$98)*(P61-T$98)/10000
=M62*O62	=M62*P62		=ABS(SR$96-N62)	=ABS(SS$96-O62)	=ABS(ST$96-P62)	=K62+M62*(W62^2+V62^2)/10000	=L62+M62*(V62^2+V62^2)/10000	=M62+M62*(V62^2+W62^2)/10000	=M62*(N62-R$98)*(O62-S$98)/10000	=M62*(N62-R$98)*(P62-T$98)/10000	=M62*(O62-S$98)*(P62-T$98)/10000
=M63*O63	=M63*P63		=ABS(SR$96-N63)	=ABS(SS$96-O63)	=ABS(ST$96-P63)	=K63+M63*(W63^2+V63^2)/10000	=L63+M63*(V63^2+V63^2)/10000	=M63+M63*(V63^2+W63^2)/10000	=M63*(N63-R$98)*(O63-S$98)/10000	=M63*(N63-R$98)*(P63-T$98)/10000	=M63*(O63-S$98)*(P63-T$98)/10000
=M64*O64	=M64*P64		=ABS(SR$96-N64)	=ABS(SS$96-O64)	=ABS(ST$96-P64)	=K64+M64*(W64^2+V64^2)/10000	=L64+M64*(V64^2+V64^2)/10000	=M64+M64*(V64^2+W64^2)/10000	=M64*(N64-R$98)*(O64-S$98)/10000	=M64*(N64-R$98)*(P64-T$98)/10000	=M64*(O64-S$98)*(P64-T$98)/10000
=M65*O65	=M65*P65		=ABS(SR$96-N65)	=ABS(SS$96-O65)	=ABS(ST$96-P65)	=K65+M65*(W65^2+V65^2)/10000	=L65+M65*(V65^2+V65^2)/10000	=M65+M65*(V65^2+W65^2)/10000	=M65*(N65-R$98)*(O65-S$98)/10000	=M65*(N65-R$98)*(P65-T$98)/10000	=M65*(O65-S$98)*(P65-T$98)/10000
=M66*O66	=M66*P66		=ABS(SR$96-N66)	=ABS(SS$96-O66)	=ABS(ST$96-P66)	=K66+M66*(W66^2+V66^2)/10000	=L66+M66*(V66^2+V66^2)/10000	=M66+M66*(V66^2+W66^2)/10000	=M66*(N66-R$98)*(O66-S$98)/10000	=M66*(N66-R$98)*(P66-T$98)/10000	=M66*(O66-S$98)*(P66-T$98)/10000
=M67*O67	=M67*P67		=ABS(SR$96-N67)	=ABS(SS$96-O67)	=ABS(ST$96-P67)	=K67+M67*(W67^2+V67^2)/10000	=L67+M67*(V67^2+V67^2)/10000	=M67+M67*(V67^2+W67^2)/10000	=M67*(N67-R$98)*(O67-S$98)/10000	=M67*(N67-R$98)*(P67-T$98)/10000	=M67*(O67-S$98)*(P67-T$98)/10000
=M68*O68	=M68*P68		=ABS(SR$96-N68)	=ABS(SS$96-O68)	=ABS(ST$96-P68)	=K68+M68*(W68^2+V68^2)/10000	=L68+M68*(V68^2+V68^2)/10000	=M68+M68*(V68^2+W68^2)/10000	=M68*(N68-R$98)*(O68-S$98)/10000	=M68*(N68-R$98)*(P68-T$98)/10000	=M68*(O68-S$98)*(P68-T$98)/10000
=M69*O69	=M69*P69		=ABS(SR$96-N69)	=ABS(SS$96-O69)	=ABS(ST$96-P69)	=K69+M69*(W69^2+V69^2)/10000	=L69+M69*(V69^2+V69^2)/10000	=M69+M69*(V69^2+W69^2)/10000	=M69*(N69-R$98)*(O69-S$98)/10000	=M69*(N69-R$98)*(P69-T$98)/10000	=M69*(O69-S$98)*(P69-T$98)/10000
=M70*O70	=M70*P70		=ABS(SR$96-N70)	=ABS(SS$96-O70)	=ABS(ST$96-P70)	=K70+M70*(W70^2+V70^2)/10000	=L70+M70*(V70^2+V70^2)/10000	=M70+M70*(V70^2+W70^2)/10000	=M70*(N70-R$98)*(O70-S$98)/10000	=M70*(N70-R$98)*(P70-T$98)/10000	=M70*(O70-S$98)*(P70-T$98)/10000
=M71*O71	=M71*P71		=ABS(SR$96-N71)	=ABS(SS$96-O71)	=ABS(ST$96-P71)	=K71+M71*(W71^2+V71^2)/10000	=L71+M71*(V71^2+V71^2)/10000	=M71+M71*(V71^2+W71^2)/10000	=M71*(N71-R$98)*(O71-S$98)/10000	=M71*(N71-R$98)*(P71-T$98)/10000	=M71*(O71-S$98)*(P71-T$98)/10000
=M72*O72	=M72*P72		=ABS(SR$96-N72)	=ABS(SS$96-O72)	=ABS(ST$96-P72)	=K72+M72*(W72^2+V72^2)/10000	=L72+M72*(V72^2+V72^2)/10000	=M72+M72*(V72^2+W72^2)/10000	=M72*(N72-R$98)*(O72-S$98)/10000	=M72*(N72-R$98)*(P72-T$98)/10000	=M72*(O72-S$98)*(P72-T$98)/10000
=M73*O73	=M73*P73		=ABS(SR$96-N73)	=ABS(SS$96-O73)	=ABS(ST$96-P73)	=K73+M73*(W73^2+V73^2)/10000	=L73+M73*(V73^2+V73^2)/10000	=M73+M73*(V73^2+W73^2)/10000	=M73*(N73-R$98)*(O73-S$98)/10000	=M73*(N73-R$98)*(P73-T$98)/10000	=M73*(O73-S$98)*(P73-T$98)/10000
=M76*O76	=M76*P76		=ABS(SR$96-N76)	=ABS(SS$96-O76)	=ABS(ST$96-P76)	=K76+M76*(W76^2+V76^2)/10000	=L76+M76*(V76^2+V76^2)/10000	=M76+M76*(V76^2+W76^2)/10000	=M76*(N76-R$98)*(O76-S$98)/10000	=M76*(N76-R$98)*(P76-T$98)/10000	=M76*(O76-S$98)*(P76-T$98)/10000
=M77*O77	=M77*P77		=ABS(SR$96-N77)	=ABS(SS$96-O77)	=ABS(ST$96-P77)	=K77+M77*(W77^2+V77^2)/10000	=L77+M77*(V77^2+V77^2)/10000	=M77+M77*(V77^2+W77^2)/10000	=M77*(N77-R$98)*(O77-S$98)/10000	=M77*(N77-R$98)*(P77-T$98)/10000	=M77*(O77-S$98)*(P77-T$98)/10000
=M78*O78	=M78*P78		=ABS(SR$96-N78)	=ABS(SS$96-O78)	=ABS(ST$96-P78)	=K78+M78*(W78^2+V78^2)/10000	=L78+M78*(V78^2+V78^2)/10000	=M78+M78*(V78^2+W78^2)/10000	=M78*(N78-R$98)*(O78-S$98)/10000	=M78*(N78-R$98)*(P78-T$98)/10000	=M78*(O78-S$98)*(P78-T$98)/10000
=M79*O79	=M79*P79		=ABS(SR$96-N79)	=ABS(SS$96-O79)	=ABS(ST$96-P79)	=K79+M79*(W79^2+V79^2)/10000	=L79+M79*(V79^2+V79^2)/10000	=M79+M79*(V79^2+W79^2)/10000	=M79*(N79-R$98)*(O79-S$98)/10000	=M79*(N79-R$98)*(P79-T$98)/10000	=M79*(O79-S$98)*(P79-T$98)/10000
=M80*O80	=M80*P80		=ABS(SR$96-N80)	=ABS(SS$96-O80)	=ABS(ST$96-P80)	=K80+M80*(W80^2+V80^2)/10000	=L80+M80*(V80^2+V80^2)/10000	=M80+M80*(V80^2+W80^2)/10000	=M80*(N80-R$98)*(O80-S$98)/10000	=M80*(N80-R$98)*(P80-T$98)/10000	=M80*(O80-S$98)*(P80-T$98)/10000
=M81*O81	=M81*P81		=ABS(SR$96-N81)	=ABS(SS$96-O81)	=ABS(ST$96-P81)	=K81+M81*(W81^2+V81^2)/10000	=L81+M81*(V81^2+V81^2)/10000	=M81+M81*(V81^2+W81^2)/10000	=M81*(N81-R$98)*(O81-S$98)/10000	=M81*(N81-R$98)*(P81-T$98)/10000	=M81*(O81-S$98)*(P81-T$98)/10000
=M82*O82	=M82*P82		=ABS(SR$96-N82)	=ABS(SS$96-O82)	=ABS(ST$96-P82)	=K82+M82*(W82^2+V82^2)/10000	=L82+M82*(V82^2+V82^2)/10000	=M82+M82*(V82^2+W82^2)/10000	=M82*(N82-R$98)*(O82-S$98)/10000	=M82*(N82-R$98)*(P82-T$98)/10000	=M82*(O82-S$98)*(P82-T$98)/10000
=M83*O83	=M83*P83		=ABS(SR$96-N83)	=ABS(SS$96-O83)	=ABS(ST$96-P83)	=K83+M83*(W83^2+V83^2)/10000	=L83+M83*(V83^2+V83^2)/10000	=M83+M83*(V83^2+W83^2)/10000	=M83*(N83-R$98)*(O83-S$98)/10000	=M83*(N83-R$98)*(P83-T$98)/10000	=M83*(O83-S$98)*(P83-T$98)/10000
=M84*O84	=M84*P84		=ABS(SR$96-N84)	=ABS(SS$96-O84)	=ABS(ST$96-P84)	=K84+M84*(W84^2+V84^2)/10000	=L84+M84*(V84^2+V84^2)/10000	=M84+M84*(V84^2+W84^2)/10000	=M84*(N84-R$98)*(O84-S$98)/10000	=M84*(N84-R$98)*(P84-T$98)/10000	=M84*(O84-S$98)*(P84-T$98)/10000
=M85*O85	=M85*P85		=ABS(SR$96-N85)	=ABS(SS$96-O85)	=ABS(ST$96-P85)	=K85+M85*(W85^2+V85^2)/10000	=L85+M85*(V85^2+V85^2)/10000	=M85+M85*(V85^2+W85^2)/10000	=M85*(N85-R$98)*(O85-S$98)/10000	=M85*(N85-R$98)*(P85-T$98)/10000	=M85*(O85-S$98)*(P85-T$98)/10000
=M88*O88	=M88*P88		=ABS(SR$96-N88)	=ABS(SS$96-O88)	=ABS(ST$96-P88)	=K88+M88*(W88^2+V88^2)/10000	=L88+M88*(V88^2+V88^2)/10000	=M88+M88*(V88^2+W88^2)/10000	=M88*(N88-R$98)*(O88-S$98)/10000	=M88*(N88-R$98)*(P88-T$98)/10000	=M88*(O88-S$98)*(P88-T$98)/10000
=M89*O89	=M89*P89		=ABS(SR$96-N89)	=ABS(SS$96-O89)	=ABS(ST$96-P89)	=K89+M89*(W89^2+V89^2)/10000	=L89+M89*(V89^2+V89^2)/10000	=M89+M89*(V89^2+W89^2)/10000	=M89*(N89-R$98)*(O89-S$98)/10000	=M89*(N89-R$98)*(P89-T$98)/10000	=M89*(O89-S$98)*(P89-T$98)/10000
=M90*O90	=M90*P90		=ABS(SR$96-N90)	=ABS(SS$96-O90)	=ABS(ST$96-P90)	=K90+M90*(W90^2+V90^2)/10000	=L90+M90*(V90^2+V90^2)/10000	=M90+M90*(V90^2+W90^2)/10000	=M90*(N90-R$98)*(O90-S$98)/10000	=M90*(N90-R$98)*(P90-T$98)/10000	=M90*(O90-S$98)*(P90-T$98)/10000
=M91*O91	=M91*P91		=ABS(SR$96-N91)	=ABS(SS$96-O91)	=ABS(ST$96-P91)	=K91+M91*(W91^2+V91^2)/10000	=L91+M91*(V91^2+V91^2)/10000	=M91+M91*(V91^2+W91^2)/10000	=M91*(N91-R$98)*(O91-S$98)/10000	=M91*(N91-R$98)*(P91-T$98)/10000	=M91*(O91-S$98)*(P91-T$98)/10000
=M92*O92	=M92*P92		=ABS(SR$96-N92)	=ABS(SS$96-O92)	=ABS(ST$96-P92)	=K92+M92*(W92^2+V92^2)/10000	=L92+M92*(V92^2+V92^2)/10000	=M92+M92*(V92^2+W92^2)/10000	=M92*(N92-R$98)*(O92-S$98)/10000	=M92*(N92-R$98)*(P92-T$98)/10000	=M92*(O92-S$98)*(P92-T$98)/10000
=M93*O93	=M93*P93		=ABS(SR$96-N93)	=ABS(SS$96-O93)	=ABS(ST$96-P93)	=K93+M93*(W93^2+V93^2)/10000	=L93+M93*(V93^2+V93^2)/10000	=M93+M93*(V93^2+W93^2)/10000	=M93*(N93-R$98)*(O93-S$98)/10000	=M93*(N93-R$98)*(P93-T$98)/10000	=M93*(O93-S$98)*(P93-T$98)/10000
=SUM97:S$2U$98	=SUM[T7:T92M98	TOTAL SPACECRAFT MOME				=SUM[Z7:Z93]	=SUM[AA7:AA93]	=SUM[AB7:AB93]	=SUM[AC7:AC93]	=SUM[AD7:AD93]	=SUM[AE7:AE93]

APPENDIX D

THIS PAGE INTENTIONALLY LEFT BLANK

THIS PAGE INTENTIONALLY LEFT BLANK

Appendix D

A. Acknowledgement

Tables D-1, D-2, and D-3 and Figures D-3 and D-4 have been reproduced from the GLOBALSTAR System Application before the Federal Communications Commission.

B. Planar Array Antenna Design

The initial algorithm used to design the payload antennas assumes that a uniform amplitude beam is generated by each element of the array and that all elements are energized in phase. This determines the highest theoretical gain achievable by the array. This algorithm was performed for each antenna. A second algorithm was developed to model an array containing elements energized in phase, but at different amplitudes. This allows the beamwidth to be increased, but at the expense of gain. The second algorithm was run only for the L-Band antennas. The L-Band antenna algorithms do not yield a particular solution to the specifications (a detailed incremental design is not possible within the allotted timeframe), however, they do show that a solution is attainable.

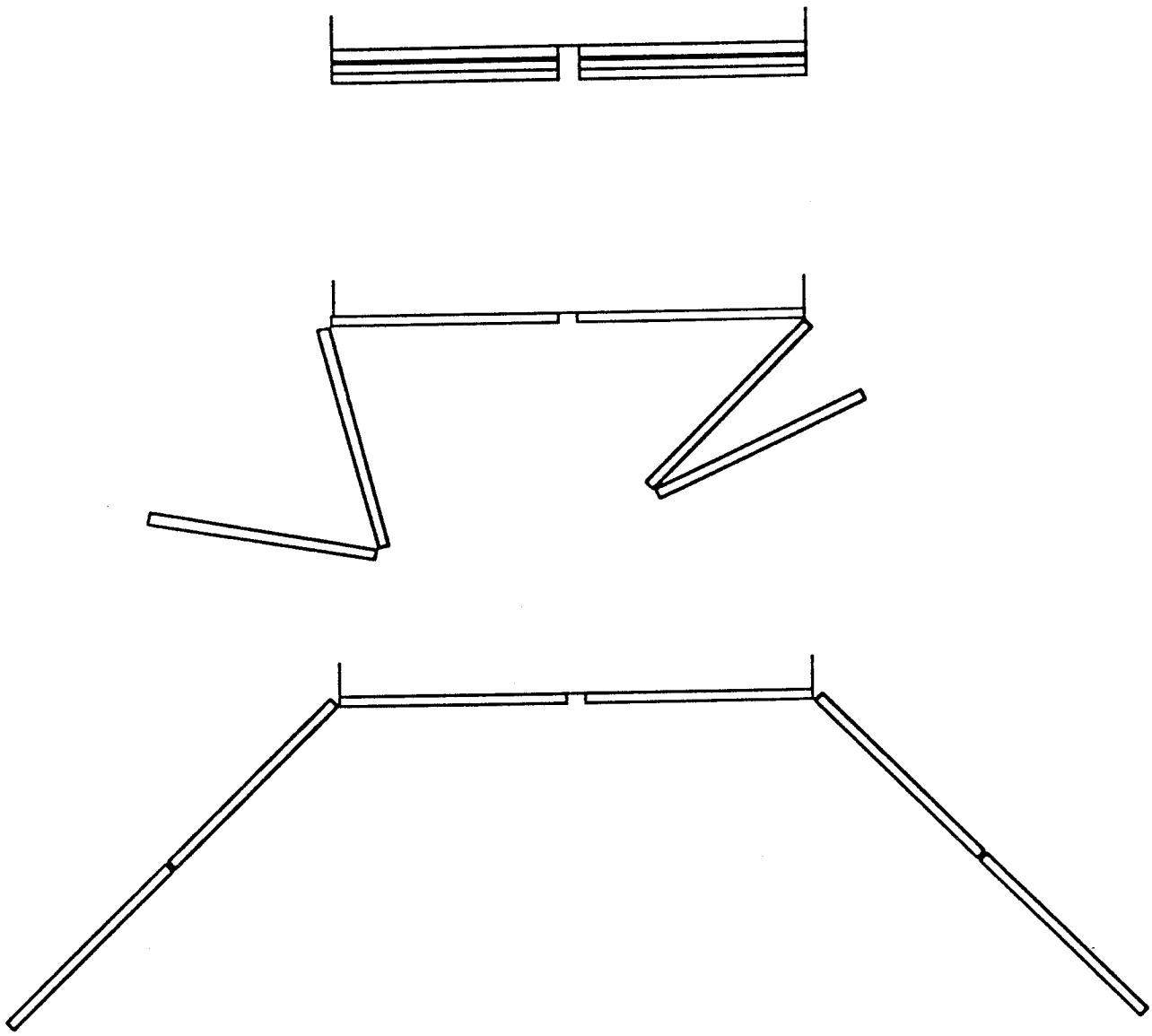

Figure D-1 Payload Planar Array Antenna Deployment

	ES to Satellite	User to Satellite			Satellite to ES	Satellite to User	
Frequency	6530.0	1625.0	MHz	Frequency	5205.0	1625.0	MHz
RF Power	0.2	6	Watts	RF Power	0.66	12	Watts
	-7.0	7.8	dBW		-1.8	10.8	dBW
Power Loss	-1.0	-1.0	dB	Power Loss	-1.5	-2.2	dB
Antenna Gain	40.2	3.0	dBI	S/C Ant. Gain (Isoflux)	3.0	6.5	dBI
EIRP	32.2	9.8	dBW	EIRP	-0.3	15.1	dBW
No. Users, u	35.0	35.0		Pilot Power	0.0	-0.2	dB
Voice Duty Cycle	37.5	37.5	%	No. Users & Interferers, u	38.0	35.0	
-10*log (u*d)	-11.2	-11.2	dB	Voice Duty Cycle, d	37.5	37.5	%
				-10*log (u*d)	-11.5	-11.2	dB
				EIRP/channel	-11.8	3.7	dBW
Satellite Altitude-750 NM	1389.0	1389.0	km	Satellite Altitude-750 NM	1389.0	1389.0	km
Elevation Angle	90.0	90.0	degrees	Elevation Angle	90.0	90.0	degrees
Range	1389.0	1389.0	km	Range	1389.0	1389.0	km
Free Space Loss	-171.6	-159.5	dB	Free Space Loss	-169.7	-159.5	dB
RX Signal Strength	-139.4	-149.8		RX Signal Strength	-181.5	-155.8	
Polarization Loss	-1.0	-0.5	dB	Polarization Loss	-1.0	-0.5	dB
Tracking Loss	-1.0	0.0	dB	Tracking Loss	-1.0	0.0	dB
S/C Ant. Gain (Isoflux)	3.0	6.5	dBI	Antenna Gain	38.2	3.0	dBI
RX Line Losses	-1.2	-1.0	dB	RX Line Losses	-1.0	-0.5	dB
Data Rate, Rb	28800.0	28800.0	bps	Data Rate, Rb	28800.0	28800.0	bps
-10*log(Rb)	-44.6	-44.6	dB/Hz	-10*log(Rb)	-44.6	-44.6	dB/Hz
Eb	-184.2	-189.4	dBW/Hz	Eb	-190.9	-198.4	dBW/Hz
LNA Temp.	170.0	75.0	degree K	LNA Temp.	65.0	75.0	degree K
Ant. Noise	290.0	290.0	degree K	Ant. Noise	150.0	200.0	degree K
Total Thermal Noise	460.0	365.0	degree K	Total Thermal Noise	178.8	264.0	degree K
Thermal Noise Density, No	-202.0	-203.0	dBW/Hz	Thermal Noise Density, No	-206.1	-204.4	dBW/Hz
Single Interferer Power	-139.6	-144.8	dBW	Single Interferer Power	-146.3	-153.8	dBW
Equivalent # of Interferers	0.0	3.0		Intra/Interbeam Interferen	-134.9	-152.6	dBW
Self Interference	-155.0	-146.0	dBW	Inter-Satellite Interferenc	0.0	0.0	%
Total Interference	-155.0	-146.0	dBW	Self Interference	-134.9	-152.6	dBW
Spreading Bandwidth	1.25	1.25	MHz	Total Interference	-134.9	-152.6	dBW
-10*log(spreading BW)	-61.0	-61.0	db/Hz	Spreading Bandwidth	1.25	1.25	MHz
Pseudo-Noise Density, Io	-216.0	-207.0	dBW/Hz	-10*log(spreading BW)	-61.0	-61.0	dB/Hz
				Pseudo-Noise Density, Io	-195.8	-213.6	dBW/Hz
Thermal, Eb/No	17.8	13.6	dB	Thermal, Eb/No	15.2	6.0	dB
Pseudo Noise, Eb/Io	31.8	17.6	dB	Pseudo Noise, Eb/Io	5.0	15.2	dB
Uplink Eb/(No+Io)	17.6	12.2	dB	Downlink Eb/(No+Io)	4.6	5.5	dB
				C/I (Intermodulation)	23.0	15.0	dB
				Overall Thermal, Eb/No	11.3	5.7	dB
				Overall Interference, Eb/Io	5.0	15.2	dB
				Overall Eb/(No+Io+IM)	4.0	4.8	dB
Number of S-Band Beams		2		Modem Implem/Doppler Los	-0.5	-0.5	dB
Number of SubBands		13		Eb/(No+Io) Required	2.5	3.5	dB
C-Band Amplifier Efficiency		18	%	Interf/Power Control Marg	1.0	1.3	dB
L-Band Amplifier Efficiency		35	%	Thermal Noise Margin	1.3	1.2	dB
Number of Beams Transmitting at On		1		DC POWER (For 1/2 of Beams)		246.7	Watts
				TOTAL Mobile BW		16.50	MHz
				TOTAL USERS (2 Beams)		910.0	

Table D-3 Link Budget, Beams 3 and 4

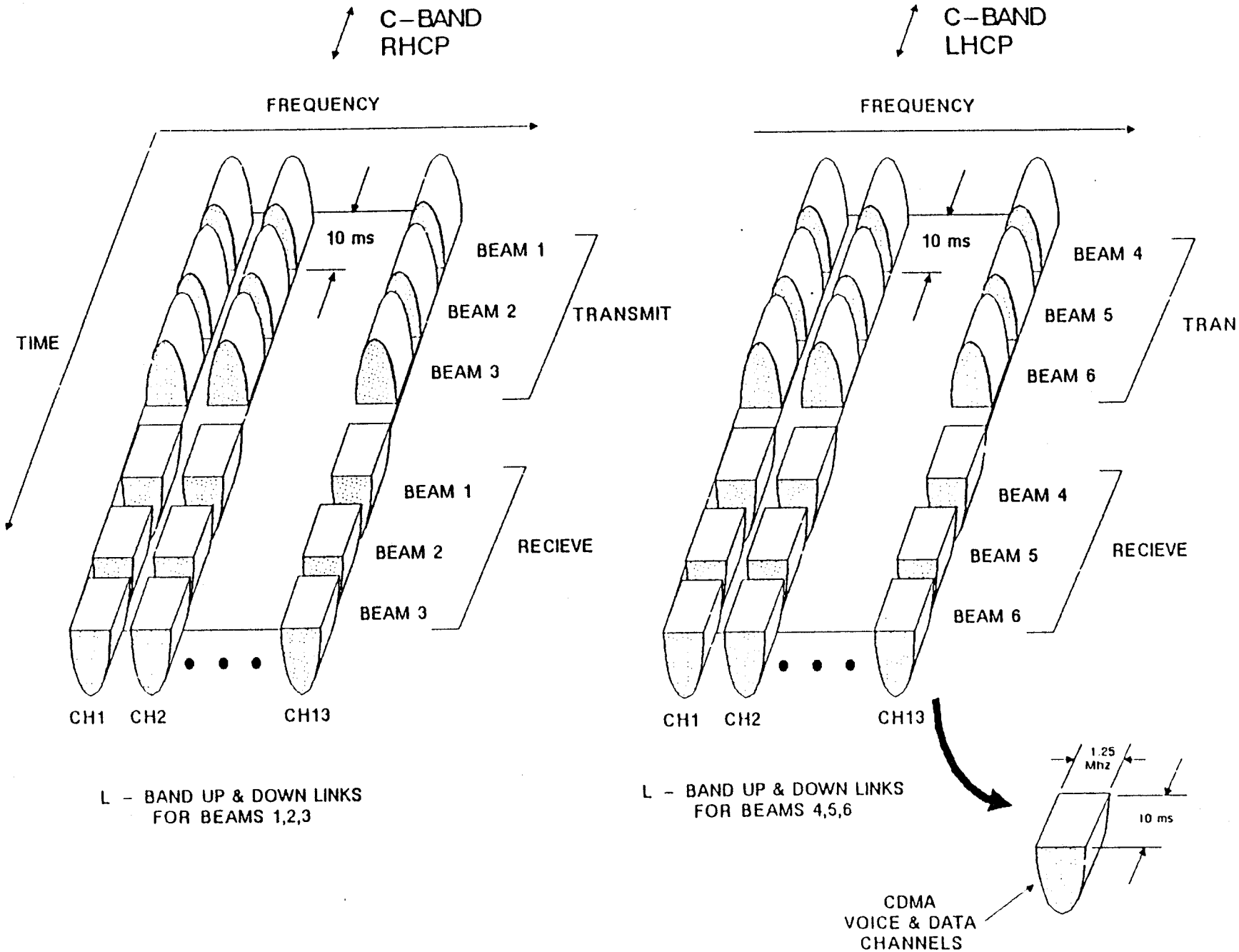

Figure D-3 Communications Multiplexing Scheme

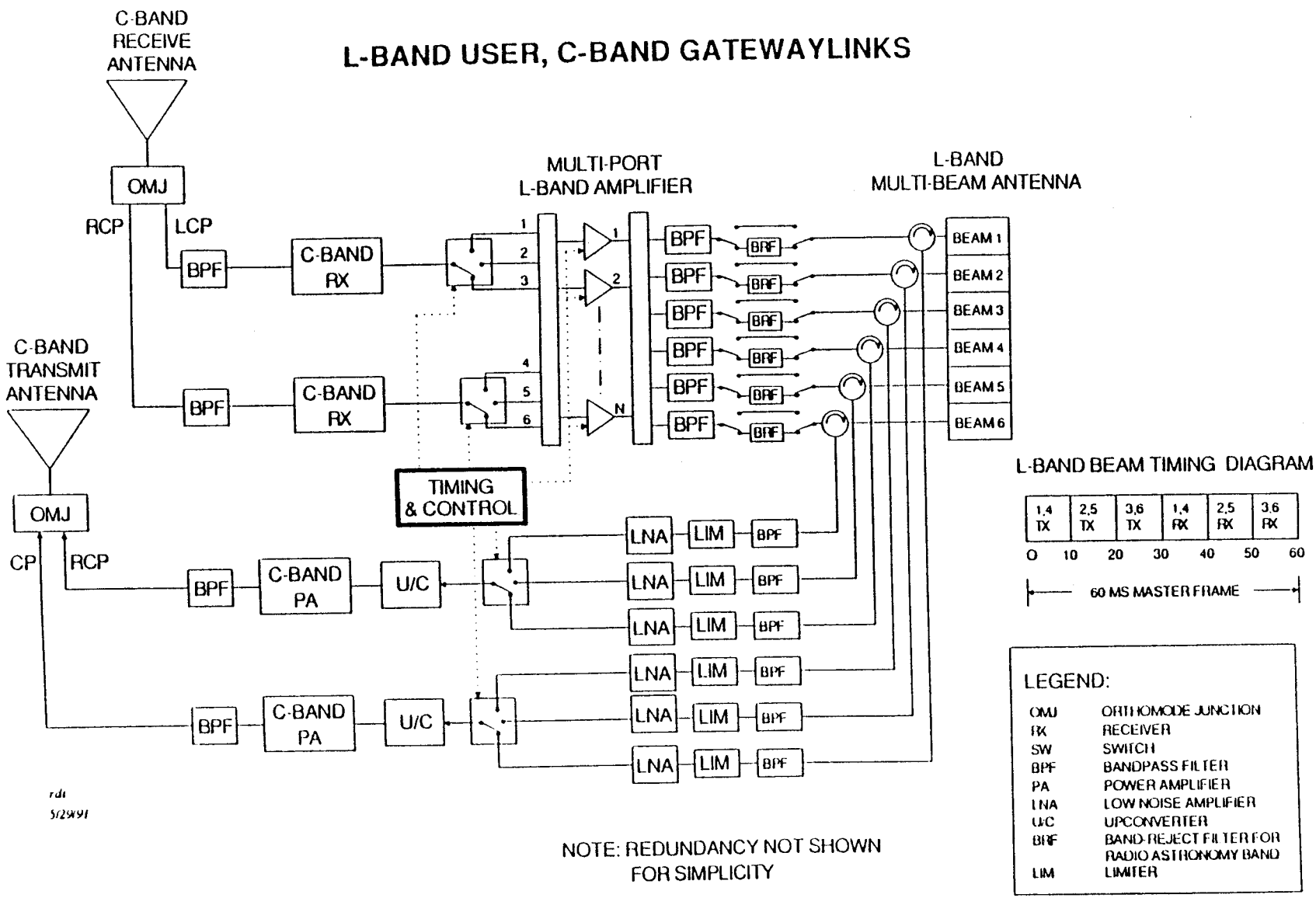

Figure D-4 Payload Block Diagram

APPENDIX E

THIS PAGE INTENTIONALLY LEFT BLANK

THIS PAGE INTENTIONALLY LEFT BLANK

L-Band Antenna Array Design (Uniform Element Amplitude)

Patch design.

The antenna array will be constructed from patches such as the one shown in figure 1.

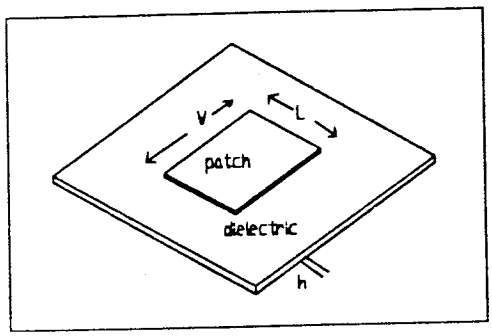

Figure 1. Rectangular patch

Given $f = 1617.75 \cdot 10^6$ Hz $\quad \varepsilon_r = 2.32$

$h = .0127\,m$ (thickness of dielectric)

$$l = \frac{3 \cdot 10^8}{f} \qquad l = 0.185 \qquad k = \frac{2 \cdot p}{l} \qquad k = 33.882$$

$$W = \frac{3 \cdot 10^8}{2 \cdot f} \cdot \left| \frac{1}{\sqrt{\frac{\varepsilon_r + 1}{2}}} \right| \qquad W = 0.072$$

The effective dielectric constant is given by

$$\varepsilon_e = \frac{\varepsilon_r + 1}{2} + \frac{\varepsilon_r - 1}{2} \cdot \left| \frac{1}{\sqrt{1 + 12 \cdot \frac{h}{W}}} \right| \qquad \varepsilon_e = 2.034$$

$$0.412 \cdot h \cdot \left(\varepsilon_e + 0.3 \right) \cdot \left(\frac{W}{h} + 0.264 \right) \cdot h$$

$\varepsilon - L$

E: 1.

$$dl = \frac{}{\left[e_e - 0.258 \right] \cdot \left[\frac{W}{h} + 0.8 \right]}$$

$dl = 0.006$

The patch length is given by $L = \frac{3 \cdot 10^8}{2 \cdot f \cdot \sqrt{e_e}} - 2 \cdot dl$

$L = 0.052$

Directivity is given by

$$D_0 = \frac{4 \cdot W^2 \cdot p^2}{\int_0^p \sin\left[\frac{k \cdot W \cdot \cos(q)}{2} \right]^2 \cdot \tan(q)^2 \cdot \sin(q)\, dq \cdot l^2}$$

$$Q = \frac{3 \cdot 10^8 \cdot \sqrt{e_e}}{4 \cdot f \cdot h}$$

Radiation resistance: $R_r = \frac{120 \cdot l}{W}$

Copper loss is given by: $R_c = .00027 \cdot \sqrt{f} \cdot \left[\frac{L}{W} \right] \cdot Q^2$

Dielectric loss is given by: $R_d = \frac{30 \cdot .0005}{e_e} \cdot \frac{h \cdot l}{L \cdot W} \cdot Q^2$

Total resistance is given by: $R_T = R_r + R_c + R_d$

$R_T = 523.659$

$h = \frac{R_r}{R_T}$

Antenna efficency: $h = 0.59$

Directivity and gain:

$D = 10 \cdot \log[D_0]$ $D = 5.186$ dB

$G = 10 \cdot \log[h \cdot D_0]$ $G = 2.899$ dB

Array design.

The number of patches is selected as $N = 9$

the patches should by spaced $d = .55 \cdot l$ apart. This gives d as:

$$d = 0.102$$

for the configuration shown in figure 2, the elements must be spaced

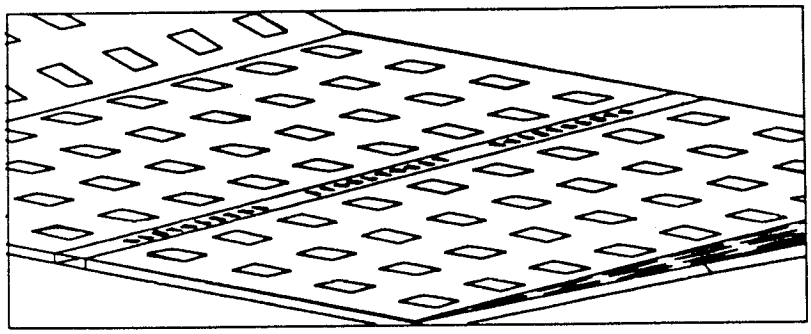

Figure 2. Array configuration

q' defines the lobe direction, set q'=desired beam direction and solve for phase shift b.

$q' = 90$ (degrees)

$$b = -\cos\left[q' \cdot \left[\frac{p}{180} \right] \right] \cdot k \cdot d \quad \text{(radians)}$$

(b in dgrees)

$$b \cdot \frac{180}{p} = -1.212 \cdot 10^{-14}$$

$$i = 0, 1 .. 360$$

$$q(i) = i$$

$$F(i) = \left[b + k \cdot d \cdot \cos\left[q(i) \cdot \frac{p}{180} \right] \right] \cdot \frac{180}{p}$$

$$j = 0, 1 .. 180$$

$$F(j) = -1 \cdot F(j)$$

$$AF(i) = \left| \frac{\sin\left[\left[N \cdot \frac{F(i)}{2} \cdot \frac{p}{180} \right] \right]}{N \cdot \sin\left[\left[\frac{F(i)}{2} \right] \cdot \frac{p}{180} \right]} \right|$$

the array factor is given by

$$q = k \cdot d \cdot \frac{180}{p} \qquad q = 198$$

the visible region is defined by b-kd<= F <=b+kd

$$j_1 = \frac{180}{N} \qquad j_2 = j_1 + (2 \cdot (k \cdot d)) \cdot \frac{180}{p}$$

(visible region)

$$j_1 = 20 \quad j_2 = 416$$

Plot of array factor vs. observation angle

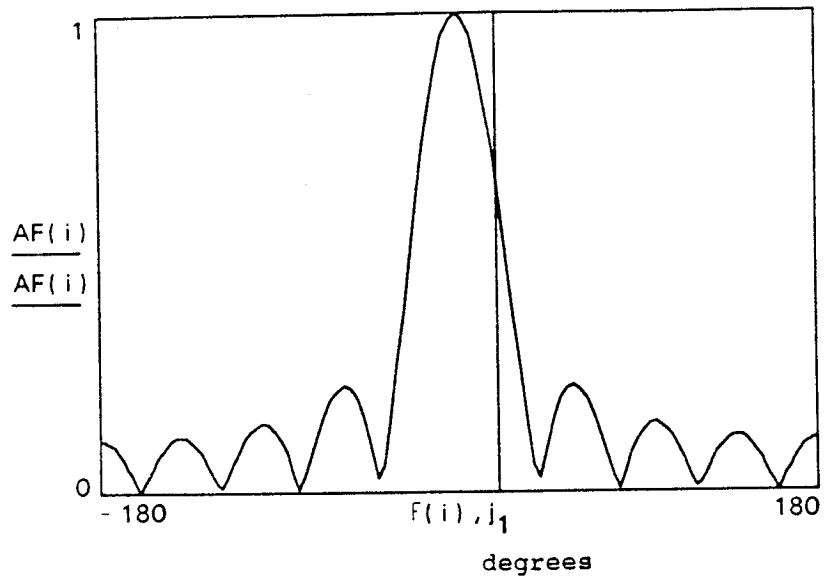

This is for a linear array with uniform amplitude. A uniform array gives the smallest half-power beamwidth, followed in order by a Dolph-Chebyshev and binomial array. The binomial array gives the smallest side lobe levels followed by the Dolph-Chebyshev then uniform array. For a given beamwidth between first nulls, a Dolph-Chebyshev array gives the smallest possibel SLL.

Beamwidth calculations

directivity calculated as follows

$j := 0, 1 .. 360$

$U(j) := AF(j)^2$

radiation intensity

$\phi := p$

$$U_{max} := \frac{\sin\left[\frac{N}{2}\cdot(k\cdot d\cdot\cos(\phi)+b)\right]}{N\cdot\sin\left[\frac{k\cdot d\cdot\cos(\phi)+b}{2}\right]}$$

$U_{max} = 0.018$

$U_{max} := 1$

$j := 0, 1 .. 360$

$$D(j) := 10\cdot\log\left[\frac{U_{max}}{U(j)}\right]$$

directivity in dB

antenna efficency is $\eta = .55$

antenna gain is given by $G_{dB}(j) = 10 \cdot \log\left[\eta \cdot \left[\frac{U_{max}}{U(j)} \right] \right]$

The total gain provided by the array at the angle $q' = 90$ is given by

$p = 1 .. (N - 1)$

$$D = \frac{N^2 \cdot (k \cdot d)}{N \cdot k \cdot d + 2 \cdot \sum_p \left[\frac{N - p}{N} \cdot \sin(p \cdot k \cdot d) \cdot \cos(p \cdot k \cdot d \cdot \cos(q')) \right]}$$

$Gain = 10 \cdot \log(\eta \cdot D)$ $\quad Gain = 6.994$ db

L-Band Antenna Array Design (Variable Element Amplitude)

A. Beam synthesis for an M x N planar array composed of microstrip patches.

The following characteristics are desired:

θ= 10 degrees ϕ= 0 degrees
beamwidth in N direction (along y axis)= 40 degrees
beamwidth in M direction (along x axis)= 120 degrees
number of elements in array M x N=

$M := 4 \qquad N := 9$

$MHz := \frac{10^6}{sec} \qquad cm := m \cdot 10^{-2}$

$c := 3 \cdot 10^8 \cdot \frac{m}{sec}$

$f := 1617.75 \cdot MHz$

The distance between patches is given by $d := .0947 \cdot m$

$\lambda := \frac{c}{(f)} \qquad \lambda = 0.185 \cdot m$

$k := \frac{(2 \cdot \pi)}{\lambda} \qquad k = 33.882 \cdot m^{-1}$

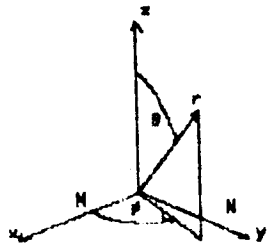

Coordinate orientation

The beams are steered by adjusting the progressive phase shift between elements. The appropriate phase shifts are calculated as follows:

for phase shift in x direction, $\phi := 90 \quad \theta := 45 \qquad \beta_\xi := -k \cdot d \cdot \sin(\theta \cdot deg) \cdot \cos(\phi \cdot deg)$

for phase shift in y direction. $\beta_\psi := -k \cdot d \cdot \sin(\theta \cdot deg) \cdot \sin(\phi \cdot deg)$

The beam pattern is defined by the total array factor which is the product of the array factor in the x direction and the array factor in the y direction. Using the fourier transform method, the array factors are found as follows:

$\theta_{\xi 1} := 55 \qquad \theta_{\xi 2} := 55 \qquad \phi_\xi := 0$ (defines pattern limits in x-z plane)

$\psi_{\xi 1} := k \cdot d \cdot \sin(\theta_{\xi 1} \cdot deg) \cdot \cos(\phi_\xi \cdot deg) + \beta_\xi$

$\psi_{\xi 2} := k \cdot d \cdot \sin(\theta_{\xi 2} \cdot deg) \cdot \cos(\phi_\xi \cdot deg) + \beta_\xi$

$\psi_\xi := k \cdot d \cdot \sin(\theta_{\xi 1} \cdot deg) \cdot \cos(\phi_\xi \cdot deg) + \beta_\xi$

$\psi_{\xi 1} = -150.594 \cdot deg$

$\psi_{\xi 2} = 150.594 \cdot deg$

$m := -\frac{M}{2} .. -1$

$a_{x_{[m+M-1]}} := \frac{1}{(2 \cdot \pi)} \cdot \left| \int_{\psi_{\xi 1}}^{\psi_{\xi 2}} e^{-j \cdot \left(\frac{2 \cdot m + 1}{2}\right) \cdot \psi_\xi} \, d\psi_\xi \right|$

m	$a_{x_{m+M-1}}$
-2	-0.152
-1	0.616

$m := 1 .. \frac{M}{2}$

$a_{x_{m+2}} := \frac{1}{(2 \cdot \pi)} \cdot \left| \int_{\psi_{\xi 1}}^{\psi_{\xi 2}} e^{-j \cdot \left(\frac{2 \cdot m - 1}{2}\right) \cdot \psi_\xi} \, d\psi_\xi \right|$

m	a_{x_m}
1	-0.152
2	0.616

The amplitude coefficents are found to be:

$m := 1..M$

m	a_{x_m}
1	-0.152
2	0.616
3	0.616
4	-0.152

In normalized form the coefficents are:

$a'_{x_m} := \frac{a_{x_m}}{\max(a_x)}$

a'_{x_m}
0.247
1
1
-0.247

The array factor in the x direction (for an even number of elements) is given by:

$m := -\frac{M}{2}..-1 \qquad n := 1..\frac{M}{2} \qquad i := 0..180 \qquad j := 0$

$\theta_i := i \qquad \phi_j := 0$

$$AF_x(\theta,\phi) := \left[\sum_m a_{x_{m+M-1}} \cdot e^{\left[\frac{2\cdot m+1}{2}\right]\cdot\left[k\cdot d\cdot\sin(\theta\cdot deg)\cdot\cos(\phi\cdot deg)+\beta_\xi\right]\cdot j}\right] + \left[\sum_n a_{x_{n+\left[\frac{M}{2}\right]}} \cdot e^{\left[\frac{2\cdot n-1}{2}\right]\cdot\left[k\cdot d\cdot\sin(\theta\cdot deg)\cdot\cos(\phi\cdot deg)+\right.}\right.$$

Let P=number of data points in the plane defined by ϕ $\qquad P := 30$

$ii := 0..P \qquad j := 0..P \qquad I := 0, \frac{180}{P}..180 \qquad i := 0, \frac{360}{P}..360$

$x_{\left[\frac{P}{2}\right]} := 10^{-10} \qquad \theta_j := -90 + I \qquad y_{\left[\frac{P}{2}\right]} := 10^{-10}$

$\phi_{ii} := -180 + i$

$f(\phi,\theta) := |AF_x(\theta,\phi)| \qquad MM_{[ii,j]} := |f(\phi_{ii},\theta_j)| \qquad MM_{[ii,j]} := \frac{MM_{[ii,j]}}{\max(MM)}$

$i := 0..180$

$\theta_i := -90 + i$

$f2_i := |AF_x(\theta_i, 0)| \qquad f2_i := \frac{f2_i}{\max(f2)}$

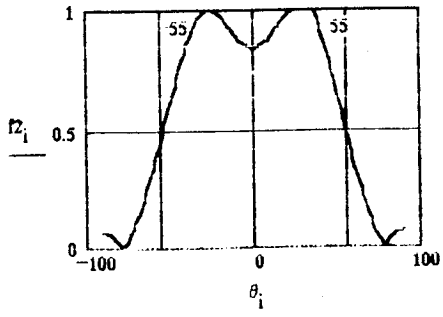

The array factor in the y direction is found in a similar manner.

$\theta_{\psi 1} := -12.5 \quad \theta_{\psi 2} := 12.5 \quad \phi_\psi := 90$ (defines pattern limits in y-z plane)

$\psi_{\psi 1} := k \cdot d \cdot \sin(\theta_{\psi 1} \cdot deg) \cdot \sin(\phi_\psi \cdot deg) + \beta_\psi \qquad \psi_{\psi 2} := k \cdot d \cdot \sin(\theta_{\psi 2} \cdot deg) \cdot \sin(\phi_\psi \cdot deg) + \beta_\psi$

$\psi_\psi := k \cdot d \cdot \sin(\theta_{\psi 1} \cdot deg) \cdot \sin(\phi_\psi \cdot deg) + \beta_\psi$

$\psi_{\psi 1} = -169.736 \cdot deg$

$\psi_{\psi 2} = -90.205 \cdot deg$

$n := \frac{(N-1)}{2} .. \frac{(N-1)}{2}$

$$a_{y\left[n+\frac{(N-1)}{2}\right]} := \frac{1}{(2 \cdot \pi)} \cdot \int_{\psi_{\psi 1}}^{\psi_{\psi 2}} (e)^{\left[j \cdot n \cdot \psi_\psi\right]} d\psi_\psi$$

The amplitude coefficents are found to be:

$n := 0 .. N-1$

n	a_{y_n}
0	$-0.027 - 0.01j$
1	$0.08 - 0.046j$
2	$0.027 + 0.154j$
3	$-0.131 - 0.156j$
4	0.221
5	$-0.131 + 0.156j$
6	$0.027 - 0.154j$
7	$0.08 + 0.046j$
8	$-0.027 + 0.01j$

In normalized form the coefficents are:

$a''y_n := a_{y_n} \qquad a'y_n := \frac{a''y_n}{\max(a''y)}$

$a'y_n$
$-0.101 + 0.027j$
$0.143 - 0.31j$
$0.246 + 0.523j$
$-0.728 - 0.192j$
$0.667 - 0.471j$
$-0.063 + 0.75j$
$0.411 - 0.407j$
$0.34 - 0.031j$
$-0.06 + 0.086j$

The array factor in the y direction (for an odd number of elements) is given by:

$n := \frac{-(N-1)}{2} .. \frac{(N-1)}{2} \qquad i := 0 .. 180 \qquad j := 0$

$\theta_i := i \qquad \phi_j := 0$

$$AF_y(\theta, \phi) := \sum_n a_{y\left[n+\frac{(N-1)}{2}\right]} \cdot e^{j \cdot \left[n \cdot \left[k \cdot d \cdot \sin(\theta \cdot deg) \cdot \sin(\phi \cdot deg) + \beta_\psi\right]\right]}$$

Let P=number of data points in the plane defined by ϕ $P := 30$

$i := 0..P$ $j := 0..P$ $l := 0, \frac{180}{P}..180$

$x_i := \frac{-P}{2} + i$ $x_{\lfloor \frac{P}{2} \rfloor} := 10^{-10}$ $y_j := \frac{-P}{2} + 2 \cdot j$ $\theta_l := -90 + l$ $y_{\lfloor \frac{P}{2} \rfloor} := 10^{-10}$

$f_y(x, y, \theta) := AF_y\left[\theta, \frac{\operatorname{atan}\left[\frac{y}{x}\right]}{\text{deg}}\right]$ $NN_{[i,j]} := \left|f_y\left[x_i, y_j, \theta_i\right]\right|$ $NN_{[i,j]} := \frac{NN_{[i,j]}}{\max(NN)}$

$i := 0..180$

$\theta_i := -90 + i$

$f2_i := \left|AF_y\left[\theta_i, 90\right]\right|$ $f2_i := \frac{f2_i}{\max(f2)}$

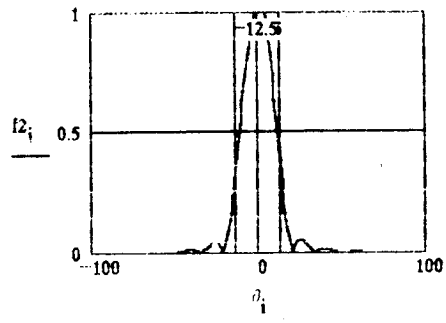

$i := 0..P$ $j := 0..P$ $l := 0, \frac{180}{P}..180$

$\theta_l := -90 + l$

$AF_t(x, y, \theta)$ $AF_x\left[\theta, \frac{\operatorname{atan}\left[\frac{y}{x}\right]}{\text{deg}}\right] \cdot AF_y\left[\theta, \frac{\operatorname{atan}\left[\frac{y}{x}\right]}{\text{deg}}\right]$

$T_{[i,j]} := \left|AF_t\left[x_i, y_j, \theta_i\right]\right|$ $T_{[i,j]} := \frac{T_{[i,j]}}{\max(T)}$

$x := 56$ $y := 56$

$i := 0..180$

$\theta_i := -90 + i$

$f2_i := \left|AF_t\left[x, y, \theta_i\right]\right|$ $f2_i := \frac{f2_i}{\max(f2)}$

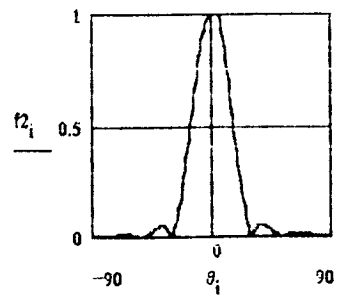

The gain of a single patch was found to be 4 d B. The maximum array gain is

$$Gain := 10 \cdot \log(2.5 \cdot \max(T)) \qquad Gain = 2.314$$

Summary.

The array is composed of M x N microstrip patches. where M=4 and N=9. The beam is shaped and steered by nonuniform patch excitation. The excitation coefficients are as follows:

$m := 1..M$ $\qquad$ $n := 0..N-1$

$$a'_{y_n} := \left[\operatorname{atan}\left(\frac{\operatorname{Im}(a_{y_n})}{\operatorname{Re}(a_{y_n})} \right) \right] \cdot deg \qquad a''_{y_n} := |a_{y_n}|$$

a_{x_m}

0.152
0.616
0.616
-0.152

a''_{y_n}	a'_{y_n}
0.028	0.006
0.092	0.009
0.157	-0.024
0.204	0.015
0.221	0
0.204	-0.015
0.157	0.024
0.092	0.009
0.028	-0.006

C-Band Downlink Antenna Array Design (Uniform Element Amplitude)

Patch design

The antenna array will be constructed from patches such as the one shown in figure 1.

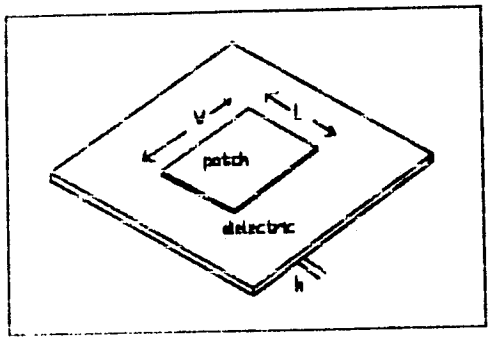

Figure 1. Rectangular patch

Given $f := 5200.0 \cdot 10^6$ Hz $\quad \varepsilon_\rho := 2.32$

$h := .0127$ m (thickness of dielectric)

$\lambda := \frac{3 \cdot 10^8}{f}$ $\quad \lambda = 0.058$ m $\quad k := \frac{2 \cdot \pi}{\lambda}$ $\quad k = 108.909$

$$W := \frac{3 \cdot 10^8}{2 \cdot f} \cdot \left| \frac{1}{\sqrt{\frac{\varepsilon_\rho + 1}{2}}} \right| \qquad W = 0.022$$

The effective dielectric constant is given by

$$\varepsilon_e := \frac{\varepsilon_\rho + 1}{2} + \frac{\varepsilon_\rho - 1}{2} \cdot \left| \frac{1}{\sqrt{1 + 12 \cdot \frac{h}{W}}} \right| \qquad \varepsilon_e = 1.896$$

$$\delta\lambda := \frac{0.412 \cdot \left[\left(\varepsilon_\varepsilon + 0.3 \right) \cdot \left[\left(\frac{W}{h} + 0.264 \right) \right] \right] \cdot h}{\left[\left(\varepsilon_\varepsilon - 0.258 \right) \cdot \left[\left(\frac{W}{h} + 0.8 \right) \right] \right]}$$

$\delta\lambda = 0.006$

The patch length is given by $L := \frac{3 \cdot 10^8}{2 \cdot f \cdot \sqrt{\varepsilon_\varepsilon}} - 2 \cdot \delta\lambda$

$L = 0.01$

Directivity is given by

$$D_0 := \frac{4 \cdot W^2 \cdot \pi^2}{\int_0^{\pi} \left[\sin\left[\frac{k \cdot W \cdot \cos(\theta)}{2} \right] \right]^2 \cdot \tan(\theta)^2 \cdot \sin(\theta)\, d\theta \cdot \lambda^2}$$

$$Q := \frac{3 \cdot 10^8 \cdot \sqrt{\varepsilon_\varepsilon}}{4 \cdot f \cdot h}$$

$$R_r := \frac{120 \cdot \lambda}{W}$$

Radiation resistance:

$$R_c := .00027 \cdot \sqrt{f} \cdot \left[\left(\frac{L}{W} \right) \right] \cdot Q^2$$

Copper loss is given by

$$R_d := \frac{30 \cdot .0005}{\varepsilon_\varepsilon} \cdot \frac{h \cdot \lambda}{L \cdot W} \cdot Q^2$$

Dielectric loss is given by:

Total resistance is given by: $R_T := R_r + R_c + R_d$

$R_T = 330.238$

$$\eta := \frac{R_r}{R_T}$$

Antenna efficency

$\eta = 0.936$

Directivity and gain

$D := 10 \cdot \log(D_0)$ $\quad D = 5.186$ dB

$G := 10 \cdot \log(\eta \cdot D_0)$ $\quad G = 4.901$ dB

Array design

The number of patches is selected as $N := 10$

the patches should by spaced $d := .55 \cdot \lambda$ apart This gives d as

$d = 0.032$

for the configuration shown in figure 2 the elements must be spaced

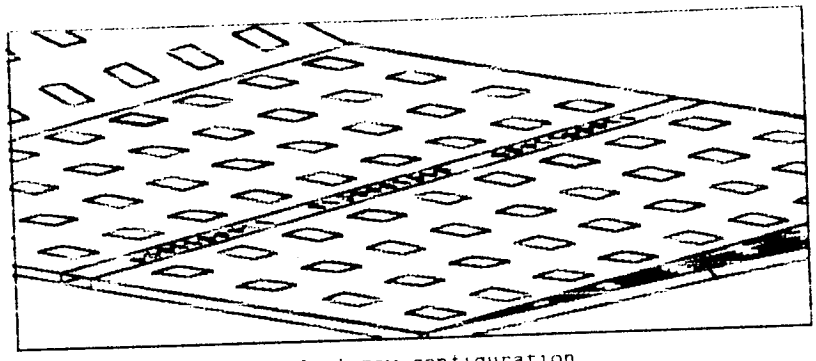

Figure 2. Array configuration

θ defines the lobe direction. set θ=desired beam direction and solve for phase shift β

$\theta_0 := 90$ (degrees)

$\beta := -\cos\left(\theta_0 \cdot \frac{\pi}{180}\right) \cdot k \cdot d$ (radians) β (degrees)

$\beta \cdot \frac{180}{\pi} = -1.212 \cdot 10^{14}$

$i := 0, 1 .. 360$

$\theta(i) := i$

$\Phi(i) := \left[\beta + k \cdot d \cdot \cos\left(\theta(i) \cdot \frac{\pi}{180}\right)\right] \cdot \frac{180}{\pi}$

$j := 0, 1 .. 180$

$\Phi(j) := -1 \cdot \Phi(j)$

$$AF(i) := \left| \frac{\sin\left(N \cdot \frac{\Phi(i)}{2} \cdot \frac{\pi}{180}\right)}{N \cdot \sin\left(\frac{\Phi(i)}{2} \cdot \frac{\pi}{180}\right)} \right|$$

the array factor is given by

C-Band Uplink Antenna Array Design (Uniform Element Amplitude)

Patch design

The antenna array will be constructed from patches such as the one shown in figure 1.

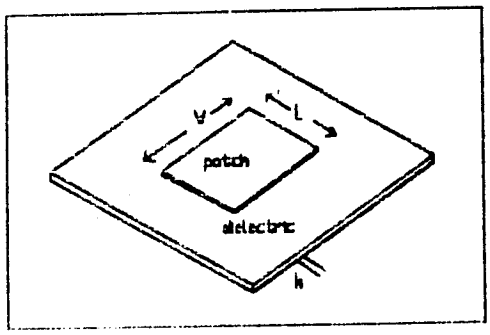

Figure 1. Rectangular patch

Given $f := 6500.0 \cdot 10^6$ Hz $\quad \varepsilon_\rho := 2.32$

$h := .0127$ m (thickness of dielectric)

$\lambda := \frac{3 \cdot 10^8}{f}$ $\quad \lambda = 0.046$ m

$k := \frac{2 \cdot \pi}{\lambda}$ $\quad k = 136.136$

$$W := \frac{3 \cdot 10^8}{2 \cdot f} \cdot \left| \frac{1}{\sqrt{\frac{\varepsilon_\rho + 1}{2}}} \right| \qquad W = 0.018$$

The effective dielectric constant is given by

$$\varepsilon_\varepsilon := \frac{\varepsilon_\rho + 1}{2} + \frac{\varepsilon_\rho - 1}{2} \cdot \left| \frac{1}{\sqrt{1 + 12 \cdot \frac{h}{W}}} \right| \qquad \varepsilon_e = 1.874$$

$$\delta\lambda = \frac{0.412 \cdot \left[\left(\varepsilon_\varepsilon + 0.3\right) \cdot \left(\frac{W}{h} + 0.264\right)\right] \cdot h}{\left[\left(\varepsilon_\varepsilon - 0.258\right) \cdot \left(\frac{W}{h} + 0.8\right)\right]}$$

$\delta\lambda = 0.005$

The patch length is given by $L = \frac{3 \cdot 10^8}{2 \cdot f \cdot \sqrt{\varepsilon_\varepsilon}} - 2 \cdot \delta\lambda$

$L = 0.006$

Directivity is given by

$$D_0 = \frac{4 \cdot W^2 \cdot \pi^2}{\int_0^{\pi} \sin\left[\frac{k \cdot W \cdot \cos(\theta)}{2}\right]^2 \cdot \tan(\theta)^2 \cdot \sin(\theta)\, d\theta \cdot \lambda^2}$$

$$Q = \frac{3 \cdot 10^8 \cdot \sqrt{\varepsilon_\varepsilon}}{4 \cdot f \cdot h}$$

$$R_r = \frac{120 \cdot \lambda}{W}$$

Radiation resistance:

$$R_c = .00027 \cdot \sqrt{f} \cdot \left[\frac{L}{W}\right] \cdot Q^2$$

Copper loss is given by

$$R_d = \frac{30 \cdot .0005}{\varepsilon_\varepsilon} \cdot \frac{h \cdot \lambda}{L \cdot W} \cdot Q^2$$

Dielectric loss is given by:

Total resistance is given by $R_T = R_r + R_c + R_d$

$R_T = 320.927$

$$\eta = \frac{R_r}{R_T}$$

Antenna efficency:

$\eta = 0.964$

Directivity and gain:

$$D := 10 \cdot \log(D_0) \qquad D = 5.186 \quad \text{dB}$$

$$G := 10 \cdot \log(\eta \cdot D_0) \qquad G = 5.025 \quad \text{db}$$

Array design

The number of patches is selected as $N := 10$

the patches should by spaced $d := .55 \cdot \lambda$ apart This gives d as:

$$d = 0.025$$

for the configuration shown in figure 2 the elements must be spaced

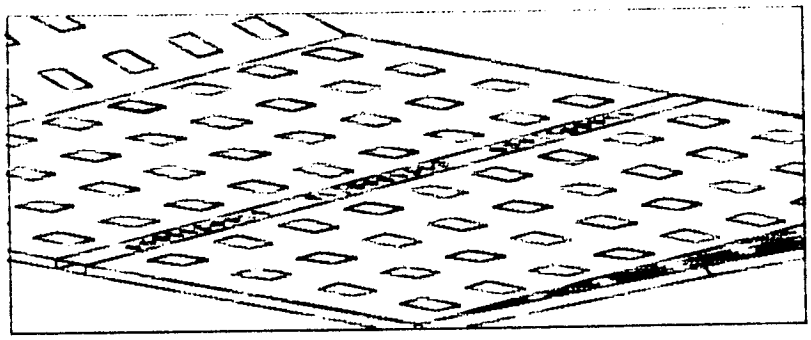

Figure 2. Array configuration

θ' defines the lobe direction, set θ'=desired beam direction and solve for phase shift β

$\theta_D := 90$ (degrees)

$\beta := -\cos\left(\theta_D \cdot \left(\frac{\pi}{180}\right)\right) \cdot k \cdot d$ (radians) β in degrees

$$\beta \cdot \frac{180}{\pi} = -1.212 \cdot 10^{-14}$$

$i := 0, 1 .. 360$

$\theta(i) := i$

$$\Phi(i) := \left[\beta + k \cdot d \cdot \cos\left(\theta(i) \cdot \frac{\pi}{180}\right)\right] \cdot \frac{180}{\pi}$$

$j := 0, 1 .. 180$

$\Phi(j) := -1 \cdot \Phi(j)$

$$AF(i) := \left| \frac{\sin\left(N \cdot \frac{\Phi(i)}{2} \cdot \frac{\pi}{180}\right)}{N \cdot \sin\left(\frac{\Phi(i)}{2} \cdot \frac{\pi}{180}\right)} \right|$$

the array factor is given by

$\alpha \quad k \cdot d \cdot \frac{180}{\pi}$ $\qquad \alpha = 198$

The visible region is defined by $\beta - kd \leq \Phi \leq \beta + kd$ (visible region)

$j_1 := \frac{180}{N}$ $\qquad j_2 := j_1 + (2 \cdot (k \cdot d)) \cdot \frac{180}{\pi}$ $\qquad j_1 = 18 \qquad j_2 = 414$

Plot of array factor vs. observation angle

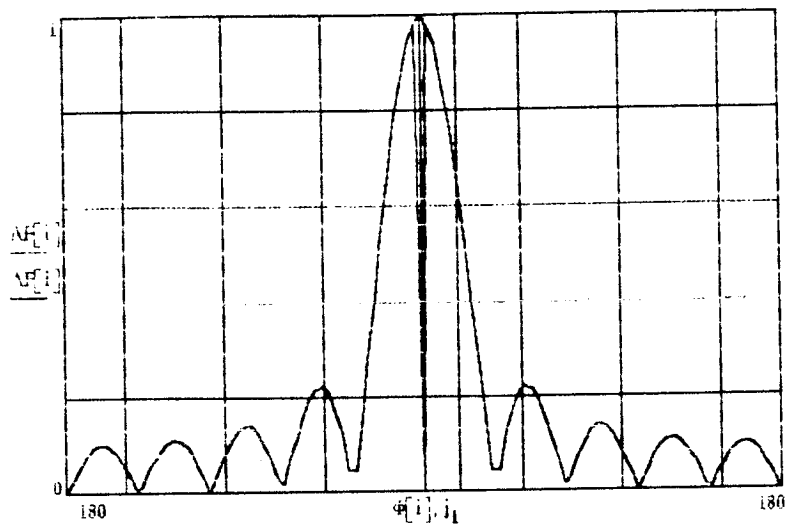

This is for a linear array with uniform amplitude. A uniform array gives the smallest half-power beamwidth, followed in order by a Dolph-Chebyshev and binomial array. The binomial array gives the smallest side lobe levels followed by the Dolph-Chebyshev then uniform array. For a given beamwidth between first nulls, a Dolph-Chebyshev array gives the smallest possibel SLL

Beamwidth calculations

Directivity calculated as follows

$j := 0, 1 .. 360$

$U(j) := AF(j)^2$ radiation intensity

$\infty := \pi$

$$U_{max} \quad \frac{\sin\left[\frac{N}{2} \cdot (k \cdot d \cdot \cos(\infty) + \beta)\right]}{N \cdot \sin\left[\frac{k \cdot d \cdot \cos(\infty) + \beta}{2}\right]}$$

$$\alpha \quad k \cdot d \cdot \frac{180}{\pi} \qquad \alpha = 198$$

the visible region is defined by $\beta - kd \le \Phi \le \beta + kd$ (visible region)

$$j_1 = \frac{180}{N} \qquad j_2 = j_1 + (2 \cdot (k \cdot d)) \cdot \frac{180}{\pi}$$

$j_1 = 18 \qquad j_2 = 414$

Plot of array factor vs. observation angle

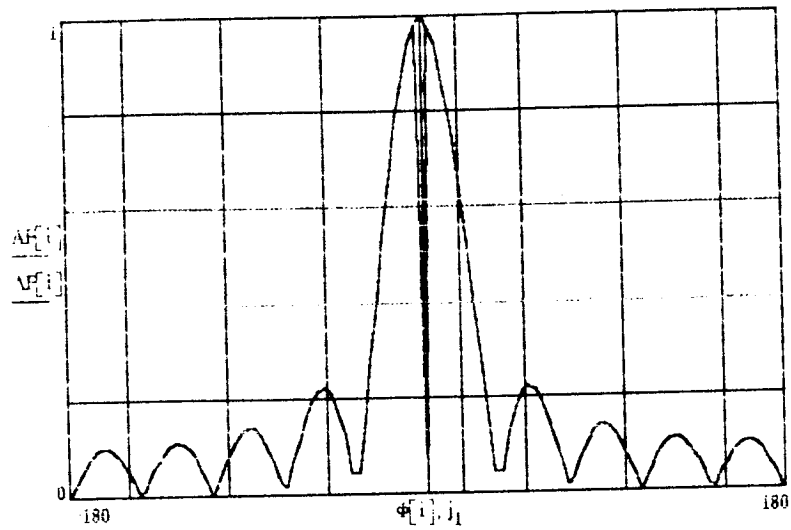

This is for a linear array with uniform amplitude. A uniform array gives the smallest half-power beamwidth, followed in order by a Dolph-Chebyshev and binomial array. The binomial array gives the smallest side lobe levels followed by the Dolph-Chebyshev then uniform array. For a given beamwidth between first nulls, a Dolph-Chebyshev array gives the smallest possibel SLL

Beamwidth calculations

Directivity calculated as follows

$$j := 0, 1 .. 360$$

$$U(j) = AF(j)^2$$

radiation intensity

$$\infty = \pi$$

$$U_{max} = \frac{\left| \sin\left[\frac{N}{2} \cdot (k \cdot d \cdot \cos(\infty) + \beta) \right] \right|}{N \cdot \left| \sin\left[\frac{k \cdot d \cdot \cos(\infty) + \beta}{2} \right] \right|}$$

$U_{max} = -0.101$

$U_{max} := 1$

$j := 0, 1 .. 360$

$$D(j) := 10 \cdot \log\left[\frac{U_{max}}{U(j)}\right]$$

directivity in dB

antenna efficency is $\eta := .55$

antenna gain is given by $$G_{dB}(j) := 10 \cdot \log\left[\eta \cdot \left[\frac{U_{max}}{U(j)}\right]\right]$$

The total gain provided by the array at the angle $\theta_3 = 90$ is given by

$p := 1 .. (N - 1)$

$$D := \frac{N^2 \cdot (k \cdot d)}{N \cdot k \cdot d + 2 \cdot \sum_p \left[\frac{N - p}{N} \cdot \sin(p \cdot k \cdot d) \cdot \cos(p \cdot k \cdot d \cdot \cos(\theta_3))\right]}$$

Gain $10 \cdot \log(\eta \cdot D)$ $\quad$ Gain = 7.443 dB

THIS PAGE INTENTIONALLY LEFT BLANK

APPENDIX F

THIS PAGE INTENTIONALLY LEFT BLANK

THIS PAGE INTENTIONALLY LEFT BLANK

I. RADIATION DEGRADATION of SOLAR ARRAY

ASEC 24 BSF/R-200 Si Solar Cells
10-ohm, 2x4cm, 200mm, 0.416g/cc
as=0.72, alt=1381km, incl=50deg

Ref(1):Solar Cell Radiation Handbook, JPL 1982
Ref(2): " " " Addendum 1. 1988

A. Front Shielding: $r_{cmx} = 2.5500$ $r_{adsv} = 1.08000$ g/cc

$t_{cmx} = 0.0152$ $t_{adsv} = 0.007640$ cm

Equivalent thickness of fused silicon: $r_{Si} = 2.290$

$$FS = \left[t_{cmx} \cdot \frac{r_{cmx}}{r_{Si}} \right] + \left[t_{adsv} \cdot \frac{r_{adsv}}{r_{Si}} \right]$$

$FS = 0.021$ cm.

B. Backshielding:

10 mils RTV-142 adhesive	1.	$t_{rtv} = .0254$	$r_{rtv} = 1.04$
Insulation: a. Glasfibre weave	2.	$t_{gf} = .0035$	$r_{gf} = 1.87$
b. kapton	3.	$t_{kap} = .0025$	$r_{kap} = 1.42$
c. Teflon(2 layers)	4.	$t_{tef} = .0025$	$r_{tef} = 2.96$
Honeycomb panel	5.	$t_{Al} = 2.20$	$r_{Al} = .026$
CFRP (2 layers)	6.	$t_{cfrp} = .012$	$r_{cfrp} = .74$
kaptn/ITO/Si paint	7.	$t_{paint} = .010$	$r_{paint} = 1.55$
Two Al facesheets	8.	$t_{Alsh} = .013$	$r_{Alsh} = 2.70$

Backshield equivalent thickness of fused Si:

$$BS = \left[\begin{array}{l} t_{rtv} \cdot r_{rtv} + t_{tef} \cdot r_{tef} + t_{kap} \cdot r_{kap} \cdots \\ + t_{gf} \cdot r_{gf} + t_{Al} \cdot r_{Al} + t_{cfrp} \cdot r_{cfrp} \cdots \\ + t_{paint} \cdot r_{paint} + 2 \cdot t_{Alsh} \cdot r_{Alsh} \end{array} \right] \cdot \left[\frac{1}{r_{Si}} \right]$$

BS = 0.085 cm Si.

III. Trapped electrons and protons.

1. Electrons; Isc, Imp, Voc, Vmp

$F1_{te} = 2.05 \cdot 10^{12}$

$F2_{te} = 1.29 \cdot 10^{12}$

$B1_{te} = 5.89 \cdot 10^{11}$

$B2_{te} = 2.62 \cdot 10^{11}$

A. Front side.
Ref(1) p6.34-6.36

F1 = 0.0152
F2 = 0.0305
B1 = 0.0764
B2 = 0.152

$$FS_{te} = \left[-\left[\frac{FS - F1}{F2 - F1} \right] \right] \cdot \left[F1_{te} - F2_{te} \right] + F1_{te}$$

$$FS_{te} = 1.785 \cdot 10^{12} \quad e-/cm\hat{}2-yr$$

B. Back

$$BS_{te} = \left[-\left[\frac{BS - B1}{B2 - B1} \right] \right] \cdot \left[B1_{te} - B2_{te} \right] + B1_{te}$$

$$BS_{te} = 5.498 \cdot 10^{11} \quad e-/cm\hat{}2-yr$$

III.2. Protons; Voc, Vmp:

$F1_{tpv} = 2.43 \cdot 10^{14}$

$B1_{tpv} = 7.75 \cdot 10^{13}$

$F2_{tpv} = 1.52 \cdot 10^{14}$

$B2_{tpv} = 5.13 \cdot 10^{13}$

A. Front side.

$$FS_{tpv} = \left[\frac{-(FS - F1)}{F2 - F1} \right] \cdot \left[F1_{tpv} - F2_{tpv} \right] + F1_{tpv}$$

$$FS_{tpv} = 2.113 \cdot 10^{14} \quad e-/cm\hat{}2-yr$$

B. Back side

$$BS_{tpv} = \left[\left[\frac{BS - B1}{B2 - B1} \right] \cdot (- 1) \right] \cdot \left[B1_{tpv} - B2_{tpv} \right] + B1_{tpv}$$

$$BS_{tpv} = 7.436 \cdot 10^{13} \quad e-/cm^2-yr$$

III. 3. Trapped Protons; Isc, Imp:

$$F1_{tpi} = 1.42 \cdot 10^{14}$$

$$B1_{tpi} = 6.16 \cdot 10^{13}$$

$$F2_{tpi} = 1.00 \cdot 10^{14}$$

$$B2_{tpi} = 4.39 \cdot 10^{13}$$

A. Front side.

$$FS_{tpi} = \left[\frac{- (FS - F1)}{F2 - F1} \right] \cdot \left[F1_{tpi} - F2_{tpi} \right] + F1_{tpi}$$

$$FS_{tpi} = 1.274 \cdot 10^{14} \quad e-/cm^2-yr$$

B. Back :

$$BS_{tpi} = \left[\frac{- (BS - B1)}{B2 - B1} \right] \cdot \left[B1_{tpi} - B2_{tpi} \right] + B1_{tpi}$$

Total equivalent 1Mev fluences, trapped protons and electrons:

Orbit life of 8 years $L = 5$

Isc, Imp: $I_{tr} = \left[\left[FS_{te} + BS_{te} \right] + \left[FS_{tpi} + BS_{tpi} \right] \right] \cdot L$

Voc, Vmp: $V_{tr} = \left[\left[FS_{te} + BS_{te} \right] + \left[FS_{tpv} + BS_{tpv} \right] \right] \cdot L$

$$I_{tr} = 9.459 \cdot 10^{14} \quad e-/cm^2$$

$$V_{tr} = 1.44 \cdot 10^{15} \quad e-/cm^2$$

IV. Solar Flare Protons.

6.39 (e-/cm^2-yr), 1974-1984 annual, 3/6/12/20 mils. + Ref(1), table

$$SP_{v30} = 1.695 \cdot 10^{12} \qquad SP_{v6} = 6.399 \cdot 10^{12} \qquad SP_{v12} = 3.581 \cdot 10^{12}$$

$$SP_{v60} = 9.34 \cdot 10^{11} \qquad SP_{i60} = 7.91 \cdot 10^{11}$$

$$SP_{v20} = 2.267 \cdot 10^{12} \qquad SP_{i30} = 1.22 \cdot 10^{12} \qquad SP_{i6} = 3.48 \cdot 10^{12}$$

$$SP_{i20} = 1.600 \cdot 10^{12} \qquad SP_{i12} = 2.258 \cdot 10^{12}$$

A. Front side:

$$FS_{spv} = \left[\left[\frac{-(FS - F1)}{F2 - F1} \right] \cdot \left[SP_{v6} - SP_{v12} \right] + SP_{v6} \right]$$

$$FS_{spi} = \left[\frac{-(FS - F1)}{F2 - F1} \right] \cdot \left[SP_{i6} - SP_{i12} \right] + SP_{i6}$$

B. Back side:

$$BS_{spv} = \left[\frac{-(BS - B1)}{B2 - B1} \right] \cdot \left[SP_{v30} - SP_{v60} \right] + SP_{v30}$$

$$BS_{spi} = \left[\frac{-(BS - B1)}{B2 - B1} \right] \cdot \left[SP_{i30} - SP_{i60} \right] + SP_{i30}$$

IV. Total equivalent 1 Mev fluence due to Solar Flare protons:

$$SP_v = \left[FS_{spv} + BS_{spv} \right] \cdot L$$

$$SP_i = \left[FS_{spi} + BS_{spi} \right] \cdot L$$

V. TOTAL equivalent 1 Mev electron fluence, 5 years:
(solar flare+trapped e- and protons).

$$V_{Mev} := [\, V_{tr} + SP_v \,] \qquad V_{Mev} = 1.475 \cdot 10^{15} \quad e\text{-}/cm\hat{}2$$

$$I_{Mev} := [\, I_{tr} + SP_i \,] \qquad I_{Mev} = 9.67 \cdot 10^{14} \quad e\text{-}/cm\hat{}2$$

VI. SOLAR ARRAY

10 ohm-cm, Si, 2x4cm, 200mm cells

Equivalent 1Mev fluence for 5 years;
V=1.475E15, I=9.67E14
Pmax= 13 mW/cm^2

EOL array power = 600 watts

Fully regulated dual bus @ 28 volts.

$I_{sc} := 0.350$

$I_{mp} := 0.330$

$V_{mp} := 0.400$

$V_{oc} := 0.495$

$K_A := .94$

$K_d := .960$

$K_{ss} := .8888$

$K_{se} := .9941$

$T_{SAs} := 64.0$

$T_{SAe} := 60.0$

$K_E := .9605$

$\alpha_I := .000$

$\alpha_V := -.0023$

$dV := .006$

$$CellI_{sol} := [\, [\, I_{mp} + \alpha_I \cdot [\, T_{SAs} - 28 \,] \,] \cdot K_A \cdot K_d \cdot K_{ss} \,]$$

$$CellI_{eqx} := [\, [\, I_{mp} + \alpha_I \cdot [\, T_{SAe} - 28 \,] \,] \cdot K_A \cdot K_d \cdot K_{se} \,]$$

$$CellV_{sol} := [\, [\, V_{mp} - dV + [\, \alpha_V \cdot [\, T_{SAs} - 28 \,] \,] \cdot K_E \,] \,]$$

$$CellV_{eqx} := [\, [\, V_{mp} - dV + [\, \alpha_V \cdot [\, T_{SAe} - 28 \,] \,] \cdot K_E \,] \,]$$

$CellV_{sol} = 0.314$ $\qquad CellI_{sol} = 0.265$

$CellV_{eqx} = 0.323$ $\qquad CellI_{eqx} = 0.296$

Current required by each bus (A):

$$Bl_{sol} = 6 \qquad V_{bus} = 28 \qquad I_{eqx} = \left[\frac{300}{28}\right] \qquad I_{sol} = \left[\frac{300}{28}\right]$$

$$EqxN_p = \left[\frac{I_{eqx}}{CellI_{eqx}}\right] \qquad SolN_p = \left[\frac{I_{sol}}{CellI_{sol}}\right]$$

$$EqxN_p = 36.193$$

$$SolN_p = 40.481$$

Number of solar cells in series.

$$EqxN_s = \left[\frac{V_{bus} + 1.8}{CellV_{eqx}}\right] \qquad SolN_s = \left[\frac{V_{bus} + 1.8}{CellV_{sol}}\right]$$

$$EqxN_s = 92.172$$

$$SolN_s = 94.762$$

Area of Solar Array (Effective).

$$A_{sae} = \left[EqxN_s \cdot EqxN_p\right] \cdot \left[2 \cdot 4 \cdot 10^{-4}\right]$$

$$A_{sae} = 2.669$$

$$A_{sas} = \left[SolN_s \cdot SolN_p\right] \cdot \left[2 \cdot 4 \cdot 10^{-4}\right]$$

$$A_{sas} = 3.069 \quad m^2 \text{ per wing}$$

Net array area, packing factor: $F_p = .87$

$$Area = \frac{A_{sas}}{F_p}$$

$Area = 3.527$ Required area on each wing.

APPENDIX G

THIS PAGE INTENTIONALLY LEFT BLANK

THIS PAGE INTENTIONALLY LEFT BLANK

APPENDIX G

A. RADIATOR SIZING CALCULATIONS

The following calculations were done in MATHCAD, by the Math Works, ver 2.4.

B. PHASE CHANGER SIZING CALCULATIONS

The following calculations were based on organic polymer properties found in Ref. 7.

The heat of fusion for $C_{22}H_{46}$ is 157.61 J/gm. The mass required to accept any heating over the average can be calculated by

$$m = \frac{Q}{L}$$
$$= \frac{Power\ t}{L}$$
$$= \frac{(870-130\ W)(20\ \text{min})(60\ s/\text{min})}{157.61\ J/gm}$$
$$= 5635\ gm = 5.7\ kg$$

Which is the mass required for both phase changers.
Each phase changer then masses 2.85 kg.

Knowing the height and width of the phase changer, the depth may be calculated.

$$w = \frac{m}{\rho\ l\ h}$$
$$= \frac{2850g}{(0.7944\frac{g}{cm^3})\ (96.12cm)\ (57.15cm)}$$
$$= 0.65cm$$

The depth is taken as 0.70 cm to account for the aluminum sheath around the paraffin.

C. THERMAL MODELING RESULTS

PC-ITAS results are summarized in the following pages. A list of equipment node numbers of interest is provided in Tables A.1 and A.2. These numbers may be matched to node numbers in the PC-ITAS output to determine the temperatures of nodes of interest. It should be noted that both steady state and transient thermal analyses were run and that all nodes stayed within their allowable temperature limits as outlined in Table 5.1.

Table A.1 Partial Model Nodes of Interest

Equipment	Nodes
Kapton Insulation	3xx

Propellent Tank Interior	399

Table A.2 Full Model Nodes of Interest

Equipment	Nodes
Transponders	45xx, 48xx
RTU's	12xx, 16xx
RCU's	10xx, 11xx
TT & C	44xx, 53xx
Battery Package #1	30xx
Battery Package #2	31xx
Battery Package #3	32xx
Battery Package #4	33xx
Propellent Tank	7xx

Power vs. time for the design scenario (slightly more dissipation than within the worst-case orbit);

```
i := 1 ..113
j := 1
k := 0 ..30
l := 0 ..19
m := 0 ..2
```

Define a matrix P, which is a 113 X 2 matrix of orbital time (minutes) and power to dissipate:

$P_{i,0} := i$

$P_{(l+31),1} := 864.28$

$P_{(l+51),1} := 130$

$P_{k,1} := 130$

$P_{(l+71),1} := 864.28$

$P_{(l+91),1} := 130$

$P_{(m+111),1} := 600$

Plotting P yields the design criterion power profile,

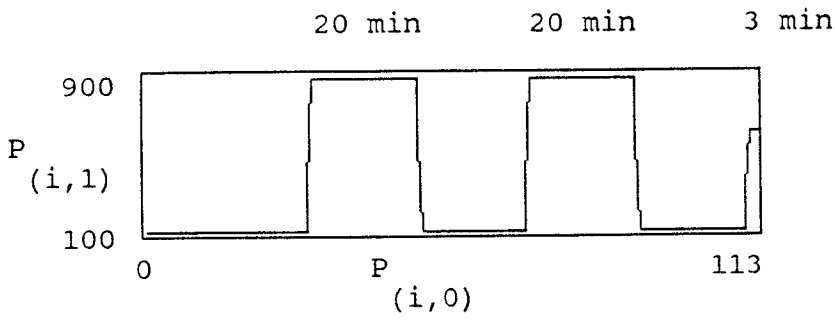

Integrating the above plot and dividing by the total time yields the average dissipated power requirement.

$$Paverage := \frac{130 \cdot (71) + 864.28 \cdot (40) + 600 \cdot (3)}{113}$$

Paverage = 403.55044 W, average power dissipation required.

The above then becomes the design criterion for determining the radiator size as shown below.

Using off-the-shelf louvers, the radiators can be designed for size by determining the power dissipated through various configurations and the temperatures associated therewith. The following represents one possible solution.

$\epsilon := 0.8$

$\sigma := 5.67 \cdot 10^{-8}$ W/m^2K^4

$\eta 1 := 0.9$ $\eta 2 := .4$

$\alpha s := 0.21$ W/m^2

$S := 1397$

$\theta := 28.5 \cdot \frac{180}{\pi}$ rad, from orbital geometry at Winter Solstice.

2 Fairchild 18-blade louvers per side (sunlit side radiating at 40% efficiency).

Area := 2 · .4806 · .5715 - .00133

Area = 0.548 m^2

High Temperature check:

$T := 100 \cdot 1.8 - 32 + 273$ = 100 F, maximum allowable temperature for the electronics.

$$Powerdis := Area \cdot \left[\epsilon \cdot \sigma \cdot T^4 \cdot \eta 1 + \epsilon \cdot \sigma \cdot T^4 \cdot \eta 2 - \alpha s \cdot \sigma \cdot (\cos(\theta) + 0.31)\right]$$

$Powerdis = 1.01513 \cdot 10^3$

Since the maximum power expected to be dissipated is less than this figure, temperatures will not exceed 100 F.

Mean temperature determination:

$T := 52 \cdot 1.8 - 32 + 273$ = 61.6 C, mean temperature.

$$Powerdis := Area \cdot \left[\epsilon \cdot \sigma \cdot T^4 \cdot \eta 1 + \epsilon \cdot \sigma \cdot T^4 \cdot \eta 2 - \alpha s \cdot \sigma \cdot (\cos(\theta) + 0.31)\right]$$

Powerdis = 405.0395 W

Temperature during low-power operations:

$T := 6.1 \cdot 1.8 - 32 + 273$ = -21.0 C, non-operational temperature.

$$Powerdis := Area \cdot \left[\epsilon \cdot \sigma \cdot T^4 \cdot \eta 1 + \epsilon \cdot \sigma \cdot T^4 \cdot \eta 2 - \alpha s \cdot \sigma \cdot (\cos(\theta) + 0.31)\right]$$

Powerdis = 130.27405 W

Cold Case:

$\eta 2 := .9$ (All louvers jammed open)

$T := -4.9 \cdot 1.8 - 32 + 273$ = -40.8 C, heaters not required for the electronics. (-40 F allowable)

$$Powerdis := Area \cdot \left[\epsilon \cdot \sigma \cdot T^4 \cdot \eta 1 + \epsilon \cdot \sigma \cdot T^4 \cdot \eta 2\right]$$

Powerdis = 130.02355 W

```
NODE      26 (REL NODE      26 ) IS BEING ADDED TO THE CURRENT LIST
NODE      27 (REL NODE      27 ) IS BEING ADDED TO THE CURRENT LIST
NODE      28 (REL NODE      28 ) IS BEING ADDED TO THE CURRENT LIST
NODE      29 (REL NODE      29 ) IS BEING ADDED TO THE CURRENT LIST
NODE      30 (REL NODE      30 ) IS BEING ADDED TO THE CURRENT LIST
NODE      31 (REL NODE      31 ) IS BEING ADDED TO THE CURRENT LIST
NODE      32 (REL NODE      32 ) IS BEING ADDED TO THE CURRENT LIST
NODE      33 (REL NODE      33 ) IS BEING ADDED TO THE CURRENT LIST
NODE      34 (REL NODE      34 ) IS BEING ADDED TO THE CURRENT LIST
NODE      35 (REL NODE      35 ) IS BEING ADDED TO THE CURRENT LIST
NODE      36 (REL NODE      36 ) IS BEING ADDED TO THE CURRENT LIST
NODE      37 (REL NODE      37 ) IS BEING ADDED TO THE CURRENT LIST
NODE      38 (REL NODE      38 ) IS BEING ADDED TO THE CURRENT LIST
NODE      39 (REL NODE      39 ) IS BEING ADDED TO THE CURRENT LIST
NODE      40 (REL NODE      40 ) IS BEING ADDED TO THE CURRENT LIST
NODE      41 (REL NODE      41 ) IS BEING ADDED TO THE CURRENT LIST
NODE      42 (REL NODE      42 ) IS BEING ADDED TO THE CURRENT LIST
NODE      43 (REL NODE      43 ) IS BEING ADDED TO THE CURRENT LIST
NODE      44 (REL NODE      44 ) IS BEING ADDED TO THE CURRENT LIST
NODE      45 (REL NODE      45 ) IS BEING ADDED TO THE CURRENT LIST
NODE      46 (REL NODE      46 ) IS BEING ADDED TO THE CURRENT LIST
NODE      47 (REL NODE      47 ) IS BEING ADDED TO THE CURRENT LIST
NODE      48 (REL NODE      48 ) IS BEING ADDED TO THE CURRENT LIST
NODE      49 (REL NODE      49 ) IS BEING ADDED TO THE CURRENT LIST
NODE      50 (REL NODE      50 ) IS BEING ADDED TO THE CURRENT LIST
NODE      51 (REL NODE      51 ) IS BEING ADDED TO THE CURRENT LIST
NODE      52 (REL NODE      52 ) IS BEING ADDED TO THE CURRENT LIST
NODE      53 (REL NODE      53 ) IS BEING ADDED TO THE CURRENT LIST
NODE      54 (REL NODE      54 ) IS BEING ADDED TO THE CURRENT LIST
NODE      55 (REL NODE      55 ) IS BEING ADDED TO THE CURRENT LIST
NODE      56 (REL NODE      56 ) IS BEING ADDED TO THE CURRENT LIST
NODE      57 (REL NODE      57 ) IS BEING ADDED TO THE CURRENT LIST
NODE      58 (REL NODE      58 ) IS BEING ADDED TO THE CURRENT LIST
NODE      59 (REL NODE      59 ) IS BEING ADDED TO THE CURRENT LIST
NODE      60 (REL NODE      60 ) IS BEING ADDED TO THE CURRENT LIST
NODE      61 (REL NODE      61 ) IS BEING ADDED TO THE CURRENT LIST
NODE      62 (REL NODE      62 ) IS BEING ADDED TO THE CURRENT LIST
NODE      63 (REL NODE      63 ) IS BEING ADDED TO THE CURRENT LIST
NODE      64 (REL NODE      64 ) IS BEING ADDED TO THE CURRENT LIST
NODE      65 (REL NODE      65 ) IS BEING ADDED TO THE CURRENT LIST
NODE      66 (REL NODE      66 ) IS BEING ADDED TO THE CURRENT LIST
NODE      67 (REL NODE      67 ) IS BEING ADDED TO THE CURRENT LIST
NODE      68 (REL NODE      68 ) IS BEING ADDED TO THE CURRENT LIST
NODE      69 (REL NODE      69 ) IS BEING ADDED TO THE CURRENT LIST
NODE      70 (REL NODE      70 ) IS BEING ADDED TO THE CURRENT LIST
NODE      71 (REL NODE      71 ) IS BEING ADDED TO THE CURRENT LIST
NODE      72 (REL NODE      72 ) IS BEING ADDED TO THE CURRENT LIST
   73 *WARNING*THIS NODE WAS PREVIOUSLY DEFINED. OVERIDES PREVIOUS INPUT.
 END OF RADIATION CONDUCTANCE & POWER PROCESSING
 ITAS THERMAL ANALYSIS:


 CHECKOUT PHASE OF PC-ITAS THERMAL ANALYSIS

 TOTAL CARDS ENCOUNTERED:    2069
================================================================================
 NO. OF THERMAL NODES=          146

 ITAS STEADY-STATE SOLUTION ALGORITHM (SUCCESSIVE POINT ITERATION) PARAMETERS:
 ARLXCA=0.50000E-03, DRLXCA=0.50000E-03 NLOOP=  9999
********************************************************************************
 ITAS STEADY-STATE SOLUTION (SUCCESSIVE POINT ITERATION)
 NO. OF ITERATIONS= 4416 TOTAL INPUT ENERGY (W)=  3.2800
 SYSTEM ENERGY BALANCE (W)=  2.2121      (  67.443     %)
********************************************************************************
 T      1=      0.78 T      2=      0.12 T      3=     -7.52 T      4=     -0.22
```

5=	0.12 T	6=	-7.60 T	7=	0.77 T	8=	0.11
9=	-7.49 T	10=	-0.22 T	11=	0.11 T	12=	-7.57
13=	1.63 T	14=	1.63 T	15=	1.63 T	16=	1.63
17=	1.63 T	18=	1.63 T	19=	1.63 T	20=	1.63
21=	1.63 T	22=	1.63 T	23=	1.63 T	24=	1.63
25=	1.63 T	26=	1.63 T	27=	1.63 T	28=	1.63
29=	1.63 T	30=	1.63 T	31=	1.63 T	32=	1.63
33=	1.63 T	34=	1.63 T	35=	1.63 T	36=	1.63
37=	1.63 T	38=	1.63 T	39=	1.63 T	40=	1.63
41=	1.63 T	42=	1.63 T	43=	1.63 T	44=	1.63
45=	1.63 T	46=	1.63 T	47=	1.63 T	48=	1.63
49=	1.63 T	50=	1.63 T	51=	1.63 T	52=	1.63
53=	1.63 T	54=	1.63 T	55=	1.63 T	56=	1.63
57=	1.63 T	58=	1.63 T	59=	1.63 T	60=	1.63
61=	1.63 T	62=	1.63 T	63=	1.63 T	64=	1.63
65=	1.63 T	66=	1.63 T	67=	1.63 T	68=	1.63
69=	1.63 T	70=	1.63 T	71=	1.63 T	72=	1.63
73=	-273.16 T	101=	0.78 T	102=	0.12 T	103=	-7.52
104=	-0.22 T	105=	0.12 T	106=	-7.60 T	201=	0.77
202=	0.11 T	203=	-7.49 T	204=	-0.22 T	205=	0.11
206=	-7.57 T	301=	1.63 T	302=	1.63 T	303=	1.63
304=	1.63 T	305=	1.63 T	306=	1.63 T	307=	1.63
308=	1.63 T	309=	1.63 T	310=	1.63 T	311=	1.63
312=	1.63 T	313=	1.63 T	314=	1.63 T	315=	1.63
316=	1.63 T	317=	1.63 T	318=	1.63 T	319=	1.63
320=	1.63 T	321=	1.63 T	322=	1.63 T	323=	1.63
324=	1.63 T	325=	1.63 T	326=	1.63 T	327=	1.63
328=	1.63 T	329=	1.63 T	330=	1.63 T	331=	1.63
332=	1.63 T	333=	1.63 T	334=	1.63 T	335=	1.63
336=	1.63 T	337=	1.63 T	338=	1.63 T	339=	1.63
340=	1.63 T	341=	1.63 T	342=	1.63 T	343=	1.63
344=	1.63 T	345=	1.63 T	346=	1.63 T	347=	1.63
348=	1.63 T	349=	1.63 T	350=	1.63 T	351=	1.63
352=	1.63 T	353=	1.63 T	354=	1.63 T	355=	1.63
356=	1.63 T	357=	1.63 T	358=	1.63 T	359=	1.63
360=	1.63 T	399=	22.46 T				

ASCENDING NODE NUMBER : TEMPERATURE

****

ITAS STEADY-STATE SOLUTION (SUCCESSIVE POINT ITERATION)
NO. OF ITERATIONS= 4416 TOTAL INPUT ENERGY (W)= 3.2800
SYSTEM ENERGY BALANCE (W)= 2.2121 (67.443 %)

****

1=	0.780 T	2=	0.115 T	3=	-7.520 T	4=	-0.215
5=	0.115 T	6=	-7.599 T	7=	0.770 T	8=	0.111
9=	-7.488 T	10=	-0.215 T	11=	0.112 T	12=	-7.568
13=	1.629 T	14=	1.629 T	15=	1.629 T	16=	1.629
17=	1.629 T	18=	1.629 T	19=	1.629 T	20=	1.629
21=	1.629 T	22=	1.629 T	23=	1.629 T	24=	1.629
25=	1.629 T	26=	1.629 T	27=	1.629 T	28=	1.629
29=	1.629 T	30=	1.629 T	31=	1.629 T	32=	1.629
33=	1.629 T	34=	1.629 T	35=	1.629 T	36=	1.629
37=	1.629 T	38=	1.629 T	39=	1.629 T	40=	1.629
41=	1.629 T	42=	1.629 T	43=	1.629 T	44=	1.629
45=	1.629 T	46=	1.629 T	47=	1.629 T	48=	1.629
49=	1.629 T	50=	1.629 T	51=	1.629 T	52=	1.629
53=	1.629 T	54=	1.629 T	55=	1.629 T	56=	1.629
57=	1.629 T	58=	1.629 T	59=	1.629 T	60=	1.629
61=	1.629 T	62=	1.629 T	63=	1.629 T	64=	1.629
65=	1.629 T	66=	1.629 T	67=	1.629 T	68=	1.629
69=	1.629 T	70=	1.629 T	71=	1.629 T	72=	1.629
73=	-273.159 T	101=	0.780 T	102=	0.115 T	103=	-7.519
104=	-0.215 T	105=	0.115 T	106=	-7.598 T	201=	0.770
202=	0.111 T	203=	-7.488 T	204=	-0.215 T	205=	0.112
206=	-7.569 T	301=	1.630 T	302=	1.630 T	303=	1.630
304=	1.630 T	305=	1.630 T	306=	1.630 T	307=	1.630

```
T   308=      1.630 T   309=      1.630 T   310=      1.630 T   311=      1.630
T   312=      1.630 T   313=      1.630 T   314=      1.630 T   315=      1.630
T   316=      1.630 T   317=      1.630 T   318=      1.630 T   319=      1.630
T   320=      1.630 T   321=      1.630 T   322=      1.630 T   323=      1.630
T   324=      1.630 T   325=      1.630 T   326=      1.630 T   327=      1.630
T   328=      1.630 T   329=      1.630 T   330=      1.630 T   331=      1.630
T   332=      1.630 T   333=      1.630 T   334=      1.630 T   335=      1.630
T   336=      1.630 T   337=      1.630 T   338=      1.630 T   339=      1.630
T   340=      1.630 T   341=      1.630 T   342=      1.630 T   343=      1.630
T   344=      1.630 T   345=      1.630 T   346=      1.630 T   347=      1.630
T   348=      1.630 T   349=      1.630 T   350=      1.630 T   351=      1.630
T   352=      1.630 T   353=      1.630 T   354=      1.630 T   355=      1.630
T   356=      1.630 T   357=      1.630 T   358=      1.630 T   359=      1.630
T   360=      1.630 T   399=     22.463 T
                    ASCENDING NODE NUMBER : IMPRESSED Q
Q     1=      0.230 Q     2=      0.140 Q     3=      0.050 Q     4=      0.170
Q     5=      0.140 Q     6=      0.050 Q     7=      0.000 Q     8=      0.000
Q     9=      0.000 Q    10=      0.000 Q    11=      0.000 Q    12=      0.000
Q    13=      0.000 Q    14=      0.000 Q    15=      0.000 Q    16=      0.000
Q    17=      0.000 Q    18=      0.000 Q    19=      0.000 Q    20=      0.000
Q    21=      0.000 Q    22=      0.000 Q    23=      0.000 Q    24=      0.000
Q    25=      0.000 Q    26=      0.000 Q    27=      0.000 Q    28=      0.000
Q    29=      0.000 Q    30=      0.000 Q    31=      0.000 Q    32=      0.000
Q    33=      0.000 Q    34=      0.000 Q    35=      0.000 Q    36=      0.000
Q    37=      0.000 Q    38=      0.000 Q    39=      0.000 Q    40=      0.000
Q    41=      0.000 Q    42=      0.000 Q    43=      0.000 Q    44=      0.000
Q    45=      0.000 Q    46=      0.000 Q    47=      0.000 Q    48=      0.000
Q    49=      0.000 Q    50=      0.000 Q    51=      0.000 Q    52=      0.000
Q    53=      0.000 Q    54=      0.000 Q    55=      0.000 Q    56=      0.000
Q    57=      0.000 Q    58=      0.000 Q    59=      0.000 Q    60=      0.000
Q    61=      0.000 Q    62=      0.000 Q    63=      0.000 Q    64=      0.000
Q    65=      0.000 Q    66=      0.000 Q    67=      0.000 Q    68=      0.000
Q    69=      0.000 Q    70=      0.000 Q    71=      0.000 Q    72=      0.000
Q    73=      0.000 Q   101=      0.000 Q   102=      0.000 Q   103=      0.000
Q   104=      0.000 Q   105=      0.000 Q   106=      0.000 Q   201=      0.000
Q   202=      0.000 Q   203=      0.000 Q   204=      0.000 Q   205=      0.000
Q   206=      0.000 Q   301=      0.000 Q   302=      0.000 Q   303=      0.000
Q   304=      0.000 Q   305=      0.000 Q   306=      0.000 Q   307=      0.000
Q   308=      0.000 Q   309=      0.000 Q   310=      0.000 Q   311=      0.000
Q   312=      0.000 Q   313=      0.000 Q   314=      0.000 Q   315=      0.000
Q   316=      0.000 Q   317=      0.000 Q   318=      0.000 Q   319=      0.000
Q   320=      0.000 Q   321=      0.000 Q   322=      0.000 Q   323=      0.000
Q   324=      0.000 Q   325=      0.000 Q   326=      0.000 Q   327=      0.000
Q   328=      0.000 Q   329=      0.000 Q   330=      0.000 Q   331=      0.000
Q   332=      0.000 Q   333=      0.000 Q   334=      0.000 Q   335=      0.000
Q   336=      0.000 Q   337=      0.000 Q   338=      0.000 Q   339=      0.000
Q   340=      0.000 Q   341=      0.000 Q   342=      0.000 Q   343=      0.000
Q   344=      0.000 Q   345=      0.000 Q   346=      0.000 Q   347=      0.000
Q   348=      0.000 Q   349=      0.000 Q   350=      0.000 Q   351=      0.000
Q   352=      0.000 Q   353=      0.000 Q   354=      0.000 Q   355=      0.000
Q   356=      0.000 Q   357=      0.000 Q   358=      0.000 Q   359=      0.000
Q   360=      0.000 Q   399=      2.500 Q
 BOLTZMANN CONSTANT: SIGMA =   0.566970E-11 W/(CM^2 K)
================================================================================
 NO. OF THERMAL NODES (CURRENT) =          146
ITAS TRANSIENT SOLUTION ALGORITHM PARAMETERS:
TIMEO = 0.00000     , TIMEND=  113.49     , OUTPUT=  2.0000
DTIMEI= 0.10000     , ARLXCA= 0.50000E-03, DRLXCA= 0.50000E-03
CSGFAC=  1.0000      , NLOOP =        9999
************************************
 THERMAL CALC CPU TIME (second)      =     6165.72
************************************
********************************************************************************
                                                          Time: 21:31:38.10
Date: 12/02/91
********************************************************************************
================================================================================
```

```
 355 *WARNING*THIS NODE WAS PREVIOUSLY DEFINED. OVERIDES PREVIOUS INPUT.
 369 *WARNING*THIS NODE WAS PREVIOUSLY DEFINED. OVERIDES PREVIOUS INPUT.
 215 *WARNING*THIS NODE WAS PREVIOUSLY DEFINED. OVERIDES PREVIOUS INPUT.
END OF RADIATION CONDUCTANCE & POWER PROCESSING
ITAS THERMAL ANALYSIS:


CHECKOUT PHASE OF PC-ITAS THERMAL ANALYSIS

TOTAL CARDS ENCOUNTERED:    6667
================================================================================
NO. OF THERMAL NODES=          456

ITAS STEADY-STATE SOLUTION ALGORITHM (SUCCESSIVE POINT ITERATION) PARAMETERS:
ARLXCA=0.50000E-03, DRLXCA=0.50000E-03 NLOOP=  9999
********************************************************************************
ITAS STEADY-STATE SOLUTION (SUCCESSIVE POINT ITERATION)
NO. OF ITERATIONS=10000 TOTAL INPUT ENERGY (W)=  801.70
SYSTEM ENERGY BALANCE (W)= -1.7652     ( 0.22019    %)
********************************************************************************
T     1=   -70.51 T     2=    45.81 T     3=   -93.33 T     4=   -72.01
T     5=    -3.57 T     6=   -35.71 T     7=   -70.48 T     8=    45.69
T     9=   -93.32 T    10=   -71.99 T    11=    -3.69 T    12=   -35.70
T    13=     0.01 T    14=     0.01 T    15=     0.01 T    16=     0.01
T    17=     0.01 T    18=     0.01 T    19=     0.01 T    20=     0.01
T    21=     0.01 T    22=     0.01 T    23=     0.01 T    24=     0.01
T    25=     0.01 T    26=     0.01 T    27=     0.01 T    28=     0.01
T    29=     0.01 T    30=     0.01 T    31=     0.01 T    32=     0.01
T    33=     0.01 T    34=     0.01 T    35=     0.01 T    36=     0.01
T    37=     0.01 T    38=     0.01 T    39=     0.01 T    40=     0.01
T    41=     0.01 T    42=     0.01 T    43=     0.01 T    44=     0.01
T    45=     0.01 T    46=     0.01 T    47=     0.01 T    48=     0.01
T    49=     0.01 T    50=     0.01 T    51=     0.01 T    52=     0.01
T    53=     0.01 T    54=     0.01 T    55=     0.01 T    56=     0.01
T    57=     0.01 T    58=     0.01 T    59=     0.01 T    60=     0.01
T    61=     0.01 T    62=     0.01 T    63=     0.01 T    64=     0.01
T    65=     0.01 T    66=     0.01 T    67=     0.01 T    68=     0.01
T    69=     0.01 T    70=     0.01 T    71=     0.01 T    72=     0.01
T    73=    45.63 T    74=    -3.75 T    75=    44.49 T    76=    -4.36
T    77=    45.63 T    78=    45.60 T    79=    45.63 T    80=    45.63
T    81=    45.63 T    82=    45.63 T    83=    -3.75 T    84=    -3.75
T    85=    -3.75 T    86=    -3.75 T    87=    -3.78 T    88=    -3.75
T    89=    46.61 T    90=    45.97 T    91=    46.61 T    92=    46.99
T    93=    46.61 T    94=    46.61 T    95=    -3.12 T    96=    -3.21
T    97=    -3.21 T    98=    -3.21 T    99=    -3.58 T   100=    -3.21
T   101=   -23.38 T   102=   -23.38 T   103=   -23.38 T   104=   -23.40
T   105=   -23.38 T   106=   -23.38 T   107=    45.60 T   108=    45.58
T   109=    45.60 T   110=    45.60 T   111=    45.60 T   112=    45.60
T   113=    45.60 T   114=    45.59 T   115=    45.60 T   116=    45.60
T   117=    45.60 T   118=    45.60 T   119=    -3.78 T   120=    -3.78
T   121=    -3.78 T   122=    -3.78 T   123=    -3.80 T   124=    -3.78
T   125=    -3.78 T   126=    -3.78 T   127=    -3.78 T   128=    -3.78
T   129=    -3.79 T   130=    -3.78 T   131=   -30.50 T   132=   -30.48
T   133=   -30.48 T   134=   -30.48 T   135=   -30.48 T   136=   -30.48
T   137=    47.36 T   138=    46.38 T   139=    47.74 T   140=    47.74
T   141=    47.74 T   142=    47.74 T   143=    -2.93 T   144=    -2.92
T   145=    -2.92 T   146=    -3.02 T   147=    -3.50 T   148=    -2.92
T   149=   -69.01 T   150=   -69.00 T   151=   -69.00 T   152=   -69.00
T   153=   -69.00 T   154=   -69.00 T   155=     0.00 T   156=     0.00
T   157=     0.00 T   158=     0.00 T   159=     0.00 T   160=     0.00
T   161=     0.00 T   162=     0.00 T   163=     0.00 T   164=     0.00
T   165=     0.00 T   166=     0.00 T   167=     0.00 T   168=     0.00
T   169=     0.00 T   170=     0.00 T   171=     0.00 T   172=     0.00
T   173=     0.00 T   174=     0.00 T   175=     0.00 T   176=     0.00
T   177=     0.00 T   178=     0.00 T   179=     0.00 T   180=     0.00
T   181=     0.00 T   182=     0.00 T   183=     0.00 T   184=     0.00
```

185=	0.00 T	186=	0.00 T	187=	0.00 T	188=	0.00
189=	0.00 T	190=	0.00 T	191=	0.00 T	192=	0.00
193=	0.00 T	194=	0.00 T	195=	0.00 T	196=	0.00
197=	0.00 T	198=	0.00 T	199=	0.00 T	200=	0.00
201=	0.00 T	202=	0.00 T	203=	0.00 T	204=	0.00
205=	0.00 T	206=	0.00 T	207=	0.00 T	208=	0.00
209=	0.00 T	210=	0.00 T	211=	0.00 T	212=	0.00
213=	0.00 T	214=	0.00 T	215=	-273.16 T	501=	-70.50
502=	45.75 T	503=	-93.32 T	504=	-72.00 T	505=	-3.63
506=	-35.70 T	601=	-70.48 T	602=	45.69 T	603=	-93.32
604=	-71.99 T	605=	-3.69 T	606=	-35.70 T	701=	0.01
702=	0.01 T	703=	0.01 T	704=	0.01 T	705=	0.01
706=	0.01 T	707=	0.01 T	708=	0.01 T	709=	0.01
710=	0.01 T	711=	0.01 T	712=	0.01 T	713=	0.01
714=	0.01 T	715=	0.01 T	716=	0.01 T	717=	0.01
718=	0.01 T	719=	0.01 T	720=	0.01 T	721=	0.01
722=	0.01 T	723=	0.01 T	724=	0.01 T	725=	0.01
726=	0.01 T	727=	0.01 T	728=	0.01 T	729=	0.01
730=	0.01 T	731=	0.01 T	732=	0.01 T	733=	0.01
734=	0.01 T	735=	0.01 T	736=	0.01 T	737=	0.01
738=	0.01 T	739=	0.01 T	740=	0.01 T	741=	0.01
742=	0.01 T	743=	0.01 T	744=	0.01 T	745=	0.01
746=	0.01 T	747=	0.01 T	748=	0.01 T	749=	0.01
750=	0.01 T	751=	0.01 T	752=	0.01 T	753=	0.01
754=	0.01 T	755=	0.01 T	756=	0.01 T	757=	0.01
758=	0.01 T	759=	0.01 T	760=	0.01 T	799=	0.01
801=	45.63 T	802=	-3.75 T	901=	45.58 T	902=	-3.80
1001=	45.63 T	1002=	45.60 T	1003=	45.63 T	1004=	45.63
1005=	45.63 T	1006=	45.63 T	1099=	45.63 T	1101=	-3.75
1102=	-3.75 T	1103=	-3.75 T	1104=	-3.75 T	1105=	-3.78
1106=	-3.75 T	1199=	-3.75 T	1201=	46.61 T	1202=	45.97
1203=	46.61 T	1204=	46.99 T	1205=	46.61 T	1206=	46.61
1299=	46.61 T	1601=	-3.12 T	1602=	-3.21 T	1603=	-3.21
1604=	-3.21 T	1605=	-3.58 T	1606=	-3.21 T	1699=	-3.21
2001=	-23.38 T	2002=	-23.38 T	2003=	-23.38 T	2004=	-23.40
2005=	-23.38 T	2006=	-23.38 T	2099=	-23.38 T	3001=	45.60
3002=	45.58 T	3003=	45.60 T	3004=	45.60 T	3005=	45.60
3006=	45.60 T	3099=	45.60 T	3101=	45.60 T	3102=	45.59
3103=	45.60 T	3104=	45.60 T	3105=	45.60 T	3106=	45.60
3199=	-3.78 T	3201=	-3.78 T	3202=	-3.78 T	3203=	-3.78
3204=	-3.78 T	3205=	-3.80 T	3206=	-3.78 T	3299=	-3.78
3301=	-3.79 T	3302=	-3.78 T	3303=	-3.78 T	3304=	-3.78
3305=	-30.49 T	3306=	-3.78 T	3399=	-3.78 T	4401=	-30.51
4402=	-30.49 T	4403=	-30.48 T	4404=	-30.48 T	4405=	-30.48
4406=	47.74 T	4499=	-30.51 T	4501=	47.36 T	4502=	46.38
4503=	47.74 T	4504=	47.74 T	4505=	47.74 T	4506=	47.74
4599=	-3.02 T	4801=	-2.93 T	4802=	-2.92 T	4803=	-2.92
4804=	-69.01 T	4805=	-3.50 T	4806=	-2.92 T	4899=	-2.92
5301=	-69.00 T	5302=	-69.00 T	5303=	-69.00 T	5304=	-69.00
5305=	0.00 T	5306=	-69.00 T	5399=	-69.00 T	5601=	0.00
5602=	0.00 T	5603=	0.00 T	5604=	0.00 T	5605=	0.00
5606=	0.00 T	5607=	0.00 T	5608=	0.00 T	5609=	0.00
5610=	0.00 T	5611=	0.00 T	5612=	0.00 T	5613=	0.00
5614=	0.00 T	5615=	0.00 T	5616=	0.00 T	5617=	0.00
5618=	0.00 T	5699=	0.00 T	5701=	0.00 T	5702=	0.00
5703=	0.00 T	5704=	0.00 T	5705=	0.00 T	5706=	0.00
5707=	0.00 T	5708=	0.00 T	5709=	0.00 T	5710=	0.00
5711=	0.00 T	5712=	0.00 T	5713=	0.00 T	5714=	0.00
5715=	0.00 T	5716=	0.00 T	5717=	0.00 T	5718=	0.00
5799=	0.00 T	6201=	0.00 T	6202=	0.00 T	6203=	0.00
6204=	0.00 T	6205=	0.00 T	6206=	0.00 T	6207=	0.00
6208=	0.00 T	6209=	0.00 T	6210=	0.00 T	6211=	0.00
6212=	0.00 T	6299=	0.00 T	6301=	0.00 T	6302=	0.00
6303=	0.00 T	6304=	0.00 T	6305=	0.00 T	6306=	0.00
6307=	0.00 T	6308=	0.00 T	6309=	0.00 T	6310=	0.00
6311=	0.00 T	6312=	0.00 T	6399=	0.00 T	7001=	-93.32

```
T  7002=    -35.70 T  7003=    -35.70 T  7101=    -93.32 T  7102=    -93.32
T  7103=    -70.50 T  7104=    -70.50 T  7105=    -72.00 T  7106=    -72.00

                    ASCENDING NODE NUMBER : TEMPERATURE
**********************************************************************
 ITAS STEADY-STATE SOLUTION (SUCCESSIVE POINT ITERATION)
 NO. OF ITERATIONS=10000 TOTAL INPUT ENERGY (W)=  801.70
 SYSTEM ENERGY BALANCE (W)= -1.7652      ( 0.22019    %)
**********************************************************************
T       1=   -70.515 T       2=    45.807 T       3=   -93.327 T       4=   -72.009
T       5=    -3.569 T       6=   -35.706 T       7=   -70.481 T       8=    45.689
T       9=   -93.325 T      10=   -71.986 T      11=    -3.688 T      12=   -35.704
T      13=     0.014 T      14=     0.014 T      15=     0.014 T      16=     0.014
T      17=     0.014 T      18=     0.014 T      19=     0.014 T      20=     0.014
T      21=     0.014 T      22=     0.014 T      23=     0.014 T      24=     0.014
T      25=     0.014 T      26=     0.014 T      27=     0.014 T      28=     0.014
T      29=     0.014 T      30=     0.014 T      31=     0.014 T      32=     0.014
T      33=     0.014 T      34=     0.014 T      35=     0.014 T      36=     0.014
T      37=     0.014 T      38=     0.014 T      39=     0.014 T      40=     0.014
T      41=     0.014 T      42=     0.014 T      43=     0.014 T      44=     0.014
T      45=     0.014 T      46=     0.014 T      47=     0.014 T      48=     0.014
T      49=     0.014 T      50=     0.014 T      51=     0.014 T      52=     0.014
T      53=     0.014 T      54=     0.014 T      55=     0.014 T      56=     0.014
T      57=     0.014 T      58=     0.014 T      59=     0.014 T      60=     0.014
T      61=     0.014 T      62=     0.014 T      63=     0.014 T      64=     0.014
T      65=     0.014 T      66=     0.014 T      67=     0.014 T      68=     0.014
T      69=     0.014 T      70=     0.014 T      71=     0.014 T      72=     0.011
T      73=    45.634 T      74=    -3.746 T      75=    44.487 T      76=    -4.364
T      77=    45.629 T      78=    45.597 T      79=    45.629 T      80=    45.629
T      81=    45.629 T      82=    45.629 T      83=    -3.749 T      84=    -3.749
T      85=    -3.749 T      86=    -3.749 T      87=    -3.784 T      88=    -3.749
T      89=    46.610 T      90=    45.970 T      91=    46.610 T      92=    46.985
T      93=    46.610 T      94=    46.610 T      95=    -3.118 T      96=    -3.215
T      97=    -3.215 T      98=    -3.215 T      99=    -3.578 T     100=    -3.215
T     101=   -23.375 T     102=   -23.376 T     103=   -23.379 T     104=   -23.396
T     105=   -23.377 T     106=   -23.376 T     107=    45.596 T     108=    45.584
T     109=    45.596 T     110=    45.596 T     111=    45.596 T     112=    45.596
T     113=    45.598 T     114=    45.586 T     115=    45.598 T     116=    45.598
T     117=    45.598 T     118=    45.598 T     119=    -3.781 T     120=    -3.781
T     121=    -3.781 T     122=    -3.781 T     123=    -3.796 T     124=    -3.781
T     125=    -3.780 T     126=    -3.780 T     127=    -3.780 T     128=    -3.780
T     129=    -3.794 T     130=    -3.780 T     131=   -30.501 T     132=   -30.482
T     133=   -30.483 T     134=   -30.483 T     135=   -30.483 T     136=   -30.482
T     137=    47.362 T     138=    46.376 T     139=    47.738 T     140=    47.738
T     141=    47.739 T     142=    47.738 T     143=    -2.925 T     144=    -2.925
T     145=    -2.925 T     146=    -3.022 T     147=    -3.495 T     148=    -2.925
T     149=   -69.007 T     150=   -68.999 T     151=   -68.999 T     152=   -68.998
T     153=   -68.999 T     154=   -68.999 T     155=    -0.002 T     156=     0.001
T     157=     0.001 T     158=     0.001 T     159=     0.001 T     160=     0.001
T     161=     0.001 T     162=     0.001 T     163=     0.001 T     164=     0.001
T     165=     0.001 T     166=     0.001 T     167=     0.001 T     168=     0.001
T     169=     0.001 T     170=     0.001 T     171=     0.001 T     172=     0.001
T     173=     0.001 T     174=     0.001 T     175=     0.001 T     176=    -0.002
T     177=     0.001 T     178=     0.001 T     179=     0.001 T     180=     0.001
T     181=     0.001 T     182=     0.001 T     183=     0.001 T     184=     0.001
T     185=     0.001 T     186=     0.001 T     187=     0.001 T     188=     0.001
T     189=     0.001 T     190=     0.001 T     191=     0.004 T     192=     0.004
T     193=     0.004 T     194=     0.004 T     195=     0.004 T     196=     0.004
T     197=     0.004 T     198=     0.004 T     199=     0.004 T     200=     0.004
T     201=     0.004 T     202=     0.004 T     203=     0.005 T     204=     0.005
T     205=     0.005 T     206=     0.005 T     207=     0.005 T     208=     0.005
T     209=     0.005 T     210=     0.005 T     211=     0.005 T     212=     0.005
T     213=     0.005 T     214=     0.005 T     215=  -273.159 T     501=   -70.497
T     502=    45.747 T     503=   -93.325 T     504=   -71.997 T     505=    -3.629
T     506=   -35.705 T     601=   -70.482 T     602=    45.690 T     603=   -93.325
T     604=   -71.986 T     605=    -3.688 T     606=   -35.704 T     701=     0.014
```

T	702=	0.014	T	703=	0.014	T	704=	0.014	T	705=	0.014
T	706=	0.014	T	707=	0.014	T	708=	0.014	T	709=	0.014
T	710=	0.014	T	711=	0.014	T	712=	0.014	T	713=	0.014
T	714=	0.014	T	715=	0.014	T	716=	0.014	T	717=	0.014
T	718=	0.014	T	719=	0.014	T	720=	0.014	T	721=	0.014
T	722=	0.014	T	723=	0.014	T	724=	0.014	T	725=	0.014
T	726=	0.014	T	727=	0.014	T	728=	0.014	T	729=	0.014
T	730=	0.014	T	731=	0.014	T	732=	0.014	T	733=	0.014
T	734=	0.014	T	735=	0.014	T	736=	0.014	T	737=	0.014
T	738=	0.014	T	739=	0.014	T	740=	0.014	T	741=	0.014
T	742=	0.014	T	743=	0.014	T	744=	0.014	T	745=	0.014
T	746=	0.014	T	747=	0.014	T	748=	0.014	T	749=	0.014
T	750=	0.014	T	751=	0.014	T	752=	0.014	T	753=	0.014
T	754=	0.014	T	755=	0.014	T	756=	0.014	T	757=	0.014
T	758=	0.014	T	759=	0.014	T	760=	0.011	T	799=	0.014
T	801=	45.634	T	802=	-3.746	T	901=	45.577	T	902=	-3.805
T	1001=	45.629	T	1002=	45.597	T	1003=	45.629	T	1004=	45.629
T	1005=	45.629	T	1006=	45.629	T	1099=	45.629	T	1101=	-3.749
T	1102=	-3.749	T	1103=	-3.749	T	1104=	-3.749	T	1105=	-3.784
T	1106=	-3.749	T	1199=	-3.749	T	1201=	46.610	T	1202=	45.970
T	1203=	46.610	T	1204=	46.985	T	1205=	46.611	T	1206=	46.610
T	1299=	46.610	T	1601=	-3.118	T	1602=	-3.215	T	1603=	-3.215
T	1604=	-3.215	T	1605=	-3.578	T	1606=	-3.215	T	1699=	-3.215
T	2001=	-23.381	T	2002=	-23.382	T	2003=	-23.379	T	2004=	-23.396
T	2005=	-23.377	T	2006=	-23.382	T	2099=	-23.379	T	3001=	45.596
T	3002=	45.584	T	3003=	45.596	T	3004=	45.596	T	3005=	45.596
T	3006=	45.596	T	3099=	45.597	T	3101=	45.598	T	3102=	45.586
T	3103=	45.598	T	3104=	45.598	T	3105=	45.598	T	3106=	45.598
T	3199=	45.598	T	3201=	-3.781	T	3202=	-3.781	T	3203=	-3.781
T	3204=	-3.781	T	3205=	-3.796	T	3206=	-3.781	T	3299=	-3.781
T	3301=	-3.780	T	3302=	-3.780	T	3303=	-3.780	T	3304=	-3.780
T	3305=	-3.794	T	3306=	-3.780	T	3399=	-3.780	T	4401=	-30.507
T	4402=	-30.488	T	4403=	-30.484	T	4404=	-30.484	T	4405=	-30.484
T	4406=	-30.488	T	4499=	-30.515	T	4501=	47.362	T	4502=	46.376
T	4503=	47.738	T	4504=	47.738	T	4505=	47.739	T	4506=	47.738
T	4599=	47.739	T	4801=	-2.925	T	4802=	-2.925	T	4803=	-2.925
T	4804=	-3.022	T	4805=	-3.495	T	4806=	-2.925	T	4899=	-2.925
T	5301=	-69.009	T	5302=	-68.999	T	5303=	-68.999	T	5304=	-69.000
T	5305=	-68.999	T	5306=	-68.999	T	5399=	-68.999	T	5601=	-0.002
T	5602=	0.001	T	5603=	0.001	T	5604=	0.001	T	5605=	0.001
T	5606=	0.001	T	5607=	0.001	T	5608=	0.001	T	5609=	0.001
T	5610=	0.001	T	5611=	0.001	T	5612=	0.001	T	5613=	0.001
T	5614=	0.001	T	5615=	0.001	T	5616=	0.001	T	5617=	0.001
T	5618=	0.001	T	5699=	0.000	T	5701=	0.001	T	5702=	0.001
T	5703=	0.001	T	5704=	-0.002	T	5705=	0.001	T	5706=	0.001
T	5707=	0.001	T	5708=	0.001	T	5709=	0.001	T	5710=	0.001
T	5711=	0.001	T	5712=	0.001	T	5713=	0.001	T	5714=	0.001
T	5715=	0.001	T	5716=	0.001	T	5717=	0.001	T	5718=	0.001
T	5799=	0.000	T	6201=	0.004	T	6202=	0.004	T	6203=	0.004
T	6204=	0.004	T	6205=	0.004	T	6206=	0.004	T	6207=	0.004
T	6208=	0.004	T	6209=	0.004	T	6210=	0.004	T	6211=	0.004
T	6212=	0.004	T	6299=	0.004	T	6301=	0.005	T	6302=	0.005
T	6303=	0.005	T	6304=	0.005	T	6305=	0.005	T	6306=	0.005
T	6307=	0.005	T	6308=	0.005	T	6309=	0.005	T	6310=	0.005
T	6311=	0.005	T	6312=	0.005	T	6399=	0.005	T	7001=	-93.325
T	7002=	-35.705	T	7003=	-35.705	T	7101=	-93.325	T	7102=	-93.325
T	7103=	-70.497	T	7104=	-70.497	T	7105=	-71.997	T	7106=	-71.997

ASCENDING NODE NUMBER : IMPRESSED Q

Q	1=	46.500	Q	2=	18.100	Q	3=	50.700	Q	4=	46.500
Q	5=	18.100	Q	6=	155.370	Q	7=	0.000	Q	8=	0.000
Q	9=	0.000	Q	10=	0.000	Q	11=	0.000	Q	12=	0.000
Q	13=	0.000	Q	14=	0.000	Q	15=	0.000	Q	16=	0.000
Q	17=	0.000	Q	18=	0.000	Q	19=	0.000	Q	20=	0.000
Q	21=	0.000	Q	22=	0.000	Q	23=	0.000	Q	24=	0.000
Q	25=	0.010	Q	26=	0.000	Q	27=	0.000	Q	28=	0.000
Q	29=	0.000	Q	30=	0.010	Q	31=	0.000	Q	32=	0.000

33=	0.010 Q	34=	0.000 Q	35=	0.010 Q	36=	0.000
37=	0.010 Q	38=	0.010 Q	39=	0.000 Q	40=	0.010
41=	0.000 Q	42=	0.010 Q	43=	0.000 Q	44=	0.000
45=	0.000 Q	46=	0.000 Q	47=	0.000 Q	48=	0.000
49=	0.000 Q	50=	0.000 Q	51=	0.000 Q	52=	0.000
53=	0.000 Q	54=	0.000 Q	55=	0.000 Q	56=	0.000
57=	0.000 Q	58=	0.000 Q	59=	0.000 Q	60=	0.000
61=	0.000 Q	62=	0.000 Q	63=	0.000 Q	64=	0.000
65=	0.000 Q	66=	0.000 Q	67=	0.000 Q	68=	0.000
69=	0.000 Q	70=	0.000 Q	71=	0.000 Q	72=	0.000
73=	0.000 Q	74=	0.000 Q	75=	0.010 Q	76=	0.010
77=	0.000 Q	78=	0.000 Q	79=	0.000 Q	80=	0.000
81=	0.000 Q	82=	0.000 Q	83=	0.000 Q	84=	0.000
85=	0.000 Q	86=	0.000 Q	87=	0.000 Q	88=	0.000
89=	0.000 Q	90=	0.000 Q	91=	0.000 Q	92=	0.000
93=	0.000 Q	94=	0.000 Q	95=	0.000 Q	96=	0.000
97=	0.000 Q	98=	0.000 Q	99=	0.000 Q	100=	0.000
101=	0.000 Q	102=	0.000 Q	103=	0.000 Q	104=	0.000
105=	0.000 Q	106=	0.000 Q	107=	0.000 Q	108=	0.000
109=	0.000 Q	110=	0.000 Q	111=	0.000 Q	112=	0.000
113=	0.000 Q	114=	0.000 Q	115=	0.000 Q	116=	0.000
117=	0.000 Q	118=	0.000 Q	119=	0.000 Q	120=	0.000
121=	0.000 Q	122=	0.000 Q	123=	0.000 Q	124=	0.000
125=	0.000 Q	126=	0.000 Q	127=	0.000 Q	128=	0.000
129=	0.000 Q	130=	0.000 Q	131=	0.000 Q	132=	0.000
133=	0.000 Q	134=	0.000 Q	135=	0.000 Q	136=	0.000
137=	0.000 Q	138=	0.000 Q	139=	0.000 Q	140=	0.000
141=	0.000 Q	142=	0.000 Q	143=	0.000 Q	144=	0.000
145=	0.000 Q	146=	0.000 Q	147=	0.000 Q	148=	0.000
149=	0.000 Q	150=	0.000 Q	151=	0.000 Q	152=	0.000
153=	0.000 Q	154=	0.000 Q	155=	0.000 Q	156=	0.000
157=	0.000 Q	158=	0.000 Q	159=	0.000 Q	160=	0.000
161=	0.000 Q	162=	0.000 Q	163=	0.000 Q	164=	0.000
165=	0.000 Q	166=	0.000 Q	167=	0.000 Q	168=	0.000
169=	0.000 Q	170=	0.000 Q	171=	0.000 Q	172=	0.000
173=	0.000 Q	174=	0.000 Q	175=	0.000 Q	176=	0.000
177=	0.000 Q	178=	0.000 Q	179=	0.000 Q	180=	0.000
181=	0.000 Q	182=	0.000 Q	183=	0.000 Q	184=	0.000
185=	0.000 Q	186=	0.000 Q	187=	0.000 Q	188=	0.000
189=	0.000 Q	190=	0.000 Q	191=	0.000 Q	192=	0.000
193=	0.000 Q	194=	0.000 Q	195=	0.000 Q	196=	0.000
197=	0.000 Q	198=	0.000 Q	199=	0.000 Q	200=	0.000
201=	0.000 Q	202=	0.000 Q	203=	0.000 Q	204=	0.000
205=	0.000 Q	206=	0.000 Q	207=	0.000 Q	208=	0.000
209=	0.000 Q	210=	0.000 Q	211=	0.000 Q	212=	0.000
213=	0.000 Q	214=	0.000 Q	215=	0.000 Q	501=	0.000
502=	0.000 Q	503=	0.000 Q	504=	0.000 Q	505=	0.000
506=	0.000 Q	601=	0.000 Q	602=	0.000 Q	603=	0.000
604=	0.000 Q	605=	0.000 Q	606=	0.000 Q	701=	0.000
702=	0.000 Q	703=	0.000 Q	704=	0.000 Q	705=	0.000
706=	0.000 Q	707=	0.000 Q	708=	0.000 Q	709=	0.000
710=	0.000 Q	711=	0.000 Q	712=	0.000 Q	713=	0.000
714=	0.000 Q	715=	0.000 Q	716=	0.000 Q	717=	0.000
718=	0.000 Q	719=	0.000 Q	720=	0.000 Q	721=	0.000
722=	0.000 Q	723=	0.000 Q	724=	0.000 Q	725=	0.000
726=	0.000 Q	727=	0.000 Q	728=	0.000 Q	729=	0.000
730=	0.000 Q	731=	0.000 Q	732=	0.000 Q	733=	0.000
734=	0.000 Q	735=	0.000 Q	736=	0.000 Q	737=	0.000
738=	0.000 Q	739=	0.000 Q	740=	0.000 Q	741=	0.000
742=	0.000 Q	743=	0.000 Q	744=	0.000 Q	745=	0.000
746=	0.000 Q	747=	0.000 Q	748=	0.000 Q	749=	0.000
750=	0.000 Q	751=	0.000 Q	752=	0.000 Q	753=	0.000
754=	0.000 Q	755=	0.000 Q	756=	0.000 Q	757=	0.000
758=	0.000 Q	759=	0.000 Q	760=	0.000 Q	799=	2.500
801=	0.000 Q	802=	0.000 Q	901=	0.000 Q	902=	0.000
1001=	0.000 Q	1002=	0.000 Q	1003=	0.000 Q	1004=	0.000

```
Q  1005=      0.000 Q  1006=      0.000 Q  1099=      5.000 Q  1101=      0.000
Q  1102=      0.000 Q  1103=      0.000 Q  1104=      0.000 Q  1105=      0.000
Q  1106=      0.000 Q  1199=      5.000 Q  1201=      0.000 Q  1202=      0.000
Q  1203=      0.000 Q  1204=      0.000 Q  1205=      0.000 Q  1206=      0.000
Q  1299=     40.000 Q  1601=      0.000 Q  1602=      0.000 Q  1603=      0.000
Q  1604=      0.000 Q  1605=      0.000 Q  1606=      0.000 Q  1699=     40.000
Q  2001=      0.000 Q  2002=      0.000 Q  2003=      0.000 Q  2004=      0.000
Q  2005=      0.000 Q  2006=      0.000 Q  2099=      1.000 Q  3001=      0.000
Q  3002=      0.000 Q  3003=      0.000 Q  3004=      0.000 Q  3005=      0.000
Q  3006=      0.000 Q  3099=      2.000 Q  3101=      0.000 Q  3102=      0.000
Q  3103=      0.000 Q  3104=      0.000 Q  3105=      0.000 Q  3106=      0.000
Q  3199=      2.000 Q  3201=      0.000 Q  3202=      0.000 Q  3203=      0.000
Q  3204=      0.000 Q  3205=      0.000 Q  3206=      0.000 Q  3299=      2.000
Q  3301=      0.000 Q  3302=      0.000 Q  3303=      0.000 Q  3304=      0.000
Q  3305=      0.000 Q  3306=      0.000 Q  3399=      2.000 Q  4401=      0.000
Q  4402=      0.000 Q  4403=      0.000 Q  4404=      0.000 Q  4405=      0.000
Q  4406=      0.000 Q  4499=      1.000 Q  4501=      0.000 Q  4502=      0.000
Q  4503=      0.000 Q  4504=      0.000 Q  4505=      0.000 Q  4506=      0.000
Q  4599=    261.630 Q  4801=      0.000 Q  4802=      0.000 Q  4803=      0.000
Q  4804=      0.000 Q  4805=      0.000 Q  4806=      0.000 Q  4899=    100.000
Q  5301=      0.000 Q  5302=      0.000 Q  5303=      0.000 Q  5304=      0.000
Q  5305=      0.000 Q  5306=      0.000 Q  5399=      1.000 Q  5601=      0.000
Q  5602=      0.000 Q  5603=      0.000 Q  5604=      0.000 Q  5605=      0.000
Q  5606=      0.000 Q  5607=      0.000 Q  5608=      0.000 Q  5609=      0.000
Q  5610=      0.000 Q  5611=      0.000 Q  5612=      0.000 Q  5613=      0.000
Q  5614=      0.000 Q  5615=      0.000 Q  5616=      0.000 Q  5617=      0.000
Q  5618=      0.000 Q  5699=      0.300 Q  5701=      0.000 Q  5702=      0.000
Q  5703=      0.000 Q  5704=      0.000 Q  5705=      0.000 Q  5706=      0.000
Q  5707=      0.000 Q  5708=      0.000 Q  5709=      0.000 Q  5710=      0.000
Q  5711=      0.000 Q  5712=      0.000 Q  5713=      0.000 Q  5714=      0.000
Q  5715=      0.000 Q  5716=      0.000 Q  5717=      0.000 Q  5718=      0.000
Q  5799=      0.300 Q  6201=      0.000 Q  6202=      0.000 Q  6203=      0.000
Q  6204=      0.000 Q  6205=      0.000 Q  6206=      0.000 Q  6207=      0.000
Q  6208=      0.000 Q  6209=      0.000 Q  6210=      0.000 Q  6211=      0.000
Q  6212=      0.000 Q  6299=      0.300 Q  6301=      0.000 Q  6302=      0.000
Q  6303=      0.000 Q  6304=      0.000 Q  6305=      0.000 Q  6306=      0.000
Q  6307=      0.000 Q  6308=      0.000 Q  6309=      0.000 Q  6310=      0.000
Q  6311=      0.000 Q  6312=      0.000 Q  6399=      0.300 Q  7001=      0.000
Q  7002=      0.000 Q  7003=      0.000 Q  7101=      0.000 Q  7102=      0.000
Q  7103=      0.000 Q  7104=      0.000 Q  7105=      0.000 Q  7106=      0.000
 BOLTZMANN CONSTANT: SIGMA =   0.566970E-11 W/(CM^2 K)
=================================================================================
 NO. OF THERMAL NODES (CURRENT) =          456
 TAS TRANSIENT SOLUTION ALGORITHM PARAMETERS:
 IMEO = 0.00000     , TIMEND=  113.60     , OUTPUT=  15.000
 TIMEI= 0.10000     , ARLXCA= 0.50000E-03, DRLXCA= 0.50000E-03
 SGFAC=  1.0000      , NLOOP =        9999
 ************************************
 THERMAL CALC CPU TIME (second)      =     4597.70
 ************************************
```

APPENDIX H

THIS PAGE INTENTIONALLY LEFT BLANK

THIS PAGE INTENTIONALLY LEFT BLANK

APPENDIX H

A. ATTITUDE CONTROL SYSTEM CALCULATIONS

The attitude control system (ACS) consists of one momentum wheel whose spin axis is aligned with the pitch axis. Another momentum wheel is installed for redundancy. Two magnetic torque rods are installed for the purposes of momentum wheel desaturation and control of disturbances in the roll-yaw plane. Thrusters are installed for satellite repositioning and will replace the torque rods in the event of their failure.

Table C.1 is a summary of satellite inertias and distance of the center of mass from the center of pressure. The contributions of the cross-products of inertia are negligible and are not shown here.

Mass (kg)	x (cm)	y (cm)	z (cm)	I_{xx} (kg-m^2)	I_{yy} (kg-m^2)	I_{zz} (kg-m^2)
400	1.1025	2.1468	0.0036	166.08	246.45	188.88

Table C.1 CP-CM offset and satellite inertias

B. DISTURBANCE TORQUES

The disturbance torques acting on the spacecraft consist of solar torque, gravity gradient torque, magnetic torque and internal torques. The magnetic disturbance torque is the primary disturbing force acting on the spacecraft and is used to calculate the time constants and gains of the attitude control system.

1. Solar Torque

The solar torque is modeled using the following equations (Agrawal, 1986, p. 135).

$$M_s = PA \begin{pmatrix} (yK1 - zK2 - xK2 \sin(\alpha)) I_o \\ (zK1 \sin(\alpha) - xK1 \cos(\alpha)) J_o \\ (-zK2 \sin(\alpha) + xK2 \cos(\alpha)) K_o \end{pmatrix}$$

Solar pressure was calculated a program written for Mathcad, which is included at the end of this appendix.

2. Gravity gradient, Magnetic and Internal torques

The gravity gradient torque is of the same order of magnitude as the solar torque. These are both approximately an order of magnitude smaller than the magnetic disturbing torques. These torques are very difficult to model and were therefore calculated for worst case values.

The following figures illustrate the sensed magnetic field in both body-fixed and inertial coordinate systems. It is seen that the magnetic disturbance is on the order of 10^{-5} Tesla for pitch and 10^{-6} Tesla for roll. In order to counter the disturbances in roll in a timely manner, a torque rod providing a 50 AMP-m^2 dipole was used. In the same vein, a torque rod of 50 AMP-m^2 is used to desaturate the momentum wheel. Since the magnetic torque is given by

$$\vec{T}_M = \vec{B} \times \vec{M}$$

Coefficient of specular reflection:..... $r_s = 0.25$

Coefficient of diffuse reflection:..... $r_d = 0.03$

CP-CM offset:..... $r = \begin{bmatrix} 0.0110253 \\ 0.02146816 \\ 0.00357446 \end{bmatrix} \cdot m$

Solar array area:..... $A = 7.0 \cdot m^2$

Solar pressure:..... $P = 4.644 \cdot 10^{-6} \cdot Newton \cdot m^{-2}$

Spacecraft moments of inertia:

$$I_{xx} = 166.08 \cdot kg \cdot m^2$$

$$I_{yy} = 246.45 \cdot kg \cdot m^2$$

$$I_{zz} = 188.88 \cdot kg \cdot m^2$$

Equations foe determining constants K1 and K2 at equinox: $d = 0$

$$K_1 = \left[\left[1 - r_s \right] \cdot \cos(d) + 2 \cdot \left[r_s \cdot \cos(d) + \frac{1}{3} \cdot r_d \right] \right] \cdot \cos(d)$$

$$K_2 = \left[1 - r_s \right] \cdot \cos(d) \cdot \sin(d)$$

$$K_1 = 1.27$$

$$K_2 = 0$$

Solar torque equations:

- Body cordinates -

$$M_{sb.E}(\alpha) = \begin{bmatrix} r_1 \cdot K_1 \cdot \cos(\alpha) - r_2 \cdot K_2 \\ r_2 \cdot K_1 \cdot \sin(\alpha) - r_0 \cdot K_1 \cdot \cos(\alpha) \\ r_0 \cdot K_2 - r_1 \cdot K_1 \cdot \sin(\alpha) \end{bmatrix} \cdot P \cdot A$$

$$M_{sb.E}(d) = \begin{bmatrix} 8.86316 \cdot 10^{-7} \\ -4.55181 \cdot 10^{-7} \\ 0 \end{bmatrix} \cdot m \cdot Newton \quad \text{Equinox}$$

- Inertial cordinates -

$$M_{si.E}(\alpha) = \begin{bmatrix} r_1 \cdot K_1 - r_2 \cdot K_2 \cdot \cos(\alpha) - r_0 \cdot K_2 \cdot \sin(\alpha) \\ r_2 \cdot K_1 \cdot \sin(\alpha) - r_0 \cdot K_1 \cdot \cos(\alpha) \\ -r_2 \cdot K_2 \cdot \sin(\alpha) + r_0 \cdot K_2 \cdot \cos(\alpha) \end{bmatrix} \cdot P \cdot A$$

$$M_{si.E}(d) = \begin{bmatrix} 8.86316 \cdot 10^{-7} \\ -4.55181 \cdot 10^{-7} \\ 0 \end{bmatrix} \cdot m \cdot Newton \quad \text{Equinox}$$

Equations for determining constants K1 and K2 at solstice: $d = 23.45 \cdot deg$

$$K_1 = \left[\left[1 - r_s \right] \cdot \cos(d) + 2 \cdot \left[r_s \cdot \cos(d) + \frac{1}{3} \cdot r_d \right] \right] \cdot \cos(d)$$

$$K_2 = \left[1 - r_s \right] \cdot \cos(d) \cdot \sin(d)$$

$$K_1 = 1.07039$$

$$K_2 = 0.27381$$

Solar torque equations

- Body coordinates -

$$M_{sb.S}(\alpha) := \begin{bmatrix} r_1 \cdot K_1 \cdot \cos(\alpha) - r_2 \cdot K_2 \\ r_2 \cdot K_1 \cdot \sin(\alpha) - r_0 \cdot K_1 \cdot \cos(\alpha) \\ r_0 \cdot K_2 - r_1 \cdot K_1 \cdot \sin(\alpha) \end{bmatrix} \cdot P \cdot A$$

$$M_{sb.S}(d) = \begin{bmatrix} 6.535 \cdot 10^{-7} \\ -3.02459 \cdot 10^{-7} \\ -1.99137 \cdot 10^{-7} \end{bmatrix} \cdot m \cdot Newton \qquad Solstice$$

- Inertial coordinates -

$$M_{si.S}(\alpha) := \begin{bmatrix} r_1 \cdot K_1 - r_2 \cdot K_2 \cdot \cos(\alpha) - r_0 \cdot K_2 \cdot \sin(\alpha) \\ r_2 \cdot K_1 \cdot \sin(\alpha) - r_0 \cdot K_1 \cdot \cos(\alpha) \\ -r_2 \cdot K_2 \cdot \sin(\alpha) + r_0 \cdot K_2 \cdot \cos(\alpha) \end{bmatrix} \cdot P \cdot A$$

$$M_{si.S}(d) = \begin{bmatrix} 6.78772 \cdot 10^{-7} \\ -3.02459 \cdot 10^{-7} \\ 7.737 \cdot 10^{-8} \end{bmatrix} \cdot m \cdot Newton \qquad Solstice$$

Maximum steady state torque occurs at equinox

$$T_s := \left[\left| M_{si.E}(0 \cdot deg)_0 \right| \right] \qquad T_s = 8.86316 \cdot 10^{-7} \cdot m \cdot Newton$$

SIZING THE MOMENTUM WHEEL

Yaw error

$F = 1.0 \cdot deg$ and $F = F_{ss} + F_2 \square$

Let $F_2 := 0.80 \cdot deg$

Then $F_{ss} := 0.20$

Roll deadband

$f_d := 0.10 \cdot deg$

CALCULATING THE ANGULAR MOMENTUM OF THE WHEEL

Wheel angular momentum:..... $h := 9 \cdot Newton \cdot m \cdot sec$

Magnetic torquer offset angle:.. $\alpha := 67.33414 \cdot deg$

Satellite angular velocity:..... $w_0 := 9.217 \cdot 10^{-4} \cdot \frac{rad}{sec}$

Constant body-fixed roll-yaw torques:

$$T_{bx} := 1.5 \cdot 10^{-5} \cdot \frac{kg}{A \cdot sec^2} \cdot [\, 1 \cdot A \cdot m^2 \,]$$

$$T_{bx} = 1.5 \cdot 10^{-5} \cdot Newton \cdot m$$

$$T_{bz} := 3.0 \cdot 10^{-5} \cdot \frac{kg}{A \cdot sec^2} \cdot [\, 1 \cdot A \cdot m^2 \,]$$

$$T_{bz} = 3 \cdot 10^{-5} \cdot Newton \cdot m$$

The maximum torque acting on the satellite is due to magnetic disturbances. The magnitude of this disturbance torque is:

$$T_m := 3.0 \cdot 10^{-5} \cdot Newton \cdot m$$

The angular momentum and offset angle must be found through iteration of the equations below.

$$F_{ss} := \frac{T_{bz} + T_{bx} \cdot \tan(\alpha)}{w_0 \cdot h} \qquad F_{ss} = 0.4553 \cdot deg$$

To determine F2, the followins\g equations are used:

Initial guesses: $v_1 := 1 \cdot rad \qquad v_2 := 2 \cdot rad$

$$F_1 := -1.4 \cdot rad \qquad F_2 := -1 \cdot 10^{-3} \cdot rad$$

Given

$$\cos[\nu_1] = \frac{w_0 \cdot f_d \cdot h}{2 \cdot T_m}$$

$$F_1 = \frac{-[T_m \cdot \sin[\nu_1]]}{w_0 \cdot h}$$

$$f_d \cdot [1 + \cos[\nu_2 - \nu_1]] + F_1 \cdot \sin[\nu_2 - \nu_1] + [\nu_2 - \nu_1] \cdot \sin[\nu_2] \cdot \frac{T_m}{w_0 \cdot h} = 0$$

$$F_1 \cdot \cos[\nu_2 - \nu_1] - f_d \cdot \sin[\nu_2 - \nu_1] + [\nu_2 - \nu_1] \cdot \cos[\nu_2] \cdot \frac{T_m}{w_0 \cdot h} = F_2$$

$$vars = Find[\nu_1, F_1, \nu_2, F_2] \qquad vars = \begin{bmatrix} 1.32709 \\ -3.50964 \cdot 10^{-3} \\ 2.8347 \\ -7.161 \cdot 10^{-3} \end{bmatrix} \cdot rad$$

$$\nu_1 = vars_0 \qquad \nu_1 = 76.03669 \cdot deg$$

$$F_1 = vars_1 \qquad F_1 = -0.20109 \cdot deg$$

$$\nu_2 = vars_2 \qquad \nu_2 = 1.14592 \cdot 10^2 \cdot deg$$

$$F_2 = vars_3 \qquad F_2 = -0.4103 \cdot deg$$

To solve for Psi:

$$F = |F_{ss}| + |F_2| \qquad F = 0.8656 \cdot deg$$

To calculate the autopilot gain:

Assume the linear range is: $LR = 3 \cdot deg$

$$M_R = 0.00106 \cdot Newton \cdot m$$

$$K = \frac{M_R}{LR} \qquad K = 0.02024 \cdot Newton \cdot m \cdot rad^{-1}$$

The correction factor is:

$$N := \frac{1}{1 + \left[\frac{h^2}{I_{zz} \cdot K \cdot \cos(\alpha)} \right]} \qquad N = 0.01787$$

Magnetic torquer offset angle is given by:

$$\alpha := \operatorname{atan}\left[2 \cdot \sqrt{\frac{I_{zz} \cdot w_0}{N \cdot h}} \right] \qquad \alpha = 64.33414 \cdot \text{deg}$$

The lead time constant is:

$$t := 2 \cdot \sqrt{\frac{I_{xx}}{N \cdot K \cdot \cos(\alpha)}} \qquad t = 2.05925 \cdot 10^{3} \cdot \text{sec}$$

The magnetic torquer impulse is determined from:

$$dh_{lower} := \frac{2 \cdot h \cdot f_d \cdot \tan(\alpha)}{\cos(\alpha)}$$

$$dh_{upper} := \frac{2 \cdot f_d \cdot h}{1 + \sin(\alpha) + 2 \cdot \sin\left[.785398 + \left[\frac{\alpha}{2} \right] \right]}$$

$dh_{upper} = 8.15706 \cdot 10^{-3} \cdot \text{Newton} \cdot \text{m} \cdot \text{sec}$ $dh_{lower} = 0.15094 \cdot \text{Newton} \cdot \text{m} \cdot \text{sec}$

The limits on the upper impulse bit should be less than:

$$t_{upper} := \frac{dh_{upper}}{M_R} \qquad t_{upper} = 7.69534 \cdot \text{sec}$$

The limits on the lower bound should be greater than:

$$t_{lower} := \frac{dh_{lower}}{M_R} \qquad t_{lower} = 1.424 \cdot 10^{2} \cdot \text{sec}$$

Magnetic torquer impulse is chosen to be:

$$t = \frac{t_{upper} + t_{lower}}{2} \qquad t = 75.0476 \cdot sec$$

PITCH AXIS CONTROL

Desaturation torque impulse:..... $M_y = 0.075 \cdot Newton \cdot m \cdot sec$

Maximum pitch error:..... $q = 0.7 \cdot deg$

The system time constant is given by:

$$t = \frac{q \cdot I_{yy} \cdot e}{M_y} \qquad t = 1.09128 \cdot 10^2 \cdot sec$$

The system gain is given by:

$$K_q = \frac{I_{yy}}{t^2} \qquad K_q = 0.02069 \cdot Newton \cdot \frac{m}{rad}$$

The lead-time constant is given by:

$$t_q = 2 \cdot \sqrt{\frac{I_{yy}}{K_q}} \qquad t_q = 2.18257 \cdot 10^2 \cdot sec$$

THIS PAGE INTENTIONALLY LEFT BLANK

THIS PAGE INTENTIONALLY LEFT BLANK

APPENDIX I

THIS PAGE INTENTIONALLY LEFT BLANK

THIS PAGE INTENTIONALLY LEFT BLANK

APPENDIX I

1. List of parametric equations used in the analysis [Ref 1].

Structure/Thermal costs = $0.0 + 92.3X^{0.65}$
TT&C costs = $99 + 175X^{0.93}$
Comm. Antenna costs = $21 + 245X^{0.59}$
Comm. electronics pkg. costs = $0.0 + 191X^{1.0}$

2. Equation for determining the total cost (U_N) to produce N units given a learning rate (S), and a TFUC U_1.

$$U_N = U_1 \left(N^{\left(1 - \frac{\ln\left(\frac{100}{S}\right)}{\ln 2}\right)} \right)$$

THIS PAGE INTENTIONALLY LEFT BLANK

APPENDIX J

THIS PAGE INTENTIONALLY LEFT BLANK

THIS PAGE INTENTIONALLY LEFT BLANK

APPENDIX J

A. INTRODUCTION

Orbital perturbation analysis was performed using the Orbital Workbench software. Perturbations were analyzed over the five year lifetime of a single satellite, with the assumption that all other satellites would be effected in a similar manner. The analysis was undertaken from 0800, 1 July 1996 until 0800, 1 July 2001. This simulation required 17 hours to complete using a 25-MHz, 486 computer.

B. PERTURBATION ANALYSIS

The Cowell Propogation Method, using fourth order Runga Kutta integration, was used. The forces included in the simulation were zonals, tesserals, lunar gravity, solar gravity, and solar pressure.

- Zonals — Zonal harmonics (J2 through J6 of the spherical harmonic gravitational potential) vary with latitude. These forces result from the oblateness of the Earth and cause changes in eccentricity, inclination, nodal right ascention, and argument of perigee. For altitudes greater than 300 kilometers and less than geosynchronous, zonal harmonics are the dominant perturbation.
- Tesserals — Spherical harmonic gravitational potential caused by longitudinal variations in the distribution of the Earth's mass. The Cowell integration uses the first 12 x 12 tesseral terms.
- Lunar Gravity — The gravitational force of the Moon.
- Solar Gravity — The gravitational force of the Sun.
- Solar Pressure — Solar radiation pressure. The magnitude of this force is directly propotional to the satellite's area.

Table J-1 lists the ephemeris parameters generated using an integration time step of 2 minutes, with ephemeris data extracted every three months. It is assumed that there are no stationkeeping maneuvers during the 5 year simulation. It can be seen that the inclination stays relatively constant at 52 ± 0.1 degrees and that the only stationkeeping required is in-plane to maintain the semi-major axis (altitude).

Table J-1 Ephemeris Parameters with Perturbations

Time (hr)	Semi Maj Ax (km)	Eccentricity	Inclination (deg)	Rt Asc Node (deg)	True Anomaly (deg)
Jul 96	7759.000	.0000000	52.00000	.0000000	.0000000
Oct 96	7747.179	.1511960E-02	51.97098	76.75061	29.44777
Jan 97	7755.166	.9083657E-03	51.99851	153.2886	13.12778
Apr 97	7752.531	.1953402E-02	51.99595	-130.3860	281.9897
Jul 97	7746.177	.1071790E-02	51.98509	-53.58741	217.0868
Oct 97	7750.141	.1819065E-02	52.00235	22.24785	28.47666
Jan 98	7738.558	.1787696E-02	51.97140	97.85960	217.6329
Apr 98	7746.370	.1259050E-02	51.99823	173.2620	359.0561
Jul 98	7743.375	.1488790E-02	51.99589	-111.5506	104.6905
Oct 98	7741.999	.7179373E-03	51.99943	-36.61902	8.691524
Jan 99	7739.987	.1301609E-02	51.99683	38.06161	238.5591
Apr 99	7728.932	.9331507E-03	51.96684	112.5455	92.40669
Jul 99	7736.780	.6732633E-03	51.99484	-173.2252	199.6741
Oct 99	7728.548	.1495671E-02	51.97702	-98.47444	350.8088
Jan 00	7725.359	.2402283E-03	51.97666	-24.70368	91.68115
Apr 00	7727.728	.1550561E-02	51.98837	48.83462	133.4879
Jul 00	7729.731	.1040971E-02	51.99676	122.1106	5.949828
Oct 00	7718.523	.1956844E-02	51.96882	-164.8025	149.4116
Jan 01	7722.038	.1046557E-02	51.98616	-91.99513	295.4624
Apr 01	7724.671	.1693590E-02	52.00174	-19.39046	14.04350
Jul 01	7722.102	.1275817E-02	51.99793	53.69950	120.0624